Department of Civil and Environmental Engineering

University of Strathclyde

Development of Novel Methods for Extended Exposure Assessment of Combustion-Related Air Pollutants in Indoor and Outdoor Locations

By

NOR ELIANI BINTI EZANI

A thesis submitted in fulfilment of the requirements for the degree of

DOCTOR OF PHILOSOPHY

March 2017

This thesis is the result of the author's original research. It has been composed by the author and has not been previously submitted for examination which has led to the award of a degree.

Signed:

Date:

Abstract

Background & Aims: There is on-going and growing concern regarding acute and chronic human health effects associated with exposure to combustion-related air pollutants. This thesis describes the development and evaluation of novel methods for assessing exposure to combustion-related air pollutants [particulate matter (PM), black carbon (BC) and nitrogen dioxide (NO_2)] in indoor and outdoor environments.

Methods: The methods that were developed and evaluated included: mass and darkness/colour analysis of airborne particle samples; passive samplers; portable real time monitors; and GC-MS analysis of particulate-bound polycyclic aromatic hydrocarbons (pPAHs). These methods were used to measure PM, BC and NO_2 in indoor offices and outdoor streets in Glasgow city centre, and an industrial hydraulic fracturing test site in Poland.

Results: Detailed evaluation and calibration of novel methods for darkness measurement of low mass particulate material specimens collected on filters were completed to allow subsequent application in BC exposure estimation. Similarly, detailed evaluation allowed the refinement of procedures for field calibration of portable real-time monitors for BC, NO_2 and O_3. Indoor concentrations of PM, BC and NO_2 measured using the calibrated monitoring instruments were influenced by outdoor sources through natural ventilation and the proximity of buildings to urban roadsides. Outdoor measurements at 2 heights indicated that children are likely to experience higher exposures to combustion-related air pollutants from vehicle emissions. Marked elevations of BC and NO_2 concentrations were observed in downwind proximity to industrial fracking equipment sources, where average BC and NO_2 concentrations (11.2 & 111.3 $\mu g/m^3$) were 2 to 3 times higher than average BC and NO_2 exposures experienced while walking in Glasgow city centre (3.7 & 42.3 $\mu g/m^3$).

Conclusions: Novel exposure science and environmental engineering approaches were developed to allow improved characterisation of short-term to medium-term personal and environmental exposures to combustion-related air pollutants in a wide range of occupational and environmental settings.

Keywords: Combustion-related air pollutants; PM; BC; NO_2, novel methods.

DEDICATION

To my parents and my late aunty, Nik Roziah Nik Ghazi.

I would not have completed this journey without your unconditional love, constant support, understanding and personal sacrifices.

ACKNOWLEDGEMENTS

All praises to Allah for the strengths and His uncountable blessing that He has bestowed upon me.

My sincerest appreciations go to both my academic supervisors, Dr. Iain Beverland (Iain) and Prof. Robert Kalin (Bob). This work would have not been possible with their enthusiasm, guidance, support and encouragement. Thank you so much for all your helps. Special mentioned also goes to Prof. Zoe and the late Dr. David Cunningham for their encouragement during the fieldwork campaign in Poland. I would like also to thanks Dr. Tara for her support. I am grateful to our 'wee' Air Pollution group in the Department of Civil and Environment Engineering; Jonathan, Nicola, Ann, Fiona and Sam. I would like to thank to Stuart and Stephen from Ricardo AEA Ltd. who have helped to gain access to the traffic trolley. In addition, I have enjoyed working with the Edinburgh folk, Dr. Mathew, Dr. Chun and Hao. I am particularly thankful to Ron, his technical depth on the IT and software is amazing. My acknowledgement also goes to all technicians and admin staffs of Department of Civil and Environmental Engineering for their co-operations. I am also grateful to the MSc students I had the pleasure to work with: Dr. David Sykes, Nur, Megan, Giorgia, Akinola and Jessica.

I am greatly indebted to Ministry of Higher Education Malaysia and the Young Lecturer Scheme University Putra Malaysia for providing me support and the finance to pursue my PhD studies. My warm thanks and sincere gratitude to my comrades for the source of support and friendship in Glasgow. Special mention goes to Sadia, Alem, Catalina, Nui, Koi, Santiago, Jaafar, Long, Chris, Amy, Ronnie and Shehla. Thank you for sharing these years with me. I also wanted to thank to all other friends who put up me through this journey, in particular Jijie, Rozaini and my Malawian buddy, Kondwani. Finally and importantly, I would like to thank to my parents, siblings and family in Malaysia for their continuous love, support and good wishes whenever I needed. Thanks to all those who have helped me directly or indirectly in the successful completion of my thesis.

Eliani Ezani

March 2017

LIST OF AUTHOR'S CONTRIBUTIONS

1. Technical & Published Works

Ezani, E., Masey, N., Gillespie, J., Beverland, I. J., Beattie, T., Kalin, R. & Shipton, Z. 2017. Assessment of air pollution exposure at an experimental unconventional natural gas operations site. *Atmospheric Environment. Manuscript is submitted.*

Masey, N., Gillespie, J., Ezani, E., Lin, C., Hao, W., Heal, M. R., Ferguson, N., Hamilton, S. & Beverland, I. J. 2017b. Temporal changes in field calibration relationships for Aeroqual S500 NO_2 and O_3 sensors. *Environmental Science & Technology. Manuscript is submitted.*

Masey, N., Ezani, E., Gillespie, J., Heal, M. R., Hamilton, S. & Beverland, I. J. 2017a. Temporal variation of peripatetic real time pollution measurements and their ability to estimate longer term concentrations. *Atmospheric Environment*. *Manuscript is submitted.*

Masey, N., Ezani, E., Gillespie, J., Lin, C., Heal, M. & Beverland, I. J. 2017. Impact of filter shadowing correction algorithms on agreement of portable AE51 micro-aethalometer and reference AE33 aethalometer black carbon measurements. *Atmospheric Environment. Manuscript is submitted*.

2. List of Conferences

Ezani, E., Beverland, I. J., Beattie, T. & Tailford, M. 2016a. Assessment of Personal Exposure to Black Carbon and Nitrogen Dioxide in Contrasting Urban (Road Traffic) and Industrial (Fracking) Environments. *International Society of Exposure Science (ISES) Annual Meeting* Utrecht, the Netherlands.

Ezani, E., Beverland, I. J. & Idowu, A. 2016b. An In-comparison of Real-time Instruments for Measurement of Personal Exposure to Black Carbon (BC) and Nitrogen Dioxide (NO_2). *BOHS Annual Occupational Hygiene Conference.* Glasgow, UK.

Ezani, E., Beverland, I. J., Masey, N., Hamilton, S. & Sykes, D. 2015. Exposure to Traffic-Related Air Pollution: Are Children More Exposed Than Adults?. *Annual Aerosol Science Conference 2015*. Birmingham, UK.

3. List of Online Article

Ezani, E. 2015. *Haze in Malaysia 2015: Same old script, new solutions* [Online]. Available: http://cleanmalaysia.com/2015/10/03/haze-in-malaysia-2015-same-old-script-new-solutions/.

4.0 List of Awards

Winner for the Best Junior Researcher Poster Contribution at Annual Aerosol Science Conference 2015.
Shortlisted for Images of Research Competition with image entitled 'Hope for Hope Street'.

TABLE OF CONTENTS

LIST OF FIGURES

Figure **Page**

LIST OF TABLES

Table **Page**

LIST OF EQUATIONS

Equation **Page**

LIST OF ABBREVIATIONS & ACRONYMS

µg	microgramme (1µg = 1 x 10^{-6} g)
µg/m^3	microgramme per metre
µm	micrometre
abs. coeff	absorption coefficient
ASE	accelerated solvent extraction
ATDSR	Agency for Toxic Substances and Disease Registry
AUN	automatic analyser
BaP	Benzo (a) pyrene
BC	black carbon
BS	black smoke
C	celcius
Conc.	concentration
COMEAP	Committee on the Medical Effects of Air Pollutants
DCEE	Department of Civil & Environmental Engineering
DEFRA	Department for Environment, Food & Rural Affairs
EC	elemental carbon
ESCAPE	European Study of Cohorts for Air Pollution Effects
g	gram

GC-MS	gas chromatography-mass spectrometry
GF/A	glass fibre
GPS	global positioning system
h	hour
HEPA	High-efficiency particulate arrestance
HSE	Health Safety & Executive
IOM	Institute of Occupational Medicine
ISC	International Study Centre
L	litre
LEO	little environmental observatory
LMICs	low- and middle-income countries
L min^{-1}	litre per minute
ln	natural logarithm
LOD	limit of detection
NiMH	nickel metal hydride
mg	miligramme
min	minute
mm	millimetre
MicroAeth	microaethlometer
mL	mililitre

mL min^{-1}	millilitre per minute
m/s^{1}	metre per second
ms	milisecond
MHDS	material safety data sheet
MNB	mean normalised bias
n	number
N/A	not available
ng	nanogramme (1×10^{-9})
NRMSE	normalised root mean square error
NIOSH	The National Institute for Occupational Safety and Health
NO	nitric oxide
NO_x	nitrous oxide
NO_2	nitrogen dioxide
NO_2^-	nitrite
O_3	ozone
OLS	ordinary least squares
PDTs	passive diffusion tubes
PAHs	polycyclic aromatic hydrocarbons
pPAHs	particle-bound polycyclic aromatic hydrocarbons
PM	particulate matter

PM_1	particulate matter with aerodynamic less than 1.0 µm
$PM_{2.5}$	particulate matter with aerodynamic less than 2.5 µm
PM_{10}	particulate matter with aerodynamic less than 10 µm
PTFE	polytetrafluoroethylene
RMA	reduced major axis
RMSE	root mean square error
s	second
SD	standard deviation
S/N	serial number
St.	street
WHO	World Health Organization
UK	United Kingdom
UNG	unconventional natural gas
US EPA	United States of Environmental Protection Act
UV-Vis	ultraviolet-visible spectrophotometry
VAT	value-added tax
vs.	versus

1 INTRODUCTION

1.0 Background

This chapter introduces: Firstly, the major constituents of combustion-related air pollutants, and their key sources responsible for air pollution in different environmental settings. Secondly, the health effects and standard guidelines for each air pollutant component. Finally, the concept of exposure assessment and basic measurement principles from traditional to real-time sensors used to measure combustion-related air pollutants.

1.1 Introduction

The ubiquitous nature of poor air quality is a key environmental health priority as it is regarded as one of the greatest dangers to human health, and has been associated with 7 million annual deaths globally (WHO, 2014). In many parts of the world (especially in developed countries) large numbers of people spent most of their time living and working indoors (Kankaria *et al.*, 2014, Lim *et al.*, 2012) where air pollution exposures are different from exposures experienced during outdoor travel and recreation activities. Key source categories include pollutants resulting from combustion of fossil fuels in stationary sources and traffic. Combustion-related air pollutants have been associated with adverse health outcomes include particulate

matter (PM), nitrogen dioxide (NO_2), black carbon (BC), ozone (O_3) and other toxic compounds including polycyclic aromatic hydrocarbons (PAHs) (Lewtas, 2007).

1.1.1 PM

Airborne particulate matter ranges in size from a sub-nanometer to micrometers, and they can have unique shapes, which affect their aerodynamic diameters. They can comprise of a single origin or can be of mixed chemical composition. Airborne particles can be derived from various sources, both natural and anthropogenic including emissions from sea salts, volcanic eruption, biomass combustion and diesel exhaust (Fuzzi *et al.*, 2015). $PM_{2.5}$ and PM_{10} describe the mass of particles with a mean diameter or less than 2.5 and 10 μm, employed as the main metrics for the purposes of ambient monitoring and regulation (Thorpe and Harrison, 2008).

1.1.2 PAHs

Polycyclic aromatic hydrocarbons (PAHs) are comprised of two or more fused aromatic rings and have received much attention in air pollution studies (Ravindra *et al.*, 2008), the pollutant is a complex mixture of particles and gaseous phase (Tiwary and Colls, 2010). There have been approximately 500 of PAHs recognised, however the US EPA has prioritised 16 PAHs compounds based on their health concerns. Mohanraj *et al.* (2012) found fine particulates comprised PAHs collected in Southern India, with their study highlighting that the major source of PAHs are from traffic emissions.

1.1.3 BC

Black carbon (BC) can be defined as a strong light-absorbing carbonaceous particle. Petzold *et al.* (2013) also described in detail BC, which includes strong light absorption at 550 nm wavelengths, refractory at high volatile temperature, insoluble in water and containing a graphite-carbon atoms element. This description manifested the measurement methods of BC proposed by Lack *et al.* (2014). The actual definition of BC is still somewhat vague, and many researchers still argue about its definition (Buseck *et al.*, 2012). Additionally, Viidanoja *et al.* (2002) when studying traffic emissions found that 90% of $PM_{2.5}$ fractions were from BC. BC has

been recognised as a climate forging agent that contributes to climate change (Novakov and Rosen, 2013) due to its unique properties as a light absorber, which leads to regional heating on the atmospheric scale (Booth and Bellouin, 2015).

1.1.4 NO_2 and O_3

NO_2 is a mixture of nitrogen and oxygen that is typically released from motor exhausts, coal burning and natural gas. The odourless gas, nitric oxide (NO) is associated with the NO_2 and the combination of these two gases are known as nitrous oxides (NO_x). NO_2 is also produced during the process of arc welding, electroplating and dynamite blasting (ATSDR, 2002). NO_2 can also be formed in the atmosphere via a chemical reaction between NO and ozone (O_3) (Equation 1.1).

$$NO + O_3 \rightarrow NO_2 + Oxygen\ (O_2) \tag{1.1}$$

Additionally, O_3 is also produced from the photochemical oxidation of volatile organic compounds in the presence of NO. The secondary NO_2 is also formed at the ground level through a chemical reaction of NO_x and O_3 from traffic emissions (DEFRA, 2004).

1.2 Contribution of combustion-related air pollutants in different environmental settings

Indoor combustion-related activity of cigarette smoking has been found degrading the indoor air quality in homes in Scotland and Ireland (Semple *et al.*, 2012). Using gas for heating has been found to contribute to increased indoor NO_2 (Lee *et al.*, 2004). In addition, cooking and candle burning is associated with increased the BC levels in an occupied house in Washington (LaRosa *et al.*, 2002). There were different distributions on personal NO_2 exposure found in the summer and winter seasons, with indoor levels measured in the workplace and home being higher during winter (Kornartit *et al.*, 2010). The highest NO_2 concentrations were found in home with smokers using gas cookers.

Indoor air pollution from fuel combustion in the modern residential property (particularly in the urban environment) is likely to be low, some pollution is likely to have originated from outdoors (Leung, 2015). The study also noted that the main sources of PM and NO_2 are from cooking stoves, tobacco smoke and outdoor air. Biomass fuels are widely used for cooking and heating in most developing countries where these household emissions have become major problems, causing 4.3 million premature deaths each year from heart conditions and respiratory illness in adults and children (WHO, 2016). However, those living near major roads are exposed to engine exhaust emissions, which include a wide range of particles (Lim *et al.*, 2011), BC (Hoek *et al.*, 2002) and NO_2 (Levy *et al.*, 1998). A study in Southeast Asia found 23% of $PM_{2.5}$ consists of combustion particles from residential biomass emissions (Shahid *et al.*, 2016).

Excluding indoor sources, outdoor and indoor environments can be closely coupled for some air pollutants. For example, a study in New York found that outdoor air pollution sources influenced indoor and personal exposures (Kinney *et al.*, 2002). Similarly, Rivas *et al.* (2014) found that the outdoor concentrations of PM, BC and NO_2 from traffic emissions were a good indicator for concentrations in indoor settings.

Meanwhile, classification of motorway tunnel emissions found that 21% of diesel exhaust emissions were released from transport emissions and majority being PM_{10} (Lawrence *et al.*, 2013), thus this highlights in-vehicle exposure of the drivers. Lawrence *et al.* (2013) observed non-exhaust emissions (including break wear, tyre wear and resuspension of road salts) and petrol exhaust emissions contribute to another 79% on source apportionment of PM_{10}. Additionally, traffic-related emissions have become the principle source of PM in the urban areas (DEFRA, 2005). It has been found that carbonaceous component comprised of 40% of particles from traffic emission in the UK (Harrison *et al.*, 2003). Exposure to traffic-related contaminants, especially for PAH pollutants can be very high in locations

with high traffic intensity. This can be associated with the emissions from motor vehicle exhaust from both gasoline and diesel engine (Jamhari *et al.*, 2014).

For particulate and carbonaceous aerosols, Gany *et al.* (2016) found the exposure of $PM_{2.5}$ (max = 49 μg/m^3) and BC (max = 10 μg/m^3) concentrations were high among taxi drivers in New York, where the awareness about air pollution particularly traffic-related emissions were still limited. A study by Hu et al. (2007) has discovered there is a significant risk of PAHs exposure and may pose potential health threat to traffic police officers in China. The exposure concentration of PAHs was found to be 867.46 ng/m^3. Another personal exposure monitoring exercise performed with vehicle inspection workers at diesel lines in three vehicle factories in China, found that the exposure levels to PAHs was 199.80 ng/m^3 (Li *et al.*, 2013).

1.3 Combustion-related air pollutants and health effects

Exposure to combustion-related air pollutants have pointed out adverse health outcomes (Brunekreef *et al.*, 1997, Lewtas, 2007, Pope *et al.*, 2009), where these pollutants were typically released from fossil fuels, biomass emissions and traffic emissions. Historically, the carcinogenic effects of combustion-related air contaminants have been reported since 1775, where the coal soot has been addressed as a cancer agent affecting the chimney sweeper (Lewtas, 2007). The uncontrolled combustion of fossil fuels from coal heating coupled with traffic emissions caused the well-known smog episodes in London (Chen and Goldberg, 2009). In the present-day, emissions from vehicles and industrial plant have had contributed to poor air quality (DEFRA, 2005).

Health impacts of combustion-related air pollutants show both short and long-term effects, and these are linked to size and composition. In the UK study, Samoli *et al.* (2016) found an association between short-term exposures to traffic-related air pollutants with adult and children hospital admissions. This highlights the greater

risk for vulnerable groups including: children, the elderly and people suffering from asthma.

Meanwhile in the occupational setting, Koh *et al.* (2015) found a link of increased risk of lung cancer from exposure to diesel exhaust fumes in professional drivers in Korea. Their study stated that characterising the diesel exhausts exposure components, including PM and carbonaceous particles still remains a challenge. Rao *et al.* (2015) highlighted that individuals exposed to combustion-related pollutants are more likely to have an increased risk to diabetes disease. Their reviews listed the principal routes that suggest facilitating the diabetes incidence, including the activation of immune response subjected to the inflammation process and insulin production.

1.3.1 PM

The size of the particles reflects their health effects to the respiratory tract. The coarse size of PM_{10} consists of both 2.5 and 10 μm diameter; and is a typical indicator for epidemiological study (WHO, 2005). European Environment Agency (2013) reported that 40 – 80% of PM_{10} is comprised of $PM_{2.5}$ components found in the Europe. However, more attention has been given to the fine particulate of $PM_{2.5}$ in recent years due to its adverse health outcome (DEFRA, 2012). Fine particulates can travel more deeply into the lungs and are thought to cause more harmful effects through association with mutagenic and carcinogenic chemicals (Dockery *et al.*, 1993). The particles passing from the breathing route can exert the effects from thoracic and respiratory areas, particularly in children, who tend to breathe via their mouth (Brown *et al.*, 2013). An epidemiological study found that exposure to the coarse particles (PM_{10}) has resulted in 6% of annual mortality (from more than 40 000 annual attributable risk). This public health assessment was subjected to a number of cases of outdoor air pollution and health outcome frequency in three Western European countries ; Austria, France and Switzerland (Künzli *et al.*, 2000).

Pope and Dockery (2006) reviewed timelines of rising knowledge regarding the epidemiology of fine particulate air pollution and cardiopulmonary health effects. This provides evidence-based understanding to bridge the gap between atmospheric particulates pollution and health. Additionally, the nucleation progression from fine to ultrafine particles may pose to cardiac risk from traffic particles. Several studies presented the elevation of PM and BC from traffic emissions linked to the conditions of cardio-respiratory disease (Adar *et al.*, 2007, Shields *et al.*, 2013, Zhao *et al.*, 2014a). Interestingly, recent studies have linked PM exposure to neurological disorders (Liu *et al.*, 2016, Ritz *et al.*, 2016). All of these findings have signified the exposure to particles may pose a serious threat to human health.

1.3.2 PAHs

It is known that exposure to PAHs has been associated with lung, skin and bladder cancers. PAHs adducts have been found involved in triggering allergic inflammation in the respiratory system from exposure of combustion fossil fuels in diesel exhausts (Bayram *et al.*, 1998, Nel *et al.*, 1998). This component of concern contains a mixture of substances and may be carcinogenic to human that includes Benzo (a) Pyrene (BaP). A study in China revealed the exposure to BaP to the coke oven workers could give effect to their neurobehavioral function including poorer behaviour, cognitive and motor performance. The average BaP levels measured from the study was 1.21 $\mu g/m^3$ with range 0.028 - 2.82 $\mu g/m^3$ (Qiu *et al.*, 2013).

1.3.3 BC

Recent reports on BC and health effects published by WHO (2012) highlighted the short-term variations of BC concentrations associated with hospital admissions relative to the short atmospheric lifespan as the climate forging agent. A study in Belgium found a correlation between increase levels of BC and cardiovascular effects in a group of nurses (Provost *et al.*, 2016). This is in line with what have been observed by Zhao *et al.* (2014b) from BC exposure with blood pressure and heart rate variability in the female patient group. However, $PM_{2.5}$ measurements did not present similar findings with cardiovascular results in their study. Janssen et al. (2011) suggested the effects of BC might be more severe than PM, where the

estimated mortality caused by BC is expected 8 times larger than PM exposure. This is because BC concentrations are majorly generated from combustion sources. A recent study found that, exposure to BC initiates lung injury in mice (Chu *et al.*, 2016). The study also suggested the interaction of O_3 and BC that yielded oxidised BC, which may exert dangerous toxicological effects to human health compared to non-oxidised BC particles.

1.3.4 NO_2

DEFRA (2004) stated the exposure to NO_2 can cause respiratory irritants, breathing difficulties including wheezing, chest tightness and dyspnoea symptom or shortness of breath. There is a proven relationship between NO_2 and pulmonary hypertension (Sim, 2010, Williams *et al.*, 2012). A group study, European Study of Cohorts for Air Pollution Effects (ESCAPE) found the exposure to NO_2 increases asthmatics symptoms (Jacquemin *et al.*, 2015). This respiratory symptom also found to be associated with indoor exposure to NO_2 among children in New Zealand study (Gillespie-Bennett *et al.*, 2011). Another study conducted in Spain with pregnant women (who spent 63% of their time indoor), showed association of the increased preterm birth incidence with increased NO_2 exposure (Estarlich *et al.*, 2016).

1.4 Standards and limits

Air pollutant measurements are made to assess the quality of the inhaled air and address the health outcomes from the monitoring activity. The regulatory values are crucial to estimate the risk of adverse health effects to the exposed receptor. Table 1.1 below shows limits for $PM_{2.5}$, PM_{10}, NO_2 and O_3 set by the UK government (DEFRA, 2012) and WHO (Krzyzanowski and Cohen, 2008).

Table 1.1: Standards of ambient air pollution concentrations sets by the UK government and WHO.

Air Pollutants	Averaging Time	Guideline Values (μg/m^3)
$PM_{2.5}$	1 year (UK)	25
	1 year (Scotland)	12
PM_{10}	1 year (UK)	40
	1 year (Scotland)	18
BaP	1 year (UK)	0.25[1]
NO_2*	1 hour	200
	1 year	40
O_3*	1 hour	120

[1]ng/m^3. * WHO guidelines.

Part of WHO guidelines above is also described in Section 8.1.

There are still certain limited standards for indoor air quality, however WHO (2010) has released the indoor guidelines for selected pollutants. Table 1.2 below shows the indoor air quality reference for $PM_{2.5}$ and PM_{10}.

Table 1.2: The reference value for indoor PM based on WHO guidelines.

Pollutants	Levels (μg/m^3)	Duration of exposure
$PM_{2.5}$ (μg/m^3)	25	24 h
	10	1 yr
PM_{10} (μg/m^3)	50	24 h
	20	1 yr
BaP (μg/m^3)	8.7 x 10^{-5}	per concentration unit

For diesel exhaust exposure at the workplace, Health Safety and Executive (HSE, 2012) has set the 8-hour time weighted average (TWA) reference values for 10 µg/m^3 of total inhalable dust and 4 µg/m^3 of respirable dust. Meanwhile, BaP has classified in Group 2A by IARC classification and the Office of Environmental Health Hazard-Assessment (OEHHA) has estimated the unit risk of inhalation exposure of BaP in the particulate matter is 1.1 µg/m^3.

1.5 Exposure assessment

Improved characterisation of combustion related air pollution in indoor and outdoor air remains scientifically important, but technically challenging in environmental health research. The concept of exposure assessment has been widely discussed in the literature where the magnitude and duration of exposure play a major role in estimating the pollutant level (Steinle *et al.*, 2013). There are five main criteria to consider when performing the method evaluation for collecting exposure data; sensitivity, precision, accuracy, selectivity and detection limit.

1.6 Techniques used to monitor and analyse combustion-related air pollutants

1.6.1 Airborne particle specimens

Samples of airborne specimens are typically collected by drawing a known volume of air through a size-selective inlet (cyclone or impactors) onto a filter media using personal samplers over short or long periods of time. The personal sampling pump is powered by an internal battery to allow the subject to carry out his or her task while being monitored. The PM samples collected are subsequently analyse for the mass concentrations (Chakrabarti *et al.*, 2004). Sampling pumps have evolved over time with new models and functions to meet new demands of air sampling techniques with sophisticated features and benefits; to improve the precision accuracy and flexibility in sampling methods (Cherrie, 2003). Besides, there have been an increasing number of personal air sampling pumps readily available in the market

these days. Wood (1977) has first described the characteristics (Table 1.3) of an ideal pump to be employed as particle airborne collection systems.

Table 1.3: Summary of personal sampling pump features.

Specification	Criteria
Flow Rate	• Constant flow rate • Free from pulsation • Pump can set to work on different flow rate
Efficiency	• Capable to run for a longer duration (i.e. working shift – 8 hours)
Design	• Light and compact • Robust against temperature and humidity
Cost Effective	• Low-cost and affordable

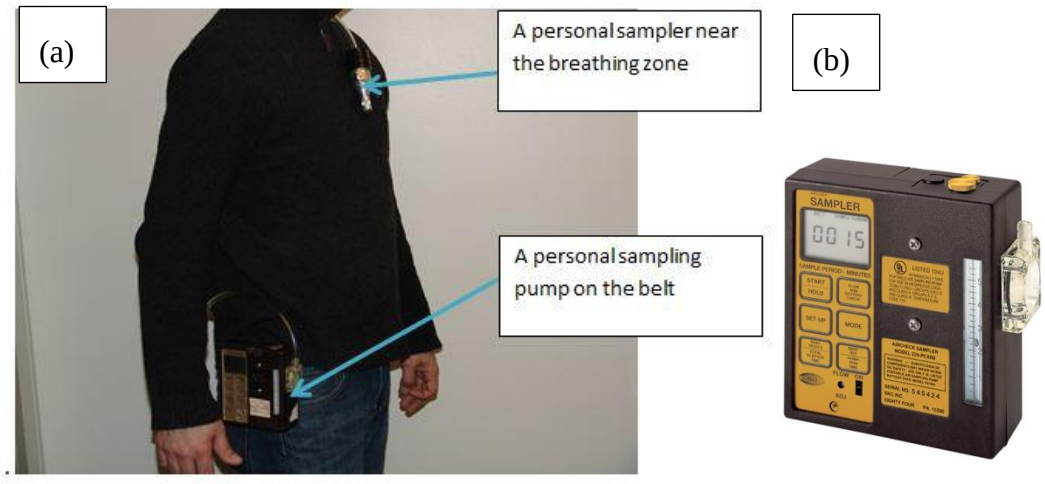

Figure 1.1: (a) Example of personal air sampling (image taken from NIOSH (2013)). (b) Example of SKC personal air sampling pump (source: www.skcinc.com)

BC concentrations are commonly measured using optical techniques established from aerosol light absorption and this procedure has been considered being non-destructive to the filter sample materials. Methods of collecting airborne particulates

to assess BC concentrations have been applied widely in a high air pollution concentration from the outdoor settings (Janssen *et al.*, 2001, Brauer *et al.*, 2003).

There is a wide variety of filters available for use in different monitoring settings. The filter media captures particulate matter within and throughout their structures, whether made from a tightly woven fibrous mat or a plastic (Chow, 1995). Chow (1995) also highlighted several features that need to be considered prior to choosing an ideal filter for air monitoring sampling. The outlined characteristics are described in Table 1.4.

Table 1.4: Outline of important characteristics of filter media for air monitoring (Chow, 1995).

Characteristics	Descriptions
1. Particle Sample Efficiency	Lower porosities and pore sizes
2. Mechanical Stability	Filter placement onto a sampling system to avoid outflows
3. Chemical Stability	Interference-free chemical from any residue
4. Temperature Stability	Able to maintain porosity and structure
5. Blank Concentrations	Free from any particulate deposit prior to analysis
6. Flow Resistance and Flow Capacity	Permit adequate amount of air flow
7. Cost and availability	Practical cost effective

The use of real time sensors to measure PM levels has aided the direct measurements, in these system the instrument records the properties of particles continuously. Koehler and Peters (2015) listed the recent PM and BC monitors with different measurement principles, including mass-based and light-scattering instruments. The key advantages and disadvantages of the instruments are also compiled, this expands the knowledge base of measurement techniques employed in

PM monitoring. In addition, Hansen *et al.* (1984) have developed a real-time optical absorption instrument called 'aethalometer' to estimate the level of the airborne BC.

Discussion on analytical methods for PAHs in airborne particulates has been broadly presented (Liu *et al.*, 2007, Szulejko *et al.*, 2014). There are a number of methods used for PAHs extraction, these include traditional Soxhlet, ultrasonication, accelerated solvent, microwave, supercritical fluid and solid-phase microextraction. Delgado-Saborit *et al.* (2010) developed a methodology to assess and enhance the measurement of particle bound PAHs collected from low airflow in the different street microenvironments. The collected samples were tested with different filter media, cleaning up techniques, extraction and GC-MS operational conditions. This study recommended mechanical shaking extraction method with dichloromethane (DCM) as the prime extraction solvent. Chantara and Sangchan (2009) collected PM_{10} in a low-volume collection system and assessed ideal techniques for PAHs in the PM_{10} specimens. Their study recommended ultrasonication method with acetonitrile as a principle technique for PAHs sample extraction.

1.6.2 Gaseous sampling

Palmes *et al.* (1976) first described the measurement of personal NO_2 using a passive sampler (Figure 1.2). A variety of tube preparation techniques are employed by coating the Triethanolamine (TEA) solutions to the grids (Figure 1.1) whether by dipping the grids with prepared TEA solutions or pipetting a known volume of TEA and water solutions onto the grids. These two methods of grid meshes treated with TEA have been influenced by the presence of NO_2 concentrations captured in the PDTs (Hamilton and Heal, 2004).

For example, study by Heal (2008) showed that the dipping method has significantly increased the efficiency of NO_2 concentrations that diffuses through the PDTs as compared to the pipetting technique. After the extraction process, the samples are analysed using a colorimetric or spectrophotometer method. Another type of passive sampler that typically uses to measure NO_2 is the Ogawa sampler, which utilised a

similar principle of Palmes type sampler where the tube is exposed for a particular period for the absorption of NO_2 that can occur to a mesh or filter. The Ogawa badge consists of a collection filter coated with reactive chemicals (ESCAPE, 2009).

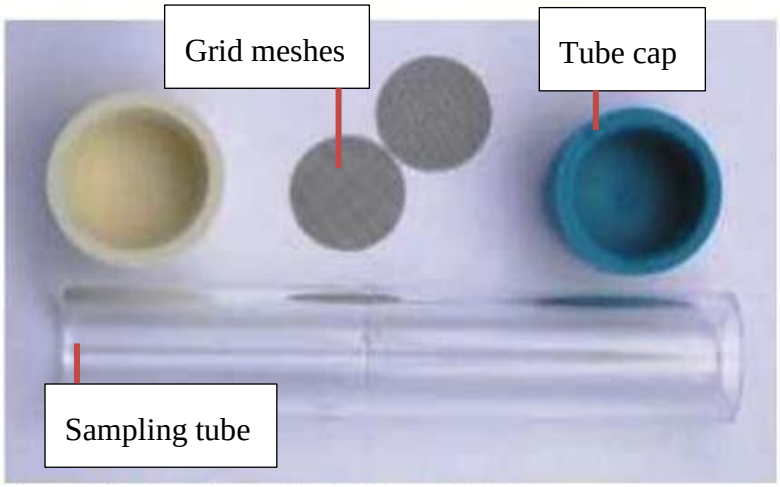

Figure 1.2: Example of NO_2 passive sampler (DEFRA, 2008).

1.7 Summary

The major components of combustion-related air pollutant consist of PM, BC, PAHs and NO_2 which are released from different combustion sources. There is growing concern being paid to the health outcomes of combustion-related air pollutants, which has in-turn led to detailed measurements of these pollutants. These pollutants have serious health effects to the individual and vulnerable groups especially children. The information on standards for outdoor, indoor and occupational reference guidelines were referred as standardisation and regulatory values for combustion-related air pollutants monitoring. Various methods were also introduced corresponding to the PM, BC, PAHs and NO_2 measurements from traditional to advanced sensors. In order to address these areas with a clear definition of combustion-related air pollutants, the examination of source contributions will better characterise and steer the implementation of mitigation strategies to minimise pollutant loads.

1.8 References

Adar, S. D., Gold, D. R., Coull, B. A., Schwartz, J., Stone, P. H. & Suh, H. 2007. Focused exposures to airborne traffic particles and heart rate variability in the elderly. *Epidemiology,* 18.

ATSDR 2002. ToxFAQs for Nitrogen Oxides. April 2002 ed.

Bayram, H., Devalia, J. L., Sapsford, R. J., Ohtoshi, T., Miyabara, Y., Sagai, M. & Davies, R. J. 1998. The effect of diesel exhaust particles on cell function and release of inflammatory mediators from human bronchial epithelial cells in vitro. *Am J Respir Cell Mol Biol,* 18**,** 441-8.

Booth, B. & Bellouin, N. 2015. Climate change: Black carbon and atmospheric feedbacks. *Nature,* 519**,** 167-8.

Brauer, M., Hoek, G., van Vliet, P., Meliefste, K., Fischer, P., Gehring, U., Heinrich, J., Cyrys, J., Bellander, T., Lewne, M. & Brunekreef, B. 2003. Estimating long-term average particulate air pollution concentrations: application of traffic indicators and geographic information systems. *Epidemiology,* 14**,** 228-39.

Brown, J. S., Gordon, T., Price, O. & Asgharian, B. 2013. Thoracic and respirable particle definitions for human health risk assessment. *Particle and Fibre Toxicology,* 10**,** 1-12.

Brunekreef, B., Janssen, N. A., de Hartog, J., Harssema, H., Knape, M. & van Vliet, P. 1997. Air pollution from truck traffic and lung function in children living near motorways. *Epidemiology,* 8**,** 298-303.

Buseck, P. R., Adachi, K., Gelencsér, A., Tompa, É. & Pósfai, M. 2012. Are black carbon and soot the same? *Atmos. Chem. Phys. Discuss.,* 2012**,** 24821-24846.

Chakrabarti, B., Fine, P. M., Delfino, R. & Sioutas, C. 2004. Performance evaluation of the active-flow personal DataRAM PM2.5 mass monitor (Thermo Anderson pDR-1200) designed for continuous personal exposure measurements. *Atmospheric Environment,* 38**,** 3329-3340.

Chantara, S. & Sangchan, W. 2009. Sensitive analytical method for particle-bound polycyclic aromatic hydrocarbons: A case study in Chiang Mai, Thailand. *Journal of the Science Society of Thailand,* 35**,** 42-48.

Chen, H. & Goldberg, M. S. 2009. The effects of outdoor air pollution on chronic illnesses. *McGill Journal of Medicine : MJM,* 12**,** 58-64.

Cherrie, J. W. 2003. Commentary: The Beginning of the Science Underpinning Occupational Hygiene. *Annals of Occupational Hygiene,* 47**,** 179-185.

Chow, J. C. 1995. Measurement Methods to Determine Compliance with Ambient Air Quality Standards for Suspended Particles. *Journal of the Air & Waste Management Association,* 45**,** 320-382.

Chu, H., Shang, J., Jin, M., Li, Q., Chen, Y., Huang, H., Li, Y., Pan, Y., Tao, X., Cheng, Z., Meng, Q., Jia, G., Zhu, T., Wei, X. & Hao, W. 2016. Comparison of lung damage in mice exposed to black carbon particles and ozone-oxidized black carbon particles. *Science of The Total Environment,* 573**,** 303-312.

DEFRA. 2004. *Nitrogen Dioxide in the United Kingdom Summary* [Online]. London. Available: https://uk-air.defra.gov.uk/assets/documents/reports/aqeg/nd-summary.pdf [Accessed 15 October 2015].

DEFRA. 2005. *Particulate Matter in Uniter Kingdom: A summary* [Online]. London. Available: https://uk-air.defra.gov.uk/assets/documents/reports/aqeg/pm-summary.pdf [Accessed 16 February 2014].

DEFRA 2008. Diffusion Tubes for Ambient NO2 Monitoring: Practical Guidance for Laboratories and User.

DEFRA. 2012. *Fine Particulate Matter PM2.5 in the United Kingdom* [Online]. Available: https://uk-air.defra.gov.uk/assets/documents/reports/aqeg/pb13837-aqeg-fine-particle-matter-20121220.pdf [Accessed 18 July 2016].

Delgado-Saborit, J. M., Aquilina, N., Baker, S., Harrad, S., Meddings, C. & Harrison, R. M. 2010. Determination of atmospheric particulate-phase polycyclic aromatic hydrocarbons from low volume air samples. *Analytical Methods,* 2**,** 231-242.

Dockery, D. W., Pope, C. A., 3rd, Xu, X., Spengler, J. D., Ware, J. H., Fay, M. E., Ferris, B. G., Jr. & Speizer, F. E. 1993. An association between air pollution and mortality in six U.S. cities. *N Engl J Med,* 329**,** 1753-9.

EEA, E. E. A. 2013. *Air Quality in Europe - 2013 report* [Online]. Denmark. Available: http://www.eea.europa.eu/publications/air-quality-in-europe-2013 [Accessed 17 October 2015 9].

ESCAPE. 2009. *Measurement of NO2 and NOx in Outdoor Air with OGAWA Badge* [Online]. Available: http://www.escapeproject.eu/manuals/ESCAPE-NOx-sop_x007E_final.pdf [Accessed 20 April 2015].

Estarlich, M., Ballester, F., Davdand, P., Llop, S., Esplugues, A., Fernández-Somoano, A., Lertxundi, A., Guxens, M., Basterrechea, M., Tardón, A., Sunyer, J. & Iñiguez, C. 2016. Exposure to ambient air pollution during pregnancy and preterm birth: A Spanish multicenter birth cohort study. *Environmental Research,* 147**,** 50-58.

Fuzzi, S., Baltensperger, U., Carslaw, K., Decesari, S., Denier van der Gon, H., Facchini, M. C., Fowler, D., Koren, I., Langford, B., Lohmann, U., Nemitz, E., Pandis, S., Riipinen, I., Rudich, Y., Schaap, M., Slowik, J. G., Spracklen, D. V., Vignati, E., Wild, M., Williams, M. & Gilardoni, S. 2015. Particulate matter, air quality and climate: lessons learned and future needs. *Atmos. Chem. Phys.,* 15**,** 8217-8299.

Gany, F., Bari, S., Prasad, L., Leng, J., Lee, T., Thurston, G. D., Gordon, T., Acharya, S. & Zelikoff, J. T. 2016. Perception and reality of particulate matter exposure in New York City taxi drivers. *J Expos Sci Environ Epidemiol*.

Gillespie-Bennett, J., Pierse, N., Wickens, K., Crane, J. & Howden-Chapman, P. 2011. The respiratory health effects of nitrogen dioxide in children with asthma. *European Respiratory Journal,* 38**,** 303-309.

Hamilton, R. P. & Heal, M. R. 2004. Evaluation of method of preparation of passive diffusion tubes for measurement of ambient nitrogen dioxide. *Journal of Environmental Monitoring,* 6**,** 12-17.

Hansen, A. D. A., Rosen, H. & Novakov, T. 1984. Carbonaceous Particles in the Atmosphere 1983 The aethalometer — An instrument for the real-time measurement of optical absorption by aerosol particles. *Science of The Total Environment,* 36**,** 191-196.

Harrison, R. M., Jones, A. M. & Lawrence, R. G. 2003. A pragmatic mass closure model for airborne particulate matter at urban background and roadside sites. *Atmospheric Environment,* 37**,** 4927-4933.

Heal, M. R. 2008. The effect of absorbent grid preparation method on precision and accuracy of ambient nitrogen dioxide measurements using Palmes passive diffusion tubes. *Journal of Environmental Monitoring,* 10**,** 1363-1369.

Hoek, G., Brunekreef, B., Goldbohm, S., Fischer, P. & van den Brandt, P. A. 2002. Association between mortality and indicators of traffic-related air pollution in the Netherlands: a cohort study. *The Lancet,* 360**,** 1203-1209.

HSE 2012. Control of diesel engine exhaust emissions in the workplace. 2 ed.

Hu, Y., Bai, Z., Zhang, L., Wang, X., Zhang, L., Yu, Q. & Zhu, T. 2007. Health risk assessment for traffic policemen exposed to polycyclic aromatic hydrocarbons (PAHs) in Tianjin, China. *Science of The Total Environment,* 382**,** 240-250.

Jacquemin, B., Siroux, V., Sanchez, M., Carsin, A. E., Schikowski, T., Adam, M., Bellisario, V., Buschka, A., Bono, R., Brunekreef, B., Cai, Y., Cirach, M., Clavel-Chapelon, F., Declercq, C., de Marco, R., de Nazelle, A., Ducret-Stich, R. E., Ferretti, V. V., Gerbase, M. W., Hardy, R., Heinrich, J., Janson, C., Jarvis, D., Al Kanaani, Z., Keidel, D., Kuh, D., Le Moual, N., Nieuwenhuijsen, M. J., Marcon, A., Modig, L., Pin, I., Rochat, T., Schindler, C., Sugiri, D., Stempfelet, M., Temam, S., Tsai, M. Y., Varraso, R., Vienneau, D., Vierkotter, A., Hansell, A. L., Kramer, U., Probst-Hensch, N. M., Sunyer, J., Kunzli, N. & Kauffmann, F. 2015. Ambient air pollution and adult asthma incidence in six European cohorts (ESCAPE). *Environ Health Perspect,* 123**,** 613-21.

Jamhari, A. A., Sahani, M., Latif, M. T., Chan, K. M., Tan, H. S., Khan, M. F. & Mohd Tahir, N. 2014. Concentration and source identification of polycyclic aromatic hydrocarbons (PAHs) in PM10 of urban, industrial and semi-urban areas in Malaysia. *Atmospheric Environment,* 86**,** 16-27.

Janssen, N. A., Hoek, G., Simic-Lawson, M., Fischer, P., van Bree, L., ten Brink, H., Keuken, M., Atkinson, R. W., Anderson, H. R., Brunekreef, B. & Cassee, F. R. 2011. Black carbon as an additional indicator of the adverse health effects of airborne particles compared with PM10 and PM2.5. *Environ Health Perspect,* 119**,** 1691-9.

Janssen, N. A. H., van Vliet, P. H. N., Aarts, F., Harssema, H. & Brunekreef, B. 2001. Assessment of exposure to traffic related air pollution of children attending schools near motorways. *Atmospheric Environment,* 35**,** 3875-3884.

Kankaria, A., Nongkynrih, B. & Gupta, S. K. 2014. Indoor Air Pollution in India: Implications on Health and its Control. *Indian Journal of Community Medicine : Official Publication of Indian Association of Preventive & Social Medicine,* 39**,** 203-207.

Kinney, P. L., Chillrud, S. N., Ramstrom, S., Ross, J. & Spengler, J. D. 2002. Exposures to multiple air toxics in New York City. *Environmental Health Perspectives,* 110**,** 539-546.

Koehler, K. A. & Peters, T. M. 2015. New Methods for Personal Exposure Monitoring for Airborne Particles. *Curr Environ Health Rep,* 2**,** 399-411.

Koh, D.-H., Kong, H.-J., Oh, C.-M., Jung, K.-W., Park, D. & Won, Y.-J. 2015. Lung cancer risk in professional drivers in Korea: A population-based proportionate cancer incidence ratio study. *Journal of Occupational Health,* 57**,** 324-330.

Kornartit, C., Sokhi, R. S., Burton, M. A. & Ravindra, K. 2010. Activity pattern and personal exposure to nitrogen dioxide in indoor and outdoor microenvironments. *Environment International,* 36**,** 36-45.

Krzyzanowski, M. & Cohen, A. 2008. Update of WHO air quality guideline. *Air Qual Atmos Health,* 1**,** 13.

Künzli, N., Kaiser, R., Medina, S., Studnicka, M., Chanel, O., Filliger, P., Herry, M., Horak Jr, F., Puybonnieux-Texier, V., Quénel, P., Schneider, J., Seethaler, R., Vergnaud, J. C. & Sommer, H. 2000. Public-health impact of outdoor and traffic-related air pollution: a European assessment. *The Lancet,* 356**,** 795-801.

Lack, D. A., Moosmüller, H., McMeeking, G. R., Chakrabarty, R. K. & Baumgardner, D. 2014. Characterizing elemental, equivalent black, and refractory black carbon aerosol particles: a review of techniques, their limitations and uncertainties. *Analytical and Bioanalytical Chemistry,* 406**,** 99-122.

LaRosa, L. E., Buckley, T. J. & Wallace, L. A. 2002. Real-time indoor and outdoor measurements of black carbon in an occupied house: an examination of sources. *J Air Waste Manag Assoc,* 52**,** 41-9.

Lawrence, S., Sokhi, R., Ravindra, K., Mao, H., Prain, H. D. & Bull, I. D. 2013. Source apportionment of traffic emissions of particulate matter using tunnel measurements. *Atmospheric Environment,* 77**,** 548-557.

Lee, K., Bartell, S. M. & Paek, D. 2004. Interpersonal and daily variability of personal exposures to nitrogen dioxide and sulfur dioxide. *J Expo Anal Environ Epidemiol,* 14**,** 137-43.

Leung, D. Y. C. 2015. Outdoor-indoor air pollution in urban environment: challenges and opportunity. *Frontiers in Environmental Science,* 2.

Levy, J. I., Lee, K., Spengler, J. D. & Yanagisawa, Y. 1998. Impact of residential nitrogen dioxide exposure on personal exposure: an international study. *J Air Waste Manag Assoc,* 48**,** 553-60.

Lewtas, J. 2007. Air pollution combustion emissions: Characterization of causative agents and mechanisms associated with cancer, reproductive, and cardiovascular effects. *Mutation Research/Reviews in Mutation Research,* 636**,** 95-133.

Li, L., Wu, J., Ghosh, J. K. & Ritz, B. 2013. Estimating spatiotemporal variability of ambient air pollutant concentrations with a hierarchical model. *Atmos Environ*, 71.

Lim, J. M., Jeong, J. H., Lee, J. H., Moon, J. H., Chung, Y. S. & Kim, K. H. 2011. The analysis of PM2.5 and associated elements and their indoor/outdoor pollution status in an urban area. *Indoor Air*, 21**,** 145-55.

Lim, S. S., Vos, T., Flaxman, A. D., Danaei, G., Shibuya, K., Adair-Rohani, H., Amann, M., Anderson, H. R., Andrews, K. G., Aryee, M., Atkinson, C., Bacchus, L. J., Bahalim, A. N., Balakrishnan, K., Balmes, J., Barker-Collo, S., Baxter, A., Bell, M. L., Blore, J. D., Blyth, F., Bonner, C., Borges, G., Bourne, R., Boussinesq, M., Brauer, M., Brooks, P., Bruce, N. G., Brunekreef, B., Bryan-Hancock, C., Bucello, C., Buchbinder, R., Bull, F., Burnett, R. T., Byers, T. E., Calabria, B., Carapetis, J., Carnahan, E., Chafe, Z., Charlson, F., Chen, H., Chen, J. S., Cheng, A. T., Child, J. C., Cohen, A., Colson, K. E., Cowie, B. C., Darby, S., Darling, S., Davis, A., Degenhardt, L., Dentener, F., Des Jarlais, D. C., Devries, K., Dherani, M., Ding, E. L., Dorsey, E. R., Driscoll, T., Edmond, K., Ali, S. E., Engell, R. E., Erwin, P. J., Fahimi, S., Falder, G., Farzadfar, F., Ferrari, A., Finucane, M. M., Flaxman, S., Fowkes, F. G., Freedman, G., Freeman, M. K., Gakidou, E., Ghosh, S., Giovannucci, E., Gmel, G., Graham, K., Grainger, R., Grant, B., Gunnell, D., Gutierrez, H. R., Hall, W., Hoek, H. W., Hogan, A., Hosgood, H. D., 3rd, Hoy, D., Hu, H., Hubbell, B. J., Hutchings, S. J., Ibeanusi, S. E., Jacklyn, G. L., Jasrasaria, R., Jonas, J. B., Kan, H., Kanis, J. A., Kassebaum, N., Kawakami, N., Khang, Y. H., Khatibzadeh, S., Khoo, J. P., Kok, C., Laden, F., et al. 2012. A comparative risk assessment of burden of disease and injury attributable to 67 risk factors and risk factor clusters in 21 regions, 1990-2010: a systematic analysis for the Global Burden of Disease Study 2010. *Lancet*, 380**,** 2224-60.

Liu, L.-b., Liu, Y., Lin, J.-m., Tang, N., Hayakawa, K. & Maeda, T. 2007. Development of analytical methods for polycyclic aromatic hydrocarbons

(PAHs) in airborne particulates: A review. *Journal of Environmental Sciences*, 19**,** 1-11.

Liu, R., Young, M. T., Chen, J. C., Kaufman, J. D. & Chen, H. 2016. Ambient Air Pollution Exposures and Risk of Parkinson Disease. *Environ Health Perspect*.

Mohanraj, R., Dhanakumar, S. & Solaraj, G. 2012. Polycyclic Aromatic Hydrocarbons Bound to PM 2.5 in Urban Coimbatore, India with Emphasis on Source Apportionment. *The Scientific World Journal*, 2012**,** 980843.

Nel, A. E., Diaz-Sanchez, D., Ng, D., Hiura, T. & Saxon, A. 1998. Enhancement of allergic inflammation by the interaction between diesel exhaust particles and the immune system. *Journal of Allergy and Clinical Immunology*, 102**,** 539-554.

NIOSH. 2013. Available: https://blogs.cdc.gov/niosh-science-blog/2013/03/26/silica-fibercementdust/ [Accessed 15 March 2017].

Novakov, T. & Rosen, H. 2013. The Black Carbon Story: Early History and New Perspectives. *Ambio*, 42**,** 840-851.

Palmes, E. D., Gunnison, A. F., DiMattio, J. & Tomczyk, C. 1976. Personal sampler for nitrogen dioxide. *American Industrial Hygiene Association Journal*, 37**,** 570-577.

Petzold, A., Ogren, J. A., Fiebig, M., Laj, P., Li, S. M., Baltensperger, U., Holzer-Popp, T., Kinne, S., Pappalardo, G., Sugimoto, N., Wehrli, C., Wiedensohler, A. & Zhang, X. Y. 2013. Recommendations for reporting "black carbon" measurements. *Atmos. Chem. Phys.*, 13**,** 8365-8379.

Pope, C. A., 3rd & Dockery, D. W. 2006. Health effects of fine particulate air pollution: lines that connect. *J Air Waste Manag Assoc*, 56**,** 709-42.

Pope , C. A. I., Ezzati , M. & Dockery , D. W. 2009. Fine-Particulate Air Pollution and Life Expectancy in the United States. *New England Journal of Medicine*, 360**,** 376-386.

Provost, E. B., Louwies, T., Cox, B., op ‘t Roodt, J., Solmi, F., Dons, E., Int Panis, L., De Boever, P. & Nawrot, T. S. 2016. Short-term fluctuations in personal

black carbon exposure are associated with rapid changes in carotid arterial stiffening. *Environment International,* 88**,** 228-234.

Qiu, C., Peng, B., Cheng, S., Xia, Y. & Tu, B. 2013. The effect of occupational exposure to benzo[a]pyrene on neurobehavioral function in coke oven workers. *Am J Ind Med,* 56**,** 347-55.

Rao, X., Montresor-Lopez, J., Puett, R., Rajagopalan, S. & Brook, R. D. 2015. Ambient Air Pollution: An Emerging Risk Factor for Diabetes Mellitus. *Current Diabetes Reports,* 15**,** 1-11.

Ravindra, K., Sokhi, R. & Van Grieken, R. 2008. Atmospheric polycyclic aromatic hydrocarbons: Source attribution, emission factors and regulation. *Atmospheric Environment,* 42**,** 2895-2921.

Ritz, B., Lee, P. C., Hansen, J., Lassen, C. F., Ketzel, M., Sorensen, M. & Raaschou-Nielsen, O. 2016. Traffic-Related Air Pollution and Parkinson's Disease in Denmark: A Case-Control Study. *Environ Health Perspect,* 124**,** 351-6.

Rivas, I., Viana, M., Moreno, T., Pandolfi, M., Amato, F., Reche, C., Bouso, L., Àlvarez-Pedrerol, M., Alastuey, A., Sunyer, J. & Querol, X. 2014. Child exposure to indoor and outdoor air pollutants in schools in Barcelona, Spain. *Environment International,* 69**,** 200-212.

Samoli, E., Atkinson, R. W., Analitis, A., Fuller, G. W., Green, D. C., Mudway, I., Anderson, H. R. & Kelly, F. J. 2016. Associations of short-term exposure to traffic-related air pollution with cardiovascular and respiratory hospital admissions in London, UK. *Occupational and Environmental Medicine*.

Semple, S., Garden, C., Coggins, M., Galea, K. S., Whelan, P., Cowie, H., Sánchez-Jimenéz, A., Thorne, P. S., Hurley, J. F. & Ayres, J. G. 2012. Contribution of solid fuel, gas combustion or tobacco smoke to indoor air pollutant concentrations in Irish and Scottish homes. *Indoor air,* 22**,** 212-223.

Shahid, I., Kistler, M., Mukhtar, A., Ghauri, B. M., Ramirez-Santa Cruz, C., Bauer, H. & Puxbaum, H. 2016. Chemical characterization and mass closure of PM10 and PM2.5 at an urban site in Karachi – Pakistan. *Atmospheric Environment,* 128**,** 114-123.

Shields, K. N., Cavallari, J. M., Hunt, M. J. O., Lazo, M., Molina, M., Molina, L. & Holguin, F. 2013. Traffic-related air pollution exposures and changes in heart rate variability in Mexico City: A panel study. *Environmental Health,* 12**,** 1-14.

Sim, J.-Y. 2010. Nitric oxide and pulmonary hypertension. *Korean Journal of Anesthesiology,* 58**,** 4-14.

Steinle, S., Reis, S. & Sabel, C. E. 2013. Quantifying human exposure to air pollution—Moving from static monitoring to spatio-temporally resolved personal exposure assessment. *Science of The Total Environment,* 443**,** 184-193.

Szulejko, J. E., Kim, K.-H., Brown, R. J. C. & Bae, M.-S. 2014. Review of progress in solvent-extraction techniques for the determination of polyaromatic hydrocarbons as airborne pollutants. *TrAC Trends in Analytical Chemistry,* 61**,** 40-48.

Thorpe, A. & Harrison, R. M. 2008. Sources and properties of non-exhaust particulate matter from road traffic: A review. *Science of The Total Environment,* 400**,** 270-282.

Tiwary, A. & Colls, J. 2010. *Air Pollution Measurement, modelling and mitigation,* Oxon, Routledge.

Viidanoja, J., Sillanpää, M., Laakia, J., Kerminen, V.-M., Hillamo, R., Aarnio, P. & Koskentalo, T. 2002. Organic and black carbon in PM2.5 and PM10: 1 year of data from an urban site in Helsinki, Finland. *Atmospheric Environment,* 36**,** 3183-3193.

WHO. 2005. *WHO Air Quality Guidelines for Particulate Matter, Ozone, Nitrogen Dioxide and Sulphur Dioxide* [Online]. Available: http://apps.who.int/iris/bitstream/10665/69477/1/WHO_SDE_PHE_OEH_06.02_eng.pdf [Accessed 20 October 2014].

WHO. 2010. *WHO Guidelines for Indoor Air Quality: Selected Pollutants* [Online]. Available:

http://www.euro.who.int/__data/assets/pdf_file/0009/128169/e94535.pdf [Accessed 5 August 2015].

WHO. 2012. *Health Effects of Black Carbon* [Online]. Denmark. Available: http://www.euro.who.int/__data/assets/pdf_file/0004/162535/e96541.pdf [Accessed 20 January 2015].

WHO. 2014. *7 million premature deaths annually linked to air pollution* [Online]. Available: http://www.who.int/mediacentre/news/releases/2014/air-pollution/en/ [Accessed 13 April 2015].

WHO. 2016. *Burning Oppurtunity: Clean Household Energy for Health, Sustainable, Development,and Wellbeing of Women and Children* [Online]. Luxemborg: WHO. Available: http://apps.who.int/iris/bitstream/10665/204717/1/9789241565233_eng.pdf?ua=1 [Accessed 18 September 2016].

Williams, R., Brook, R., Bard, R., Conner, T., Shin, H. & Burnett, R. 2012. Impact of personal and ambient-level exposures to nitrogen dioxide and particulate matter on cardiovascular function. *International Journal of Environmental Health Research,* 22**,** 71-91.

Wood, J. D. 1977. A Review of Personal Sampling Pumps. *Annals of Occupational Hygiene,* 20**,** 3-17.

Zhao, X., Sun, Z., Ruan, Y., Yan, J., Mukherjee, B., Yang, F., Duan, F., Sun, L., Liang, R., Lian, H., Zhang, S., Fang, Q., Gu, D., Brook, J. R., Sun, Q., Brook, R. D., Rajagopalan, S. & Fan, Z. 2014a. Personal Black Carbon Exposure Influences Ambulatory Blood Pressure: Air Pollution and Cardio-metabolic Disease (AIRCMD-China) Study. *Hypertension,* 63**,** 871-877.

Zhao, X., Sun, Z., Ruan, Y., Yan, J., Mukherjee, B., Yang, F., Duan, F., Sun, L., Liang, R., Lian, H., Zhang, S., Fang, Q., Gu, D., Brook, J. R., Sun, Q., Brook, R. D., Rajagopalan, S. & Fan, Z. 2014b. Personal black carbon exposure influences ambulatory blood pressure: air pollution and cardiometabolic disease (AIRCMD-China) study. *Hypertension,* 63**,** 871-7.

2 LITERATURE REVIEW

2.0 Background

This chapter reviews current employed measurement techniques and addressed challenges to characterise combustion-related air pollutants. This chapter intends to fill important knowledge gaps of combustion-related to air pollutants.

2.1 Current approaches for the exposure assessment of combustion-related air pollutants

Atmospheric specimens can be collected across multiple monitoring sites over a period of study to examine the relationship between pollution exposure and potential health effects. The collection system may be limited by time-resolution, human activity patterns, and timing/duration of monitoring (Fan, 2011). However, recent advances in the technology of personal monitors provide specific opportunities to assess combustion related air pollutants in different environmental locations.

Over the years, a variety of modern low cost sensors were applied in the indoor (Semple *et al.*, 2013) and urban environment (Mead *et al.*, 2013) studies to measure personal exposure to particulate matter (PM). Their results showed the proposed instruments are straightforward to use and allow a robust personal measurements of

particles and gases. There is also new generation of personal air quality sensors using the smart phone to capture, upload image of carbonaceous particles, and subsequently quantify the BC data (Ramanathan *et al.*, 2011). The use of global positioning system (GPS) to track location, coupled with direct sensor measurements has also been applied to measure black carbon (BC) and nitrogen dioxide (NO_2) in the real world (Steinle *et al.*, 2015, Wu *et al.*, 2015). Likewise, the individual health status and biology are also incorporated in the current studies to better understanding the relationship between exposure to combustion-related pollutants and health effects. Table 2.1 below shows summary of combustion-related air pollutant monitoring coupled with the heart rate activity. Their measurements have provided the additional evidence of traffic-related exposure to the cardiovascular disease.

Table 2.1: Summary of studies highlighted the measurement of air pollution and health status.

Study	Air Pollutant	Study design	Health monitor	Subject
Adar *et al.* (2007)	$PM_{2.5}$ & BC	Personal activity level from in-vehicle & ME measurements[1]	Heart rate variability	44 non-smoking senior
Shields *et al.* (2013)	$PM_{2.5}$, CO_2, CO, NO_2, NOx, O_3,& formaldehyde	In-vehicle measurements	Heart rate variability	16 researchers (age between 22-56)
Zhao *et al.* (2014)	$PM_{2.5}$ & BC	Personal & fixed site measurements	Blood pressure & heart rate variability	65 patients

[1]ME = microenvironment

Koehler and Peters (2015) have connected the understanding of the application of high-resolution monitors relative to the personal exposure data. Figure 2.1 shows the outline of the relationship between the integrated exposure data and target group who have a major interest in the higher level processing information.

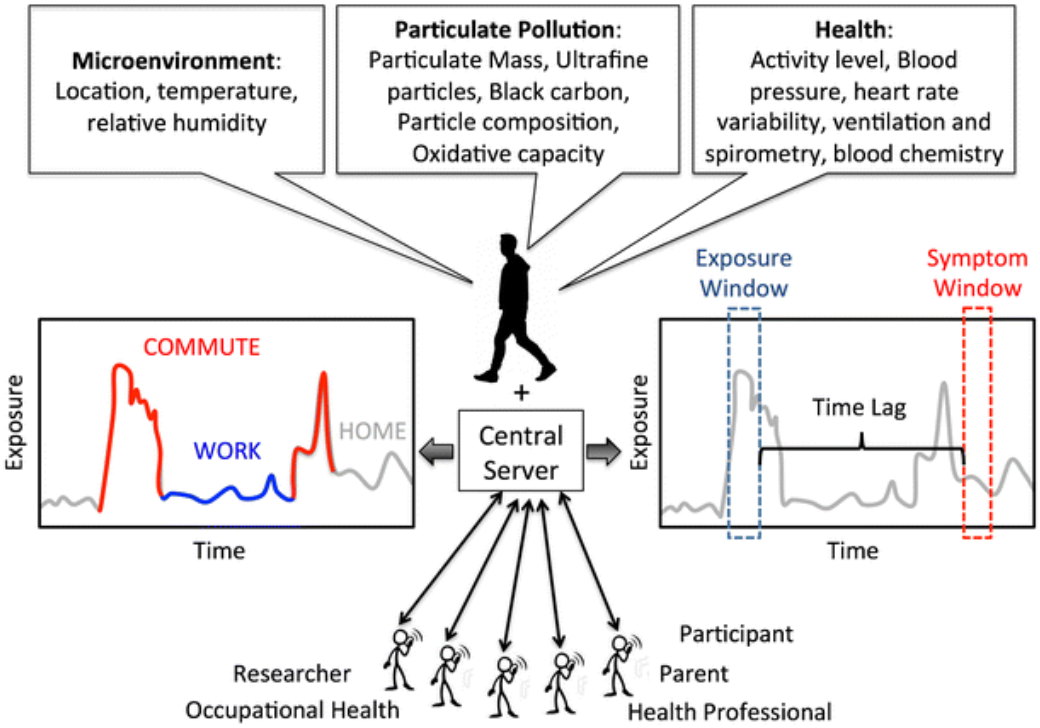

Figure 2.1: The framework of personal exposure data proposed by Koehler and Peters (2015) (Image taken with permission granted from the authors).

Several studies have incorporated the advanced technology to engage citizens to have access to instrumentation to enhance exposure science and improve air quality management (Piedrahita *et al.*, 2014, Castell *et al.*, 2015). One such instrument called 'M-Pod' accompanied by mobile application has undergone performance evaluation in the lab and real-world environments (Piedrahita *et al.*, 2014). This study demonstrated the use of the sensor package to be shared with the public and decision makers. This has opened a new paradigm for air monitoring to better understand the communities exposure to air pollutants and safeguard their health.

2.2 Challenges in sampling and analysis of combustion-related air pollutants

2.2.1 Traditional sampling methods

Volckens *et al.* (2016) raised the issue of physical load (noise, appearance, and weight) and flow rate consistencies suffered by the personal air samplers during the monitoring exposure to PM. These have led to limitation of sample size and loss to the sample mass. It is therefore essential to have a reliable and the most suitable filter material, and utilise careful filter handling techniques (Jantunen *et al.*, 2002). Typically, the smallest mass of particles collected using a filter are in the order of 10 µg (Jantunen *et al.*, 2002), this mass is sufficient to adopt analytical methods to determine the particle constituents.

Furthermore, the analytical sensitivity for low volume samples is difficult especially for particulate-bound PAHs pollutants. Samples taken from low volume monitoring are typically from the personal exposure samples or in the microenvironment settings (Delgado-Saborit *et al.*, 2010). The blackness of particulate matter has also been used to measure particle metrics in a few studies to associate BC concentrations from combustion-derived particles (Cyrys *et al.*, 2003). Nonetheless, studies to identify simple indicators of particle to specific chemical compositions are still limited. There are several downsides to the use of passive diffusion tubes despite their low-cost and straightforward application. These include their performance delivering precise and accurate measurements as compared to real time instruments (Nash and Leith, 2010), and variation with environmental conditions (i.e. wind direction) (Lin *et al.*, 2011).

2.2.2 Innovative air monitors

While there have been considerable sensor technology advancement, challenges remain to provide a foundation for characterization of different sources or components of combustion-related air pollutants. The study of BC, PM and NO_2 has resulted in the use of instruments using direct measurements and modelling to understand their component behaviour and sources of emissions (Lawrence *et al.*,

2013, Misra *et al.*, 2013). However, much effort was focused on a single pollutant, while the contribution of other components in combustion-related derived pollutants is often neglected.

2.2.3 Low-cost reliable

Weidemann *et al.* (2016) highlighted research needs for the innovative diagnostics and measurement techniques, which linked the common themes in The 14th International Congress on combustion by-products and health effects in Sweden. The meeting also emphasised the design of the monitors that include the size, weight and cost. There are varieties of portable, hand-held and miniaturised air monitors on the market, however, they are expensive, despite performing relatively well and providing sophisticated measurements. However, with the emerging technologies for low-cost sensors, are these monitors can generate data quality and can be used interchangeably with the gold standard relevance for exposure assessment?

Snyder *et al.* (2013) noted that the ability of an instrument to work in real-time, have low-cost is simple to use and can provide high time resolution, would have the potential to enhance air pollution monitoring capabilities. In the present day, the growing number of low-cost commercial instruments is inspiring. Lewis and Edwards (2016) noted the use of low-cost sensors has expanded globally and also have been used extensively in the developing countries. However, there is no current standard method to synthesize and analyse the deriving data from low-cost air quality sensing (Kotsev *et al.*, 2016), which will limit the establishment of scientifically-sound results. Castell *et al.* (2015) listed the key challenges of the use of low cost sensors including: (i) differences between laboratory and field calibration; (ii) long-term performance; (iii) response to varying weather conditions; and (iv) effect of deployment location and proximity to sources.

There are several downsides to the use of passive diffusion tubes despite their low-cost and straightforward application. These include their performance delivering precise and accurate measurements as compared to real time instruments (Nash and

Leith, 2010), and variation with environmental conditions (i.e. wind direction) (Lin *et al.*, 2011).

2.3 Development needs

Further to the features highlighted by Monn (2001) and Jantunen *et al.* (2002), they have exclusively described the characteristics of preferred PM monitoring requirements in their review. Table 2.2 shows the summary of monitoring and development needs for PM monitoring. The monitoring conditions refer to benefits to achieve methodological precision, adjustability in different sampling conditions and provide cost-effectiveness for the researcher. Furthermore, dedicated low-volume samplers are normally preferred since they are practical for micro environmental monitoring and other meteorological factors can be disregarded (Chow *et al.*, 2002).

Table 2.2: The preconditions of sampling monitors and development for PM sampling (Jantunen *et al.*, 2002).

Monitoring conditions	Development requirements
1. Sensitive to change - precision ± 5% & easy to calibrate	1. Small sampler, light and low noise level - reflects to sampling system & analysis (i.e flow rate used and filters)
2. Selective	2. Provide continuous measurement
3. Rapid	3. Microenvironment sensing based on standard sensors
4. Portable	
5. Cost effective	

In addition, Kumar *et al.* (2016) highlighted the challenge of data analysis using advanced sensor technologies. A major issue is presented includes the capacity of the sensor to measure indoor and outdoor and produce data quality. Typically, the device used to measure in the outdoor will have higher detection range compared to the lower concentrations in the indoor. Lewis and Edwards (2016) highlighted that more validation experiments would be required in order to provide robust datasets and communicate air pollution information. In their reviews, researchers are encouraged to conduct alternative experimental design with detailed processing and validation in order to safeguard data quality of low-cost sensor technology. Manufacturers and governments are also noted to play their key role for being transparent to provide adequate information of the sensor and implementing standards to improve sensor performance.

2.4 Gaps in the research

Innovative sampling systems can improve the collection of airborne specimens, which can analyse time-weighted average over the sampling period. However, there are still number of challenges that need to be addressed from the above review, and include:

- There is a need for effective monitoring strategies that include the application of additional air pollutants data, and short-term health assessment to estimate the exposure of combustion-related air pollutants.
- The contributions of different sources of combustion-related air pollutants subsequently generate the misclassification of personal exposure assessment.
- There is no simple technique to use the sensor that is publically accessible to engage the assessment methodology.
- It may become necessary to develop innovative experimental methods with the use of flexible traditional and state-of-the-art monitoring devices and appropriate validation techniques.

2.5 Summary

The urgent need for a progressive monitoring design and data utilisation are highlighted from the personal assessment context to the complex combustion-related air pollutants. Therefore, improving the measurement technique using arrays of air monitors, which are portable, straightforward, cost-effective, and provide high temporal resolution, which are appropriate in different environmental settings are deemed to facilitate the estimation of combustion-related pollutants to the individual exposure. All of these elements are important for the development of the state-of-art methods to assess combustion related air pollutants and enable the author to design or develop novel techniques for accurate exposure assessment. This will be described in the methods design of this thesis.

2.6 References

Adar, S. D., Gold, D. R., Coull, B. A., Schwartz, J., Stone, P. H. & Suh, H. 2007. Focused exposures to airborne traffic particles and heart rate variability in the elderly. *Epidemiology*, 18.

Castell, N., Kobernus, M., Liu, H.-Y., Schneider, P., Lahoz, W., Berre, A. J. & Noll, J. 2015. Mobile technologies and services for environmental monitoring: The Citi-Sense-MOB approach. *Urban Climate*, 14, Part 3**,** 370-382.

Chow, Engelbrecht, J. P., Freeman, N. C., Hashim, J. H., Jantunen, M., Michaud, J. P., Saenz de Tejada, S., Watson, J. G., Wei, F., Wilson, W. E., Yasuno, M. & Zhu, T. 2002. Chapter one: exposure measurements. *Chemosphere*, 49**,** 873-901.

Cyrys, J., Heinrich, J., Hoek, G., Meliefste, K., Lewne, M., Gehring, U., Bellander, T., Fischer, P., van Vliet, P., Brauer, M., Wichmann, H. E. & Brunekreef, B. 2003. Comparison between different traffic-related particle indicators: elemental carbon (EC), PM2.5 mass, and absorbance. *J Expo Anal Environ Epidemiol*, 13**,** 134-43.

Delgado-Saborit, J. M., Aquilina, N., Baker, S., Harrad, S., Meddings, C. & Harrison, R. M. 2010. Determination of atmospheric particulate-phase

polycyclic aromatic hydrocarbons from low volume air samples. *Analytical Methods,* 2**,** 231-242.

Fan, Z.-H. T. 2011. Passive Air Sampling: Advantages, Limitations, and Challenges. *Epidemiology,* 22**,** S132.

Jantunen, M., Hänninen, O., Koistinen, K. & Hashim, J. H. 2002. Fine PM measurements: personal and indoor air monitoring. *Chemosphere,* 49**,** 993-1007.

Koehler, K. A. & Peters, T. M. 2015. New Methods for Personal Exposure Monitoring for Airborne Particles. *Curr Environ Health Rep,* 2**,** 399-411.

Kotsev, A., Schade, S., Craglia, M., Gerboles, M., Spinelle, L. & Signorini, M. 2016. Next Generation Air Quality Platform: Openness and Interoperability for the Internet of Things. *Sensors (Basel, Switzerland),* 16**,** 403.

Kumar, P., Martani, C., Morawska, L., Norford, L., Choudhary, R., Bell, M. & Leach, M. 2016. Indoor air quality and energy management through real-time sensing in commercial buildings. *Energy and Buildings,* 111**,** 145-153.

Lawrence, S., Sokhi, R., Ravindra, K., Mao, H., Prain, H. D. & Bull, I. D. 2013. Source apportionment of traffic emissions of particulate matter using tunnel measurements. *Atmospheric Environment,* 77**,** 548-557.

Lewis, A. & Edwards, P. 2016. Validate personal air-pollution sensors. *Nature,* 535**,** 29-31.

Lin, C., Becker, S., Timmis, R. & Jones, K. C. 2011. A new flow–through directional passive air sampler: design, performance and laboratory testing for monitoring ambient nitrogen dioxide. *Atmospheric Pollution Research,* 2**,** 1-8.

Mead, M. I., Popoola, O. A. M., Stewart, G. B., Landshoff, P., Calleja, M., Hayes, M., Baldovi, J. J., McLeod, M. W., Hodgson, T. F., Dicks, J., Lewis, A., Cohen, J., Baron, R., Saffell, J. R. & Jones, R. L. 2013. The use of electrochemical sensors for monitoring urban air quality in low-cost, high-density networks. *Atmospheric Environment,* 70**,** 186-203.

Misra, A., Roorda, M. J. & MacLean, H. L. 2013. An integrated modelling approach to estimate urban traffic emissions. *Atmospheric Environment,* 73**,** 81-91.

Monn, C. 2001. Exposure assessment of air pollutants: a review on spatial heterogeneity and indoor/outdoor/personal exposure to suspended particulate matter, nitrogen dioxide and ozone. *Atmospheric Environment,* 35**,** 1-32.

Nash, D. G. & Leith, D. 2010. Use of Passive Diffusion Tubes to Monitor Air Pollutants. *Journal of the Air & Waste Management Association,* 60**,** 204-209.

Piedrahita, R., Xiang, Y., Masson, N., Ortega, J., Collier, A., Jiang, Y., Li, K., Dick, R. P., Lv, Q., Hannigan, M. & Shang, L. 2014. The next generation of low-cost personal air quality sensors for quantitative exposure monitoring. *Atmos. Meas. Tech.,* 7**,** 3325-3336.

Ramanathan, N., Lukac, M., Ahmed, T., Kar, A., Praveen, P. S., Honles, T., Leong, I., Rehman, I. H., Schauer, J. J. & Ramanathan, V. 2011. A cellphone based system for large-scale monitoring of black carbon. *Atmospheric Environment,* 45**,** 4481-4487.

Semple, S., Apsley, A. & Maccalman, L. 2013. An inexpensive particle monitor for smoker behaviour modification in homes. *Tob Control,* 22**,** 295-8.

Shields, K. N., Cavallari, J. M., Hunt, M. J. O., Lazo, M., Molina, M., Molina, L. & Holguin, F. 2013. Traffic-related air pollution exposures and changes in heart rate variability in Mexico City: A panel study. *Environmental Health,* 12**,** 1-14.

Snyder, E. G., Watkins, T. H., Solomon, P. A., Thoma, E. D., Williams, R. W., Hagler, G. S. W., Shelow, D., Hindin, D. A., Kilaru, V. J. & Preuss, P. W. 2013. The Changing Paradigm of Air Pollution Monitoring. *Environmental Science & Technology,* 47**,** 11369-11377.

Steinle, S., Reis, S., Sabel, C. E., Semple, S., Twigg, M. M., Braban, C. F., Leeson, S. R., Heal, M. R., Harrison, D., Lin, C. & Wu, H. 2015. Personal exposure monitoring of PM2.5 in indoor and outdoor microenvironments. *Science of The Total Environment,* 508**,** 383-394.

Volckens, J., Quinn, C., Leith, D., Mehaffy, J., Henry, C. S. & Miller-Lionberg, D. 2016. Development and evaluation of an ultrasonic personal aerosol sampler. *Indoor Air*.

Weidemann, E., Andersson, P. L., Bidleman, T., Boman, C., Carlin, D. J., Collina, E., Cormier, S. A., Gouveia-Figueira, S. C., Gullett, B. K., Johansson, C., Lucas, D., Lundin, L., Lundstedt, S., Marklund, S., Nording, M. L., Ortuno, N., Sallam, A. A., Schmidt, F. M. & Jansson, S. 2016. 14th congress of combustion by-products and their health effects-origin, fate, and health effects of combustion-related air pollutants in the coming era of bio-based energy sources. *Environ Sci Pollut Res Int,* 23**,** 8141-59.

Wu, H., Reis, S., Lin, C., Beverland, I. J. & Heal, M. R. 2015. Identifying drivers for the intra-urban spatial variability of airborne particulate matter components and their interrelationships. *Atmospheric Environment,* 112**,** 306-316.

Zhao, X., Sun, Z., Ruan, Y., Yan, J., Mukherjee, B., Yang, F., Duan, F., Sun, L., Liang, R., Lian, H., Zhang, S., Fang, Q., Gu, D., Brook, J. R., Sun, Q., Brook, R. D., Rajagopalan, S. & Fan, Z. 2014. Personal black carbon exposure influences ambulatory blood pressure: air pollution and cardiometabolic disease (AIRCMD-China) study. *Hypertension,* 63**,** 871-7.

3 RESEARCH AIMS & OBJECTIVES

3.0 Background

This chapter summarises the aims and objectives of this PhD research, and outlines the overall structure of the chapters in the thesis.

3.1 Aims and objectives

This research aimed to develop novel methods for assessment of exposure to combustion-related air pollutants within indoor and outdoor settings.

Specific objectives for this study included:

(i). To develop innovative sampling methods using portable low power samplers for estimation of exposure to combustion-related air pollutants.

(ii). To evaluate BC and NO_2 exposure estimation methods in the field settings.

(iii). To assess exposure to PM, BC and NO_2 concentrations within indoor and outdoor microenvironments.

(iv). To interpret environmental and personal exposures to PM, BC and NO_2.

(v). To investigate whether it is possible to use estimates of the concentration of particular constituents of combustion-related air pollutants (PM, BC and NO_2) as simple markers for different combustion sources.

3.2 Scope of the study

This PhD research focuses on the development of novel approaches to characterise exposure to combustion related air pollutants including PM, BC and NO_2 and to subsequently assess human exposure to these pollutants in both indoor and outdoor settings. The exposure assessment methods included collection of airborne particle specimens and optical analysis to estimate black carbon concentration. Passive nitrogen dioxide (NO_2) devices, and portable real-time sensors for PM_{10}, $PM_{2.5}$, PM_1, NO_2, ozone (O_3) and black carbon (BC) were also evaluated and deployed. Sampling applications were extended from laboratory tests to indoor offices (University of Strathclyde), urban walking (Glasgow city centre) and a fracking test site (Poland).

In the first part of the project, methods were developed to collect particle and gaseous specimens using portable filter-based and passive samplers. Analytical techniques to make exposure assessment simpler and more practicable involved PM, BC and NO_2 are much in demand compared to more sophisticated systems for particulate-bound polycyclic aromatic hydrocarbons (pPAHs). Specifically, this research developed a non-destructive and low-cost optical analysis of sequentially loaded filter air samples to illustrate how BC can be estimated from filter reflectance calibrated against co-located micro-aethalometer observations. The method was then evaluated in different field micro-environments. Portable real-time NO_2 and O_3 monitor were compared to reference analysers under representative outdoor conditions prior to deployment in mobile measurements.

The above methods for estimating pollutant concentrations were used in different environmental settings. An indoor air quality study was conducted in two office

buildings in the University of Strathclyde involving assessment of exposure to PM, BC and NO_2. To assist understanding of the indoor exposures other air pollutants were also measured, including ozone (O_3) and nitric oxide (NO). Using similar methods, exposure assessment was extended to urban outdoor roadside environments in Glasgow city centre. The study examined exposure of PM, BC and NO_2 in adults and children in relation to vertical variation from combustion sources of city traffic. These measurements in urban streets were observed during different 'peak traffic' and 'non-peak traffic' periods; morning, mid-afternoon and afternoon rush-hour.

Pollutant measurements from automatic analysers in the UK air monitoring national network were used as a reference to mobile monitoring exercises. This research also assessed personal exposure to diesel engine exhaust combustion from industrial fracking equipment at an experimental hydraulic fracturing (HF) test site in Poland. This showed how the instruments can be deployed in complex industrial environments, and also allowed detailed insight into the short-term exposure of combustion related air pollutants experienced by the site operators.

3.3 Outline of thesis

This thesis comprises of nine chapters including this chapter (Chapter 3).

Chapter 1 set the scene for the study by giving relevant background information on the components of combustion-related air pollutants and their health effects. This introductory chapter describes briefly the methods of measuring these pollutants.

Chapter 2 reviews the current approaches of monitoring combustion-related air pollutants, which are relevant to human health. The chapter highlights the need and challenges for state-of-art methods to assess and characterise exposure.

Chapter 3 presents the research objectives and the scope of the study.

Chapter 4 describes the development of sampling and analysis techniques with the use of specific instruments to measure PM, BC, NO_2 and pPAHs. The pilot tests are also outlined.

Chapter 5 presents further field evaluation of some of the above methods in the indoor and outdoor settings, to estimate concentrations of BC and NO_2 using cost-effective and portable real-time techniques.

Chapter 6 describes the assessment of PM, BC and NO_2 in university offices with different ventilation methods using filter-based, passive samplers and real-time monitors. Additional measurements for O_3 and NO are also described.

Chapter 7 describes the assessment of PM, BC and NO_2 using static and mobile platforms and wearable real-time sensors in urban microenvironments in Glasgow city centre, using some of the systems described above.

Chapter 8 presents a field study of the measurement of BC and NO_2 exposure using portable air monitors at hydraulic fracking site in Poland.

Chapter 9 summarises the key findings, the contribution of this thesis to scientific knowledge, and possible avenues for future research to enhance the understanding of key pollutants from combustion sources. This chapter also illustrates how health-relevant exposures can be estimated in a more comprehensive way by combining knowledge from exposure science and environmental engineering.

A number of papers have been completed from the work described in chapter 5 (as the co-author) (details can be found from appendix 10A(1) & 10A(2)), chapter 7 (as the co-author) (details can be found from appendix 10A(3)) and chapter 8 (as the first author).

4 DEVELOPMENT OF METHODS

4.0 Background

Koehler and Peters (2015) describe how recent improvements in sampling instruments and sensor technologies have facilitated estimation of personal exposure to air pollutants. Sample collection and real-time monitoring systems require to be accurate, precise, lightweight and battery-powered. Flexible and effective methods for deployment of such systems are also required.

This chapter gives details of development of exposure assessment methods using combinations of simple and relatively inexpensive systems with more sophisticated techniques to measure PM, BC and NO_2 concentrations. The chapter provides a brief description of the operating principle of the instruments and subsequent data analysis procedures. The agreement between portable monitors (suitable for personal exposure assessment) and reference samplers was characterised. The chapter describes the reference sites used during the study and the initial sampling designs used to improve understanding of the portable monitoring systems. A new technique to estimate exposures to combustion-related pollutants is described.

4.1 Measurement of BC and PM

4.1.1 Preparation of filter media and samplers

25-mm-diameter and 37-mm-diameter 2.0 µm pore size polytetrafluoroethylene (PTFE) filters (Zefluor; Gelman Sciences, USA) were inspected for damage before use and conditioned in part-opened petri dishes for 24 hours, prior to reflectance measurement and weighing (procedures described in Section 4.1.3). When not being used for sampling or analysis, filters were stored in plastic clamshell filter holders (labelled with sample identification codes) within archiving trays (SKC Ltd, UK) in the Department of Civil & Environmental Analytical Laboratory.

Two types of cyclones were used to collect airborne particle specimens: Higgins-Dewell respirable cyclone (Casella Ltd, UK) and BGI Triplex $PM_{2.5}$ cyclone (BGI, USA). The Higgins-Dewell cyclone contains a plastic cassette, for either 25-mm or 37-mm diameter filters. Filters were placed in the cassette with tweezers. Procedures for respirable cyclone sampling in Health, Safety and Executive guidelines (HSE, 2000) were followed. The BGI Triplex cyclone has a push-fit filter cassette for 37-mm diameter filters, which was hand tightened after the installation of the filter, and opened after sampling using a stainless steel ‘SureSeal’ cassette opener (SKC Ltd, Dorset, UK).

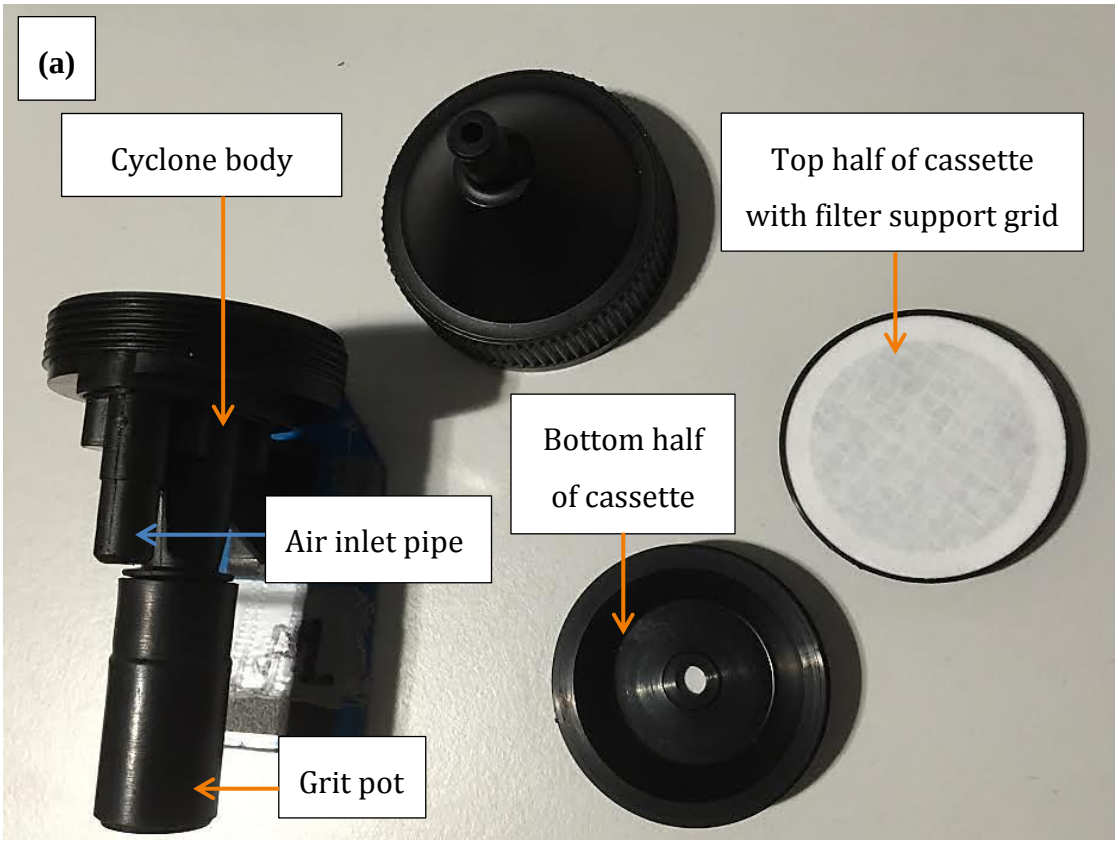

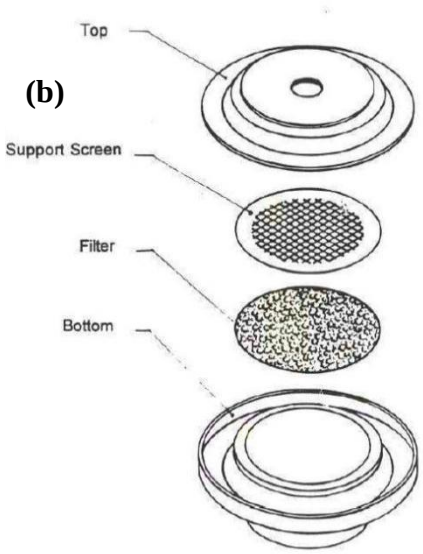

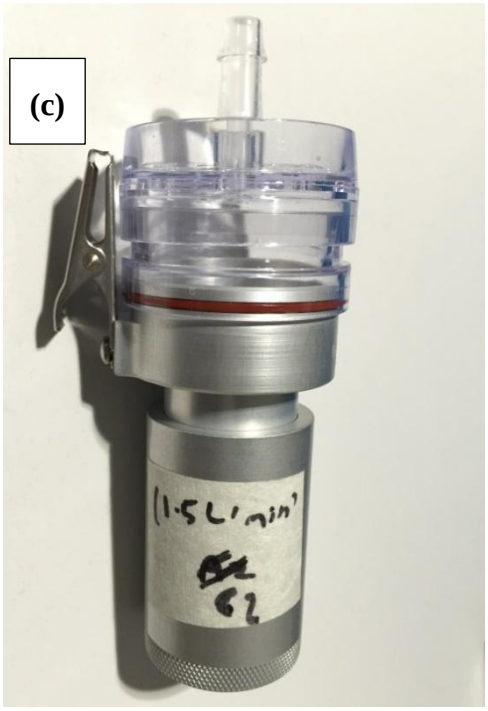

Figure 4.1: (a) Casella Higgins-Dewell respirable cyclone with 37-mm filter cassette; (b) cassette fitted in Casella Higgin-Dewell respirable cyclone Source: (HSE, 2000); (c) BGI triplex $PM_{2.5}$ cyclone.

4.1.1.1 Flow Rate Calibration

Two flowmeters were used to record and verify flow rates: a rotameter (SKC Ltd, UK); and a volumetric calibrator (DryCal Defender 530, BIOS International Corp., USA). Flow rates were measured using the rotameter from the position of a float on a 0.6 to 5.0 L min^{-1} vertical scale. The rotameter was positioned vertically using a spirit level and a laboratory stand. Sampling pumps were connected to the rotameter using ¼ inch Tygon® tubing to allow the flow to be adjusted to the required rate.

The use of the digital volumetric calibrator enabled flow rates to be measured directly by the transit time of a frictionless float. The calibrator has a specified accuracy of ± 1%. The 'suction' port of the calibrator was attached to the cyclone inlet using ¼ inch Tygon® tubing. A low flow resistance HEPA filter was connected to the 'pressure' port to prevent contamination of the calibrator during the flow rate measurement. The majority of measurements were made in 'burst' mode, where measurements continued automatically until a preset number of measurements had been made, and then the last reading and average were displayed. Flow calibration followed guidelines provided by MDHS 14/3 (HSE, 2000) which requires adjustment of the flow rate to within ± 0.1 L min^{-1}.

4.1.2 Selection of personal sampling pumps

Four personal sampling pumps were evaluated for sampling of particles airborne in the present research project: AFC 400S (BGI, USA); Apex Pro & Tuff Pro (Casella Ltd, UK); and GilAir Plus (Sensidyne, USA). These pumps are small, lightweight and portable (Table 4.1).

Table 4.1: Summary of technical information for personal air pumps.

Personal sampler	Mass (g)	Flow Range (L min^{-1})	Battery Type	Charging Duration (hour)	Software
Apex Pro (Casella)	500	0.8 - 4.0	NiMH	~4.5	Casella Insight V.0.0.0.7.0
Tuff Pro (Casella)	475	0.5 - 4.5	4.8 NiMH	~3.0	Casella Insight V.0.0.0.7.0
BGI 400S (BGI)	900	2.0 – 6.0	NiMH	No data	None
GilAir Plus (Sensidyne)	580	0.02 – 5.0	NiMH	< 3.5	Gillian Pump Data Management V.1.0.2.2

4.1.3 Analysis of particle samples

4.1.3.1 Filter Reflectance Measurements

The darkness of filter samples was measured using a smoke stain reflectometer (Model EEL MD43, Diffusion Systems Ltd, UK) consisting of measurement head with monochromatic light source, detector & circular mask; digital display; and calibration tile with white & grey sections (Figure 4.2). A non-lint cloth and ethanol were used to clean the measuring head mask and calibration tile prior to measurements.

A filter holder was designed from black paper to ensure that the reflectometer measurements were consistently made in the centre of the 25-mm filters. The holder

was fixed on the calibration tile so that calibration measurements were always made on the same part of the white and grey sections of the tile. The filter holder was based on a similar idea outlined by Kinney *et al.* (2002) who used a PTFE filter holder to reduce potential contamination problems from the circular mask coming into direct contact with filters.

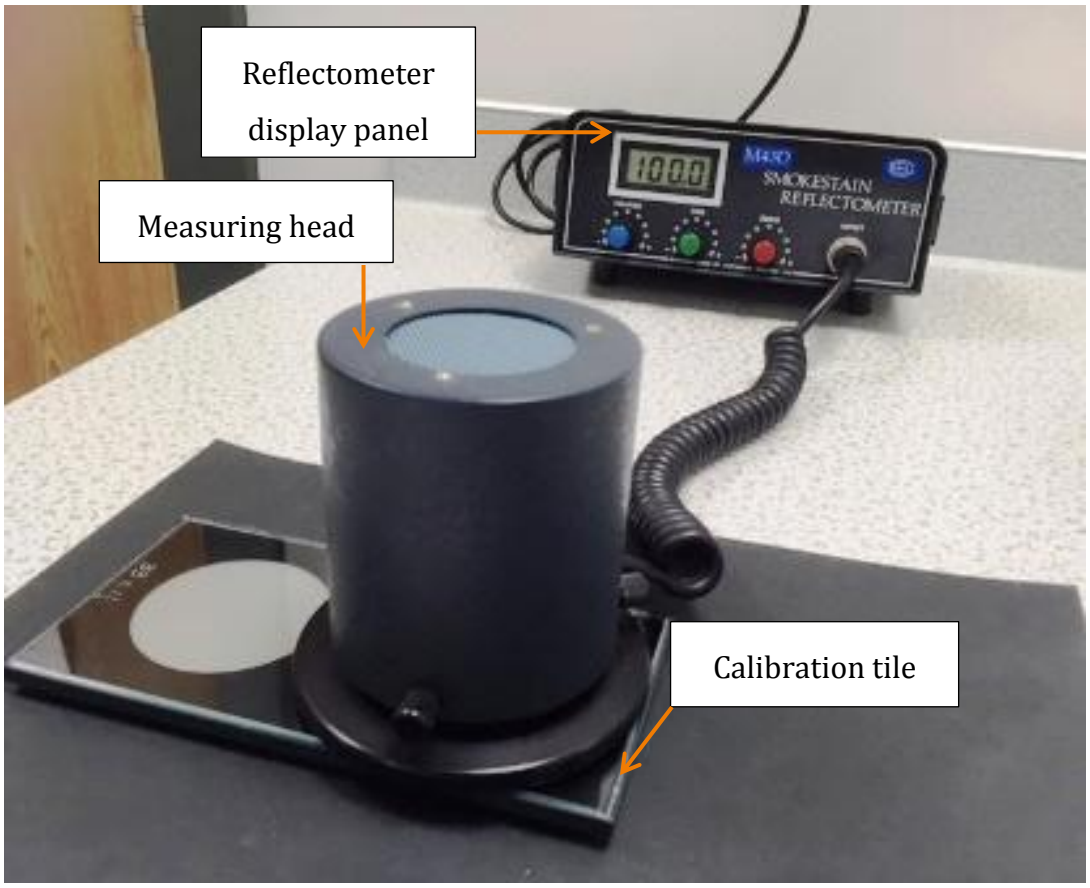

Figure 4.2: EEL MD43 smoke stain reflectometer with calibration tile.

The reflectometer was switched on and set to zero without the measurement head attached. The instrument was then switched off to allow the measurement head to be attached and placed on the grey tile of the standard plate, and then switched back on again to 'warm up' for a further 30 minutes before measurements were made. The 'COARSE' and 'FINE' knobs were used to adjust the display to a value of 100 for the white section of the calibration tile. The head was moved to the grey tile and the

display set to a value of 33 using the 'ZERO' control knob. The light source was moved between the white and grey sections of the calibration tile, and the values re-adjusted until consistent readings of 100 ± 0.2 and 33 ± 1.5 were achieved for the white and grey sections respectively (demonstrating linearity of response).

The darkness of filters was measured before and after sampling. Measurements were made three times until readings deviated by not more than 0.5 units. Blank filters had reflectances exceeding 100 units, which were not reset to 100 (analogous to the method of Penttinen *et al.* (2000). After every six filters, the white and grey sections of the calibration tile were re-measured and the display adjusted to values of 100 and 33 respectively.

4.1.3.2 Absorption coefficient

Absorption coefficients (ISO, 1993) were calculated from filter darkness measurements as follows:

$$a = \frac{A}{2V} * \ln(\frac{Ro}{Rs}) \quad \textbf{(4.1)}$$

where:

a = absorption coefficient (m^{-1})

R_0 = average darkness (reflectance) of field blank filter(s)

R_s = average darkness (reflectance) of sample filter

V = volume of air filtered through sample filter (m^3)

A = the area of the stain on the filter (m^2)

4.1.3.3 Digital image analyses

An office scanner (EPSON Model GT-1500) was used to scan filters before and after sampling. The darkness of filter samples was quantified from the red values in the digital images of the filters. The red wavelength has been shown a strong relationship with a total loading of BC that accumulates on the filter (Cheng *et al.*,

2011, Ramanathan *et al.*, 2011). A filter holder was made from white A4 paper to hold 25-mm sample, blank, and reference filters in a consistent position in the scanner during repeated measurements.

The scanner glass surface was cleaned using a lint-free cloth prior to measurements. Scanned images of filter were saved in JPEG format at 600 pixels per inch resolution. A computer program (using Delphi V.5 software) was used to sample 600 pixels from the central part of the scanned image of the filter and compute the red values for three times. The average red values were entered into an Excel spreadsheet to allow calculation of the mean of repeat measurements.

4.1.3.4 Gravimetric analysis

Filter and airborne particle masses were measured with a microbalance (MC5; Sartorius AG, Goettingen, Germany) in a temperature controlled laboratory (Figure 4.3). The microbalance has display resolution of 1 μg and a maximum weighing capacity of 5.1 g. Masses recorded by the microbalance were transferred automatically to an Excel spreadsheet using software provided by the balance manufacturer (Sarto Wedge).

The weighing facility area and plastic tweezers used for handling filters were cleaned regularly with lint-free paper wipes, and the microbalance switched on an allowed to 'warm up' for 1 hour prior to the start of measurements. Just before measurements were started, the balance door was opened and closed for three times, to equilibrate the air within the microbalance chamber and the laboratory. The microbalance was calibrated following procedures in the Sartorius operating manual.

A piece of folded aluminium foil was used to avoid the filter touching the balance weighing pan, while allowing for discharge of any residual electrostatic charge during the weighing of filters (Brown *et al.*, 2006). The mass of the foil was tared to zero before measurements were made.

Filters were conditioned for 24 hours, in part-opened petri dishes prior to weighing to equilibrate with the laboratory ambient environment. Filters were placed under an anti-static blower (Stat-Attack, Static Solutions, UK) for 20 seconds to minimise potential errors from electrostatic charge build-up. Such electro-static charges may result from relatively low humidity in the air in the weighing chamber and should be controlled prior to weighing sessions (Kulkarni *et al.*, 2011). Each of the filters was weighed three times per weighing session. The weighing procedure followed a protocol adapted from MHDS 14/3 (HSE, 2014) and (Hammond, 2012).

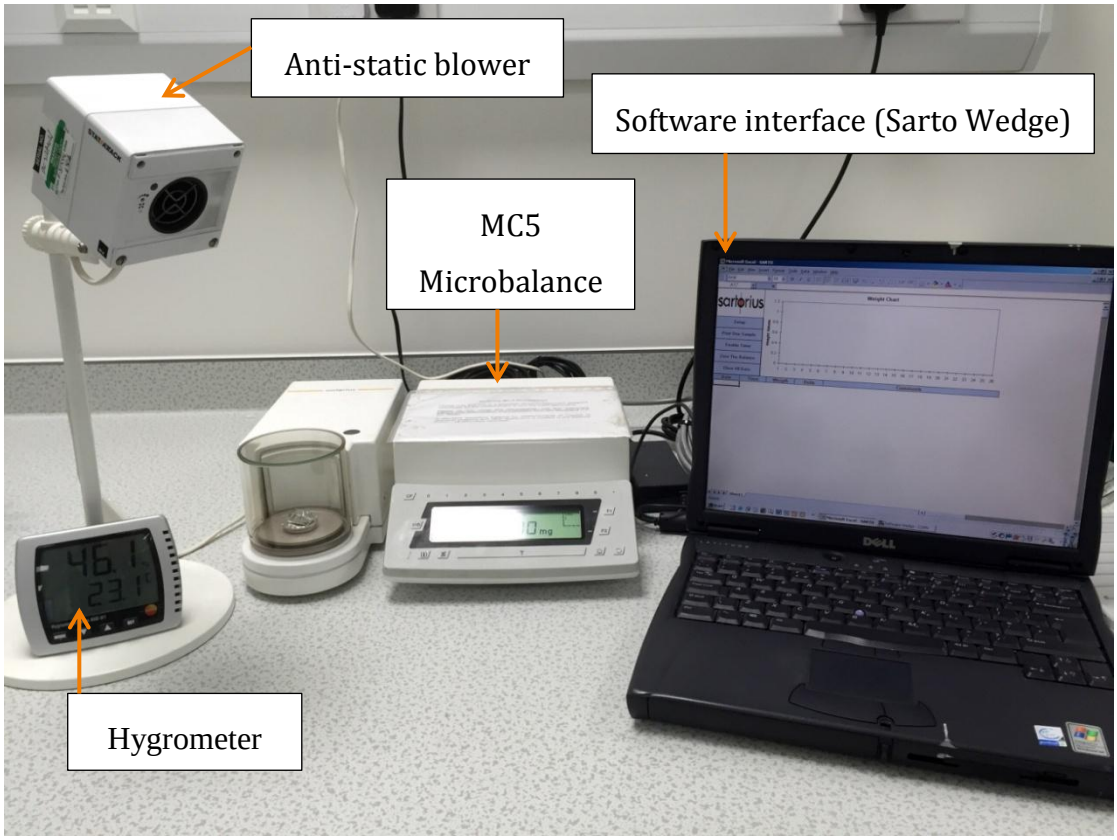

Figure 4.3: Microbalance in Department of Civil and Environmental Engineering Analytical Laboratory.

4.1.3.5 Climate monitoring in the weighing laboratory

Relative humidity (RH) and room temperature were recorded using a hygrometer (Testo 608-HI; Testo Ltd., UK) during weighing sessions. All the recordings were

conducted in accordance to the British Standards for 'Controlling and characterizing errors in weighing collected aerosols' (ISO, 1993). Barometric pressure was recorded using a barometer to quantify the effects of air buoyancy on mass measurement.

4.1.3.6 Mass concentrations

The average of filter weight before and after sampling is calculated and adjusted for the deviation of the control filter weights.

$$Ms = W2 - W1 - B \tag{4.2}$$

where:

Ms = mass on filter

W1 = adjusted filter weight before sampling

W2 = adjusted filter weight after sampling

B = mean adjusted filter weight change of field and lab blanks filters

Two field blank and two lab filters were used for every collected samples. The mean values were calculated and subtracted from the respective sample mass.

Mass concentrations are calculated from the mass on filter and sampler volume:

$$PM = Ms/V \tag{4.3}$$

where:

PM = PM mass concentrations

Ms = mass on filter (post weighed – pre weighed)

V = filter volume (calculated from average flow rate and duration of sampling)

4.1.4 Real-time monitors

4.1.4.1 BC real-time monitor: AE51 Aethalometer

Aethlabs microAeth AE51 portable Aethalometer (Model AE51 Aethlabs, San Francisco, CA, USA) were used to make continuous measurements of BC (Figure 4.4). This device measures the rate of change of transmitted 880 nm light through PTFE coated glass fibre filters as dark particles are deposited on the filter surface. The flow rate can be set from 50 to 200 ml min^{-1} and the logging time intervals can be set from 30 seconds to 5 minutes depending on sampling conditions. The AE51 Aethalometer can run off an internal battery or can be operated from an external 5V source. The battery run time is dependent on flow rate and the accumulation of particles on the filter strip.

The light transmission after passing the filter is inversely proportional to the attenuation of the light (ATN) (Virkkula *et al.*, 2007). The accumulation of loaded BC aerosols on the filter caused the ATN to increase and the degree of ATN variations is used to estimate BC concentrations.

$$ATN = -\ln(\frac{I}{I_o}) \quad \textbf{(4.4)}$$

where:

ATN = the attenuation of the filter

I = the light intensity after passing the filter

I_o = the light intensity of incoming light

Prior to sampling, the ATN value of the filter was checked using microAethCOM software (v2.1.0.1 and v2.2.4.0). The filter was renewed when the ATN was greater than 45. The date and time of sampling were synchronised to the researcher's

desktop computer clock. BC data was downloaded from the AE51 Aethalometer via a software interface in csv file format.

Downloaded data were processed to reduce noise using software from the manufacturer's website (https://www.aethlabs.com/dashboard). This software implements an Optimised Noise-Reduction Averaging (ONA) smoothing technique developed by Hagler *et al.* (2011a). A smoothing value of 0.01 was selected for ONA processing. The output data were then further processed using a correction equation (Equation 4.5) to account for changes in filter attenuation value as the filter became darker from the increased load of particles during continuous BC measurements (Apte *et al.*, 2011) :

$$BC\ (\mu g/m^3) = BC_0(0.88Tr + 0.12)^{-1} \quad \textbf{(4.5)}$$

where:

$Tr = \exp(-\frac{ATN}{100})$,

BC_0 = BC concentration measured by instrument after smoothing by ONA

ATN = attenuation value

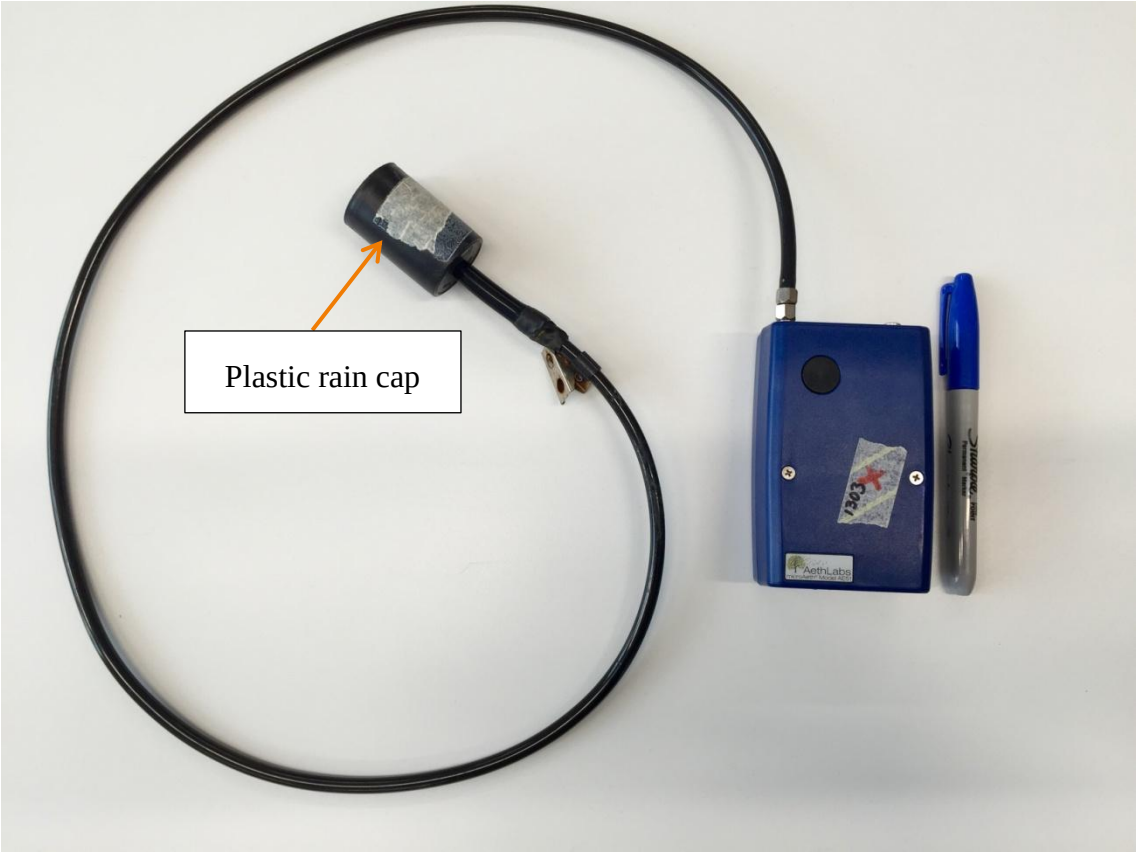

Figure 4.4: Portable AE51 Aethalometer and sampling tube with plastic rain cap.

The above method for BC measurement using AE51 Aethalometer re described in section 8.4.3.

4.1.4.2 PM sensor: Turnkey OSIRIS

The Turnkey OSIRIS monitor (Turnkey Instruments Ltd, England) uses light scattering technology to measure continuous real-time of PM mass concentrations which include TSP, $PM_{2.5}$, PM_1 and PM_{10} using the built-in microprocessor. The OSIRIS has been used and evaluated in both indoor (Tasić *et al.*, 2012) and mobile outdoor studies (Gulliver and Briggs, 2004). The filters in the Osiris unit were changed prior to deployment at the monitoring site. Flow rates were set at 600 cc min^{-1} (TurnkeyInstrument, 2006). The internal clock units were synchronised and each Osiris units was set to log data for one-minute averaging period. The collected data were downloaded through a software interface (AirQ), and saved in an Excel spreadsheet.

4.1.4.3 PM sensor: MicroPEM

$PM_{2.5}$ concentrations were measured using a portable light-scattering monitor (MicroPEM model V.3.2, RTI International, NC, USA). This lightweight PM monitor provides continuous $PM_{2.5}$ measurement using a 780 nm laser nephelometer, and collects particles on a 25-mm 3-µm pore size Teflo PTFE filter. The MicroPEM records $PM_{2.5}$ concentrations at up to 10 second time resolution and can run for approximately 40 hours using fully charged alkaline batteries. The MicroPEM flow rate can be set to 0.45, 0.50 or 0.55 L min^{-1}. The time and date were synchronised from the software interface (microPEM Docking Station).

4.1.5 Analysis of chemical composition of particle specimens analysis using GC-MS

4.1.5.1 Sample extraction and evaporation

The extraction method was based on previous PAHs analysis conducted by Tadsanaprasittipol (2016). The filter sample was stored in labelled petri dishes before being transferred to a 5 mL extraction cell. The chemical constituents of the sampled particles were extracted using an ASE 350 accelerated solvent extraction system (Dionex, Camberley, UK).

The accelerated solvent extraction (ASE) extraction cell was prepared by placing the filter on the lower lid and the cell was filled with clean-up agents (Sigma-Aldrich Company Ltd., Dorset, UK): 3.0 g of silica gel and 5.0 g of nitrogen sulphate (Na_2SO_4). These clean-up agents were prepared by heating at 450 °C for 8 h and deactivation with water at 10% w/w. The filter sample was fold with tweezers and placed inside the cell body. The remaining cell volume was packed with an inert filtration agent, called the diatomaceous earth. The cell lid with embedded filter was twisted closed by hand. Extraction cells were placed in the ASE sample carousel.

Deuterated surrogates of D8-naphthalene, D10-fluorene, D10-fluoranthene and D12-chrysene (Sigma-Aldrich Company Ltd., Dorset, UK) were prepared prior to

extraction. The ASE system was set up at 100 °C with a static time of 6 minutes, 1500 psi extraction pressure and extracted in 3 cycles. The rinse volume for the cell was 60% using the extraction solvent mixture of hexane and toluene (HPLC grade; Fisher Scientific UK Ltd., Loughborough, UK) with 4:1 ratio and 100 seconds of purge. Both extraction cells and vials were rinsed and cleaned (with acetone) after each use to prevent contamination of samples.

Sample extracts were concentrated using a Büchi Syncore Analyst (Oldham, UK) prior to quantitative analysis using gas chromatography-mass spectrometry (GC-MS). This recovery system was set for 250 rpm speed and switched on for 15 minutes before placing the extracts inside the sample racks. The rack lid temperature was set to 70 °C with a cooling temperature of 8 °C and sample rack temperature maintained at 60 °C. This system was set for 3 hours recovery time. Extracts were stored at -80 °C in 0.5 µL vials. Low concentration samples were concentrated further using a nitrogen blower at the room temperature.

4.1.5.2 GC-MS Analyses

A gas chromatograph (Trace Ultra GC) with quadrupole mass spectrometer (DSQ II) and autosampler (TriPlus) (Thermo Scientific, Inc) was used to analyse the extracts for USEPA defined 'target' PAHs. Separation was achieved using a 30 m Rxi®-5Sil MS capillary column (0.25 mm i.d., 0.25 µm film thickness). The inlet temperature was set to 250 °C and splitless mode was selected to inject 1 µL sample. All standards and extracts were analysed with the oven temperature programmed at 60 °C from 55 °C (maintained for 3 min), increased at 1 °C min^{-1} to 80 °C, increased at 5 °C min^{-1} to 230 °C and finally increased at 10 °C min^{-1} to 310 °C (maintained for 6.5 min). Benzo[a]pyrene (BaP) in the sample extracts was quantified using GC-MS SIM mode and Xcalibur® software for 16 US EPA priority pollutant PAHs.

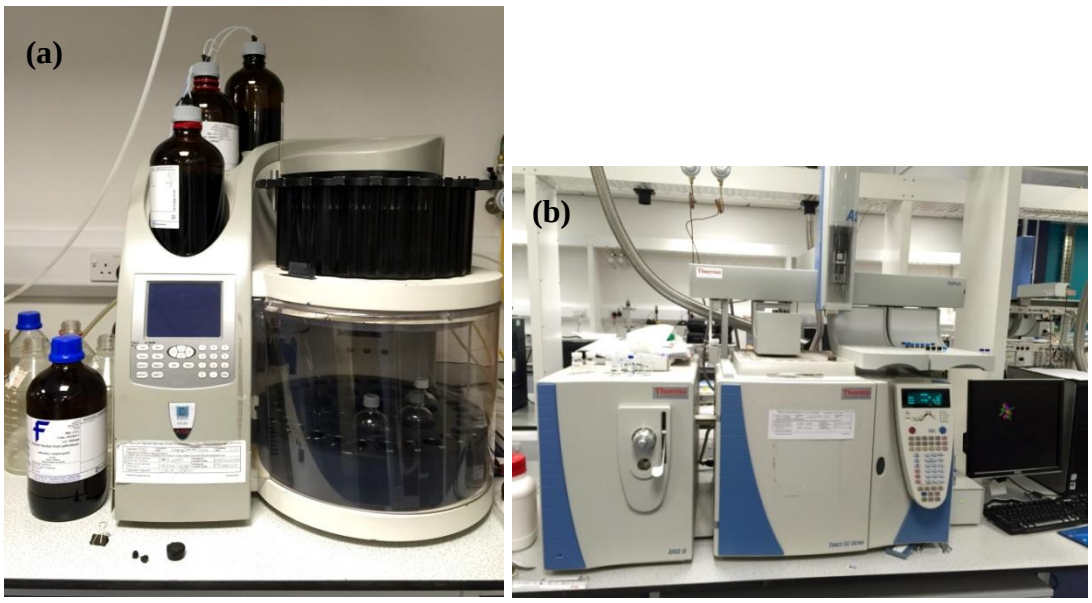

Figure 4.5: (a) ASE instrument and (b) GC-MS system in the Analytical Laboratory, Department of Civil and Environmental Engineering, University of Strathclyde.

4.2 Gaseous measurements

4.2.1 Preparation of passive samplers

Palmes-types diffusion tubes (Figure 4.6 (a)) are passive samplers commonly used to measure NO_2 concentrations in the UK (DEFRA, 2008). The transparent acrylic tube has a white end cap at the bottom (removed during sampling), and a grey cap on top to retain absorbent material during sampling. NO_2 diffuses along the length of the tube to be absorbed in triethanolamine (TEA) coated on stainless meshes inside the grey cap. The absorbed nitrite is extracted and quantified by spectrophotometric techniques or ion chromatography (Nash and Leith, 2010).

The following methods for PDT preparation and analysis are based on UK guidelines (DEFRA, 2008). PDTs were obtained from Gradko International Ltd (www.gradko.com). Clean stainless steel meshes were handled using tweezers and dipped in a 50:50 v/v solution of triethanolamine (TEA) and acetone for 5 minutes. Two mesh grids coated with TEA solution were placed inside the closed ends of the

grey cap (Jiménez *et al.*, 2011). The tubes were securely capped at the top and bottom and stored in double zip locked polythene bags in a refrigerator. PDTs were deployed for use within two weeks of preparation.

4.2.1.1 Storage, deployment and retrieval of PDTs

Duplicate PDTs were mounted vertically with foam padding keeping the tube clear of the structure on which they were secured (e.g. lampposts: Figure 4.6 (b)) below. The dates and times of exposure periods were recorded manually. Heal *et al.* (1999) suggest that an exposure time of 2-3 days is sufficient to obtain sufficient absorbed nitrite to estimate NO_2 personal exposure. After retrieval, PDTs were stored double bagged in a vertical position in the refrigerator prior to extraction and analysis.

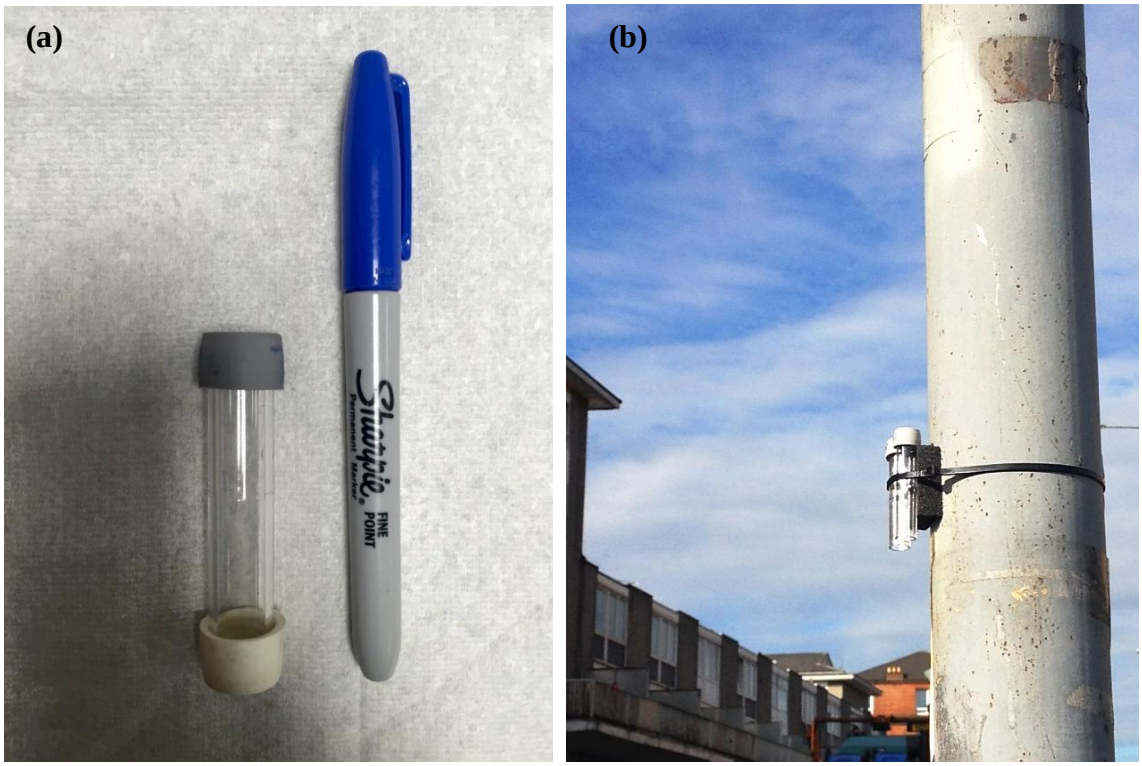

Figure 4.6: (a) Passive diffusion tube (PDT) with grey cap on top and white cap at the bottom. (b) Duplicate PDTs deployed on a lamppost for outdoor measurement.

4.2.1.2 PDT extraction and analysis

PDTs were analysed according to a standard protocol (Heal, 2013). The tubes were placed in a rack with the grey caps pointing downwards. White caps were removed

from the base of the tubes and 2.0 mL of deionised water and was transferred by pipette into each tube. The white caps were refitted and the tubes shaken by hand prior to being left to stand for 30 minutes in rack at the room temperature to extract absorbed nitrite.

Nitrite standards were prepared in six separate tubes to derive a calibration curve for quantification of nitrite concentrations in the sample tubes. Calibration tubes were prepared while the sample tubes were undergoing extraction. 1.50 mL of sulphanilamide solution was added to each sample and calibration tubes. 0.150 mL of NEDA solution was then added to each tube. All tubes were shaken briefly by hand and allowed to stand for a further 30 minutes to allow the coloured reaction product dye to develop in the tubes.

PDT sample and calibration solutions were transferred to clean cuvettes to quantify optical absorbance using UV-Visible spectrophotometry at a wavelength of 542 nm. All samples and calibration standards were measured twice and mean absorbance values calculated

The concentration of NO_2 measured using the above process was determined using the equation below:

$$C_0 = \frac{QL}{DAt} \quad \textbf{(4.6)}$$

where,

C_0 = average NO_2 concentration during PDT exposure ($\mu g/m^3$)

Q = nitrite mass measured in each PDT by UV-Vis (ng)

L = length of the PDT (7.1 cm)

D = diffusion coefficient of NO_2 (0.151 $cm^2\ s^{-1}$)

A = area of the PDT (0.916 cm^2)

t = duration when the PDT was exposed (seconds)

4.2.2 Real-time NO_2 sensors

Handheld portable sensors (Series 500 Aeroqual Ltd., Auckland, New Zealand) were used to record real-time NO_2 concentrations (Figure 4.7). These monitors use an electrochemical sensor to measure NO_2 and a metal oxide semiconductor sensor to measure ozone (O_3) (re described in section 8.4.4). External air is brought into contact with the sensors by an internal fan therefore, the sensor is not waterproof. This monitor has the capability to measure NO_2 and O_3 in the range between 1-200 ppb. The internal instruments clocks were synchronised with internet time. Data were logged at 1-minute temporal resolution prior to downloading with Aeroqual S500 software (V.6.4). Data were corrected using a method suggested by Lin *et al.* (2015) involving monthly calibration against reference analysers (further details are described in section 5.2.1).

Figure 4.7: Handheld Aeroqual NO_2 (left) and O_3 (right) monitors.

The above techniques using Aeroqual sensors re described in section 5.2 & 8.4.4.

4.3 Reference analysers

Reference air pollution data were downloaded from a database of measurements from the Automatic Urban Network (AUN) of fixed monitoring sites operated by the Scottish Government and Local Authorities (http://www.scottishairquality.co.uk/). The portable instruments were deployed at AURN measurements sites and compared to reference $PM_{2.5}$, BC and NO_2 measurements at hourly resolution. Three AUN sites were used to provide reference measurements during this research (Table 4.2).

Table 4.2: Summary of AUN reference sites used in this research.

	Glasgow Kerbside	High St.	Townhead
Type:	Urban traffic	Urban traffic	Urban background
Location:	55.859170,-4.258889	55.860936,-4.238214	55.865782,-4.243631
Pollutants measured:	$PM_{2.5}$, PM_{10}, NO, NO_2 and NO_x as NO_2	$PM_{2.5}$, PM_{10},BC, NO, NO_2 and NO_x as NO_2	$PM_{2.5}$, PM_{10}, NO, NO_2 and NO_x as NO_2

The Scottish air quality database website only provided PM and NO_2 data. BC data were downloaded from https://uk-air.defra.gov.uk/data/data_selector.

4.4 Pilot study: evaluation of instruments

Preliminary experiments to evaluate commercially available air monitoring equipment described below.

4.4.1 Sampling pump evaluation test

A technical study was undertaken to evaluate 4 commercially available sampling pumps for personal and peripatetic sampling (Table 4.3). This was prompted by the need to replace 6 sampling pumps lost from the Department of Civil and Environmental Engineering laboratory.

The four pumps tested were fully charged prior to field tests in an office in the James Weir Building, University of Strathclyde. Respirable (Higgins-Dewell) cyclones (Casella Ltd, Bedford, UK) were fitted with cassettes containing two types of filter; 25-mm glass fibre (GF/A) (Whatman) and 37-mm 2-µm pore size PTFE (Pall Ltd, Portsmouth, UK). The cyclone samplers were connected to the pumps using ¼ inch ID Tygon® tubing. Air was sampled through the cyclones and the flow calibrated using a rotameter. The pumps were run at different flow rates (1.50, 2.00 and 3.65 L min^{-1}) until their batteries were exhausted. The Casella pump run durations were logged by the pump and retrieved using the pump manager software provided by the manufacturer. The run times for the BGI pumps were manually recorded from the small display panel screen on the pump.

The BGI pump enabled sampling over a 48-hour period using GF/A filter at 2.0 L min^{-1} powered by an external USB battery pack. The Apex Pro pump provided the longest sampling duration at 1.5 L min^{-1} flow rate. The software in GilAir pump failed during the test, could not be completed properly.

Table 4.3: Summary of personal pump evaluation test.

Pump Model	Serial Number	Type of filter	Flow Rate (L min^{-1})	Volume Sampled (L)	Pump on duration (hh:mm:ss)
Apex Pro	3133073	25mm GF/A	1.5	5920.78	65:43:10
		25mm GF/A	2.0	4561.9	38:00:12
		37mm PTFE	1.5	5662.75	62:55:10
		37mm PTFE	1.5[1]	6457.52	71:45:01
		37mm PTFE	3.65	2719.98	12:25:12
Tuff 4 Pro	1011855	25mm G/FA	1.5	3863.12	40:58:36
		25mm G/FA	2.0	3565.97	29:42:20
BGI AFC 400S	None	25mm G/FA	2.0	5760	48:00:00
GilAir Plus	20110930050	37mm PTFE	1.5	Nil	<48:00:00

[1]repeat measurement on a different day.

In addition to relatively long internal battery life, the Casella Apex Pro pump (Figure 4.8) is relatively lightweight, simple to operate, and can provide intermittent sampling capability with external batteries (with minor electrical modification) for extended run times. However, this pump does also have drawbacks: we noticed that it did not always maintain higher flow-rates (> 3 L min^{-1}); it is noisy at higher flow rates; and it is not waterproof.

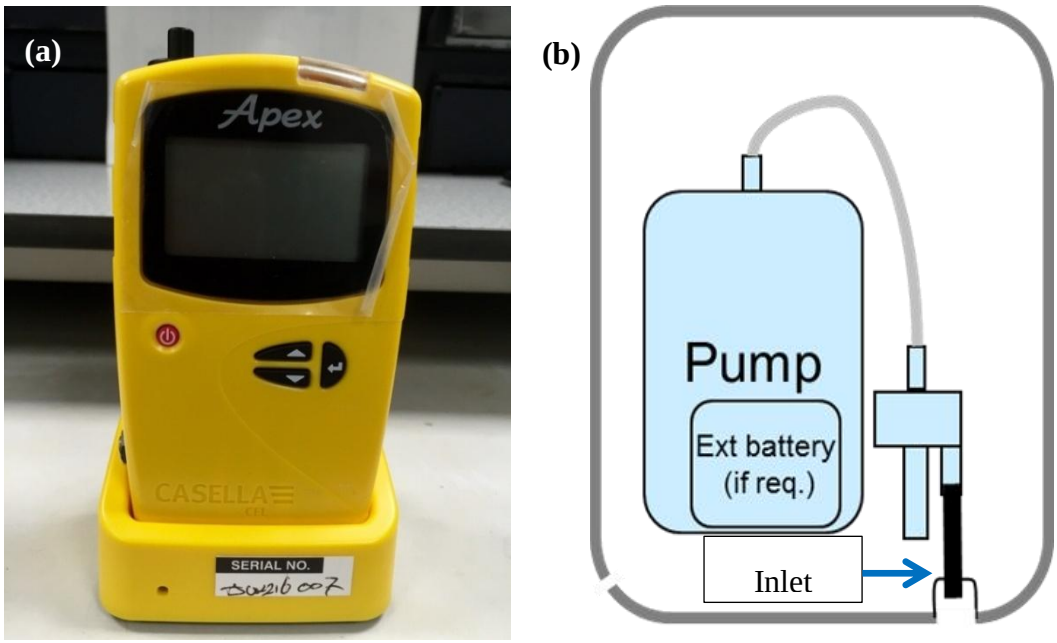

Figure 4.8: (a) Casella Apex Pro pump with charging dock. (b) Outdoor sampling configuration with pump in water-proof enclosure.

4.4.1.1 Evaluation of consistency of Casella Apex Pro pump flow rates

The resistance to air flow can become relatively high when small diameter filters are used in sampling. Therefore, it is important to calibrate and check pump flow rates to allow accurate estimates of the volume of air sampled through filter specimens for subsequent calculation of atmospheric concentrations (NIOSH, 1998). Tests were conducted to determine if the Casella Apex Pro pump could reliably maintain the low flow rates as the pressure drop increased across the filter during the course of sampling.

Four new Apex Pro pumps were used to sample air at a flow rate of 1.0 L min^{-1} through 25-mm diameter 2-µm pore size PTFE filters (Teflo, Gelman Sciences) fitted in a conductive plastic sampler of the Higgins-Dewell cyclone (Casella Ltd, Bedford, UK). The pumps were used to sample air from an office room in the Department of Civil and Environmental Engineering at the University of Strathclyde between 10-13 August 2015. Flow rates were measured using a piston displacement flowmeter (DryCal Defender 530, Mesa Labs, USA). Flow rate measurements were made 5 minutes after the pump started. The initial flow rate measurement was used

to calibrate and set the pump flow to 1.0 L min^{-1} using the procedure provided by the pump manufacturer. Subsequent flow measurements were made at the start, middle and end of 24-hour sampling periods. The same filter was used throughout to provide total run times of 24, 48, and 72 hour periods as the tests progressed

The average flow rate for all pumps fell below 1.0 L min^{-1} at the end of the first and second days of measurements (10 & 12 Aug 2015; Figure 4.9 & Table 4.4). Pump 4 had the most consistent flow rate over the three days of observations. In contrast, Pump 1 exhibited relatively large flow rate reductions on each sampling day (Figure 3.8). On 13 August 2015 the flow rates for Pumps 2, 3 and 4 decreased slightly during the middle of flow rate measurements and increased at the end of measurements.

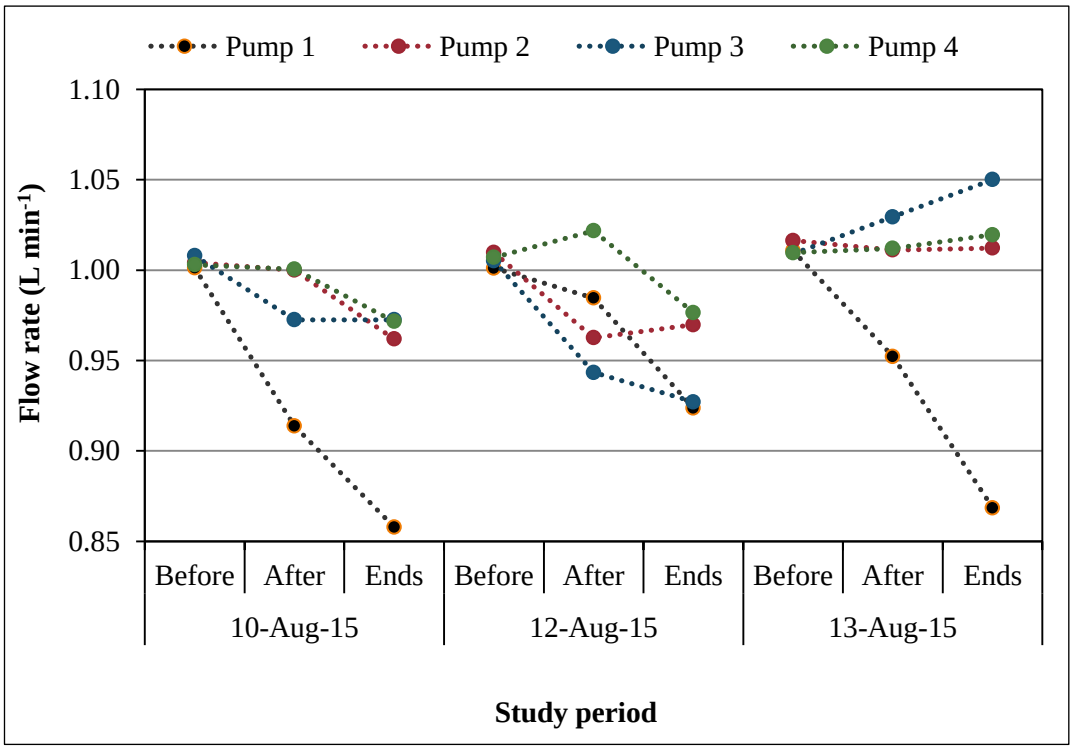

Figure 4.9: Measured flow rates (L min^{-1}) for 4 Casella Apex Pro personal air pumps over three 24-hour sampling periods.

Table 4.4: Measured flow rates (L min^{-1}) for four Casella Apex Pro personal air pumps over three 24-hour sampling periods.

Pump	**S/N**	**10-Aug-15**	**12-Aug-15**	**13-Aug-15**
		Mean ± SD	Mean ± SD	Mean ± SD
Pump 1	3541022	0.92 ± 0.07	0.97 ± 0.04	0.94 ± 0.07
Pump 2	3540918	0.99 ± 0.02	0.98 ± 0.03	1.01 ± 0.00
Pump 3	3541013	0.98 ± 0.02	0.96 ± 0.04	1.03 ± 0.02
Pump 4	3540907	0.99 ± 0.02	1.00 ± 0.02	1.01 ± 0.01

Although some of the pumps did not maintain specified airflow rates, the average flow rates remained within ± 5% of the value set. This test confirmed that it is important to measure flow rates in personal sampling pumps before and after sampling.

4.4.2 Selection of a cost-effective filter media

Following practice in other studies (ESCAPE, 2009, Rasmussen *et al.*, 2010, Koistinen *et al.*, 1999), PTFE filters were selected because of their non-hygroscopic, lower chemical reactivity and temperature resistance characteristics. However, PTFE filters are expensive compared to the other type of filters. The costs of 37-mm PTFE filters were compared from different UK suppliers (Table 4.5).

Table 4.5: Filter Costs: 37mm diameter 2 μm pore size PTFE filters (50 filter packs).

Supplier	Name of Product	Support Rings	Price (pack of 50)	Catalogue No.
Frontline Safety https://www.frontline-safety.co.uk/	Casella PTFE Filter	PTFE	£150.00 (Ex VAT)	P102088
VWR International Ltd (UK Distributor for Pall) https://uk.vwr.com/store/	Zefluor™ with support pads	PMP with support pads	£270.00	516-8902
Sigma-Aldrich http://www.sigmaaldrich.com/united-kingdom.html/	Gelman Zefluor filter membrane with pads	No information	£196.50	23390-U
SKC Ltd http://www.skcltd.com/	PTFE	PTFE with support pad	£139	225-27-07

4.4.3 Measurement precision - filter blanks

4.4.3.1 Filter reflectance

The reflectometer was used to make repeat measurements of the reflectance of 6 blank PTFE filters over 6 separate days. The filters were conditioned for 24 hours with part-opened petri dishes. The reflectometer was set up and calibrated against a standard plate (details in section 4.1.3.1 above). The blank filter were placed on the white tile of the standard plate and the reflectance reading taken after 30 seconds, or after a unchanging value was obtained. The measurement was taken at 5-spots on the filter (ESCAPE, 2002). Each filter was measured in duplicate and the mean and standard deviations were calculated. The reflectometer was recalibrated using the standard plate after every second blank filter was measured.

The average reflectance measurement of each blank filter was greater than 100 (Table 4.6). Other researchers have taken the alternative approach of adjusting the blank filter to 100 ± 2 prior to measuring the sample reflectance (Adams *et al.*, 2002, ESCAPE, 2002, Cyrys *et al.*, 2003). However, we chose not to reset the unloaded filter to a reflectance value of 100, but instead relied on the white tile to set the 100 value as the tile is much less likely than the filter to change in reflectance between measurement sessions.

Table 4.6: Summary of repeat reflectance measurements of 37-mm Teflon blank filters.

Blank Teflon 37mm	Mean ± SD	RSD (%)
1	102.1 ± 0.05	0.05
2	101.4 ± 0.10	0.10
3	102.3 ± 0.19	0.19
4	101.7 ± 0.07	0.07
5	102.1 ± 0.11	0.11
6	101.9 ± 0.11	0.11

The standard deviation for each blank filter (1-6) was lower than the allowed tolerance of ± 0.2 in the reflectance measurement's protocol (ESCAPE, 2002). The mean SD of day-to-day change in reflectance for all blank filters was 0.1 and the corresponding LoD was 0.3.

The reflectometer measuring head was positioned over 5 different areas of the filter. This procedure is likely to introduce random variation during repeat reflectance measurements. Early research in Finland (Penttinen *et al.*, 2000) measured the reflectance of one-half of folded 42.5 mm diameters Whatman 1 on the centre point to reduce measurement errors associated with positioning of the reflectometer mask.

Consistent, placement of the reflectometer head between different measurement sessions is important to improve precision. A more systematic approach using a cardboard filter holder was developed from this repeat measurement exercise and applied in the case study (section 4.5.1). Loss and/or contamination of particles deposited on the filter media may also occur. To deal with these latter problems Kinney *et al.* (2002) developed a custom filter holder to avoid the reflectometer mask coming into contact with the deposited particles on the filter.

4.4.3.2 Filter mass

The precision of 37-mm PTFE filter weighing was assessed in four separate weighing sessions in the Analytical Laboratory. The laboratory was air conditioned to maintain a constant temperature. Relative humidity was not controlled by the air conditioning system. Details of the weighing procedure are described in Section 4.1.3.5. The limit of detection (LoD) of the weighing system was calculated using the method of Vaughan *et* al., (1989) as follows:

$$LoD = 3 \times \overline{(n+1)/n} \times SD\ (day\ to\ day\ change\ in\ \boldsymbol{n}\ blank\ filters) \quad \textbf{(4.7)}$$

where:

LoD = limit of detection

n = number of filter

Table 4.7: Summary of weighing precision measurements using 37mm blank Zeflour filters.

Weighing Month (2014)	Number of filters used	No of weighing days	SD (μg)	LoD (μg)	RSD (%)
January	6	2	1.7	5.6	0.001
February	2	6	2.0	8.0	0.001
April	6	6	2.3	7.0	0.015
August	6	6	3.0	9.0	0.002

The weighing precision data were compared with Tsai *et al.* (2002) measurements of 47-mm Teflon filters under uncontrolled environment and without the charge of electrostatic eliminators. Stacey *et al.* (2002) compared mass measurement of 25 mm filters to investigate repeatability and reproducibility from different laboratory. Their reported SD was from 0.022 to 0.069 mg.

4.4.3.3 Temperature and relative humidity in weighing room

Factors that may affect filter weighing measurements include temperature, relative humidity and the buoyancy effects. Average temperature and relative humidity were recorded during the weighing experiments (Figure 4.10). Temperature varied between 20°C and 23°C, with a pronounced drop on 3 February 2014. Relative humidity varied between 24% and 57.8%.

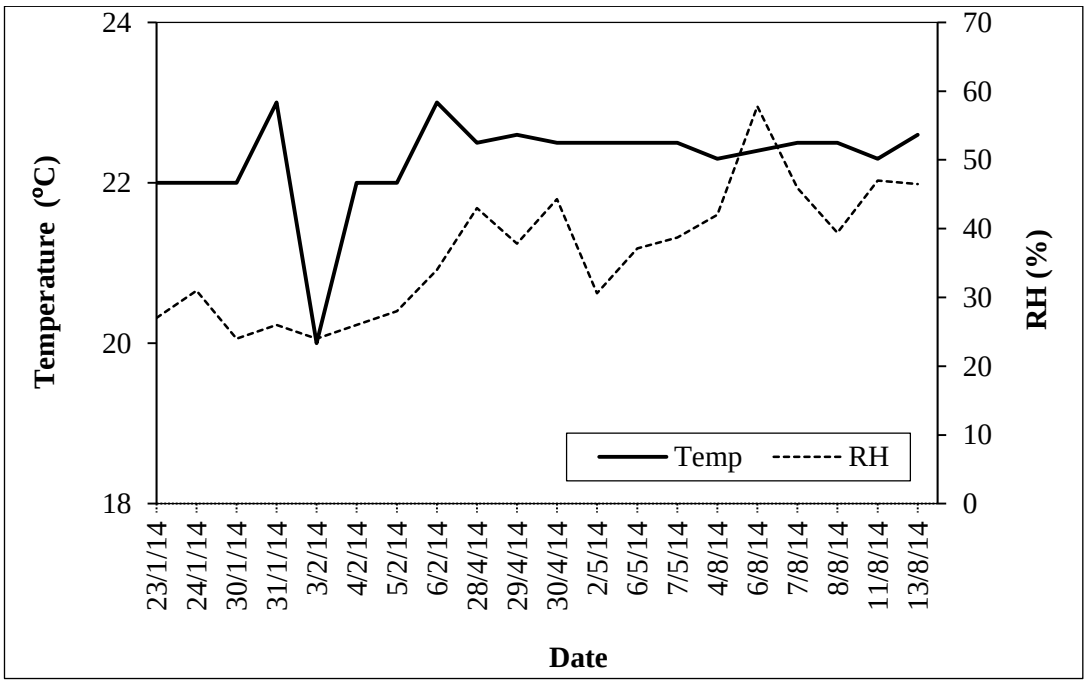

Figure 4.10: Temperature (ºC) and relative humidity (%) recorded between January and August 2014.

It is important to ensure that the RH in the weighing room is kept below 65% to minimise the variation of filter and particle masses through hygroscopic growth (Koistinen *et al.*, 1999). This was achieved in the above measurements. Kuo *et al.* (2015) has highlighted the importance of wearing gloves to avoid the moisture from the bare hands influencing the RH during the filter weighing analysis.

4.4.4 MicroAeth BC

BC concentrations were measured by two AE51 micro-aethalometers (MicroAeth 1303 and MicroAeth 1204) operated side-by-side in the Analytical Laboratory between 1 and 16 April 2014. The flow rate was set at 50 ml min^{-1} and measurements logged at 5-minute time intervals for both instruments. The filter strips were changed for both sensors prior to starting the sampling session. The final changes in attenuation (Δ ATN) for both instruments were below the suggested upper limit of 75 units (Virkkula *et al.*, 2007). All data were downloaded and post-processed as described in Section 4.1.4.1.

The two micro-aethalometers units provided very similar measurements of the temporal pattern of BC concentrations (Figure 4.11(a)). MicroAeth 1303 fell to zero between 13:30 to 14:30 on 13 April 2014 (red box). However, this was the only artefact noticed during the measurements. MicroAeth 1303 and 1204 measurements were highly correlated (R^2 = 0.99; Figure 4.11(b)). This test demonstrated excellent agreement between the micro-aethalometer units at relatively low BC concentrations.

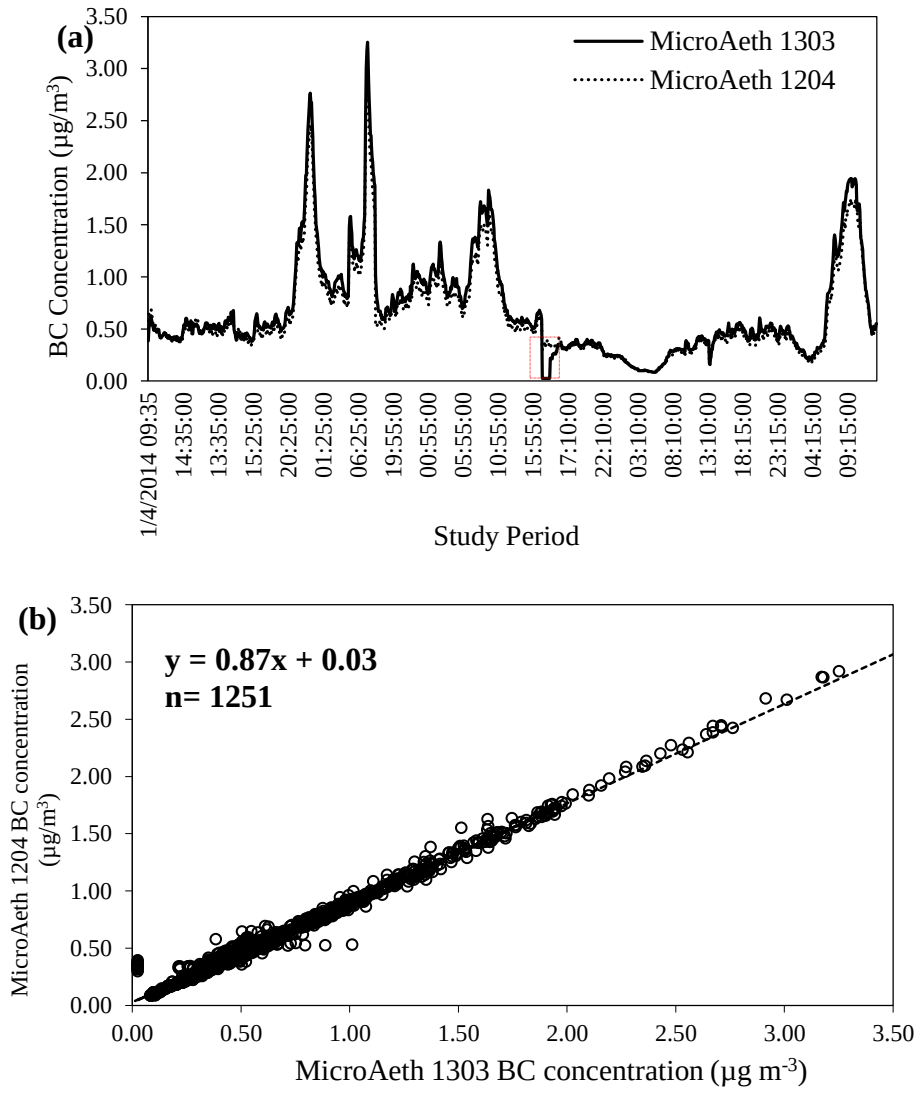

Figure 4.11(a). Time series (5-minute time resolution) of two AE51 micro-aethalometers deployed side-by-side during April 2014. Red box shows where a minor discrepancy occurred. (b). BC concentrations (µg/m^3) measured by MicroAeth 1303 and MicroAeth 1204.

4.4.5 Osiris PM measurements

Three OSIRIS units (2226, 2224, and 2205) were deployed side-by-side in an office (level 5, James Weir Building, University of Strathclyde) between 4-5 August 2014. The instruments were set up as described in Section 4.1.4.2 and were operated from mains power. Osiris 2226 was used as a reference for both Osiris 2224 and 2205 and data recorded as 1-minute averages (Figure 4.12). Both instrument pairs (2224 *vs.* 2226) and (2205 *vs.* 2226) had highly correlated PM_1, $PM_{2.5}$ and PM_{10} concentrations, with correlations for the latter pair being slightly higher than the former. Osiris 2205 stopped logging data during the experiment for unknown reasons resulting in the different numbers and ranges of data in the graphs below.

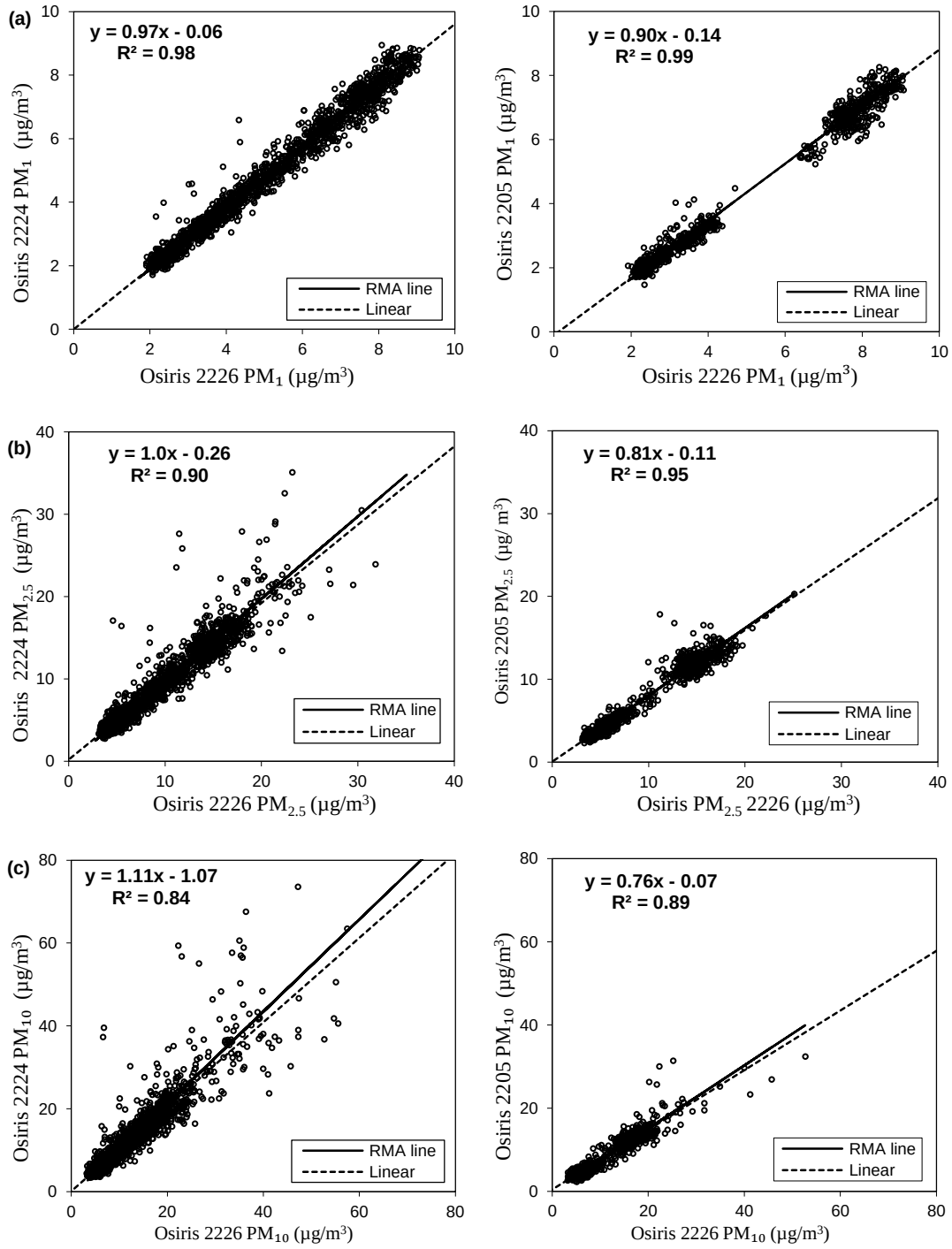

Figure 4.12: Comparisons between OSIRIS 2226 vs. 2224 and 2226 vs. 2205 monitors using RMA lines: (a) PM_1 concentrations; (b) $PM_{2.5}$ concentrations; (c) PM_{10} concentrations.

4.4.6 PAH analysis

An archived sample of an unknown mass concentration and one blank 37-mm Teflon filter were extracted using the ASE 350 system following extraction, cleaning and concentration methods described in Section 4.1.5.1. The extract was stored in GC vials at -80 ℃ in the freezer. 0.5 µL of extract solution was injected into the GC. The GC-MS system was programmed in splitless mode condition described in Section 4.1.5.2 to analyse BaP concentrations.

The BaP profile was highlighted from 16 pPAHs profiles detected from the GC-MS system (Figure 4.13). Most of the 16 compounds were lower than blank concentrations. The sample limits of detection (LoD) was 0.021 ng/sample and the LoD estimated from blanks was 0.013 ng m³. BaP was not detected. It was concluded that the sampled particle masses were too low for this configuration of GC-MS analysis

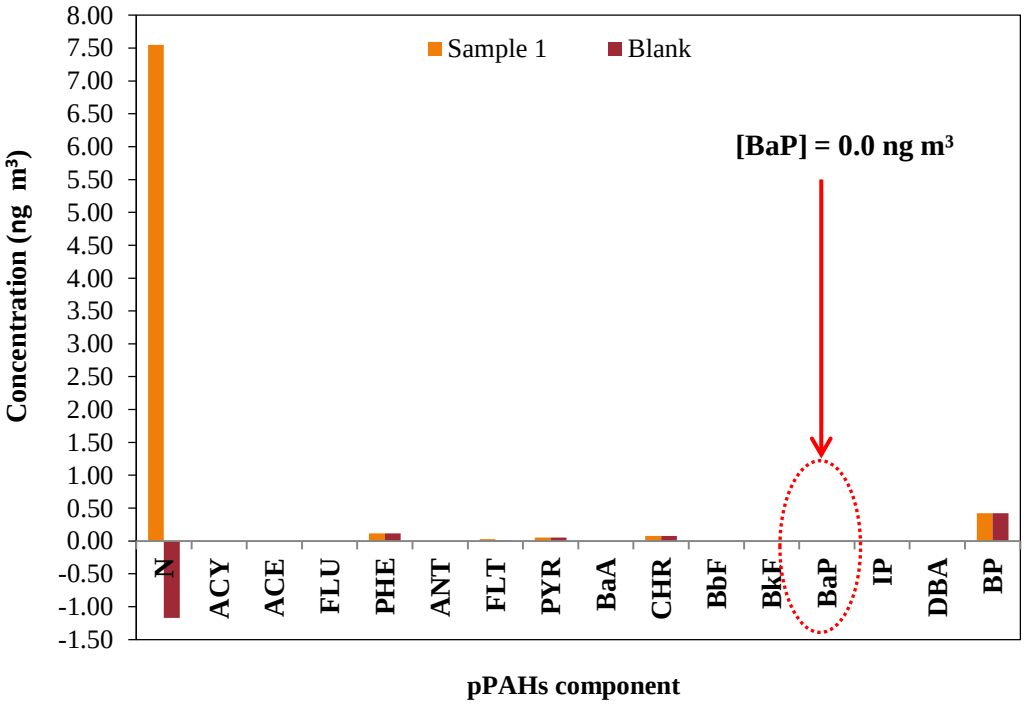

Figure 4.13: Concentrations of pPAHs detected by the GC-MS system. The 'red arrow' indicates BaP analysis.

The pre-treatment steps for GC-MS analysis were found to be time consuming and expensive. For a meaningful result, it would be necessary to test the method with simplified techniques and reduce the number of steps in the analysis to minimise uncertainties in the experimental data (Albinet *et al.*, 2014).

4.4.7 Pilot test: NO_2 measurements

4.4.7.1 Initial NO_2 analysis using calibration tubes

Six calibration tubes were prepared as described in Section 4.2.1. Mean absorbance was quantified from duplicate absorbance measurements using a UV-Visible spectrophotometer (Thermo Fisher Scientific Inc.) (Table 4.8).

Table 4.8: Mean absorbance values for calibration tubes.

Calibration Tube	Abs1[1]	Abs2[2]	Mean (ng/cm^3)
1	0.027	0.027	0.027
2	0.084	0.091	0.088
3	0.142	0.146	0.144
4	0.204	0.215	0.210
5	0.259	0.267	0.263

[1]absorbance value 1. [2]absorbance value 2.

A five-point calibration graph was constructed using the mean absorbance of duplicate tubes against for calibration solutions with different masses of nitrite (NO_2^-); 0, 375, 750, 1125 and 1500 ng (Figure 3.14).

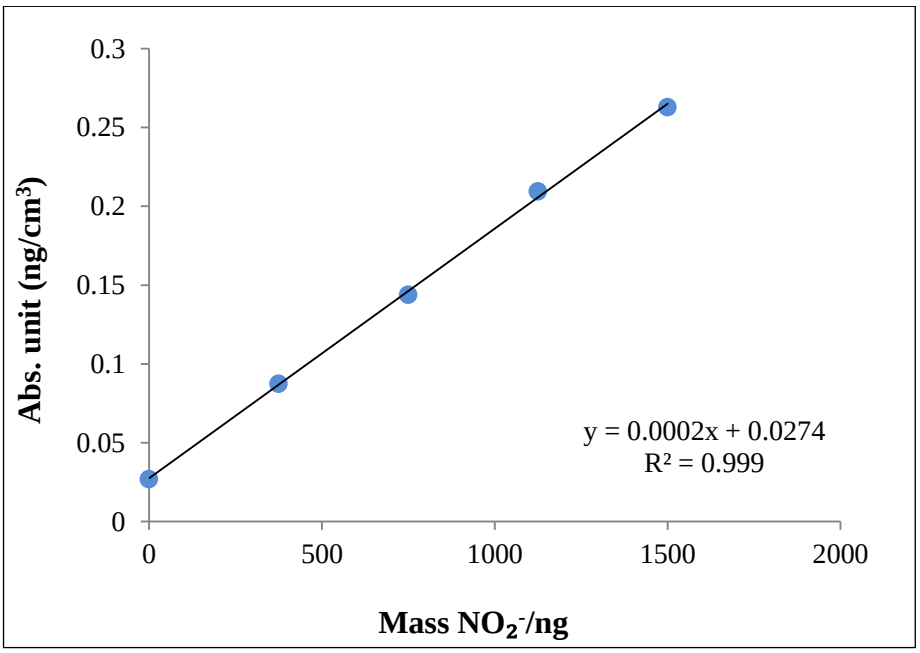

Figure 4.14: Example of calibration graph obtained from absorbance values from calibration tubes during August 2014 experiment.

This calibration data demonstrates a clear linear relationship between the mass of NO_2^- and absorbance values measured by the UV-Vis spectrophotometer (R^2 = 0.999). The NO_2^- mass in each tube sample (Q) was estimated from the calibration equation derived above. This mass estimate was then used in Equation 3.3 to estimate NO_2 concentrations in field samples.

4.4.7.2 An in-comparison of Aeroqual NO_2

Two NO_2 sensors (Aeroqual 1 and 2) and O_3 sensors (Aeroqual 3 and 4) were deployed side-by-side on the rooftop at the Townhead Automatic Analyser site between 31 March 2016 and 4 April 2016. This was part of a series of monthly NO_2 calibrations used to compare NO_2 sensor output against the chemiluminescence NO_2 analyser (further details in section 5.2). The instruments were set to log data at 1-min intervals and operated on mains power during the sampling period. Instruments were placed inside waterproof boxes with fan-assisted ventilation. Data were downloaded using Aeroqual software (Section 4.2.2).

Figure 4.15 (a) shows the NO_2 concentrations measured by both Aeroquals in 1-minute time resolutions. The pattern of NO_2 measurements exchange minute-by-minute individually was clearly identified the event of Aeroqual 1 and 2. Over the whole time period, the two Aeroqual units showed a relative difference in the NO_2 measurements with a similar trend coinciding against each other. The observed NO_2 concentrations from Aeroqual 2 were higher than Aeroqual 1, with average concentration of 96.2 $\mu g/m^3$ (Aeroqual 2) and 19.3 $\mu g/m^3$ (Aeroqual 1).

The general trend in NO_2 observed by both Aeroquals was due to the location of monitoring site, which influenced by meteorology and pollutant sources. NO_2 concentrations observed by Aeroqual 1 and 2 were moderately correlated (R^2= 0.66; Figure 4.15 (b)). NO_2 concentrations measured by the Aeroqual 1 showing constant '0' value in between 11:09 to 11:39 on 31 March 2016. A similar observation was noted for the Aeroqual 2 during the same day of measurements (between 11:11 to 11:18).

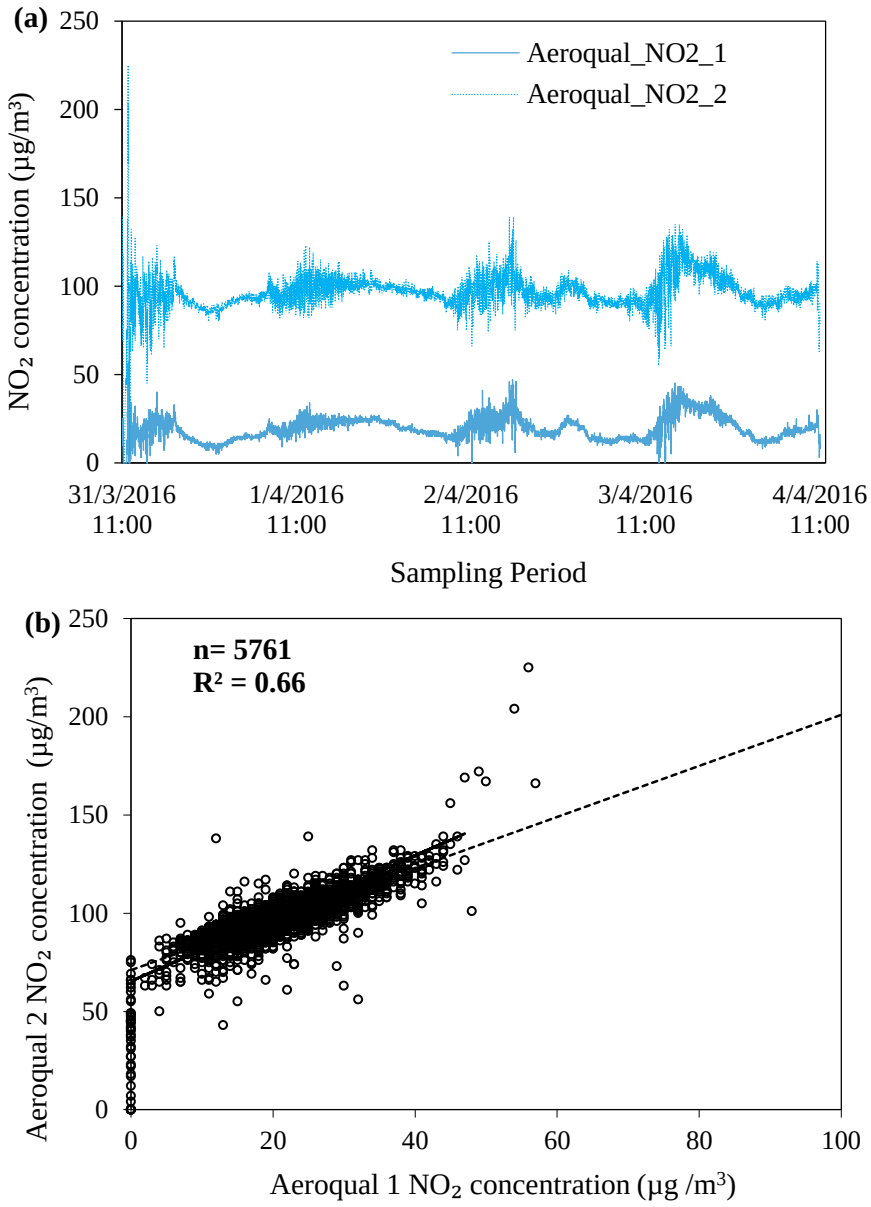

Figure 4.15: (a) Time-series of uncorrected NO_2 concentrations measured by Aeroqual 1 and Aeroqual 2. (b). Scatter plot of NO_2 measurements by Aeroqual 1 and 2 in 1-minute intervals under RMA line.

4.5 Estimation of exposure to BC: A pilot experiment

This pilot study used simple methods for non-destructive and low-cost optical analysis of sequentially loaded filter air samples collected in two separate studies, to

illustrate how black carbon (BC) can be estimated from filter reflectance and digital imaging calibrated against co-located micro-aethalometer observations.

4.5.1 Reflectometer versus AE51 Aethalometer

A preliminary laboratory experiment was conducted to investigate the suitability of flow rates and filter sizes to estimate black carbon exposure using personal air sampling pumps. Duplicate Apex Pro pumps with respirable cyclone inlets and real-time AE51 Aethalometer were used to estimate BC concentrations from filter specimens collected in the Analytical Laboratory. Different filters and flow rates were used to collect filter samples (Table 4.9).

Table 4.9: Summary of filters and flow rates used during pilot experiment.

Filter media:	Flow rate (L min^{-1})	Cyclone:
25 mm Teflon	1.0	Higgins-Dewell
37 mm Teflon	1.5	BGI triplex
37 mm Teflon	2.2	Higgins-Dewell

The sampling equipment was placed in a fibreglass enclosure with inlet tubes attached to a laboratory stand located 1.5 m above floor height (Figure 4.16). The duration of exposure was incremented during this experiment to allow particles to accumulate on filter samples (using a similar approach to Ramanathan *et al.* (2011)). Darkness measurements were made on duplicate air specimens collected at 6, 12, 24, 48 and 96 hour intervals.

Flow rates were recorded with a piston-displacement flow meter (Defender 530, MesaLabs, USA) at the beginning and end of each sampling period. Two AE51 Aethalometer were used to measure black carbon concentrations every 5 minutes at flow rate of 50 ml min^{-1}. Pumps and AE51 Aethalometer were operated over identical time periods and sampling durations were accurately measured.

Incremental changes in optical reflectance were measured (using procedure described in Section 4.1.3.1.) on sequentially loaded filters using a smoke stain reflectometer and compared to accumulated BC mass estimated from the co-located micro-aethalometer measurements. The unloaded filter darkness measurement (R_o) was divided by the loaded filter reflectance measurement (R) to provide a normalised metric of darkening that took into account the original optical characteristics of the filter:

$$Filter\ Loading = \ln \frac{R_o}{R} \quad \textbf{(4.8)}$$

where:

Ro = the reflectance measurement from unloaded filter sample

R = the reflectance measurement from loaded filter sample

AE51 Aethalometer BC data were processed using the Optimised Noise-Reduction Algorithm (ONA) with ΔATN = 0.01 from the Aethlabs website and corrected for 'shadowing' effects using the equation suggested by Apte et al. (2011). These data-processing methods are described in Section 4.1.4.1.

The BC concentration data were used to calculate the BC loading (BC surface density):

$$BC\ loading\ [\mu g/cm^2] = \frac{BC\ \ AE51\ Aethalometer\ [\mu g/m^3] = \times V\ [m^3]}{A\ [cm^2]} \quad \textbf{(4.9)}$$

where:

[BC] (µg/m^3) = BC concentrations corrected by methods published by Apte *et al.* (2011) and Hagler *et al.* (2011b)

V (m^3) = the volume sampled (flow rate (m^3 min^{-1}) x sampling duration (min)

A (cm^2) = the area of the stain on the filter, (25-mm filter = 2.4 cm^2 and 37-mm filter = 7.8 cm^2)

This normalised metric of darkening was plotted against BC loading and data fitted with a quadratic function to allow for the curvature introduced by 'shadowing' effects on the filters (Presser *et al.*, 2014) as particle loading increased.

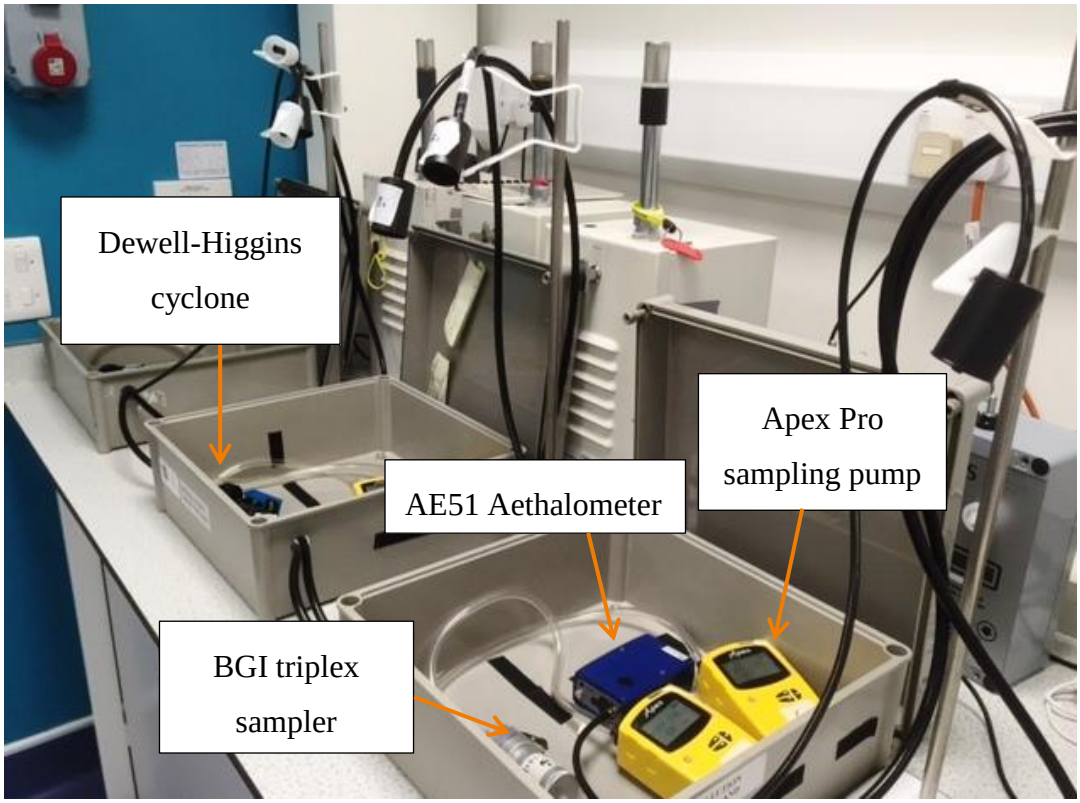

Figure 4.16: Co-located personal sampling pumps and microaethalometers in the Analytical Laboratory.

4.5.1.1 Results and discussion

All filter reflectance values for unloaded filters (R_0) exceeded the darkness metric of 100% set from the white section of the standard tile provided by reflectometer manufacturer (average R_0 = 102.2% (SD = 0.1) and 100.6% (SD = 0.1) for 37-mm and 25-mm filter size respectively (Table 4.10). The average reflectance ranged from 101.8 (unloaded filter) to 75.1% at different flow rates at 6 to 96 hours monitoring duration. Average filter darkness changes measured at a flow rate of 1.0 L min^{-1} were 0.9 & 1.8% over 6 & 24-hour sampling durations respectively.

Filter reflectance increased with BC loading (Figure 4.17). Duplicate measurements made at flow rate of 1.0 L min^{-1} and 1.5 L min^{-1} were comparable, where the data points from duplicate measurements were agreed to each other. This contrasted with sampling at 2.2 L min^{-1}, where data points were diverged from the duplicate measurements. Figure 4.17 (d) shows the data points from all measurements were combined to compare the relationship between filter reflectance and BC loading at different flow rates.

Reflectance measurements on incrementally loaded filters showed clear positive relationships with BC loading estimated by AE51 Aethalometer measurements across all sampling conditions, however there was considerable divergence between different replicates and different flow rates (Figure 4.18). Filter reflectance values changed more markedly at higher flow rates. This is related to the face velocities resulting from the combination of air flow rate and exposed filter area (McDade *et al.*, 2009). The face velocities for 25-mm diameter filters at flow rates of 1.0, 1.5 and 2.2 L min^{-1} were 3.5, 2.3 and 7.5 cm s^{-1} respectively.

Use of a 1.5 L min^{-1} sampling flow rate with the BGI Triplex cyclone allows direct $PM_{2.5}$ sampling. However, problems with leaking filter cassettes and uneven deposition patterns have been reported with this cyclone. Baron *et al.* (2002) reported that the filter cassettes must assembled in a way that avoids leakage (through insufficient tightening) and filter damage (through over-tightening). The

correct degree of tightening can be achieved using a specialised filter cassette press to avoid potential (investigator specific) problems associated with hand-assembled cassettes; however such devices may be prohibitively expensive for the average research laboratory. Yan *et al.* (2011) reported problems with uneven particle distribution on filters when the fitting tube was pressed too far into the filter cassette.

Pumps did not always reliably maintain higher flow rates. The effects of this can be seen from the divergent data points from duplicate filter samples during measurement at 2.2 L min^{-1} (Figure 4.17 (c)). In contrast, it was clear from the charts that the two filter samples collected on 25-mm filters at 1.0 L min^{-1} showed good consistency with each other. Use of a respirable cyclone at 1.0 L min^{-1} approximates PM_{10} sampling.

Table 4.10: Reflectance measurements of incrementally loaded filter samples at different flow rates and PTFE filter sizes (25-mm & 37-mm).

Date of Sampling	Duration (hour)	1.0 LPM (25-mm)				1.5 LPM (37-mm)				2.2 LPM (25-mm)			
		Mean[1] A	± SD[1]	Mean B	± SD	Mean A	± SD	Mean B	± SD	Mean A	± SD	Mean B	± SD
31st March 2015 (unloaded)	0	100.7	± 0.2	101.0	± 0.1	100.7	± 0.4	100.9	± 0.5	101.0	± 0.1	101.8	± 0.1
1st Apr 2015	6	99.8	± 0.1	100.1	± 0.1	100.5	± 0.3	100.5	± 0.3	99.5	± 0.3	100.3	± 0.1
7th Apr 2015	12	99.0	± 0.1	99.1	± 0.0	100.3	± 0.2	100.2	± 0.2	97.8	± 0.1	97.3	± 0.0
8 - 9th Apr 2015	24	96.3	± 0.0	96.4	± 0.1	100.2	± 0.2	99.9	± 0.2	94.5	± 0.1	90.6	± 0.1
9 - 10th Apr 2015	48	93.8	± 0.1	93.8	± 0.1	100.1	± 0.3	99.7	± 0.3	89.4	± 0.0	80.6	± 0.1
13 - 14th Apr 2015	72	92.0	± 0.2	91.7	± 0.1	100.1	± 0.2	99.7	± 0.4	88.4	± 0.1	78.0	± 0.1
15 - 16th Apr 2015	96	90.9	± 0.1	91.1	± 0.2	100.0	± 0.2	99.7	± 0.3	85.8	± 0.0	75.1	± 0.0

[1]The mean and standard deviation (SD) of duplicate filter samples (A & B) were calculated from repeated measurement of filter reflectance.

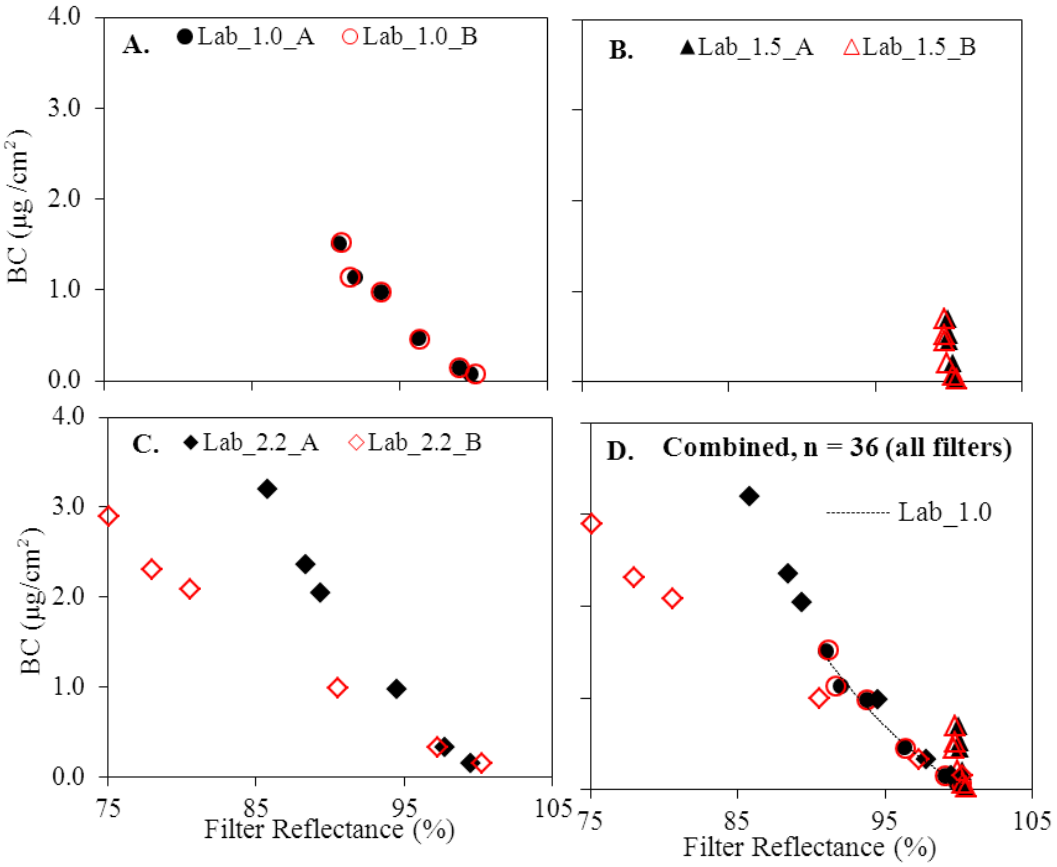

Figure 4.17: (a) – (d) Comparison between filter reflectance (%) and BC loading (µg cm^{-2}) at different flow rates.

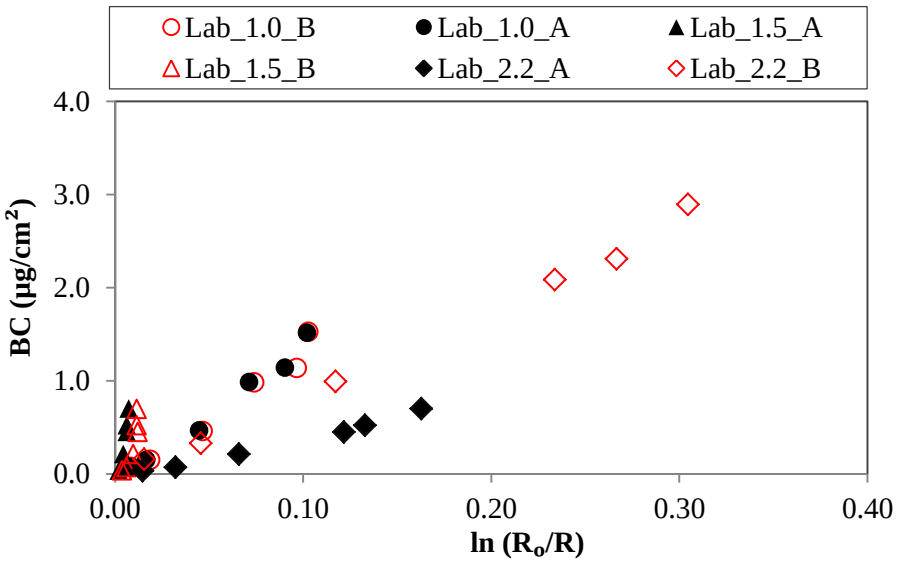

Figure 4.18: Comparison between sequential filter loading and BC loading (BC surface density) (µg/cm^2) measured at different flow rates.

4.5.2 Office scanner versus AE51 Aethalometer

An alternative approach is to measure the filter darkness using digital imaging methods. The use of flat-bed scanners to estimate BC concentrations has been applied in several studies (Cheng *et al.*, 2011, Forder, 2014, Lalchandani *et al.*, 2016). An office scanner was used to quantify the red values from the images of particles deposited on filters (Section 4.1.3.3). The red values scanned from the filter image were used to describe the incremental change of loading BC particles using equation below:

$$Filter\ Loading\ Scanner = \frac{S_\circ}{S} \qquad \textbf{(4.10)}$$

where,

S_0 = red value from unloaded filter

S = red value from loaded filter sample

The results of these additional analyses are described in detail in section 5.1.1.

4.6 Summary

This chapter describes developments of sampling and analysis methods ranging from the relative simplicity of colour analysis for particle darkness, through portable real time monitors, to complex GC-MS analysis of pPAH constituents. Similarly, for gases, the chapter describes methods for determination of NO_2 and O_3 concentrations involving both passive samplers and real-time sensors.

A common focus relates to the field evaluation of portable low power systems against reference methods. The preliminary experiments described here helped to identify suitable sampling pumps for stationary and peripatetic sampling methods to replace six units of pumps lost from Department of Civil and Environmental

Engineering laboratories. A follow-up evaluation of flow rate consistency identified reliability and practical advantages of operating these pumps at lower flow rates (1.0 – 2.0 L min^{-1}), including how different sampling inlets and filter media influence the finite run time of the internal system batteries.

The preliminary evaluation of real-time monitoring systems provided reassurance that the systems were suitable for the more extensive fieldwork described later in this thesis. Post processing steps for real-time BC and NO_2 measurements were examined. Calibration and inter-comparison of the instruments allowed a number of measurement problems to be overcome sufficiently to give useful additional measurement capacity. The preliminary research on sequentially loaded filter samples collected under different sampling conditions has provided practical information on flow rates and filter type/size that are useful for this type of measurement.

Samples collected in different microenvironments were used to construct calibration curves for reflectance measurements and digital scanned images; which in turn has considerable potential to provide a simple and low cost method that can be used to estimate exposures to combustion-related air pollutants. Methods for increasing the precision of reflectance and scanned image analysis were discussed, with systematic approaches using blank filters and calibration tiles to reduce the effects of instrument signal drift. The use of portable low power instruments have considerable potential to improve characterisation of personal exposure to PM, BC and NO_2 in microenvironments affected by combustion-related air pollutants. Further field evaluation of these type of measurement system were discussed in the next chapter.

4.7 References

Adams, H. S., Nieuwenhuijsen, M. J., Colvile, R. N., Older, M. J. & Kendall, M. 2002. Assessment of road users' elemental carbon personal exposure levels, London, UK. *Atmospheric Environment,* 36**,** 5335-5342.

Albinet, A., Nalin, F., Tomaz, S., Beaumont, J. & Lestremau, F. 2014. A simple QuEChERS-like extraction approach for molecular chemical characterization of organic aerosols: application to nitrated and oxygenated PAH derivatives (NPAH and OPAH) quantified by GC–NICIMS. *Analytical and Bioanalytical Chemistry,* 406**,** 3131-3148.

Apte, J. S., Kirchstetter, T. W., Reich, A. H., Deshpande, S. J., Kaushik, G., Chel, A., Marshall, J. D. & Nazaroff, W. W. 2011. Concentrations of fine, ultrafine, and black carbon particles in auto-rickshaws in New Delhi, India. *Atmospheric Environment,* 45**,** 4470-4480.

Baron, P. A., Khanina, A., Martinez, A. B. & Grinshpun, S. A. 2002. Investigation of Filter Bypass Leakage and a Test for Aerosol Sampling Cassettes. *Aerosol Science and Technology,* 36**,** 857-865.

Brown, A. S., Yardley, R. E., Quincey, P. G. & Butterfield, D. M. 2006. Studies of the effect of humidity and other factors on some different filter materials used for gravimetric measurements of ambient particulate matter. *Atmospheric Environment,* 40**,** 4670-4678.

Cheng, J. Y. W., Chan, C. K. & Lau, A. P. S. 2011. Quantification of Airborne Elemental Carbon by Digital Imaging. *Aerosol Science and Technology,* 45**,** 581-586.

Cyrys, J., Heinrich, J., Hoek, G., Meliefste, K., Lewne, M., Gehring, U., Bellander, T., Fischer, P., van Vliet, P., Brauer, M., Wichmann, H. E. & Brunekreef, B. 2003. Comparison between different traffic-related particle indicators: elemental carbon (EC), $PM_{2.5}$ mass, and absorbance. *J Expo Anal Environ Epidemiol,* 13**,** 134-43.

DEFRA 2008. Diffusion Tubes for Ambient NO_2 Monitoring: Practical Guidance for Laboratories and User.

ESCAPE 2002. Determination of Absorption Coefficient using Reflectometric Method.

ESCAPE 2009. Standard Operating Procedure- Weighing of Teflon Filters to determine particle mass concentrations

Forder, J. A. 2014. Simply scan--optical methods for elemental carbon measurement in diesel exhaust particulate. *Ann Occup Hyg,* 58**,** 889-98.

Gulliver, J. & Briggs, D. J. 2004. Personal exposure to particulate air pollution in transport microenvironments. *Atmospheric Environment,* 38**,** 1-8.

Hagler, G. S. W., Yelverton, T. L. B., Vedantham, R., Hansen, A. D. A. & Turner, J. R. 2011a. Post-processing Method to Reduce Noise while Preserving High Time Resolution in Aethalometer Real-time Black Carbon Data *Aerosol and Air Quality Research,* 11**,** 546.

Hagler, G. S. W., Yelverton, T. L. B., Vedantham, R., Hansen, A. D. A. & Turner, J. R. 2011b. Post-processing Method to Reduce Noise while Preserving High Time Resolution in Aethalometer Real-time Black Carbon Data. *Aerosol Air Qual Res,* 11**,** 539–54.

Hammond, M. 2012. *Characterisation of carbonaceous particulate matter in Edinburgh.* PhD.

Heal, M. R. 2013. *RE: Protocol for Preparation and Analysis of Palmes-NO_2 Passive Diffusion Tubes.*

Heal, M. R., O'Donoghue, M. A., Agius, R. M. & Beverland, I. J. 1999. Application of passive diffusion tubes to short-term indoor and personal exposure measurement of NO_2. *Environment International,* 25**,** 3-8.

HSE. 2000. *MDHS 14/3 General methods for sampling and gravimetric analysis of respirable and inhalable dust* [Online]. Available: https://www.vent-tech.co.uk/sites/vent-tech.co.uk/files/user/mdhs_14-3_general_methods_for_sampling_and_gravimetric_analysis_of_respirable_and_inhalable_dust.pdf [Accessed 10 January 2014].

HSE. 2014. *MHDS 14/4 General methods for sampling and gravimetric analysis of respirable, thoracic and inhalable aerosols* [Online]. Available: http://www.hse.gov.uk/pubns/mdhs/pdfs/mdhs14-4.pdf [Accessed 10 July 2014].

ISO 1993. Ambient Air-Determination of A Black Smoke Index. International Organization for Standardization.

Jiménez, A. S., Heal, M. R. & Beverland, I. J. 2011. Intercomparison study of NO_x passive diffusion tubes with chemiluminescence analysers and evaluation of bias factors. *Atmospheric Environment,* 45**,** 3062-3068.

Kinney, P. L., Chillrud, S. N., Ramstrom, S., Ross, J. & Spengler, J. D. 2002. Exposures to multiple air toxics in New York City. *Environmental Health Perspectives,* 110**,** 539-546.

Koehler, K. A. & Peters, T. M. 2015. New Methods for Personal Exposure Monitoring for Airborne Particles. *Curr Environ Health Rep,* 2**,** 399-411.

Koistinen, K. J., Kousa, A., Tenhola, V., Hanninen, O., Jantunen, M. J., Oglesby, L., Kuenzli, N. & Georgoulis, L. 1999. Fine particle ($PM_{2.5}$) measurement methodology, quality assurance procedures, and pilot results of the EXPOLIS study. *J Air Waste Manag Assoc,* 49**,** 1212-20.

Kulkarni, P., Baron, P. A. & Willeke, K. 2011. Introduction to Aerosol Characterization. *Aerosol Measurement.* John Wiley & Sons, Inc.

Kuo, Y.-M., Hsu, C.-W., Chen, J.-Y., Huang, S.-H., Lee, L.-H. & Chen, C.-C. 2015. Development of a Reliable and Cost-Effective Weighing Chamber for Aerosol Sample Analyses. *Aerosol and Air Quality Research,* 15**,** 749–758.

Lalchandani, V., Tripathi, S. N., Graham, E. A., Ramanathan, N., Schauer, J. J. & Gupta, T. 2016. Recommendations for calibration factors for a photo-reference method for aerosol black carbon concentrations. *Atmospheric Pollution Research,* 7**,** 75-81.

Lin, C., Gillespie, J., Schuder, M. D., Duberstein, W., Beverland, I. J. & Heal, M. R. 2015. Evaluation and calibration of Aeroqual series 500 portable gas sensors

for accurate measurement of ambient ozone and nitrogen dioxide. *Atmospheric Environment,* 100**,** 111-116.

McDade, C. E., Dillner, A. M. & Indresand, H. 2009. Particulate Matter Sample Deposit Geometry and Effective Filter Face Velocities. *Journal of the Air & Waste Management Association,* 59**,** 1045-1048.

Nash, D. G. & Leith, D. 2010. Use of Passive Diffusion Tubes to Monitor Air Pollutants. *Journal of the Air & Waste Management Association,* 60**,** 204-209.

NIOSH. 1998. *General considerations for sampling airborne airborne contaminants* [Online]. Available: http://www.cdc.gov/NIOSH/DOCS/2003-154/pdfs/chapter-d.pdf [Accessed 12 April 2014].

Penttinen, P., Alm, S., Ruuskanen, J. & Pekkanen, J. 2000. Measuring reflectance of TSP-filters for retrospective health studies. *Atmospheric Environment,* 34**,** 2581-2586.

Presser, C., Conny, J. M. & Nazarian, A. 2014. Filter Material Effects on Particle Absorption Optical Properties. *Aerosol Science and Technology,* 48**,** 515-529.

Ramanathan, N., Lukac, M., Ahmed, T., Kar, A., Praveen, P. S., Honles, T., Leong, I., Rehman, I. H., Schauer, J. J. & Ramanathan, V. 2011. A cellphone based system for large-scale monitoring of black carbon. *Atmospheric Environment,* 45**,** 4481-4487.

Rasmussen, P. E., Gardner, H. D. & Niu, J. 2010. Buoyancy-corrected gravimetric analysis of lightly loaded filters. *J Air Waste Manag Assoc,* 60**,** 1065-77.

Stacey, P., Revell, G. & Tylee, B. 2002. Accuracy and Repeatability of Weighing for Occupational Hygiene Measurements: Results from an Inter-laboratory Comparison. *Annals of Occupational Hygiene,* 46**,** 693-699.

Tadsanaprasittipol, A. 2016. *Development of Analytical Methods for Particulate-bound Polycyclic Aromatic Hydrocarbons (PAHs) in Thailand.* PhD, University of Strathclyde.

Tasić, V., Jovašević-Stojanović, M., Vardoulakis, S., Milošević, N., Kovačević, R. & Petrović, J. 2012. Comparative assessment of a real-time particle monitor against the reference gravimetric method for PM_{10} and $PM_{2.5}$ in indoor air. *Atmospheric Environment,* 54**,** 358-364.

Tsai, C. J., Chang, C. T., Shih, B. H., Aggarwal, S. G., Li, S. N., Chein, H. M. & Shih, T. S. 2002. The effect of environmental conditions and electrical charge on the weighing accuracy of different filter materials. *Sci Total Environ,* 293**,** 201-6.

TurnkeyInstrument. 2006. *Osiris Operating Instruction* [Online]. Available: http://www.turnkey-instruments.com/images/documents/Osiris-Operating-Instructions.pdf [Accessed 28 June 2014].

Virkkula, A., Mäkelä, T., Hillamo, R., Yli-Tuomi, T., Hirsikko, A., Hämeri, K. & Koponen, I. K. 2007. A Simple Procedure for Correcting Loading Effects of Aethalometer Data. *Journal of the Air & Waste Management Association,* 57**,** 1214-1222.

Yan, B., Kennedy, D., Miller, R. L., Cowin, J. P., Jung, K.-h., Perzanowski, M., Balletta, M., Perera, F. P., Kinney, P. L. & Chillrud, S. N. 2011. Validating a nondestructive optical method for apportioning colored particulate matter into black carbon and additional components. *Atmospheric Environment,* 45**,** 7478-7486.

5 FIELD EVALUATION OF FILTER-BASED BC MEASUREMENTS AND NO_2 SENSORS

5.0 Background

Field measurements using three of the methods described in the previous chapter were evaluated to determine to what extent combustion-related air pollutants can be characterised using portable low power instrumentation. Specifically, this chapter describes: comparison of reflectometer and scanner measurements of particle specimens collected on filters *vs.* reference AE51 Aethalometer observations; comparison of two AE51 Aethalometer *vs.* reference AE21 aethalometer observations; and comparison of two pairs of Aeroqual Series 500 portable ozone and nitrogen dioxide monitors *vs.* reference gas analysers.

5.1 BC measurements

5.1.1 Extended reflectance and scanner measurements

The results from the pilot study described in sections 4.5.1 & 4.5.2 informed the design of a field experiment to calibrate reflectance and scanner measurements of particles collected on filters to estimate BC concentrations. Between 10 - 24 August 2015, particles were collected on 25-mm 2-µm PTFE filters over 24-hour sampling intervals at 1.0 L min^{-1} with Casella Apex sampling pumps in an office building and a nearby outdoor urban background environment. The darkness of the filter specimens was measured as reflectance (*R*) using a smoke stain reflectometer (section 4.1.3.1 and 4.5.1) and as a scanned red value (*S*) using an office scanner (Epson, Model GT-1500; section 4.5.2).

The relationships observed between BC surface density (µg/cm^2) on filters (estimated from co-located AE51 Aethalometer measurements) and $ln(R_0/R)$ and $ln(S_0/S)$ [where R_0 and S_0 were the initial reflectance and scanned red values for each filter before sampling] were fitted with quadratic functions to allow for non-linearity associated with filter darkening. The equations derived from the fitted curves were used to estimate atmospheric BC concentrations (µg/m^3) for the calibration dataset and for other reflectance and scanner measurements, which were then compared with AE51 Aethalometer measurements. Filter measurements with inconsistent airflow rates during sampling periods were excluded from this data analysis.

5.1.2 Results

Accumulated BC surface density (µg/cm^2) was compared to reflectance, *R* (%), scanner red value (*S*), normalised reflectance (*ln (Ro/R)*) and normalised scanned red value (*ln (So/S)*) (Figure 5.1). Reflectance and scanner measurements decreased gradually with increased BC loading, consistent with observations in previous laboratory tests (section 4.5.1.1). The quadratic functions explained 99% and 97% of the variation in accumulated BC surface density from normalised reflectance and scanner values respectively (Figure 5.1).

Figures 5.2 & 5.3 illustrate relationships between normalised reflectance and scanned red values with BC surface density from each sampling location. The best-fit quadratic equation from filters sequentially loaded by sampling in the indoor location was used to calibrate the reflectometer and scanner measurements against BC surface density.

The calibration curve determined from the sequentially loaded indoor measurements was then applied to the remaining data from other locations. The estimated BC concentrations from reflectometer measurements of sequentially loaded filters in combined outdoor and campus measurements explained 78% of the variation of black carbon concentrations measured concurrently with the AE51 Aethalometer, with a root mean square error (RMSE) of 1.1 $\mu g/m^3$ (Figure 4.2) [when the combined dataset was extended further to include measurements collected in the laboratory the explained variation increased further to 84%, RMSE = 0.92 $\mu g/m^3$ (Figure 5.5)]. In contrast, the scanner measurements of the same outdoor and campus filters explained 54% of the variation of black carbon concentrations measured concurrently with the microaethalometer, with a root mean square error (RMSE) of 2.6 $\mu g/m^3$ (Figure 5.3).

To allow for possible changes in scanner output between measurements a blank filter was scanned at the time of each measurement. This allowed adjustment for small changes in scanner output by multiplication of each measurement by the ratio of the scanned blank red value prior to sampling to the scanned blank red value during each measurement. The revised calibration lines and comparisons with micro-aethalometer measurements are illustrated in Figure 5.4. This adjustment process resulted in increases explained variation for the independent outdoor and campus test data [64% explained variation, and RMSE = 1.9 $\mu g/m^3$, for adjusted calibration data (Figure 5.4) *vs.* 54% explained variation, and RMSE = 2.6 $\mu g/m^3$, for unadjusted calibration data (Figure 5.3)]. However the adjustment process reduced explained variation for the calibration data [69% explained variation, and RMSE = 0.25 $\mu g/m^3$, for adjusted calibration data (Figure 5.4) *vs.* 97% explained variation, and RMSE = 0.25 $\mu g/m^3$, for unadjusted calibration data (Figure 5.3)].

The somewhat ambiguous effect of adjustment using repeated single blank filter measurements suggests that adjustment for changes in scanner output is likely to be important, but that more detailed adjustment may be required. One possible way of doing this might be to repeatedly scan a range of greyscale image sections to allow changes in scanner output to be quantified across the range of filter darkness that is likely to be encountered. This may be possible by creating a paper template to hold the filters on the scanner that includes grey scale images. Some possible templates are illustrated in Figure 5.6. Although these templates would get dirty, and possibly fade, over time; their main use would be to allow adjustment of scanner output between the before and after sampling measurements on the same filter. Hence any soiling or fading is likely to have negligible effect over these relatively short timescales.

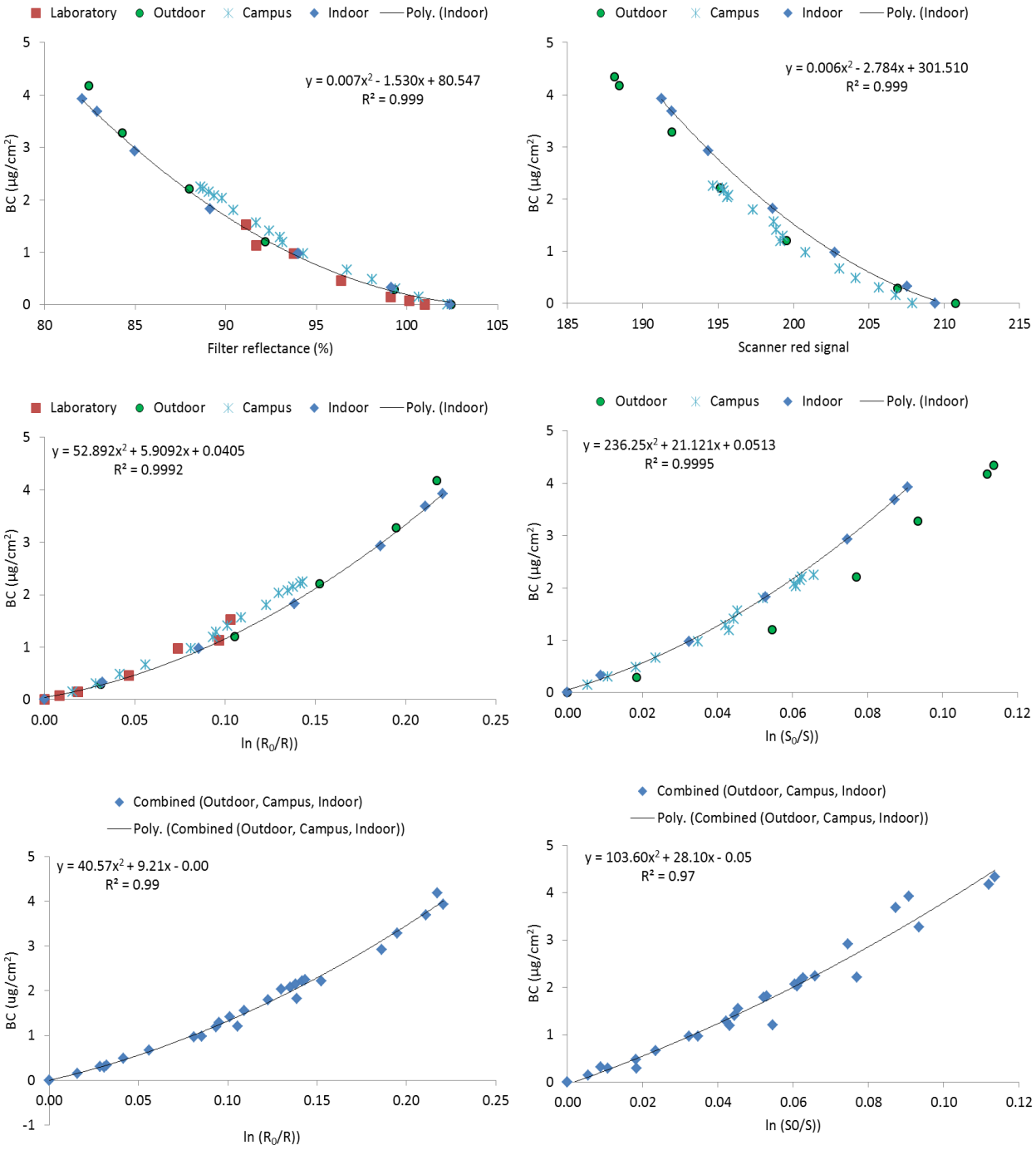

Figure 5.1: Comparison of reflectance, R (%), scanner red value (S), normalised reflectance (ln (Ro/R)) and normalised scanned red value (ln (So/S)) with black carbon (BC) surface density (µg/cm^2).

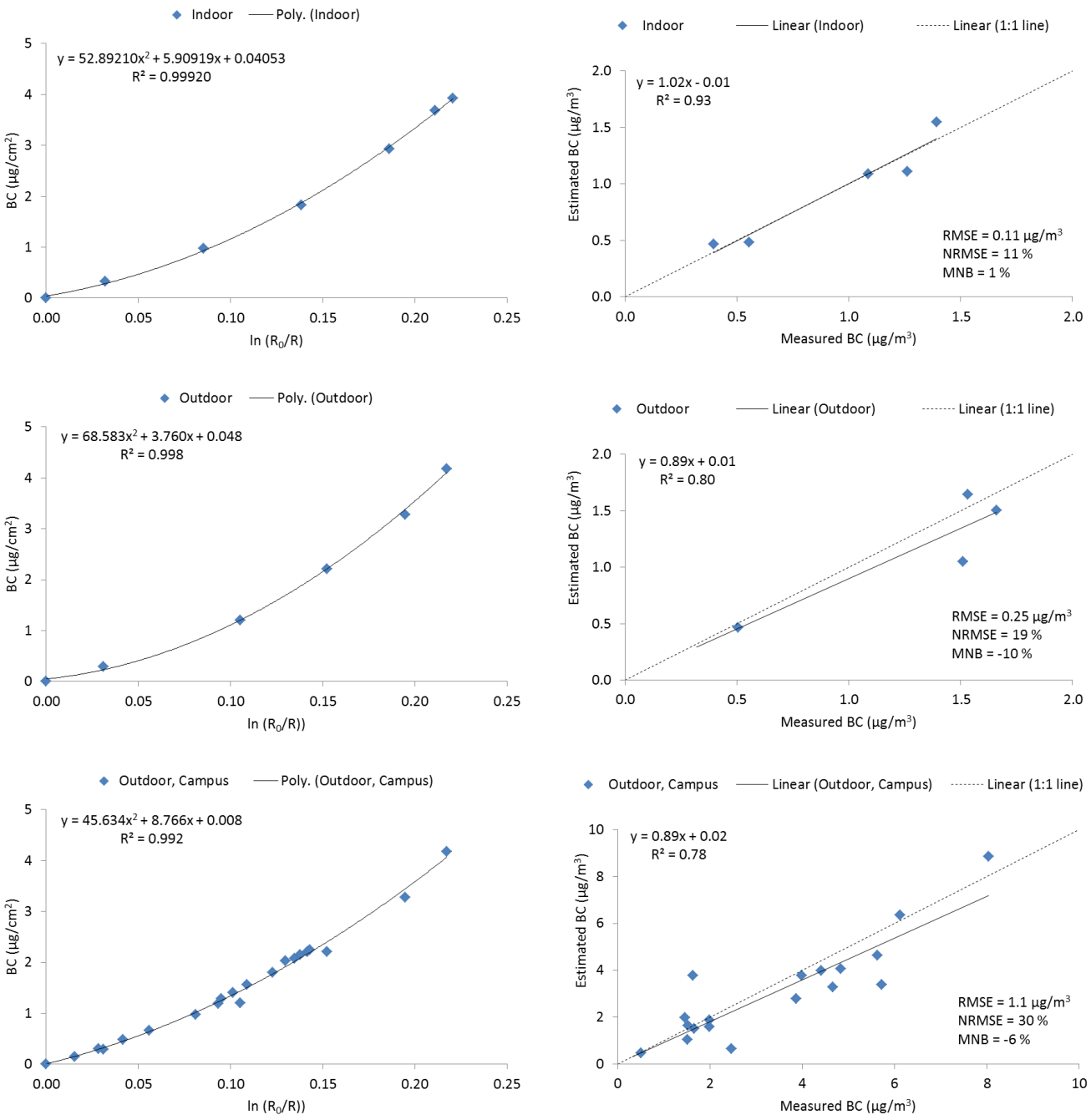

Figure 5.2: Comparison between BC concentrations estimated by reflectometer and BC measured by micro-aethalometer. BC concentrations in right hand graphs were estimated from indoor measurements using calibration plot in top left hand graph.

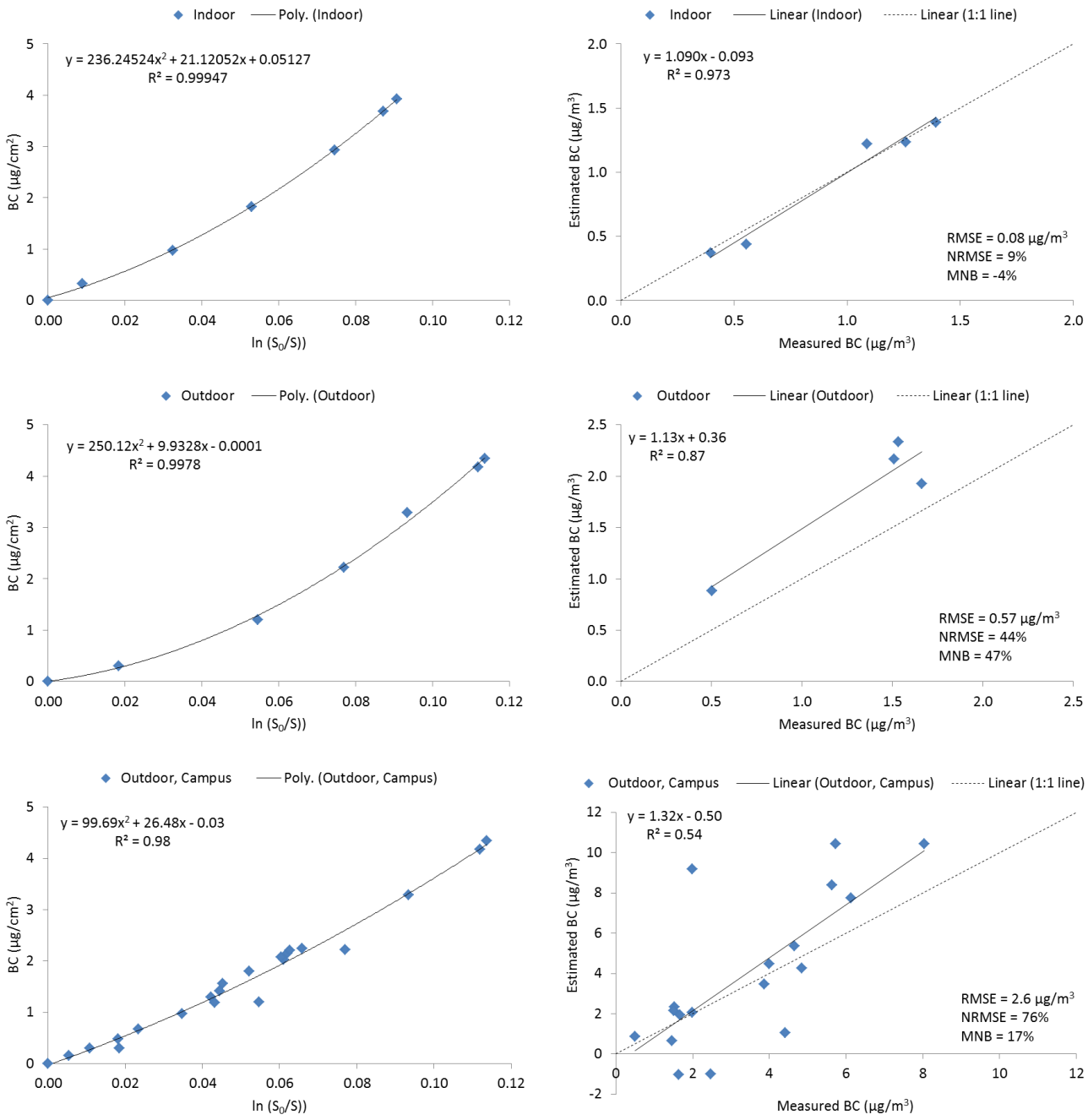

Figure 5.3: Comparison between BC concentrations estimated by scanner and BC measured by micro-aethalometer. BC concentrations in right hand graphs were estimated from indoor measurements using calibration plot in top left hand graph.

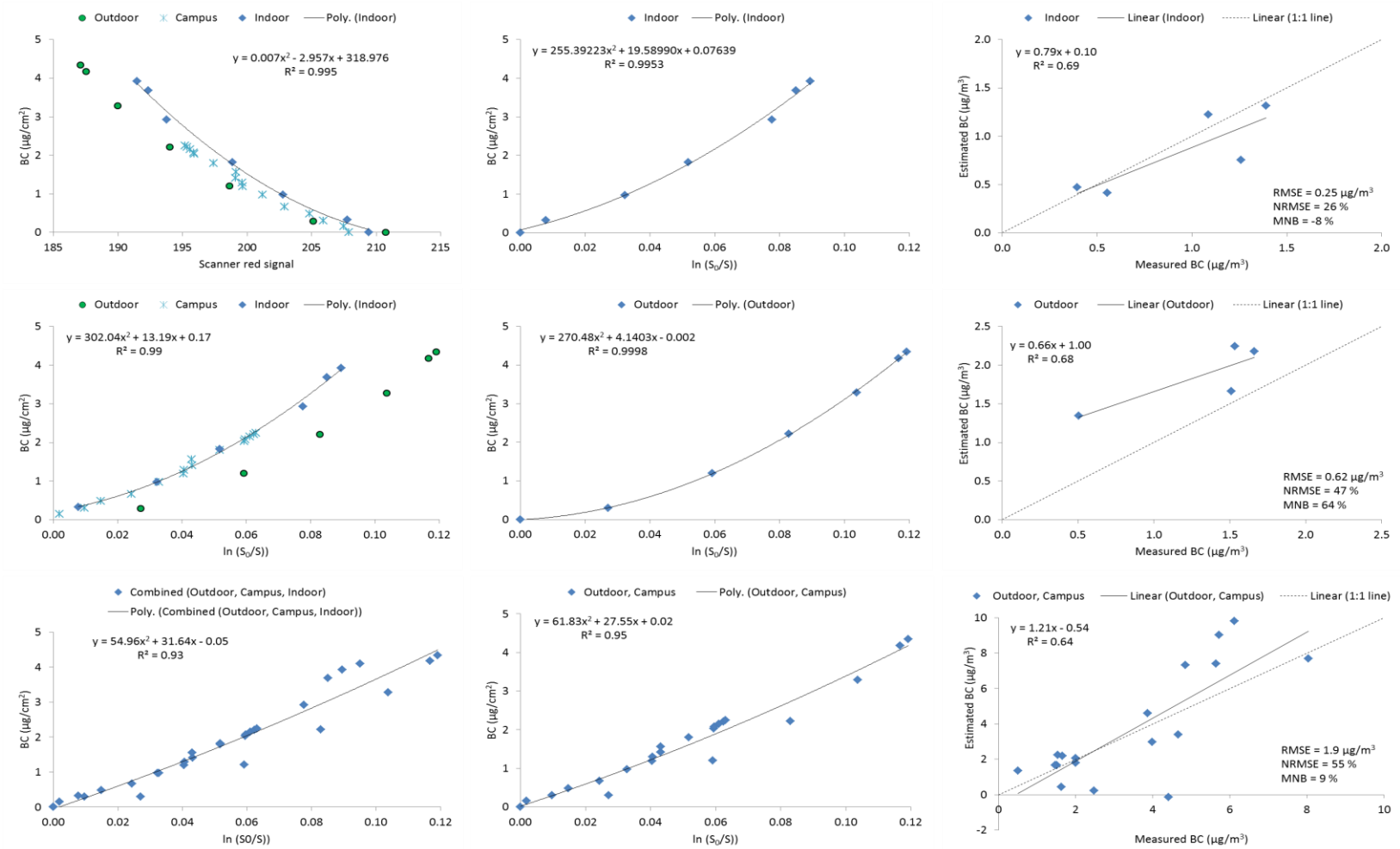

Figure 5.4: BC concentrations estimated by scanner after adjustment for changes in repeatedly scanned blank filter. BC concentrations in right hand graphs estimated from indoor calibration (top middle).

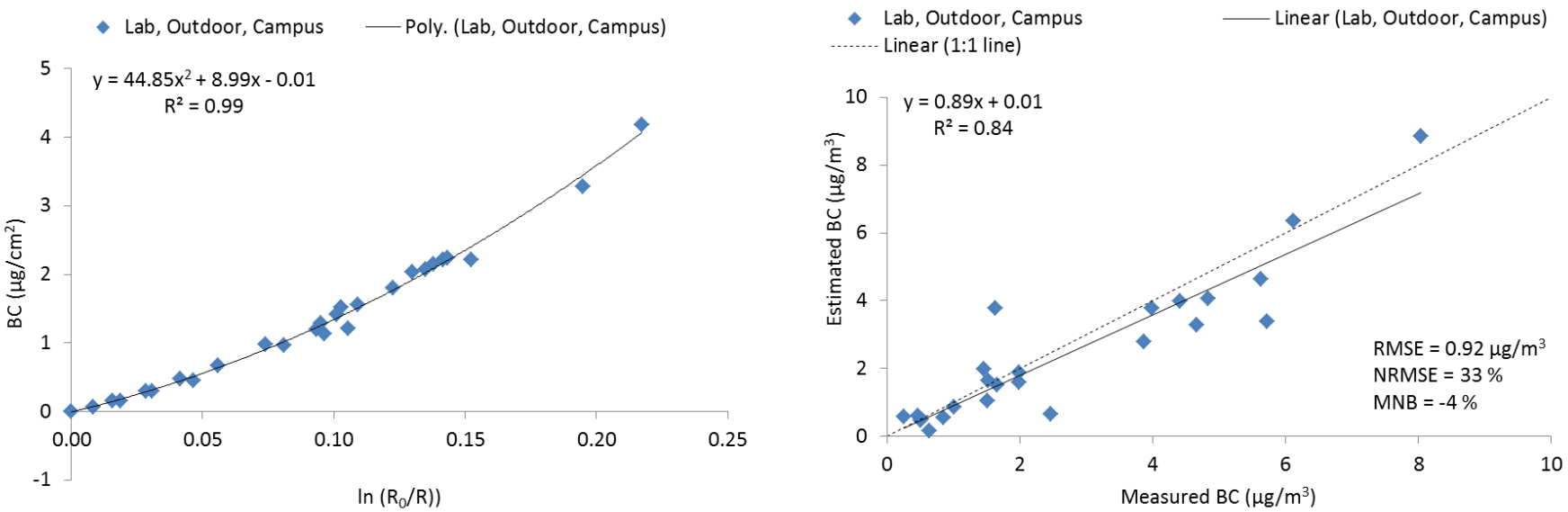

Figure 5.5: Comparison between BC concentrations estimated by reflectometer and BC measured by microaethalometer, including additional data from Environmental Engineering Laboratory. BC concentrations in right hand graphs were estimated from indoor measurements using calibration plot in top left hand graph in Figure 5.2.

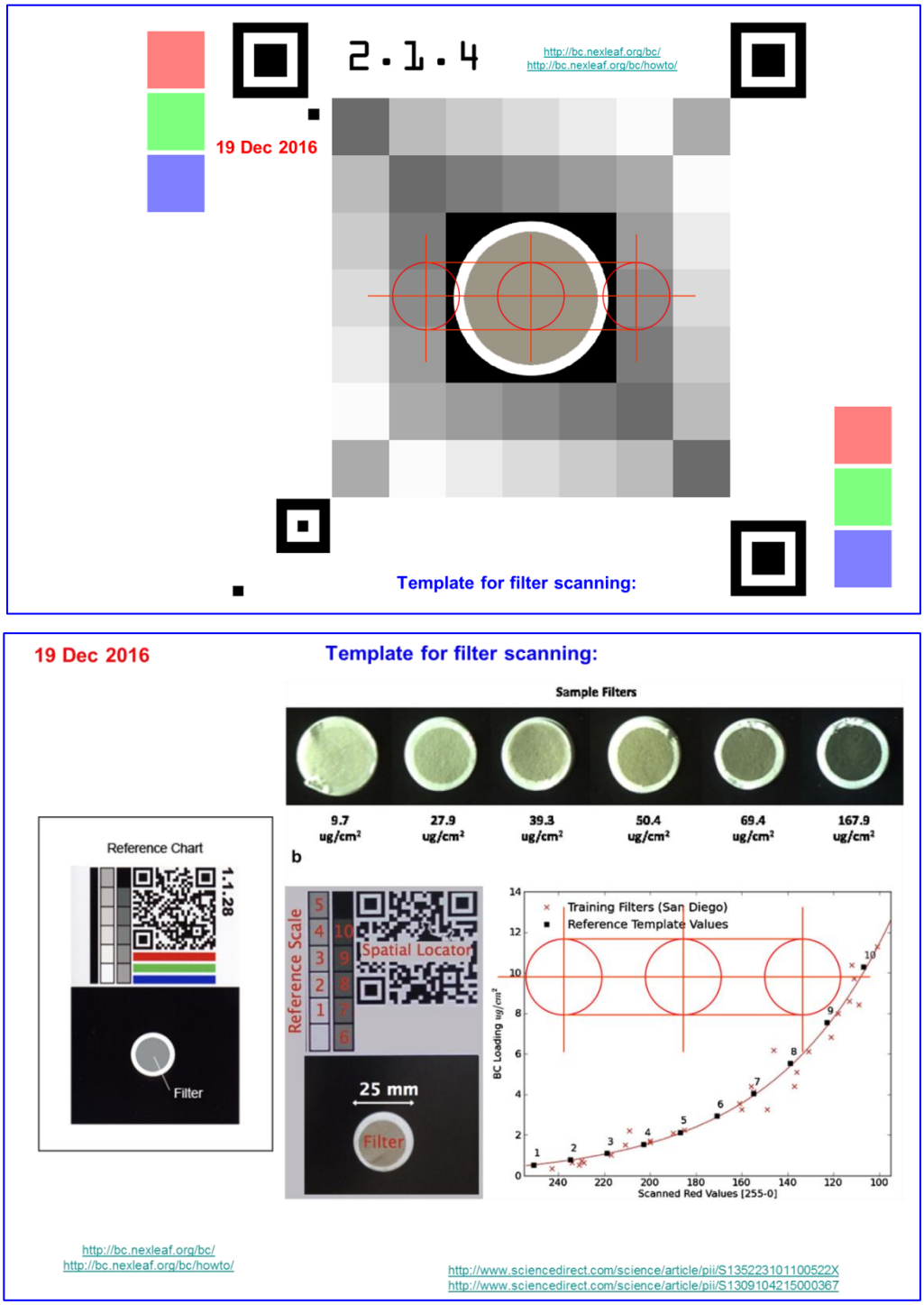

Figure 5.6: Two alternative experimental templates to hold filters for scanning and simultaneously provide a grey-scale calibration image to allow check of, and possible adjustment for, changes in scanner output. The red circles are cut out on the template to allow simultaneous scanning of grey-scale images, sample filter and reflectometer calibration tile before and after sampling.

5.1.3 Discussion

In this work, the two reflected light techniques studied; reflectometer and scanner, showed responses to the total loading of BC. It is observed that the spread of data points from reflectance and red scanner values displayed stronger relationship with the BC surface density when the light reflected back. The reflectance and red scanner measurements obtained from the collection of aerosol particles were considered low, as a result provide a good linear relationship. The variations of reflectance and scanner values from the filter samples appeared to be related to the accumulated duration of exposure, magnitude of filter sources and air monitoring approaches. A longer sampling duration was employed in this study to provide a broad range of BC loading data points and facilitates to derive an equation from the fitted curve. For this reason, the filter source from indoor measurements provide the longest sampling duration compared to other filter samples.

Additionally, the inconsistency level of measurements in the Campus shows a much wider spread of data points in Figure 5.2 & 5.3 ((a) iii) resulted from mobile outdoor monitoring exercises performed. The spatial coverage from the mobile outdoor measurements may complicate the demonstration of the quadratic functions to generate the best-fit equation for BC quantification. Much of recent work on alternative low cost optical measurements has conducted in a higher pollutant sources using high flow rates for the sampling system compared to this study. Table 5.1 below shows the comparison from this work to the other similar studies. In these studies, the BC loading values were reported higher compared to loading values collected from our filter. Forder (2014) suggested the type of samplers used may affect the BC relationship with the proposed optical methods. The collected particles were deposited more on the centre of the filter surface for cyclone sampler, therefore may introduced gradient of deposition density on the filter surface.

Table 5.1: Summary of collection system, optical methods and filter sources used from this study and other studies.

Comparison	Collection system (sampler, filter, flow rate)	Optical methods	Filter sources	Max loading ($\mu g/cm^2$)
This study	Casella Apex Pro Teflon filter(25 mm) 1.0 L min^{-1}	Reflectometer Office Scanner	Office building Urban background (Glasgow, UK)	4.34
Cheng *et al.* (2011)	High volume air samplers (Graseby, GMWT 2200) Quartz filter 40 ft min^{-1}	Office Scanner	Rooftop of residential building (Hong Kong & China)	22.12
Ramanathan *et al.* (2011)	The MAS system[1] Quartz filte(25 mm) 625 cc min^{-1}	Office Scanner	Urban areas (U.S.A)	167.9
Forder (2014)	Quartz filter (25 mm) 2.0 L min^{-1}	Office Scanner BOSCH meter Microcolor 11[2] OT 21[3]	Crane exhaust Mine air	60.0
Lalchandani *et al.* (2016)	High volume air samplers Quartz filter (47 mm) 15 L min^{-1}	Office Scanner Colorimeter	Industrial area (India) Urban areas (U.S.A)	20-35

[1]Minituarized Aerosol filter Sampler (MAS).

[2]The DR-Lange Microcolor 11. Transmissometer.

[3]The SootScan™ Model OT21

BC loading collected from our filters was considered lower from the narrow measurement range. This may introduce a fair performance of those proposed methods, however the lower loading values from less darker filter samples collected during the monitoring campaigns will avoid saturation error. Lalchandani *et al.* (2016) reported their filter samples were relatively dark and may have greater error at very high loading values (> 20 μg/cm^2). Therefore, the need for additional measurements is necessary in order to investigate the limit of our proposed techniques at which the system can accurately estimate the BC concentrations. To the best of found knowledge, this is the first work that shows the feasibility of the reflectometer and office scanner to estimate BC concentrations by sequentially loading the airborne particle specimens on a single filter. The corresponding reflectance and scanner measurements may interfere with overloading of the particle deposited on the same filter will result in saturation issue. It is estimated that the saturation effect will occur for Teflon filter when the reflectance value reached less than 20% (Janssen *et al.*, 2001). However, in the current study the minimum reflectance value reported was 82.1%. Janssen *et al.* (2001) also reported that reflectance value below 15% gave erroneous reading from their filter samples to estimate absorption coefficients. Fortunately, the use of Teflon filter in this work has its own advantages where the filter surface is less occluded and the carbon particle will easily trap within the filter matrix (Taha *et al.*, 2007).

The estimated BC concentrations of red scanner values were observed a divergence scatter points compared to BC data points estimated by reflectometer. Note that the applied digital imaging did not convert the optical signal into an electrical response in the same way as the reflectometer. The presence of other metal (i.e aluminium or iron) in the carbon particles compositions may give rise to the intensity of red value, which produced longer wavelength (Cheng *et al.*, 2011). This work demonstrates the monitoring exercise and analysis protocols for low-cost reflectometer and scanner methods, which are comparable to the high-end of BC real-time sensors. The derived equation can be used to estimate BC levels in different microenvironments. However, some drawbacks could reduce from the variability of measurements where a stronger follow-up measurement is required to optimise the proposed methods.

5.1.4 Field calibration of BC sensors at AUN site

Two AE51 Aethalometer [BC1303 & BC1204] were compared to a static government AE21 reference aethalometer at the Townhead urban background site over four separate deployment periods between April - August 2016 (Table 5.2). Both AE51 monitors were logged at 5-minute intervals and set at 50 ml min^{-1} flow rate. This enabled continuous monitoring of BC and before recommended laser light attenuation (ATN) limits associated with filter loading in the monitor were exceeded. The internal micro-aethalometer clocks were synchronised to internet time. The filter strip for each micro-aethalometer was renewed prior to each deployment period.

The micro-aethalometer units were deployed in a waterproof enclosure (green box - Figure 5.9 b), connected to mains power. The air inlets to the micro-aethalometers consisted of conductive silicone tubes with waterproof inlets attached to the railing surrounding the AUN site roof. Hourly concentrations from BC analyser (the UK BC network)[1] were downloaded from https://uk-air.defra.gov.uk/data/data_selector (section 4.3). BC data from both micro-aethalometers were downloaded using MicroAeth software and post-processed (Apte *et al.*, 2011, Hagler *et al.*, 2011) (details in section 4.1.4.1). BC statistical analyses were provided by Nicola Masey (*personal communication*) (see manuscript in Appendix 9D for full details).

Precautions were taken when working at Townhead AUN site (refer to appendix 10B(1) for appropriate Risk Assessment forms).

[1] The UK BC network was run by DEFRA and installed the monitor (aethalometer AE21) in 2013 to determine BC levels in the urban area including Glasgow (NPL, 2015).

Table 5.2: Dates of field deployment of microaethalometer instruments at the Townhead.

Study name	Monitoring period
April	31/03/2016 - 04/04/2016
May	29/04/2016 - 29/05/2016
July	01/07/2016 - 04/07/2016
August	08/08/2016 - 22/08/2016

5.1.5 Results and discussion

Measurements from the two AE51 micro-aethalometer units (BC 1303 & BC 1204) were in close agreement with each other (R^2 = 0.93, Figure 5.7 (a) & (b)), and the reference aethalometer (R^2 mostly greater than 70%, Figure 5.8). One period of lower correlation observed between BC 1303 and the reference aethalometer in the July monitoring period was associated with a small number of low concentration measurements over a small range of low concentrations. These observations are consistent with the findings of a similar field comparison study in Barcelona between microaethalometer units (AE51) and a Multi-Angle Absorption Photometer (MAAP) reference black carbon monitor (Viana *et al.*, 2015). It may be beneficial to examine the effect of changes of relative humidity and temperature on agreement between instruments in future research (Cai *et al.*, 2014).

(a)

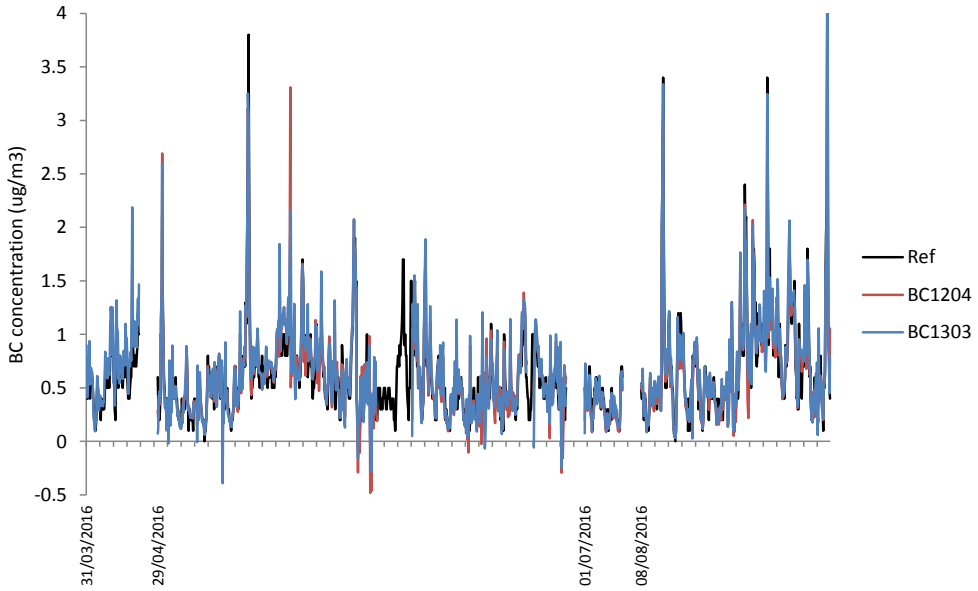

(b)

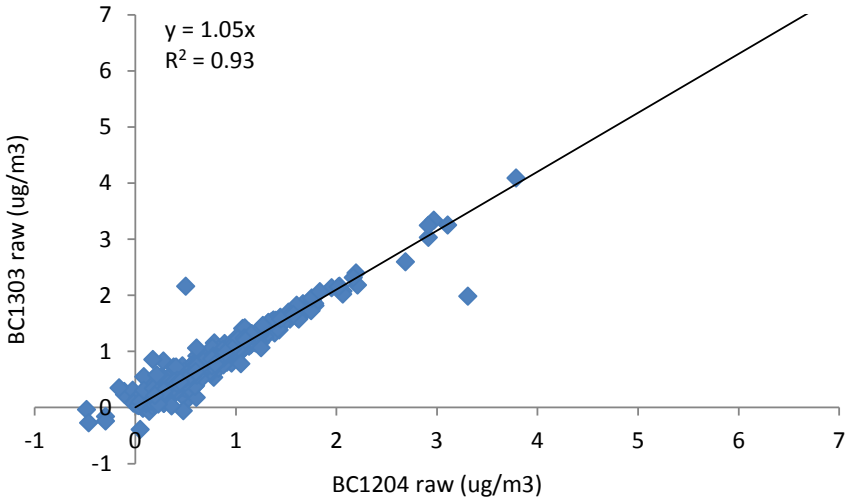

Figure 5.7: (a) Time series from measurement made by the BC instruments (BC 1303 & BC 1204 and BC reference analyser. (b) The Reduced Major Axis (RMA) regression between BC1303 and BC1204 raw black carbon concentrations at hourly resolution. [BC data and analyses provided by Nicola Masey, *personal communication*].

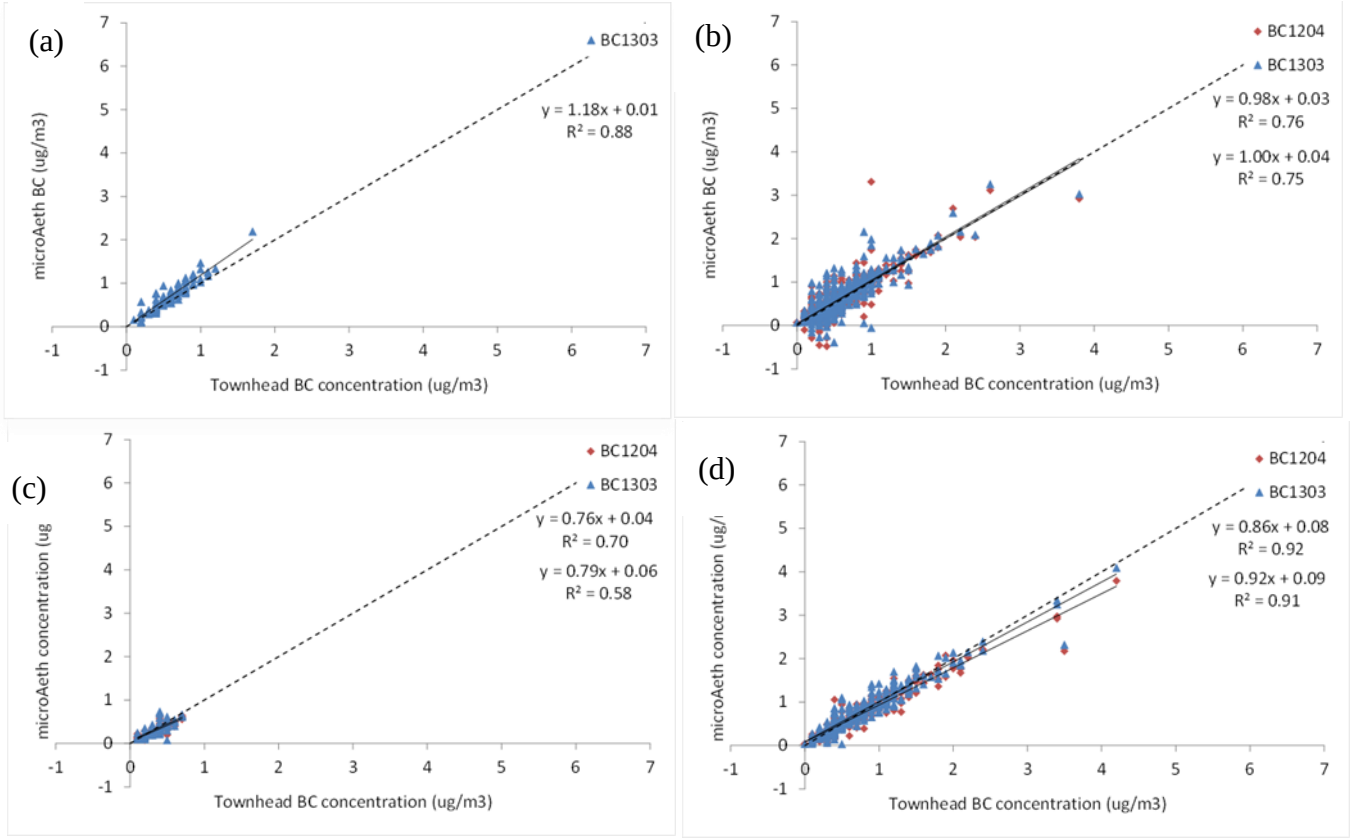

Figure 5.8: Ordinary Least Squares (OLS) regression between the BC instruments (BC 1303 & BC 1204) and the reference analyser for each monitoring period; (a) April; (b) May; (c) July; and (d) August. The dashed line represents 1:1 concentrations. [BC data and analyses provided by Nicola Masey, personal communication].

5.2 NO_2 and O_3 measurements

5.2.1 Field calibration of O_3 and NO_2 sensors at AUN site

We made intermittent comparisons (6 times over a 6-month period between November 2015 and May 2016) of gas concentrations measured by Aeroqual gas sensitive semiconductor ozone (O_3) and electrochemical nitrogen dioxide (NO_2) sensors to reference gas analysers in the UK Automatic Urban Network (AUN). These measurements were made at an urban background AUN site located within a residential area in Townhead, Glasgow close to the University of Strathclyde campus. The surrounding area is gated and the instruments housed are well secured on the roof of this AUN site. Four Aeroqual instruments were housed inside waterproof casing provided by Aeroqual Ltd. Four units of casing boxes were securely attached with cable ties vertically to the railings facing east (Figure 5.9 (a)) and west (Figure 5.9 (b)) on the AUN roof. All Aeroqual units were connected to mains power and set to log for 1 minute of measurement and during the period of deployment. Precautions were taken when working at AUN site (as stated in section 5.1.4).

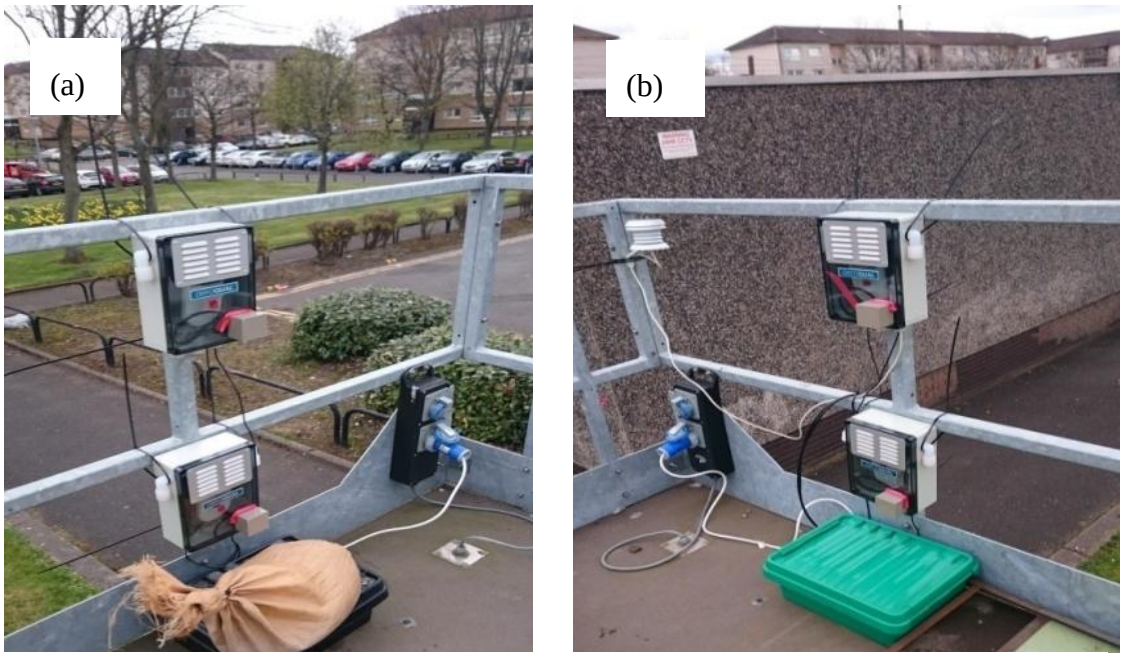

Figure 5.9: The setup of Aeroqual deployment facing (a) east and (b) west on the roof top of AUN monitoring site at Townhead, Glasgow.

5.2.2 Results and discussion

We observed clear functional relationships between *Aeroqual O_3 vs. Reference O_3* concentrations, and *(Aeroqual NO_2 – Reference NO_2) vs. Aeroqual O_3* concentrations allowing the Aeroqual sensors to be calibrated against the reference analysers (see details in Appendix A). The calibration relationships changed over time, primarily as a result of gradual reduction in the sensitivity Aeroqual O_3 sensors. The accuracy of calibrated estimates of gas concentrations was improved by repeated intermittent calibration over time, and application of the most recent calibration relationships to test data (Figure 5.10 - 5.11 – see manuscript in Appendix 10A(1) & 10A(2) for full details).

(a)

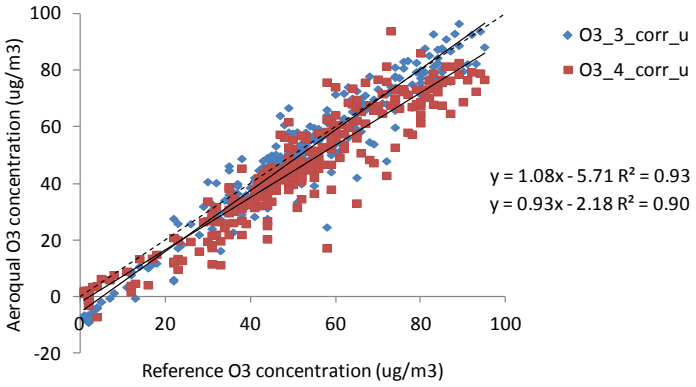

(b)

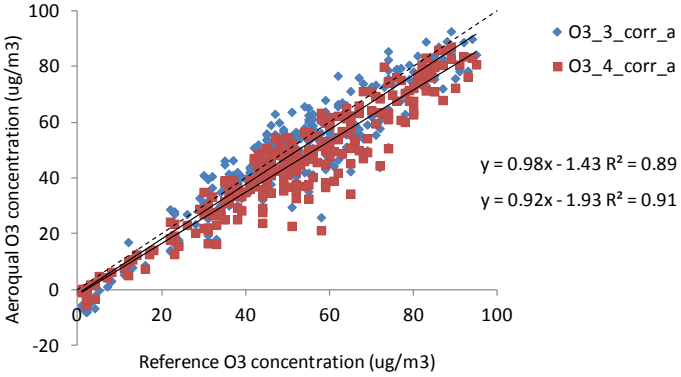

(c)

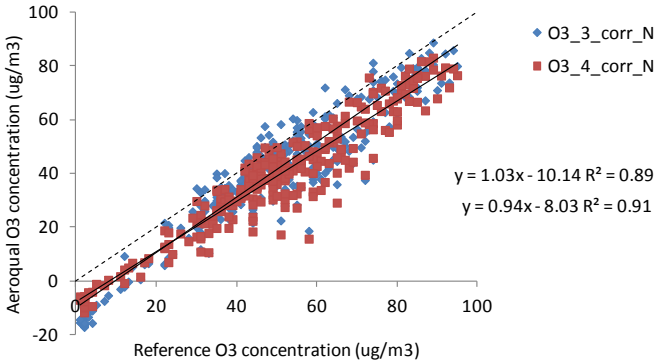

Figure 5.10: Scatter plots of adjusted Aeroqual O_3 concentration estimates *vs.* concentrations measured by the reference analyser for test data (i.e. 2nd half of deployment periods only) [O_3 data and analyses provided by Nicola Masey, *personal communication*]. (a) *O_3_aq* adjusted using calibration derived from training data in each unique deployment period (*O_3_aq_corr_u*). (b) *O_3_aq* adjusted using calibration derived from training data combined from all deployment periods (*O_3_aq_corr_a*). (c) *O_3_aq* adjusted using calibration derived from the first deployment period (November) only (*O_3_aq_corr_N*).

(a)

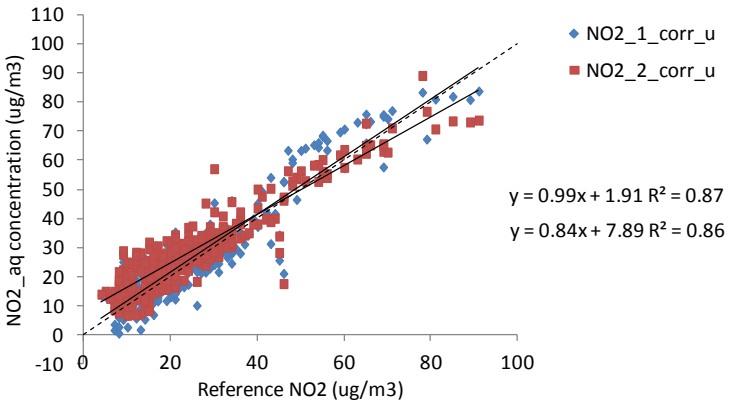

(b)

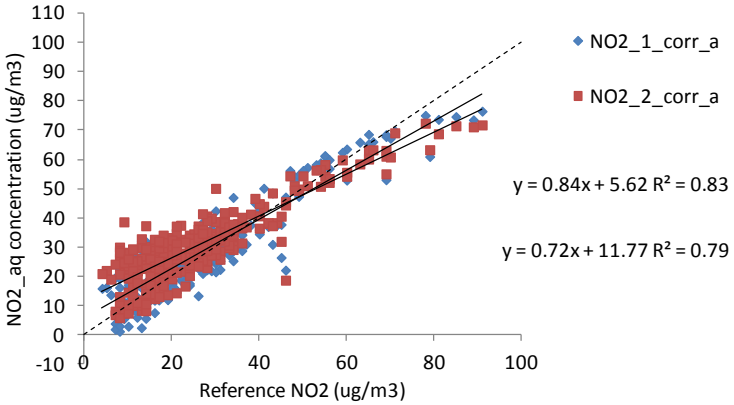

(c)

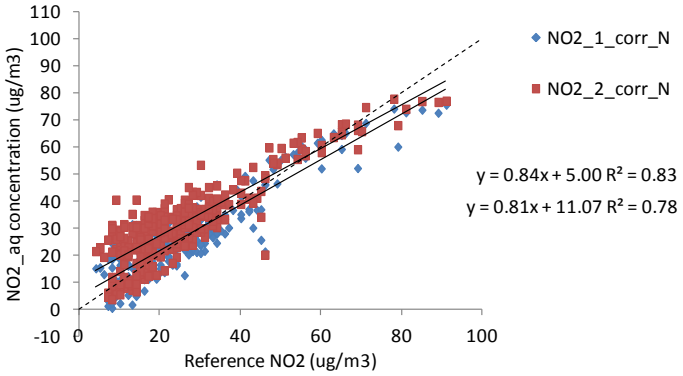

Figure 5.11: Scatter plots of adjusted Aeroqual NO_2 concentration estimates *vs.* concentrations measured by the reference analyser for test data (i.e. 2nd half of deployment periods only) [NO_2 data and analyses provided by Nicola Masey, *personal communication*]. (a) Aeroqual data adjusted using calibration derived from training data in each unique deployment period (*aq_corr_u*). (b) Aeroqual data adjusted using calibration derived from training data combined from all deployment periods (*aq_corr_a*). (c) Aeroqual data adjusted using calibration derived from the first deployment period (November) only (*aq_corr_N*).

5.3 Summary

The reflectance and scanner measurements show that they were beneficial to estimate BC concentrations between different environments. The performance of these measurement system were further assessed for outdoor air exposure assessment and described in chapter 6. The intermittent comparisons between the real-time sensors (O_3 & NO_2) and reference analysers highlight the importance of field calibration of these types of sensors. The microaethalometer AE51 units were evaluated demonstrated robust and valid data capture. This suggests that the microaethalometer could be potentially useful to characterise personal exposure to BC. In addition, both Aeroqual and microaethalometer were comparable with the reference analyser in stationary condition. Further test via peripatetic and mobile sampling designs in indoor and outdoor settings will provide a broader spatial coverage to characterise the personal exposure to combustion-related air pollution. All of these are described and illustrated in detail in the subsequent chapters.

5.4 References

Apte, J. S., Kirchstetter, T. W., Reich, A. H., Deshpande, S. J., Kaushik, G., Chel, A., Marshall, J. D. & Nazaroff, W. W. 2011. Concentrations of fine, ultrafine, and black carbon particles in auto-rickshaws in New Delhi, India. *Atmospheric Environment,* 45**,** 4470-4480.

Butterfield, D. M., Beccaceci, S., Quincey, P., Sweeney, B., Lilley, A., Bradshaw, C., Fuller, G. W., Green, D. C. & Font, A. 2016. *2015 Annual Report for the UK Black Carbon network* [Online]. Available: https://uk-air.defra.gov.uk/assets/documents/reports/cat13/1611011539_2015_Black_Carbon_Network_Annual_Report_Final_18082016.pdf [Accessed 5 January 2017].

Cai, J., Yan, B., Ross, J., Zhang, D., Kinney, P. L., Perzanowski, M. S., Jung, K., Miller, R. & Chillrud, S. N. 2014. Validation of MicroAeth® as a Black Carbon Monitor for Fixed-Site Measurement and Optimization for Personal Exposure Characterization. *Aerosol and air quality research,* 14**,** 1-9.

Cheng, J. Y. W., Chan, C. K. & Lau, A. P. S. 2011. Quantification of Airborne Elemental Carbon by Digital Imaging. *Aerosol Science and Technology,* 45**,** 581-586.

Forder, J. A. 2014. Simply scan--optical methods for elemental carbon measurement in diesel exhaust particulate. *Ann Occup Hyg,* 58**,** 889-98.

Hagler, G. S. W., Yelverton, T. L. B., Vedantham, R., Hansen, A. D. A. & Turner, J. R. 2011. Post-processing Method to Reduce Noise while Preserving High Time Resolution in Aethalometer Real-time Black Carbon Data. *Aerosol Air Qual Res,* 11**,** 539–54.

Janssen, N. A. H., van Vliet, P. H. N., Aarts, F., Harssema, H. & Brunekreef, B. 2001. Assessment of exposure to traffic related air pollution of children attending schools near motorways. *Atmospheric Environment,* 35**,** 3875-3884.

Lalchandani, V., Tripathi, S. N., Graham, E. A., Ramanathan, N., Schauer, J. J. & Gupta, T. 2016. Recommendations for calibration factors for a photo-

reference method for aerosol black carbon concentrations. *Atmospheric Pollution Research,* 7**,** 75-81.

Masey, N., Ezani, E., Gillespie, J., Lin, C., Heal, M. & Beverland, I. J. 2017a. Impact of filter shadowing correction algorithms on agreement of portable AE51 micro-aethalometer and reference AE33 aethalometer black carbon measurements. *Atmos Environ.(in preparation)*

Masey, N., Gillespie, J., Ezani, E., Lin, C., Hao, W., Heal, M. R., Ferguson, N., Hamilton, S. & Beverland, I. J. 2017b. Temporal changes in field calibration relationships for Aeroqual S500 NO2 and O3 sensors.*(in preparation)*

Ramanathan, N., Lukac, M., Ahmed, T., Kar, A., Praveen, P. S., Honles, T., Leong, I., Rehman, I. H., Schauer, J. J. & Ramanathan, V. 2011. A cellphone based system for large-scale monitoring of black carbon. *Atmospheric Environment,* 45**,** 4481-4487.

Taha, G., Box, G. P., Cohen, D. D. & Stelcer, E. 2007. Black Carbon Measurement using Laser Integrating Plate Method. *Aerosol Science and Technology,* 41**,** 266-276.

Viana, M., Rivas, I., Reche, C., Fonseca, A. S., Pérez, N., Querol, X., Alastuey, A., Álvarez-Pedrerol, M. & Sunyer, J. 2015. Field comparison of portable and stationary instruments for outdoor urban air exposure assessments. *Atmospheric Environment,* 123, Part A**,** 220-228.

6 INDOOR AIR QUALITY IN UNIVERSITY OFFICES

6.0 Background

It is important to assess exposure to indoor pollutants as people spend more than 90% of their time in the indoor environment particularly in the emerging countries (Mohammed *et al.*, 2015). A report released by WHO (2002) stated that indoor air pollution is responsible for 2.7% of disease burden globally. Several studies involving office buildings show that the indoor particulate matter (PM) (including carbonaceous particle specimens) were influenced by the outdoor levels (Mohammadyan *et al.*, 2010, Quang *et al.*, 2012, Lappalainen *et al.*, 2013).

Indoor concentrations of pollutants depend on other factors, including type of building, ventilation system, and floor level. Collectively, this highlights the importance of characterising determinants of indoor-outdoor concentration relationships, and sources and processes directly influencing indoor concentrations, when assessing personal exposure to air pollution. Accurate quantification of relatively low concentrations of gaseous and particulate air pollution can result in measurement challenges (Barrese *et al.*, 2014a). The combined use of passive and real-time sensors may be beneficial in addressing these challenges.

This chapter describes field experiments in two office buildings on the University of Strathclyde campus. Measurements included the following variables: particulate matter (PM_1, $PM_{2.5}$ and PM_{10}); black carbon (BC); gaseous pollutants (including NO_2 and O_3); temperature (T); and relative humidity (RH). Indoor and outdoor measurements were compared. The average measurements of PM, BC and NO_2 during 8-hour working periods were calculated to estimate exposure experienced by people working in the offices.

6.1 Experimental Design

6.1.1 Sampling location

The University of Strathclyde campus is situated in Glasgow city centre. The university is located between urban streets where traffic includes private cars, taxis, buses and goods vehicles. The offices included in this study were in the Department of Civil and Environmental Engineering (DCEE) and International Study Centre (ISC). The newly DCEE refurbished offices are on the fifth floor of the James Weir Building, which is between Cathedral Street and George Street. The ISC offices are approximately 300 m south-east of the James Weir building on eighth floor of Graham Hill building (Figure 6.1).

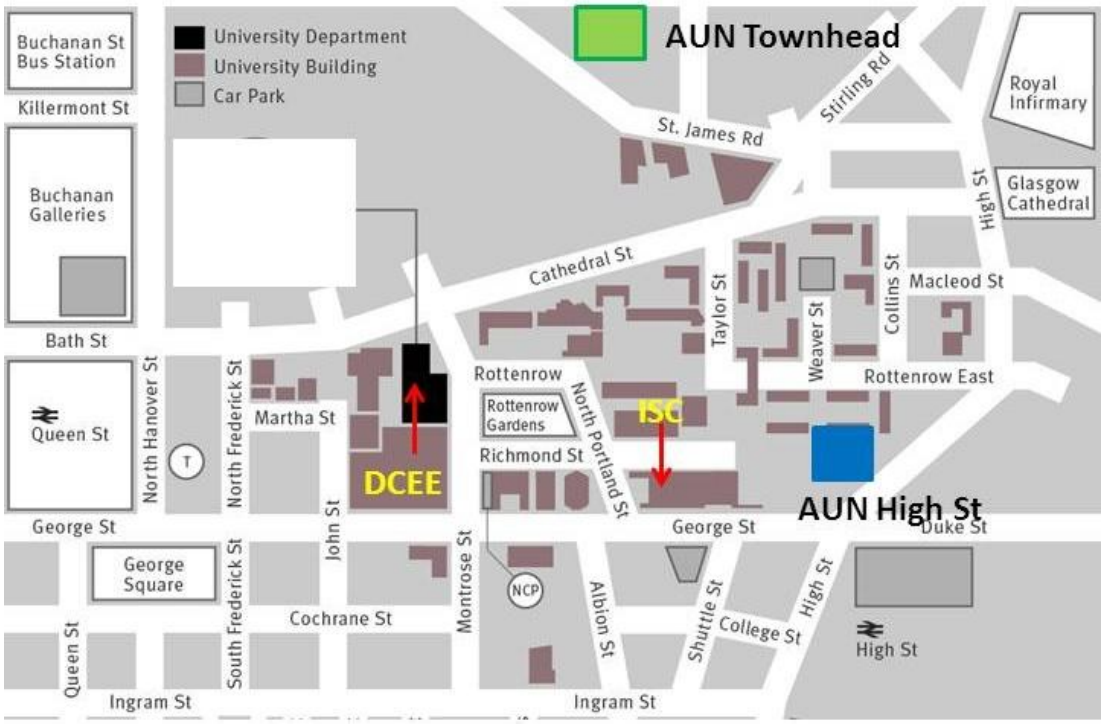

Figure 6.1: Sampling locations at DCEE and ISC. Two AUN monitoring sites were also shown (green box) for AUN Townhead and (blue box) AUN High St. (Image taken from http://www.strath.ac.uk/maps/).

6.1.2 Indoor air measurements at DCEE

Four 48-hour sampling periods were conducted in naturally ventilated open-plan offices, mechanically ventilated cubicle offices, and a nearby outdoor urban background location (accessed via an open window) between 24 July 2014 & 4 August 2014.

Airborne particle specimens were collected on 37-mm Teflon filters at 3.65 L min^{-1} using two BGI 400 pumps (BGI, USA) and one SKC pump (SKC Ltd, UK) to estimate $PM_{2.5}$ and BC concentrations from filter mass and darkness measurements respectively (as described in sections 4.1.3.1 & 4.1.3.4). NO_2 concentrations were measured using triplicate passive diffusion tubes (PDT) (section 4.2.1). PM_{10}, $PM_{2.5}$ and PM_1 concentrations were also recorded at 1-minute intervals using OSIRIS light-

scattering monitors (Turnkey Instruments Ltd, UK). Sampling pumps were placed inside a sound-proof box. Sampling tubes with plastic rain caps were hung out the window for measurement of outdoor concentrations (Figure 6.2). Details of instruments used are provided in section 4.1.4.2.

6.1.3 Indoor air measurements at ISC

48-hour indoor measurements were made in the teacher's room (27 June 2016 - 29 June 2016) and administration office (12 July 2016 - 14 July 2016). The teachers and administration staff spend most of their time during working hours (9.00 am - 5.00 pm) in these rooms. Both office rooms were located next to each other and were naturally ventilated by opening windows. The office staffs in each room were asked to fill in the observation sheet to record the time and frequency of window opening. The real-time sampling equipment used for this study is summarised in Table 6.1.

Table 6.1: Summary of real-time sensors used during the study.

Instrument	Air Pollutant/Measurement
Aeroqual series 500 (Aeroqual Ltd., NZ)	NO_2 and O_3
CP 11 (Rotronic AG, Switzerland)	RH and T
LEO (Ateknea Solutions, Spain)	NO_2, O_3, NO, RH and T
AE51 Aethalometer (Aethlabs, USA)	BC
MicroPEM (model V.3.2, USA)	$PM_{2.5}$

All sensors were set to 1-minute logging intervals except for MicroPEM instruments which logged measurements at 30 seconds during the first monitoring event (27 June

2016 - 29 June 2016), and 10 seconds during the second monitoring event (12 July 2016 - 14 July 2016) to allow computation of 1-minute averages from 2 and 6 spot measurements respectively. Prior to deployment, the internal clocks of all instruments were synchronised with internet time from the researcher's PC.

The operation of Aeroqual, MicroAeth and MicroPEM instruments is described in section 4.1.4. NO_2 measurements made by Aeroqual instruments were corrected from monthly field calibrations (discussed in section 5.2). The CP11 instrument measured temperature and relative humidity (RH). This lightweight (290 g) instrument operates on four AA alkaline batteries. Thermistor and hygrometer sensors within the CP11 instrument measure temperature and relative humidity in the ranges of -20 to 60°C and 0.1 to 99.5% respectively. This device can operate from battery power over 50 to 66 hours. The Institute of Occupational Medicine (IOM) provided Little Environment Observatory (LEO) sensors for field evaluation as part of the CITI-SENSE project. CITI-SENSE is citizen science project that actively engages the public to assess the environmental quality within their locality (Bortonova, 2016). The sensor measures NO_2, NO and O_3 using electrochemical sensors. The LEO instrument also records temperature (T) and relative humidity (RH). Data were downloaded using ExpoApp on an android smart phone via Bluetooth connection.

6.1.4 Health and safety

The risk assessments were conducted prior to deploy all instruments in the office room (appendix 10B (2) & 10B (3)).

6.1.5 Data analysis

Provisional hourly average data from the automatic urban network (AUN) monitoring sites at Townhead, High St and Glasgow Kerbside were downloaded from Scottish air quality website (details in section 4.3). All data were exported from instrument-supplied software to an Excel 2010 spreadsheet for simple descriptive statistics analysis. Inter-pollutant scatterplot matrices were constructed using R model2, dplyr and reshape2 packages (R Core Team, 2012).

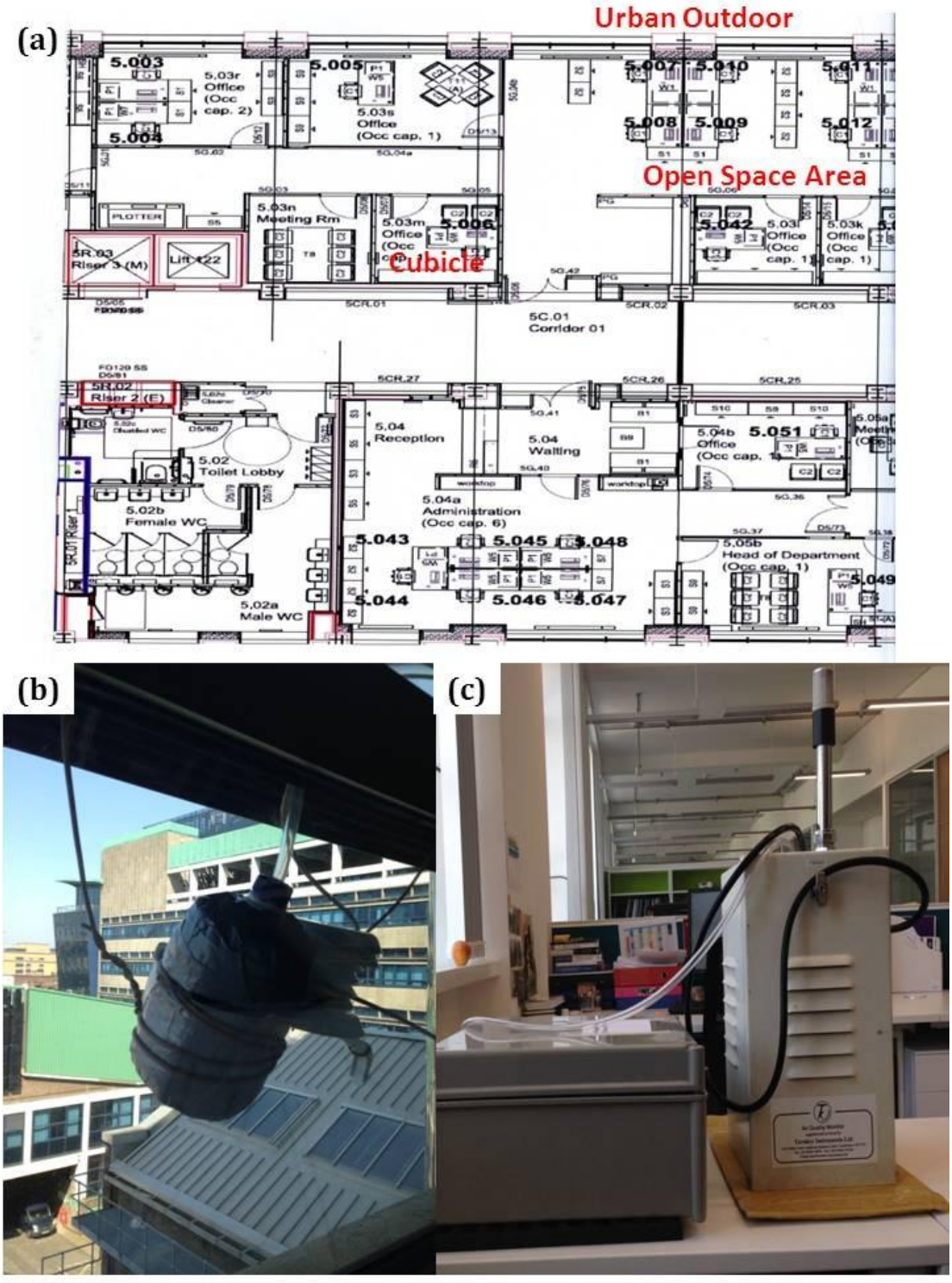

Figure 6.2: Indoor and outdoor air measurements: (a) the office floor plan; (b) outdoor urban samplers mounted outside of window; (c) indoor air pollution measurements in open-plan office.

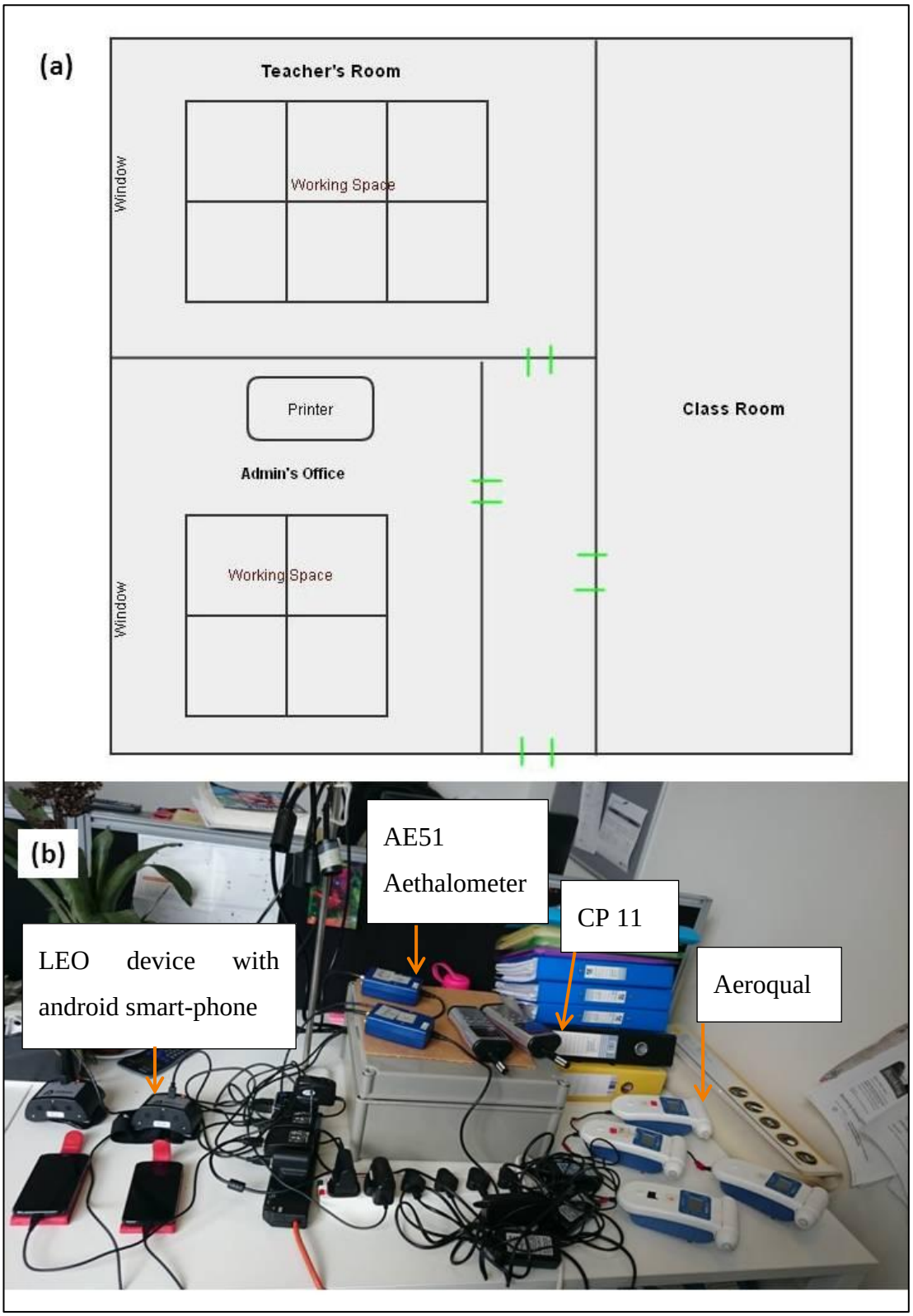

Figure 6.3: Administrative office at ISC: (a) Floor plan; (b) Pairs of instruments set up for indoor air monitoring.

6.2 Results

6.2.1 Indoor air measurement at DCEE

A summary of $PM_{2.5}$ absorption coefficient, $PM_{2.5}$ mass and NO_2 concentrations collected from filter samples and exposed PDTs at each sampling location is shown in Table 6.2. 12 filter samples and 28 passive tubes were collected across sampling events. $PM_{2.5}$ mass concentrations varied from 2.1 - 13.6 $\mu g/m^3$ across sampling periods. $PM_{2.5}$ absorption coefficient and NO_2 exhibited modest variations with values ranging from 1.2 - 8.6 for absorption coefficient (10^{-5} m^{-1}) and from 11.5 - 40.2 for NO_2 concentrations ($\mu g/m^3$). The mean coefficient of variation for triplicate NO_2 passive tubes was 9%.

Variations for all pollutants in the average concentrations were more pronounced when compared to each sampling location. The average outdoor measurements for $PM_{2.5}$ mass and NO_2 concentrations were higher in the outdoor compared to the open space and cubicle room. Conversely, $PM_{2.5}$ absorption coefficient was higher in the open space compared to the outdoor (17% higher) and cubicle room (27% higher). This suggests the sources of outdoor pollutants influenced the pollution levels of urban background measured near the office window and in the open space. NO_2 concentrations in the cubicle office were higher than the open plan office in one set of measurement (24 - 26 July 2014). A similar pattern has been observed for $PM_{2.5}$ absorption coefficient, where one set of measurement between 2 - 4 August 2014 in the cubicle office was higher than outdoor and the open plan office.

Table 6.2: Descriptive statistics: $PM_{2.5}$ mass concentration ($\mu g/m^3$), $PM_{2.5}$ absorption coefficient (10^{-5} m^{-1}) and NO_2 concentration ($\mu g/m^3$) stratified by sampling periods and locations.

Pollutant	Location	24/7/14- 26/7/14	26/7/14 - 28/7/14	31/8/14 - 2/8/14	2/8/14- 4/8/14	Mean ± SD
	Outdoor	11.9	4.8	7.1	4.7	7.1 ± 3.4
$PM_{2.5}$	Open	13.6	5.1	2.1	4.6	6.4 ± 5.0
	Cubicle	10.2	4.1	6.0	4.2	6.1 ± 2.9
	Outdoor	7.9	6.5	1.2	5.4	5.3 ± 2.9
PM abs. coeff	Open	8.6	6.7	1.2	4.4	5.2 ± 3.2
	Cubicle	6.7	5.4	1.9	4.8	4.7 ± 2.0
	Outdoor	29.5	40.2	27.6	22.1	29.9 ± 7.6
NO_2	Open	18.8	26.8	18.0	11.5	18.8 ± 6.3
	Cubicle	25.2	19.7	15.0	10.6	17.6 ± 6.3

Figure 6.4 (a) - (c) show the time series of 1-minute intervals PM_1, $PM_{2.5}$ and PM_{10} data recorded during the simultaneous measurement by three Osiris located in separate sampling areas; outdoor (urban background), open space and cubicle room. The results being presented were not corrected for humidity (Tasić *et al.*, 2012). Note that the measurement time and date for each sampling event has merged in the sampling period (x-axis) to represent the continuous monitoring. The observed data from PM_1, $PM_{2.5}$ and PM_{10} captured general trends in concentrations for each monitoring location across the sampling period. All PM levels recorded in the open area were consistently showing higher mass values than measurements recorded in the cubicle office.

Average PM_1 levels were 5.7, 4.4 and 2.7 $\mu g/m^3$ in the outdoor background, open plan and cubicle room. For $PM_{2.5}$, the average concentrations were 11.9, 8.8 and 4.8 $\mu g/m^3$. In addition, the average PM_{10} were 15.5, 12.4 and 6.4 $\mu g/m^3$. Although $PM_{2.5}$ and PM_{10} concentrations were considered lower in the cubicle room, higher peaks were noticed during the monitoring periods. There were overlapping trends for PM_1, $PM_{2.5}$ and PM_{10} measurements between outdoor and open plan area with several peaks observed during the monitoring period. Similarities in variation within these two sampling areas indicate the effects of the outdoor emissions to the natural ventilated indoor open plan. The unusual peaks were noted in two monitoring events within outdoor background observations (25 July 2014 for $PM_{2.5}$ & 28 July 2014 for PM_{10}; Figure 6.4a).

Unfortunately, the Osiris has failed to record PM_1 and $PM_{2.5}$ on 25th July 2014 (between 2:36 to 9:45 a.m) for outdoor and open plan monitoring areas due to power failures. Another Osiris located in the cubicle room has suffered from instrument failure and failed to record data for PM_{10} measurements from 1 August - 2 August 2014 (between 2:11 and 12:56) which has caused 2000 missing data (1-min time stamp) from this malfunctioned sensor.

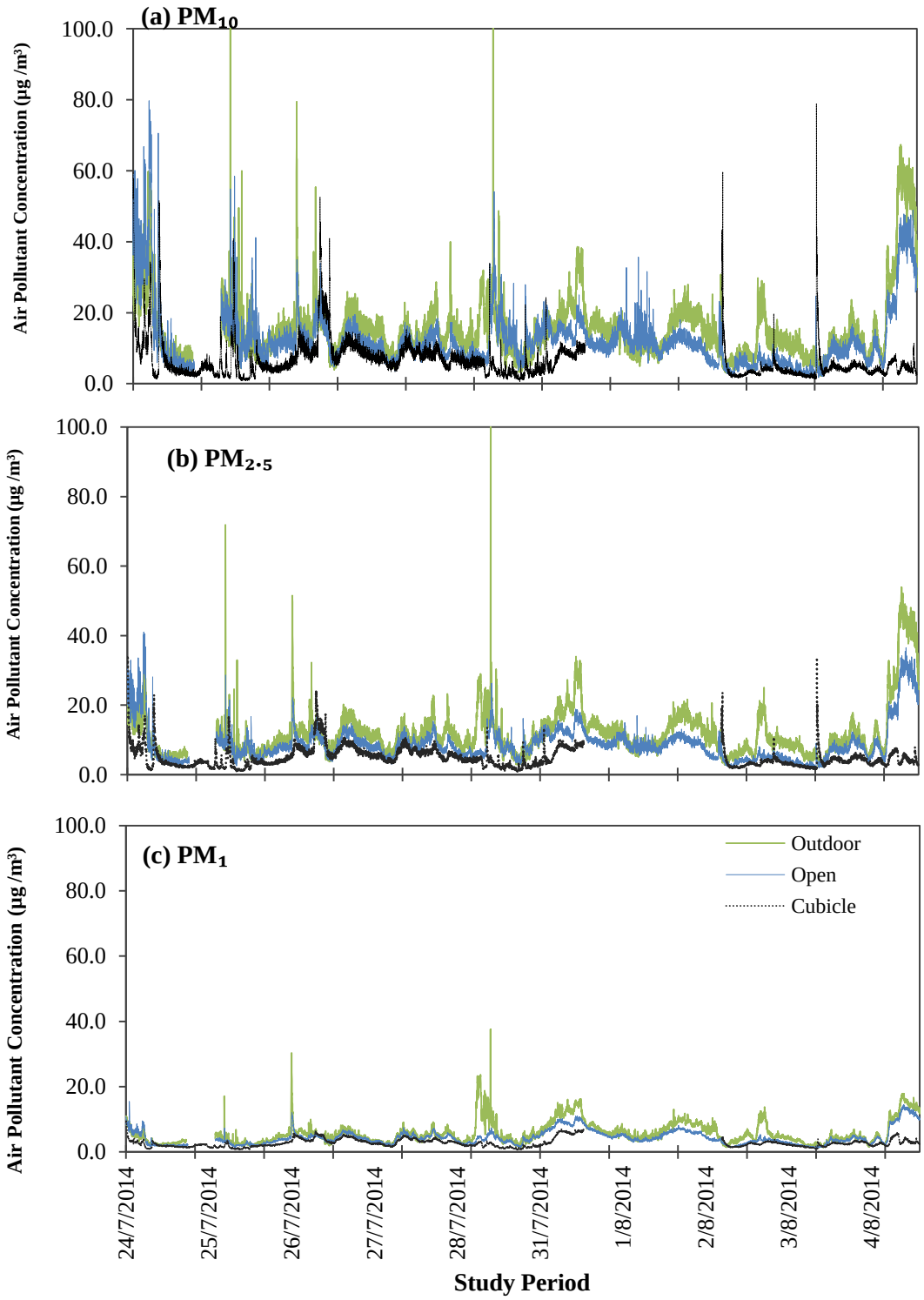

Figure 6.4: 1-min (a) PM_{10}, (b) $PM_{2.5}$ and (c) PM_1 mass concentrations measured by Osiris real-time monitors in urban outdoor, open space and cubicle room. All PM data were corrected using calibration derived from Osiris in-comparison test (as described in section 4.4.5).

Figure 6.5 (a) & (b) show the comparison of $PM_{2.5}$ measurements between filter-based methods and Osiris monitor for 48-hour average. The continuous $PM_{2.5}$ measurements from Osiris showed no relationship between filter-based methods of gravimetric ($PM_{2.5}$ mass concentrations) and reflectance (absorption coefficient). Since few Osiris instruments have failed to operate in particular period during the observations, the average concentrations observed by this sensor have given unreliable results to be compared with the accumulated 48-hour filter mass concentrations.

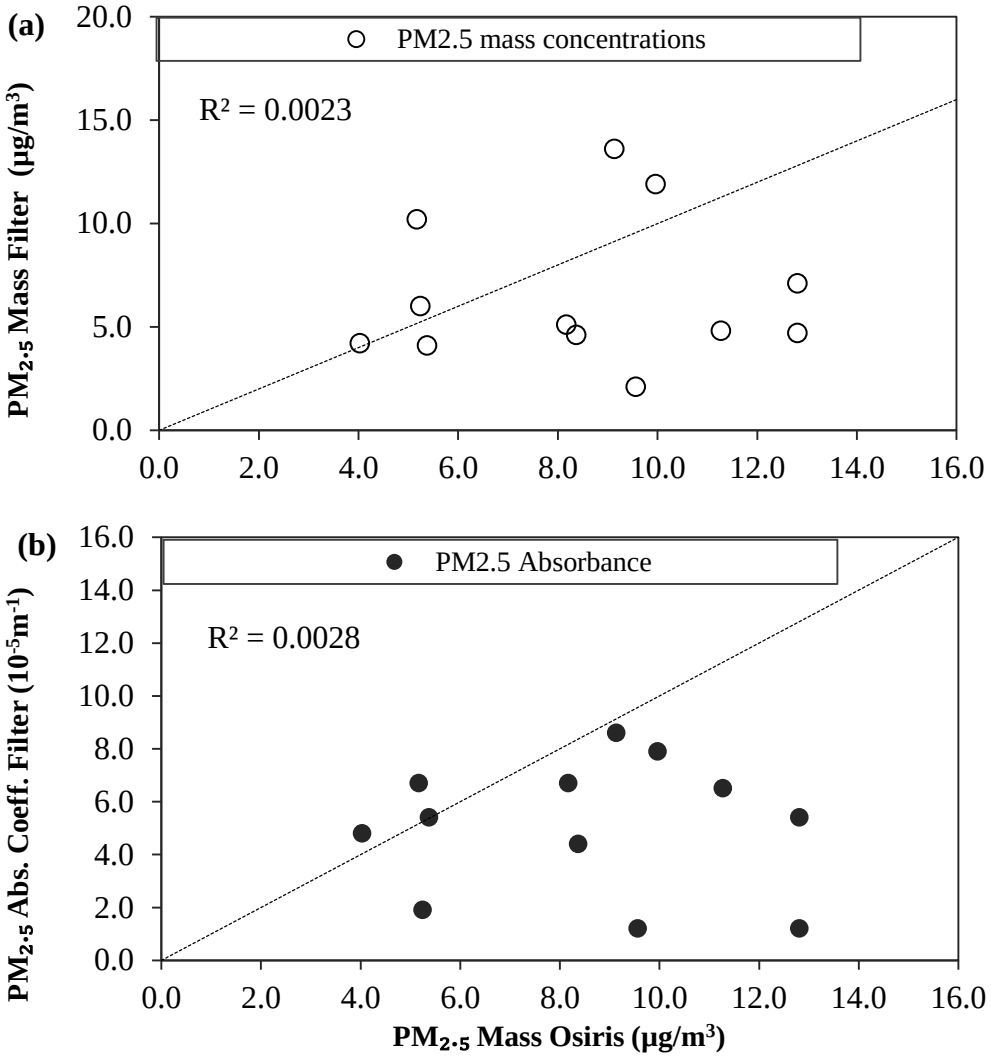

Figure 6.5: Comparison between average $PM_{2.5}$ mass concentrations measured by Osiris and (a) $PM_{2.5}$ gravimetric and (b) $PM_{2.5}$ reflectance methods, n = 12.

Figure 6.6 (a) - (c) show summary of the comparison between measurement made by the filter-based methods and PDTs. Additional time series at the right side y-axis show the air pollutant levels recorded in the AUN site ($PM_{2.5}$ and BC). $PM_{2.5}$ measurements from AUN Townhead were overestimated (10% higher) compared to the filter-based $PM_{2.5}$ mass. NO_2 measurements made by PDTs had overestimated NO_2 concentrations recorded by both AUN in Glasgow Kerbside and Townhead. $PM_{2.5}$ absorption coefficients measured during the study period were following the same trend of BC concentrations recorded from Townhead AUN site.

The continuous 1-min measurements of $PM_{2.5}$ and PM_{10} in outdoor background and open space were averaged to hourly levels to be compared with hourly BC, $PM_{2.5}$ and PM_{10} measurements obtained from the Townhead AUN site. Figure 6.7 (a) & (b) show the time series of instantaneous measurements made between hourly mean indoor and AUN monitoring site. PM_1 mass concentrations measured by Osiris were not included in this comparison due to missing number of data during the sampling periods. The instrument recording PM_{10} levels in AUN site have failed to provide data on 24 July 2014. Major trends show both $PM_{2.5}$ and PM_{10} levels recorded at both AUN sites to have underestimated the Osiris measurements. However, the trends observed from the AUN sites (BC, $PM_{2.5}$ and PM_{10}) have showed similarity in the variation recorded by the Osiris ($PM_{2.5}$ and PM_{10}). This suggests the outdoor particle emissions may influence the indoor air monitoring nearby the window (outdoor background).

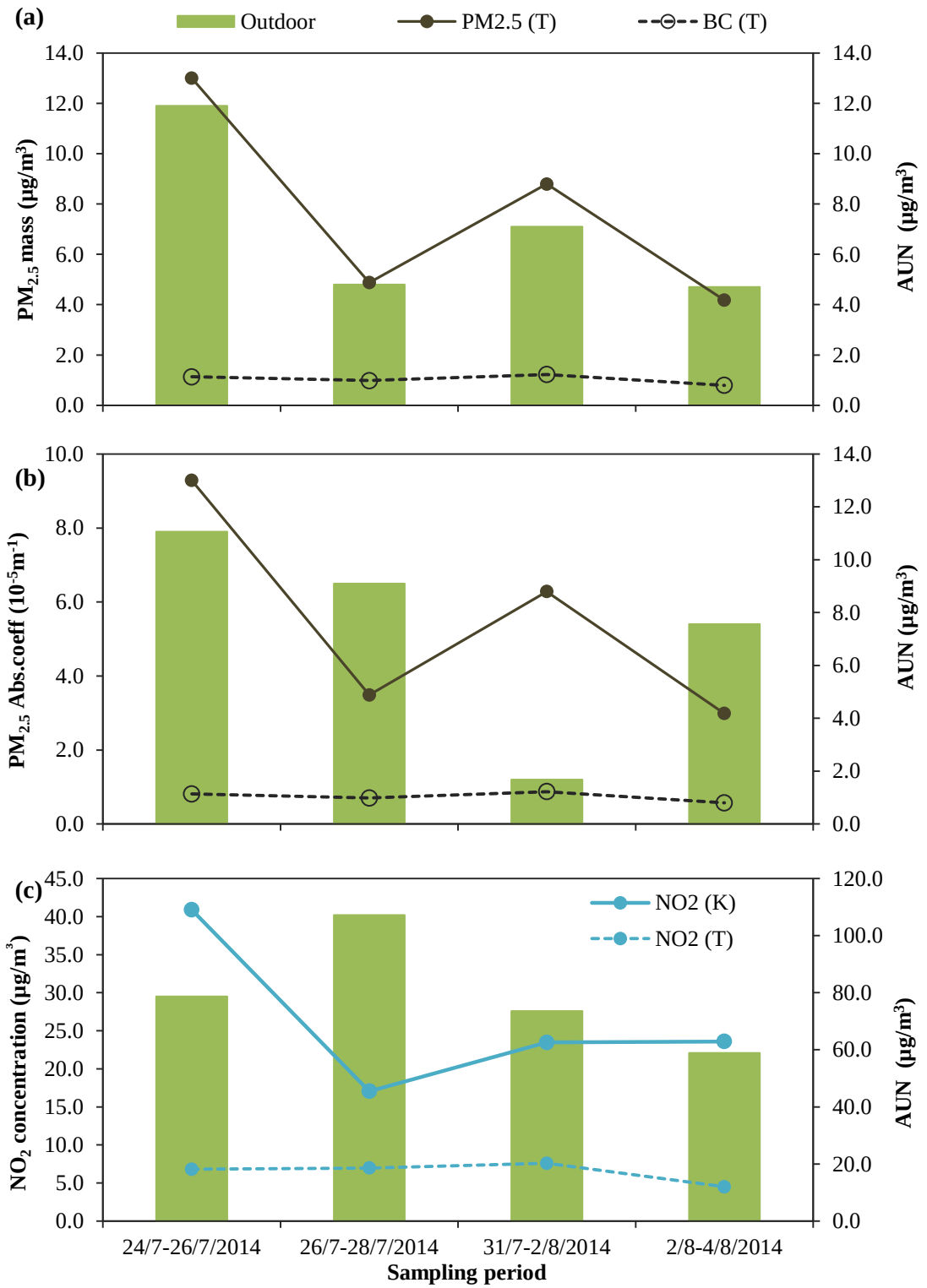

Figure 6.6: Filter-based methods of (a) $PM_{2.5}$ mass and (b) $PM_{2.5}$ absorption coefficient and PDTs measurement of (c) NO_2 concentrations in outdoor background were compared to air pollutants measured at AUN Kerbside (K) and Townhead (T).

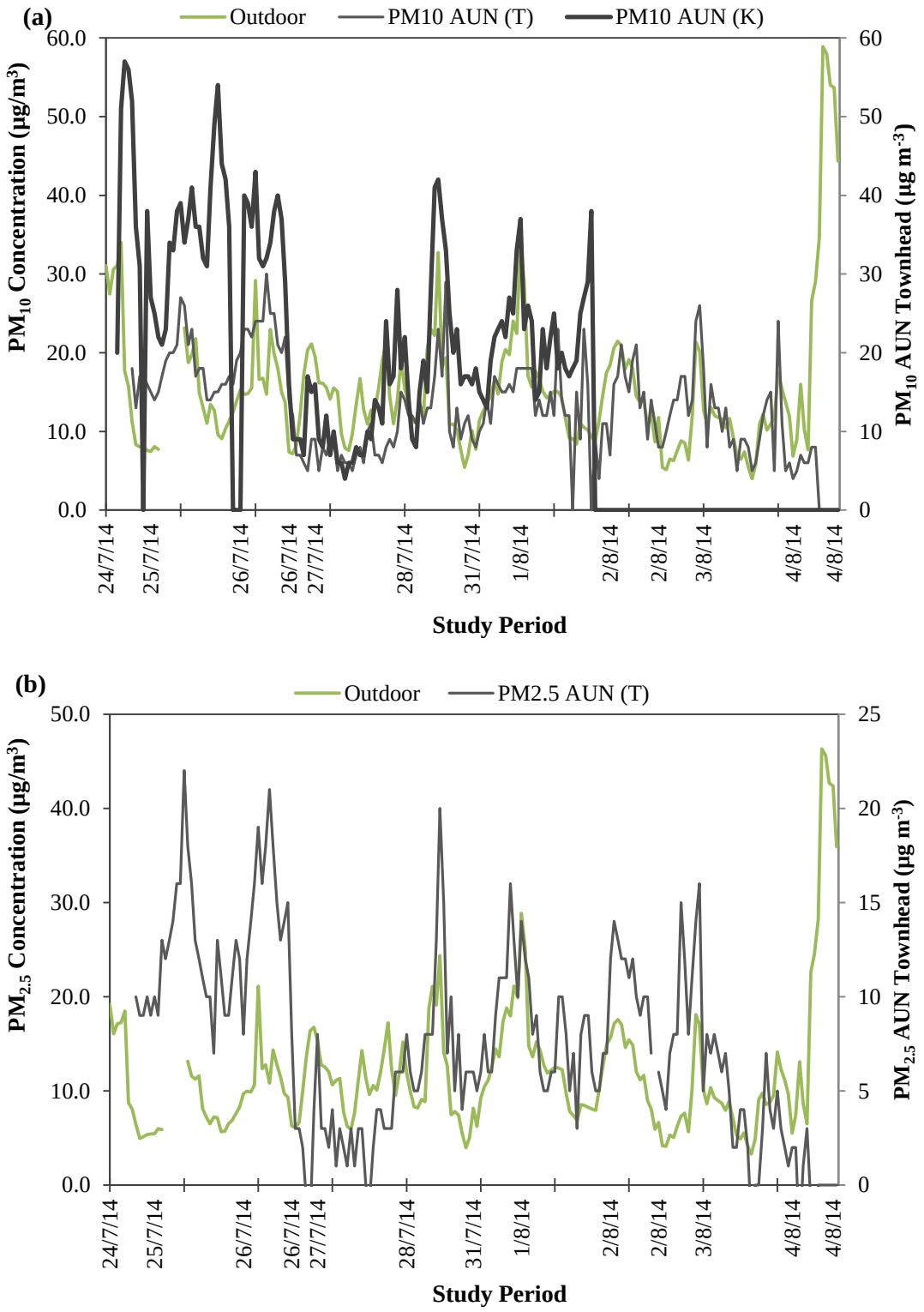

Figure 6.7: Real-time Osiris measurements for (a) PM_{10} and (b) $PM_{2.5}$ mass concentrations in outdoor background were compared with PM_{10} and $PM_{2.5}$ levels measured at Glasgow Kerbside (K) and Townhead (T).

Figure 6.8 below shows the average $PM_{2.5}$ mass, $PM_{2.5}$ absorption coefficient and NO_2 average concentrations across four monitoring periods. A good correlation coefficient (r = 0.61) was found between $PM_{2.5}$ mass and $PM_{2.5}$ absorption coefficient. For NO_2 concentrations, lower correlation was found when compared with $PM_{2.5}$ mass and $PM_{2.5}$ absorption coefficient (r = 0.21 and r = 0.32 respectively).

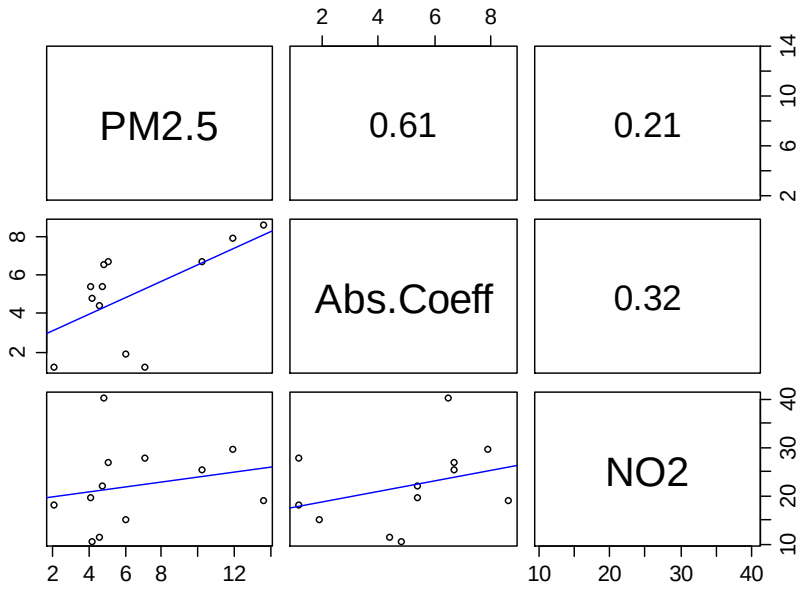

Figure 6.8: Scatter plots for (a) $PM_{2.5}$ mass concentrations ($\mu g/m^3$), $PM_{2.5}$ absorption coefficient (10^{-5} m^{-1}) and NO_2 concentrations ($\mu g/m^3$) in four monitoring sets (n = 12).

6.2.2 Indoor air measurements at ISC

Figure 6.9 (a) – (c) show the relationship between $PM_{2.5}$ BC and NO_2 concentrations measured by pairs of MicroPEM, AE51 Aethalometer and Aeroqual instruments. The instrument pairs used in this study were referred based on the instrument ID. The regression values were derived from the linear equation from 1-min intervals and average of 5-min with each instrument pair. The average 5-min data for MicroPEM (142026 *vs.* 141351) and AE51 Aethalometer (1303 *vs.* 1204) showed a good relationship between the duplicate instruments (R^2 = 0.62 and R^2 = 0.89

respectively). For NO_2 levels, the Aeroqual had only 2881 data points (1-minute intervals) due to faulty data retrieval from the instruments.

RMA regression was performed for pair of LEO 9801266 *vs.* 9801275 and shown in Table 6.3. The comparison was made for 24-hour in the teacher's room and 48-hour in the administration office. The concentration values provided by the two LEO were correlated in both monitoring sites with $R^2 > 0.70$. However, the correlation was poor for NO concentrations measured in the administration office with $R^2 = 0.34$. The NO_2 concentrations recorded by both LEO were all in negative values (min = -88.0 ppb and max = -7.4 ppb) and the O_3 concentrations were too high (min = 24.0 ppb and max = 80.2 ppb). Note that, all measurements were compared without correction and using raw data retrieved from the device.

The correlation of measured RH and temperature from the CP 11 monitor pair are shown in Table 6.4. The RMA regression for temperature had a slightly increased slope of 1.11 compared to RH (1.04). The R^2 values were high for RH and temperature with pair of CP 11 71412146 and CP 11 71412147 ($R^2 \geq 0.99$). This suggests the CP 11 instruments used in this study are reliable for measuring RH and temperature in the indoor environment.

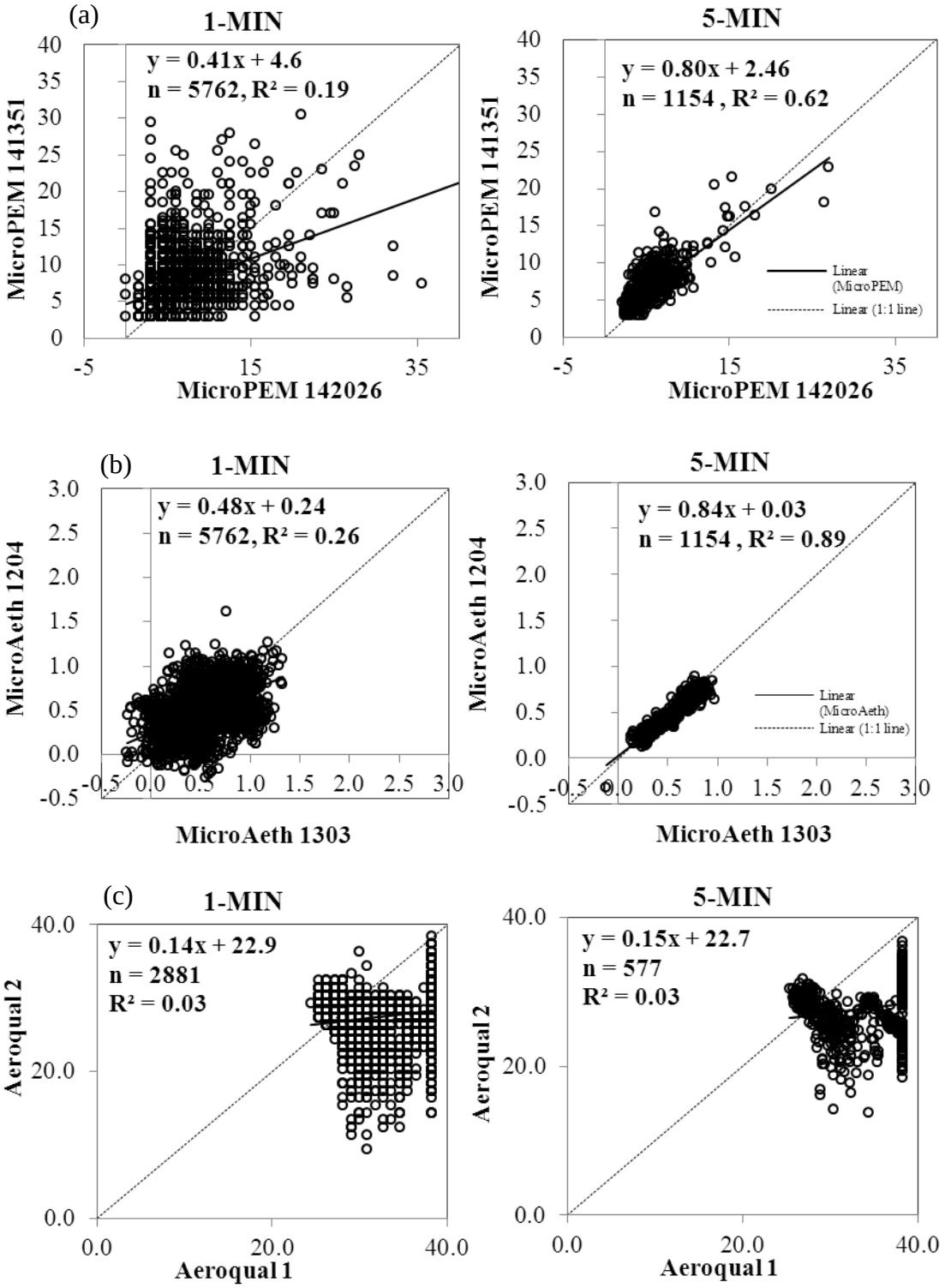

Figure 6.9: Scatter plots of 1-min and 5-min average of: (a) $PM_{2.5}$ concentrations ($\mu g/m^3$) measured by MicroPEM 142026 *vs.* 141351, (b) BC concentrations ($\mu g/m^3$) measured by MicroAeth 1303 *vs.* 1204; and (c) NO_2 concentrations ($\mu g/m^3$) measured by Aeroqual 1 *vs.* 2.

Table 6.3: Summary of inter-comparison LEO 9801266 *vs.* 9801275 sampling instruments for NO_2 (ppb), O_3 (ppb), NO (ppb), T (°C) and RH (%). All measurements were made at 1-min time resolution.

Instrument	n	R^2	RMA Slope (m)	RMA Intercept (c)
Teacher's Room (28 – 29 June 2016)				
LEO NO_2 (9801266 *vs.* 9801275)	1214	0.73	0.36	12.68
LEO O_3 (9801266 *vs.* 9801275)	1214	0.82	0.18	13.27
LEO NO (9801266 *vs.* 9801275)	1214	0.91	0.16	-9.13
LEO T (9801266 *vs.* 9801275)	1214	0.89	0.89	4.51
LEO RH (9801266 *vs.* 9801275)	1214	0.96	0.91	3.3
Admin Office (12 – 14 July 2016)				
LEO NO_2 (9801266 *vs.* 9801275)	2861	0.89	0.81	1.51
LEO O_3 (9801266 *vs.* 9801275)	2861	0.77	0.48	12.84
LEO NO (9801266 *vs.* 9801275)	2861	0.34	1.03	-0.99
LEO T (9801266 *vs.* 9801275)	2861	1.00	1.10	-0.67
LEO RH (9801266 *vs.* 9801275)	2861	0.97	1.07	-1.27

Table 6.4: : Summary of inter-comparison CP 11 71412146 *vs.* 71412147 sampling instruments for temperature (°C) and RH (%). All measurements were taken in 1-min time resolution.

Instrument CP 11	n	R^2	RMA Slope (m)	RMA Intercept (c)
T (71412146 *vs.* 71412147)	11544	0.99	1.11	-3.98
RH (71412146 *vs.* 71412147)	11544	0.99	1.04	-1.17

Table 6.5 shows summary of air pollutants and environmental conditions for the period when all instruments were recorded in indoor and outdoor settings. All indoor measurements from duplicate instruments at teacher's room and administration office were presented in 1-min averaged of data pairs (n = 2881). Hourly measurements from two AUN monitoring sites (Townhead and High Street) were also shown. Note that the summary of descriptive statistics below shows all candidate real-time instruments except for LEO device. The CP11 devices failed recording for 24-hours measurements (12 July 2016) because the instruments had exceeded their memory capacities. The data presented between 12 & 14 July 2016 were recorded from only one set of Aeroqual measurements (NO_2 and O_3). Another replicate set failed to record a valid measurement.

Indoor concentrations of averaged $PM_{2.5}$ were slightly higher in the teacher's room compared to the outdoor measurements made by AUN analysers in Townhead (6.6 $\mu g/m^3$ and 5.0 $\mu g/m^3$ respectively). This is contrary to what was observed in the administration office where $PM_{2.5}$ concentrations were lower than both AUN monitoring sites. Hourly $PM_{2.5}$ and PM_{10} concentrations from 27 - 29 June 2016 were higher compared to measurements recorded between 12 & 14 July 2016 in both AUN monitoring sites. This indicates that outdoor measurements may influence the PM concentrations measured in the teacher's room between 27 & 29 June 2016.

The average NO_2 levels measured in the teacher's room and the administration office were higher than AUN Townhead. The mean BC in both office rooms were similar to each other, 0.5 $\mu g/m^3$ where teacher's room ranged from -0.2 to 1.2 $\mu g/m^3$ and administration office ranged from -0.6 to 1.3 $\mu g/m^3$. Hourly measurements recorded in two AUN monitoring sites for $PM_{2.5}$, BC and NO_2 were higher than instantaneous 1-minute measurements measured by the candidate real-time instruments.

Table 6.5: Summary of all measurements made in the indoor and outdoor environments. 1-min time intervals recorded in the indoor measurement and hourly observations were made in the AUN monitoring sites.

Measurement	27-29 June 2016						12 - 14 July 2016				
	n	Mean	±	SD	Range		n	Mean	±	SD	Range
Teacher's Room						**Admin Office**					
$PM_{2.5}$ ($\mu g/m^3$)	2881	6.6	±	6.7	2.3 - 31.1	$PM_{2.5}$ ($\mu g/m^3$)	2881	2.8	±	1.2	0.0 - 13.6
BC ($\mu g/m^3$)	2881	0.5	±	0.2	-0.2 - 1.2	BC ($\mu g/m^3$)	2881	0.5	±	0.2	-0.6 - 1.3
NO_2 ($\mu g/m^3$)	2881	30.3	±	3.3	2.1 - 54.3	NO_2 ($\mu g/m^3$)	2881	35.5	±	4.9	27.6 - 58.7
T (°C)	2881	20.4	±	1.1	18.8 - 23.4	T (°C)	1441	22.4	±	1.7	20.3 - 20.6
RH (%)	2881	47.8	±	2.9	40.8 - 52.2	RH (%)	1441	43.5	±	2.9	35.9 - 47.0
AUN Townhead (Outdoor)						**AUN Townhead (Outdoor)**					
$PM_{2.5}$ ($\mu g/m^3$)	48	5.0	±	1.3	2.0 - 8.0	$PM_{2.5}$ ($\mu g/m^3$)	48	4.2	±	1.3	2.0 - 7.0
PM_{10} ($\mu g/m^3$)	48	12.4	±	4.4	6.0 - 23.0	PM_{10} ($\mu g/m^3$)	48	8.6	±	2.2	4.0 - 15.0
BC ($\mu g/m^3$)	48	1.2	±	0.6	0.0 - 3.2	BC ($\mu g/m^3$)	48	0.4	±	0.2	0.2 - 1.0
NO_2 ($\mu g/m^3$)	48	14.5	±	5.2	6.0 - 32.0	NO_2 ($\mu g/m^3$)	48	15.2	±	5.5	6.0 -29.0
AUN High Street (Outdoor)						**AUN High Street (Outdoor)**					
$PM_{2.5}$ ($\mu g/m^3$)	48	7.6	±	2.2	2.0 - 13.0	$PM_{2.5}$ ($\mu g/m^3$)	48	7.2	±	2.2	2.0 - 12.0
PM_{10} ($\mu g/m^3$)	48	14.6	±	3.9	7.0 - 24.0	PM_{10} ($\mu g/m^3$)	48	11.4	±	3.2	4.0 - 20.0
BC ($\mu g/m^3$)	48	0.5	±	0.3	0.1 - 1.4	BC ($\mu g/m^3$)	48	1.7	±	1.1	0.0 - 6.5

Figure 6.10 (a) & (b) show the time-series for hourly $PM_{2.5}$, BC and NO_2 concentrations in teacher's room and administration office. The hourly $PM_{2.5}$ and NO_2 levels measured in both AUN monitoring sites were variable with the same trend being followed by the indoor measurements in both office rooms. The BC levels recorded for the whole period of indoor measurement appeared to be relatively low. The major peaks in BC concentration were generally matched with NO_2 concentrations observed in AUN Townhead.

Figure 6.11 (a) & (b) show time series of the levels of NO_2, NO and O_3 monitored by two LEO devices at the teacher's room and admin room. These measurements were compared with NO_2, NO and O_3 recorded by the nearest AUN monitoring sites in Townhead and High St. Both of NO_2 and NO levels were showing in negative values recorded by two LEO. O_3 concentrations from the reference sites in Townhead and High St. exceeded the measurements monitored by LEO sensors. NO_2, NO and O_3 levels measured by two LEO were unlikely to show much temporal changes in hourly peak.

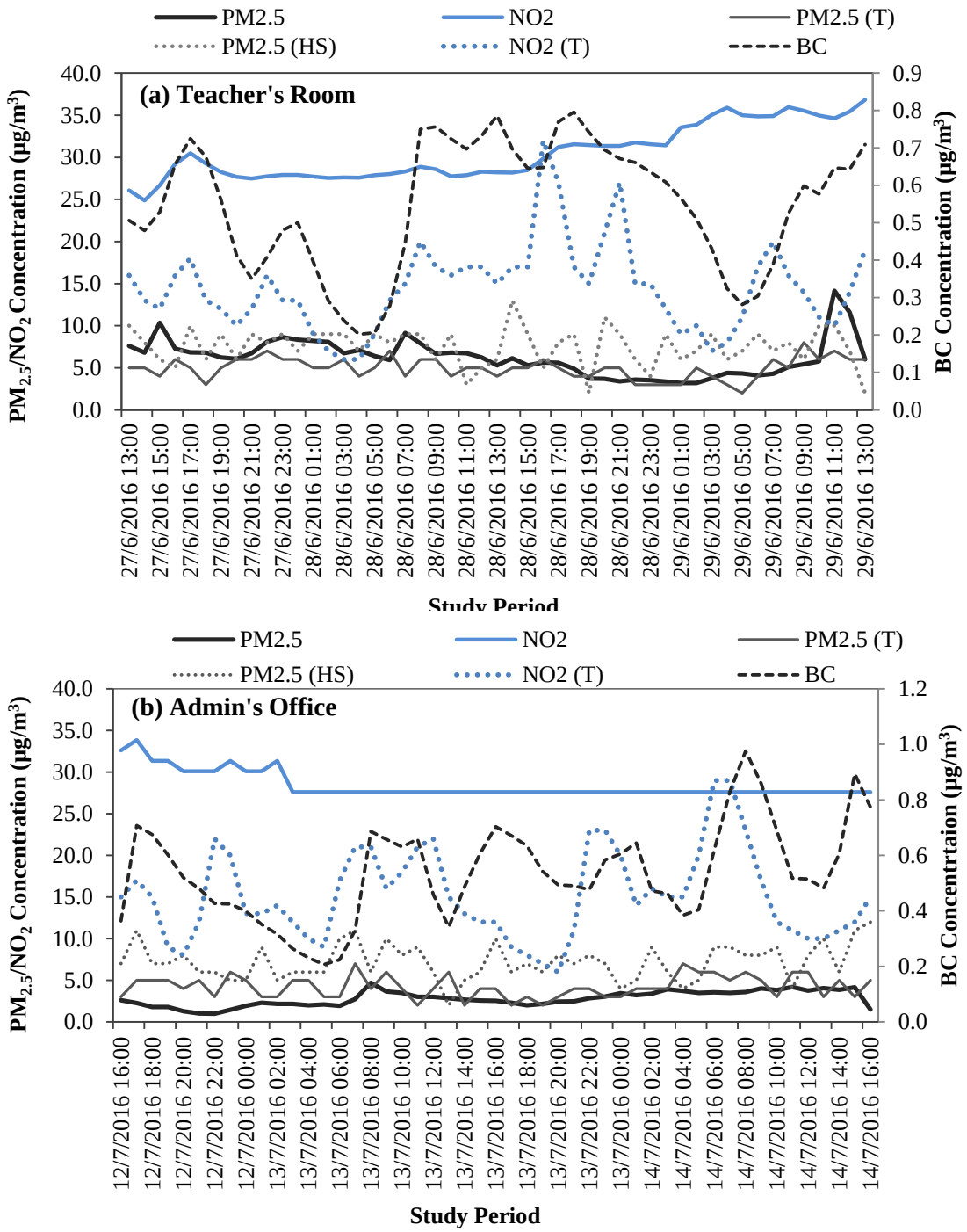

Figure 6.10: Time series of $PM_{2.5}$ (MicroPEM), BC (MicroAeth) and NO_2 (Aeroqual) measured in (a) teacher's room and (b) admin's office compared with measurements made in AUN Townhead (T) and AUN High St. (HS) monitoring sites. All measurements were in hourly averaged.

(a) Teacher's Room

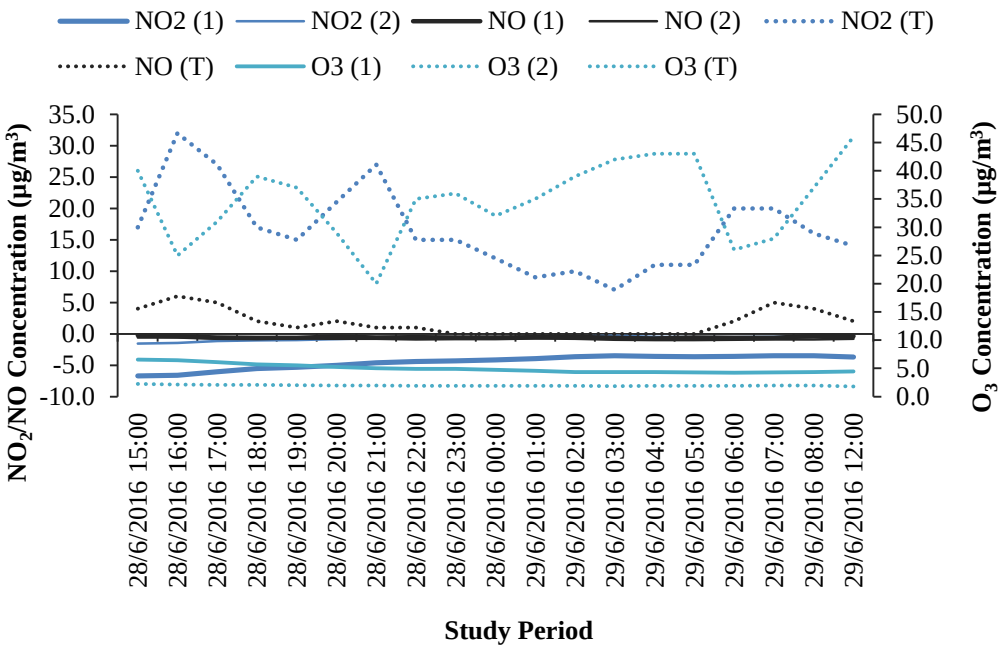

(b) Admin Office

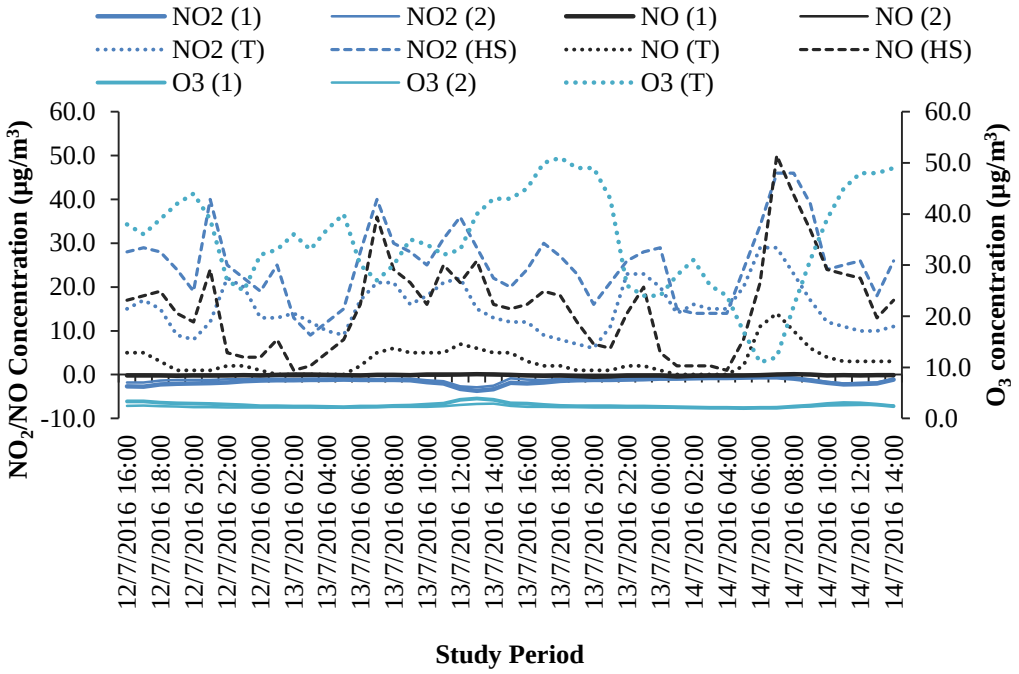

Figure 6.11: Time series of NO_2, NO and O_3 measured by LEO 1 (9801266) and LEO 2 (9801275) in (a) teacher's room and (b) admin office compared with measurements made in AUN monitoring sites in Townhead (T) and High St. (HS). All measurements were in hourly averaged.

Figure 6.12 (a) & (b) shows the scatter plot matrices between $PM_{2.5}$, BC and NO_2 from indoor (teacher's room and administration office) and outdoor (AUN monitoring sites) measurements. There was a moderate correlation (R^2 = 0.44) between $PM_{2.5}$ in teacher's room and at AUN Townhead. The urban background site at AUN Townhead was located approximately 1 km from the building office and far from the nearest busy road. This suggests that $PM_{2.5}$ concentrations are likely to be reduced through the dilution process before it gets infiltrated into the building.

There was no correlation observed between $PM_{2.5}$ in the administration office and at an urban background site in AUN Townhead. A correlation was observed for $PM_{2.5}$ with NO_2 and BC concentrations in the administration office (r = 0.51 and r = 0.38 respectively). Note that the windows in the administration office were closed due to a broken seal from the window's pane. This may imply that the pollutants were being generated from the room. The $PM_{2.5}$ detected at the administration office could have come from the printer located in the room, which would explain a reasonable correlation between $PM_{2.5}$ and BC (r = 0.38).

The NO_2 concentrations measured in the teacher's room showed high correlation with NO_2 observed at two AUN monitoring sites. There was a good correlation between the BC and NO_2 levels measured in the teacher's room and both AUN monitoring sites. They showed a common trend in BC and NO_2 concentrations that was being followed by the indoor environment. This could be attributed to the fact that the BC and NO_2 concentrations in the teacher's room might have originated from traffic emissions. However, such relationship was not observed for both pollutants in the administration office and AUN monitoring sites. This is likely to be as a result of the Aeroqual that malfunctioned during 12 – 14 July 2016 observations.

(a) Teacher's room (27 – 29 June 2016)

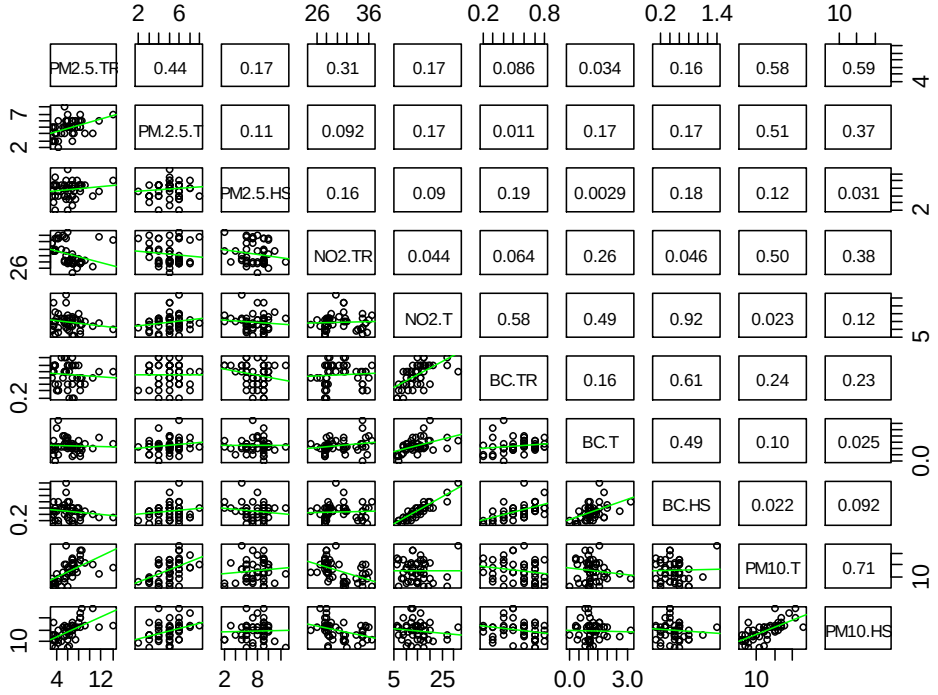

(b) Admin's office (12 – 14 July 2016)

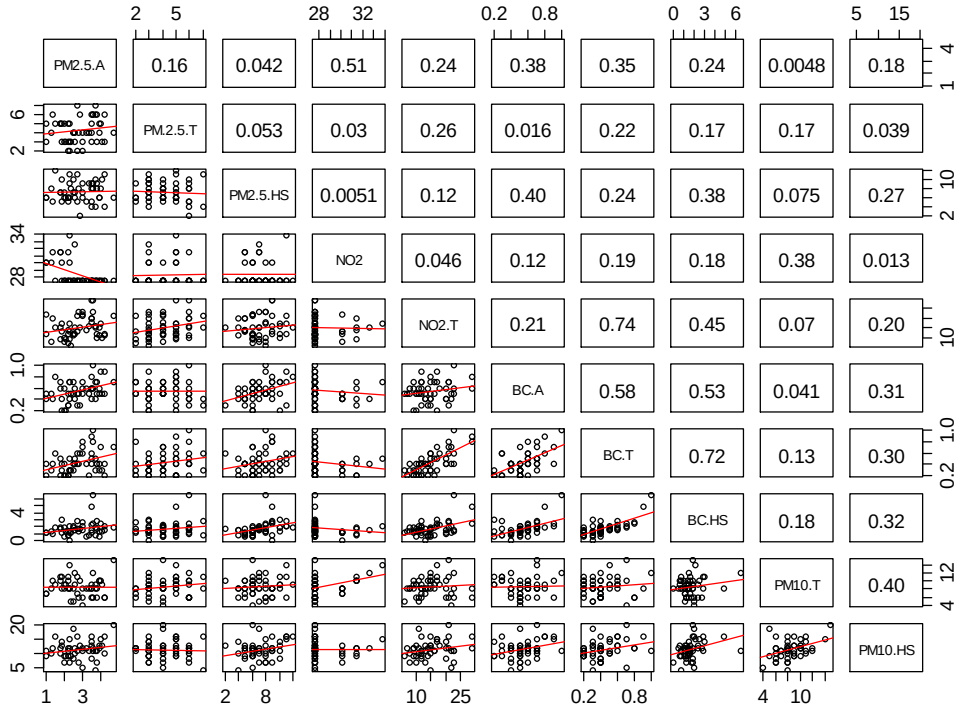

Figure 6.12: Relation between $PM_{2.5}$, PM_{10}, BC and NO_2 concentrations in AUN Townhead and AUN High Street compared with indoor (a) teacher's room and (b) admin's office measurements, (n = 48). All measurements were averaged in one-hour time-interval.

Summary of the average 8-hour of PM, BC and NO_2 concentrations are shown in Table 6.6. A worker in teacher's room would be exposed to 2.4 times the $PM_{2.5}$ concentrations of a worker in the administration office during the same working period. The study only involved short measurement periods due to security issues. There was no safety guarantee for the instruments to be left in the ISC offices overnight. The presence of office occupants during daytime was also considered to possibly influence the particle concentrations.

Table 6.6: Average air pollutant concentrations for $PM_{2.5}$, BC and NO_2 during working hours (09:00 – 17:00). All measurements were averaged in hourly observations.

Measurement	Teacher's Room (26 - 29 July 2016)				Admin Office (12 - 14 July 2016)			
Pollutant	Mean	SD	Min	Max	Mean	SD	Min	Max
$PM_{2.5}$ ($\mu g/m^3$)	7.2	25.0	4.9	14.2	3.0	0.8	1.5	4.2
BC ($\mu g/m^3$)	0.7	0.1	0.5	0.8	0.6	0.1	0.4	0.9
NO_2 ($\mu g/m^3$)	30.2	3.1	24.9	35.5	28.4	1.9	27.6	33.8

6.3 Discussion

6.3.1 Validation of integrated filter-based PM measurements

The gravimetric method used in this study suggests to be a reliable technique to estimate $PM_{2.5}$ personal exposures in the indoor environment. This is supported by the excellent correlation ($r = 0.96$) between 48-hour mean $PM_{2.5}$ mass concentrations in the urban outdoor and the AUN Townhead during the first monitoring event. Note that this method has been a fundamental technique for reference measurements of $PM_{2.5}$ and PM_{10} in Europe and USA (Tasić *et al.*, 2012).

Absorption coefficients were moderately correlated with $PM_{2.5}$ mass concentrations ($r = 0.61$, $n = 12$). This shows that the general trend of carbonaceous particle emissions was not majorly contributed from the fine mass particles of $PM_{2.5}$. Conversely, Hsu *et al.* (2012) observed high correlations between $PM_{2.5}$ mass and BC outdoors. The different sources of elemental carbon concentrations and seasonal factor may explain the discrepancy of correlations between $PM_{2.5}$ mass and fine particles absorbance. Gotschi *et al.* (2002) highlighted that the reflectance measurements of particle specimens can be a proxy of PM outdoor emissions. This also allows recommendation for additional low-cost reflectance measurements to measure BC exposure in a coarse particle size (PM_{10}).

6.3.2 Validation of passive samplers for NO_2 indoor air monitoring

Results for NO_2 concentrations measured by triplicate PDTs in the urban outdoor showed 63% overestimation when compared to NO_2 measured by the chemiluminescent analyser in Townhead site. In contrast, the NO_2 levels measured in Glasgow Kerbside were higher than the urban outdoor measurements. This result is unsurprising as this monitoring station measured urban traffic emissions that gave rise to the recorded pollutant levels.

Cape (2005) has outlined advantages of using passive samplers to measure NO_2 in the indoor environment including no significant effects can be observed from the wind turbulence and direct sunlight exposure. The disadvantages also outlined in the study included lack of wind mixing inside the tube which may affect the diffusion rate of NO_2 and that PDTs sampling may produce large spatial variability in the indoor. However, the mean variation of the coefficient for triplicate tubes used in this study was lower than what has been observed by Heal *et al.* (1999) during short-term indoor measurements. In Heal *et al.* (1999) study, the duplicate PDTs were analysed using a colorimetric technique whereas in this study, all PDTs were quantified using UV-Vis absorbance methods.

6.3.3 The real-time sensors evaluation in the indoor environment

The arithmetic mean of $PM_{2.5}$ mass concentrations across all sampling periods observed by Osiris monitors was 31% higher than $PM_{2.5}$ filter specimens. A higher underestimation of the Osiris monitors $PM_{2.5}$ measurements over filter-based methods that showed 67% difference was observed by Tasić *et al.* (2012). Their study has suggested that the Osiris monitor provided a valuable relationship between continuous PM_{10} measurements and filter-based PM_{10} mass. Conversely, the continuous $PM_{2.5}$ measurements made by a tapered element oscillating microbalance (TEOM) system has found underestimation of $PM_{2.5}$ mass concentrations using filter-based methods (Lee *et al.*, 2005). The Osiris instrument provided real-time profiles for PM_1, $PM_{2.5}$, and PM_{10} of temporal variations, despite experiencing instrument failure during the study period. The incomplete capture of particle size distribution may result in the poor Osiris measurements.

MicroPEM and AE51 Aethalometer sensors provided stronger correlation when compared to each pair in 5-min average of data points. Wider scatter was noticeable during 1-min and narrow scatter for 5-min average data points were observed for both inter-comparison instruments. This may imply that both sensors of MicroPEM and AE51 Aethalometer were performing better in 5-min time intervals. It is also possible that, with averaged 5-min, the fewer data points would give rise to increased correlation. The BC data were showing negative values despite that raw data being treated by Hagler *et al.* (2011) to reduce noise and post-processed with equation adopted from Apte *et al.* (2011). This is because the MicroAeth instruments were performed in very low BC concentrations and applied in a high time resolution (1-min).

Cheng and Lin (2013) found that 5-min averaged level reduced the noise in the BC measurements. In the indoor kitchen measurement conducted by Chartier *et al.* (2016), the results reported by the MicroPEM measurements found a minor bias from the modelling evaluated in lower indoor levels compared to personal exposure measurements. The instruments were deployed near the combustion sources (1.5 m

away from the cook stove) and this was potentially a source of bias in their study. The need for additional investigation is essential especially using MicroPEM in the indoor office.

During the Aeroqual evaluation, it was noted that an equipment for measuring NO_2 and O_3 malfunctioned during the second phase of monitoring. The two NO_2 instruments did not relate to each other although the same correction equation was applied to the values of NO_2. The correction equations were derived from the calibration experiment at AUN Townhead from 1 - 4 June 2016. The corrected NO_2 concentrations measured during the monitoring periods overestimated the measurement made from the AUN background site. The established correction methods adopted from (Lin *et al.*, 2015) where the instruments were collocated in the outdoor environment could have potentially over-adjusted the measurements applied in the lower indoor concentrations. The difference may also be as a result of the distance of the collocated site from the office building. This suggests that the collocated measurements for the indoor environment should be sited near to the indoor Aeroqual.

The LEO test results showed that the correlation between the pair of LEO instruments was good for O_3, temperature, and relative humidity measurements. However, the short inter-comparison period and poor measurements indicated from the negative drift values of NO_2 had suggested that there has been an issue with the LEO to measure pollutants in lower concentrations and thus periodic calibration is needed for this instrument. As mentioned earlier, the LEO sensors were still under field test and no established correction methods were published in any study yet. This electrochemical sensor is typically less sensitive to the environmental changes and requires a longer response time compared to other types of indoor sensors. Kim *et al.* (2016) highlighted that the ability of the real-time sensor to process information was still minimal, although the monitor may measure more than one pollutant on one occasion. Note that, this sensor is not specifically designed to evaluate the quality of indoor environment.

6.3.4 Outdoor sources to the indoor settings

Overall, the indoor pollutant concentrations measured during the course of this study were generally lower compared to the outdoor pollution criteria specified in the UK National Air Quality Strategy and associated EU directives (DEFRA, 2007). Indoor monitoring at the DEE showed that concentrations of all the pollutant metrics were higher outdoors compared to the open plan office, and in turn concentrations in the open plan office were (in all but one set of NO_2 measurements) higher than the cubicle office. Yahya (2014) measured bioaerosols concentrations in the same building within the same period when the measurement took place. The number of microbes was found highest in the outdoor (measured near the office window) (Figure 6.13 (a) & (b)). This is similar to what have been observed from NO_2 measurements during the study period.

The averaged particulates levels in the cubicle area were relatively low and this confirmed that the filtration system within the mechanical means was in good working condition. The pattern of exposure may have resulted from supply and filtration of initially cleaner from rooftop level (4 floors higher than offices studied) to the ventilation system for the cubicle offices. This is in line with the variation of indoor and outdoor PM levels observed by Gotschi *et al.* (2002) in the opened window.

Schembari *et al.* (2013) found a high correlation between $PM_{2.5}$ and absorption coefficients ($r = 0.78$). Their study has suggested a high infiltration that appeared from indoor and outdoor pollution levels. Apart from that, the carbonaceous particles are predominantly originating from outdoor emissions, where the correlation between urban outdoor and the open area was relatively high for BC measurements from 10 - 24 August 2015. This is similar to what has been found by Gotschi *et al.* (2002) and Baxter *et al.* (2007), where black smoke (BS) and elemental carbon (EC) concentrations in the indoor were influenced by the outdoor sources.

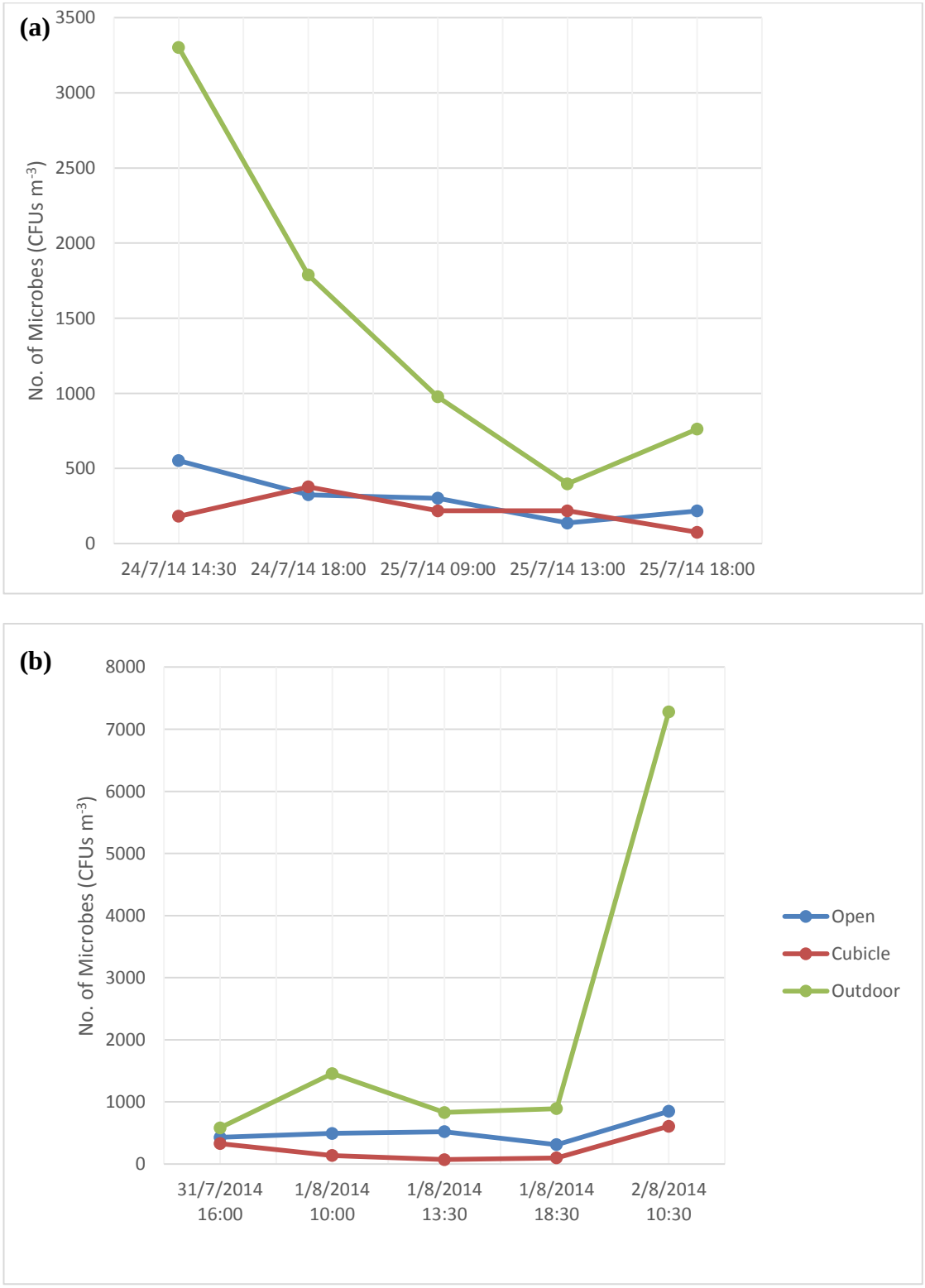

Figure 6.13: Number of microbes over two sampling periods (a) 24/7/2014 – 25/7/2014 and (b) 31/7/2014 – 2/8/2014 (Yahya, 2014).

For measurements at the ISC, the concentrations of $PM_{2.5}$, BC and NO_2 observed differences between the teacher's room and the administration office measurements, although a similar ventilation system was employed but the proportion of windows opened varied in both rooms. Windows were always opened in the teacher's room and reported closed in the administration office during the observation periods. In addition, the observation sheet of window opening behaviour was provided to the occupants in both rooms to record the frequency of window opening during working hours. Unfortunately, none of the occupants filled the observation form due to the limited number of sampling days.

The occupants were expected to open the windows, particularly during the heating season (Dutton and Shao, 2010). Air exchange rates were found highest in the summer and lowest in the winter from window opening behaviour that supplied the outside air (Bekö *et al.*, 2016). The window opening behaviour study was highlighted by Rim *et al.* (2013) as a determinant for the infiltration factor, penetration effects and deposition rate of the outdoor particles to the indoor air concentrations especially to the ultrafine PM. Their study only accounts for the particle counts and such elevations of fine particles less than 2.5 μm were likely generated by the presence of the occupants combined with the outdoor concentrations.

Apart from that, comparing seasonal variations will allow the estimation of infiltration capacity between indoor and outdoor levels. This also permits for the consideration of meteorological conditions (i.e. the wind, precipitation, and temperature) undertaken as supplementary information (Hanninen *et al.*, 2011). Kearney *et al.* (2014) also found that the indoor $PM_{2.5}$ concentrations were affected by the outdoor concentrations due to the high infiltration rate during the summer season. However, this indoor study was only done during summer compared to Gotschi *et al.* (2002) study, which conducted in both winter and summer seasons.

The distance of the building to the roadside intersection may suggest the traffic sources influence the indoor pollutant concentrations observed in this study. Thus, the mixing and dilution of the outdoor sources may penetrate to the office rooms through the opening of the windows. Huang *et al.* (2015) reported $PM_{2.5}$ concentrations were highly correlated with the urban residential area, which located near to the traffic roads. As described above, both office buildings are located close to roads. During the first monitoring exercise at DCEE building, $PM_{2.5}$ mass concentrations and $PM_{2.5}$ absorption coefficient in the mechanically ventilated cubicle office were highly correlated with urban outdoor and the open space office.

Similarly, correlations between BC and NO_2 concentrations measured in the teacher's room at ISC and outdoor AUN High St monitoring site are of particular interest, where high correlation has been observed ($r = 0.91$) at ISC building. This is almost similar to those reported by Underhill *et al.* (2015), where the high agreement of BC concentrations was observed between indoor and outdoor in the peri-urban residences located near the roadways. Oxides of nitrogen were found to correlate well with the BC concentrations from the traffic pollution observed by (Atkinson *et al.*, 2016). In contrast, Levy *et al.* (2010) found no relationship between indoor $PM_{2.5}$ and outdoor traffic, however, one should bear in mind that other factors such as particles dispersion and dilution from the wind speed may influence the variations in PM concentrations.

In residential building study in an urban environment, Jung *et al.* (2011) suggested that the ground level released from the traffic and emissions from the chimney may spread their maximum concentrations between third and fifth-floor level. The low-rise building is also suggested susceptible to expose to the business-related emissions for example mixed building with restaurant and storefront. In the present study, the both of office buildings were located on the fifth and eighth floor level at DCEE and ISC respectively.

6.3.5 Indoor sources

The use of office equipment including desktop computers, printers and copiers were reported to emit a range of indoor aerosols (Destaillats *et al.*, 2008, Barrese *et al.*, 2014b). A similar observation was reported from the printer emissions in the office room that influenced indoor pollutant levels (He *et al.*, 2010). Viana *et al.* (2011) also found 25 to 30% of BC concentrations were derived from printer emissions located near to their study area. Several sharp peaks were observed from continuous PM Osiris monitoring in the cubicle office at DCEE building, this is probably from the printing and copying activities undertaken in this room. However, the cubicle room was unoccupied by the academic staff during the course of the sampling events.

The obtained data showed the presence of correlation between $PM_{2.5}$, BC, and NO_2 in the administration office at ISC building, which indicates that these pollutants could have been influenced by indoor sources. During the study period, the administration staff did not frequently use the printer. However, the intensity of copying and printing activities is expected to be higher after the semester break and the printer perhaps being used by the teacher as well. There is also a possibility of the airborne particles to transport the volatile compounds released from the office equipment. Elango *et al.* (2013) found that the printer emitted a greater amount of PM and may cause chronic health effects to the photocopier staff. It would have been informative to record the frequencies of printer activities during the monitoring session. Apart from that, the occupant's activities in the indoor environment are likely to contribute to the pollutant sources (Lai *et al.*, 2006).

6.3.6 Other indoor air quality studies in the UK

Table 6.7 presents measured $PM_{2.5}$ from this study and another indoor air pollution studies in the UK.

Table 6.7: Comparison of average $PM_{2.5}$ measurements ($\mu g/m^3$) from this study and another studies in the UK.

Study	Location	Mean
Semple *et al.* (2012)	Non-smoking & smoking home (Aberdeen & Galway)	6-7 $\mu g/m^3$(non-smoking home) 99 $\mu g/m^3$(smoking home)
Semple *et al.* (2013)	Non-smoking & smoking home (Aberdeen)	4.4 $\mu g/m^3$(non-smoking home) 33.3 $\mu g/m^3$(smoking home)
Steinle *et al.* (2015)	Home and private residential buildings (Edinburgh)	8.4 $\mu g/m^3$(non-smoking home) 10.2 $\mu g/m^3$(private residential building) 3.0 $\mu g/m^3$(office building)
This study	Existing & refurbished office buildings (Glasgow)	2.8- 6.6 $\mu g/m^3$

The average concentrations of $PM_{2.5}$ measured in two offices were similar with mean exposures of $PM_{2.5}$ reported in UK non-smoking homes and office building. This concentration is below recommended WHO guidance for annual exposure to $PM_{2.5}$ (10 $\mu g/m^3$) (WHO, 2005). The concentration of $PM_{2.5}$ measured in the office building is 5 to 15 times lower than smoking homes in Ireland and Scotland.

6.4 Summary

This chapter demonstrates an understanding on the characterization of indoor air pollution through application of low power instrument using traditional and real-time exposure measurement techniques. $PM_{2.5}$ measurements using dedicated filter-based instruments for $PM_{2.5}$ mass concentrations and absorption coefficient of carbonaceous particles have contributed to assess the short-term indoor and personal exposure, even though the detailed analysis of the airborne particles constituent was not performed in this study (i.e: the profile of PAHs especially BaP). Additionally,

the results from the repeated NO_2 measurements had determined the reliability of the PDTs technique, nonetheless, by increasing the number exposure days of measurements may increase the accuracy of the method. Although, the use of these conventional analytical instruments would not provide spatial indoor pollutant data and are labour-intensive, incapable to provide a high degree of resolution to estimate temporal patterns and longer sampling period were required. However, the data can still be utilised to evaluate the health impact assessment, especially to the integrated doses of occupational hazards despite the lower cost compared to the real-time sensor.

The evaluations of real-time sensors have been found to be potentially useful to provide instantaneous indoor PM, BC, NO_2 and CO_2 levels and they are easy to operate. However, a limited number of observations in the dataset and instrument failure explain the lack of consistency in the analyses, especially for PM and NO_2 concentrations evaluated from the Osiris and Aeroqual sensors. The uncorrected LEO data showed poorer measurements and further investigation should focus on the performance and field calibration to provide data correction of this real-time sensors within the indoor environment. The application of the real-time sensors is anticipated to provide high temporal and spatial indoor air pollutant data (Kumar *et al.*, 2016), if the empirical correction and the limiting factor of the operating principal of different sensors can be tackled in the first place. The investigation of calibration and inter-comparison of AE51 Aethalometer and Aeroqual are expanded in the outdoor field test in the next chapter in order to provide good inter-instrument precision and a similar spatio-temporal pattern to simultaneous BC and NO_2 measurements.

The indoor measurements in both refurbished and existing building offices described in this chapter have shown that the indoor pollutant concentrations were strongly influenced by the outdoor combustion-related emissions of PM, BC and NO_2. This is due to the location of the building adjacent to the roadside and coupled with the natural ventilation means. A similar but not entirely consistent pattern was noted

with the PM concentrations and NO_2 observed during the first study (urban outdoor > open-plan > cubicle). It is anticipated that this pattern of exposure resulted from a supply and filtration of initially cleaner air from rooftop level to the ventilation system for the cubicle offices. The results described in this chapter suggests that air quality within office environments can be improved by siting the air intake inlet at increased elevation; and/or that the mechanical ventilation used in this setting may offer some advantage in reduction of exposure to the above pollutants compared to natural ventilation.

In addition, the efficiency of the air change rates, the occupant activities and the presence of the office printers have been observed to contribute to the indoor pollutants measured in the office building at ISC. The average of 8-hour PM, BC and NO_2 levels measured at the ISC building can be used as preliminary levels to estimate the exposure of indoor air pollutants to the office worker. However, the sample size in this indoor study was very small and therefore more measurements are needed for future work. People may be exposed to the different levels of air pollutants where they spent 90% of their time indoor and simultaneously affected by the outdoor emissions in the indoor environment. Apart from that, the individuals are constantly moving in time and space and expose to a great variety of possible sources of pollution in the outdoor environment particularly from traffic exhaust combustion. Consideration of monitoring the indoor-outdoor emissions from field-tests with the state-of-art sampling and analysis methods described from this chapter has bring about the determination of personal exposure at the urban outdoor settings, which described in the next chapter.

6.5 References

Apte, J. S., Kirchstetter, T. W., Reich, A. H., Deshpande, S. J., Kaushik, G., Chel, A., Marshall, J. D. & Nazaroff, W. W. 2011. Concentrations of fine, ultrafine, and black carbon particles in auto-rickshaws in New Delhi, India. *Atmospheric Environment,* 45**,** 4470-4480.

Atkinson, R. W., Analitis, A., Samoli, E., Fuller, G. W., Green, D. C., Mudway, I. S., Anderson, H. R. & Kelly, F. J. 2016. Short-term exposure to traffic-related air pollution and daily mortality in London, UK. *J Expos Sci Environ Epidemiol,* 26**,** 125-132.

Barrese, E., Gioffrè, A., Scarpelli, M., Turbante, D., Trovato, R. & Iavicoli, S. 2014a. Indoor Pollution in Work Office: VOCs, Formaldehyde and Ozone by Printer. *Occupational Diseases and Environmental Medicine*.

Barrese, E., Gioffrè, A., Scarpelli, M., Turbante, D., Trovato, R. & Iavicoli, S. 2014b. Indoor Pollution in Work Office: VOCs, Formaldehyde and Ozone by Printer. *Occupational Diseases and Environmental Medicine*

Baxter, L. K., Clougherty, J. E., Paciorek, C. J., Wright, R. J. & Levy, J. I. 2007. Predicting residential indoor concentrations of nitrogen dioxide, fine particulate matter, and elemental carbon using questionnaire and geographic information system based data. *Atmospheric environment (Oxford, England : 1994),* 41**,** 6561-6571.

Bekö, G., Gustavsen, S., Frederiksen, M., Bergsøe, N. C., Kolarik, B., Gunnarsen, L., Toftum, J. & Clausen, G. 2016. Diurnal and seasonal variation in air exchange rates and interzonal airflows measured by active and passive tracer gas in homes. *Building and Environment,* 104**,** 178-187.

Cape, J. N. 2005. Review of the use of passive diffusion tubes for measuring concentrations of nitrogen dioxide in the air

Chartier, R., Phillips, M., Mosquin, P., Elledge, M., Bronstein, K., Nandasena, S., Thornburg, V., Thornburg, J. & Rodes, C. 2016. A comparative study of human exposures to household air pollution from commonly used cookstoves in Sri Lanka. *Indoor Air*.

Cheng, Y.-H. & Lin, M.-H. 2013. Real-Time Performance of the microAeth® AE51 and the Effects of Aerosol Loading on Its Measurement Results at a Traffic Site. *Aerosol Air Qual Res,* 13**,** 1853-1863.

DEFRA. 2007 *The Air Quality Strategy for England, Scotland, Wales and Northern Ireland*[Online].Available:

https://www.gov.uk/government/uploads/system/uploads/attachment_data/file/69336/pb12654-air-quality-strategy-vol1-070712.pdf [Accessed 23 May 2016].

Destaillats, H., Maddalena, R. L., Singer, B. C., Hodgson, A. T. & McKone, T. E. 2008. Indoor pollutants emitted by office equipment: A review of reported data and information needs. *Atmospheric Environment,* 42**,** 1371-1388.

Dutton, S. & Shao, L. Window opening behaviour in a naturally ventilated school. SimBuild 2010, 4th National Conference of IBPSA-USA, August 11-13, 2010, 2010 2010 New York, NY.

Elango, N., Kasi, V., Vembhu, B. & Poornima, J. G. 2013. Chronic exposure to emissions from photocopiers in copy shops causes oxidative stress and systematic inflammation among photocopier operators in India. *Environmental Health,* 12**,** 1-12.

Gotschi, T., Oglesby, L., Mathys, P., Monn, C., Manalis, N., Koistinen, K., Jantunen, M., Hanninen, O., Polanska, L. & Kunzli, N. 2002. Comparison of black smoke and PM2.5 levels in indoor and outdoor environments of four European cities. *Environ Sci Technol,* 36**,** 1191-7.

Hagler, G. S. W., Yelverton, T. L. B., Vedantham, R., Hansen, A. D. A. & Turner, J. R. 2011. Post-processing Method to Reduce Noise while Preserving High Time Resolution in Aethalometer Real-time Black Carbon Data. *Aerosol Air Qual Res,* 11**,** 539–54.

Hanninen, O., Hoek, G., Mallone, S., Chellini, E., Katsouyanni, K., Gariazzo, C., Cattani, G., Marconi, A., Molnár, P., Bellander, T. & Jantunen, M. 2011. Seasonal patterns of outdoor PM infiltration into indoor environments: review and meta-analysis of available studies from different climatological zones in Europe. *Air Quality, Atmosphere & Health,* 4**,** 221-233.

He, C., Morawska, L., Wang, H., Jayaratne, R., McGarry, P., Richard Johnson, G., Bostrom, T., Gonthier, J., Authemayou, S. & Ayoko, G. 2010. Quantification of the relationship between fuser roller temperature and laser printer emissions. *Journal of Aerosol Science,* 41**,** 523-530.

Heal, M. R., O'Donoghue, M. A., Agius, R. M. & Beverland, I. J. 1999. Application of passive diffusion tubes to short-term indoor and personal exposure measurement of NO2. *Environment International,* 25**,** 3-8.

Hsu, S.-I., Ito, K., Kendall, M. & Lippmann, M. 2012. Factors affecting personal exposure to thoracic and fine particles and their components. *Journal of exposure science & environmental epidemiology,* 22**,** 439-447.

Huang, L., Pu, Z., Li, M. & Sundell, J. 2015. Characterizing the Indoor-Outdoor Relationship of Fine Particulate Matter in Non-Heating Season for Urban Residences in Beijing. *PLoS ONE,* 10**,** e0138559.

Jung, K. H., Bernabé, K., Moors, K., Yan, B., Chillrud, S. N., Whyatt, R., Camann, D., Kinney, P. L., Perera, F. P. & Miller, R. L. 2011. Effects of Floor Level and Building Type on Residential Levels of Outdoor and Indoor Polycyclic Aromatic Hydrocarbons, Black Carbon, and Particulate Matter in New York City. *Atmosphere,* 2**,** 96-109.

Kearney, J., Wallace, L., MacNeill, M., Héroux, M.-E., Kindzierski, W. & Wheeler, A. 2014. Residential infiltration of fine and ultrafine particles in Edmonton. *Atmospheric Environment,* 94**,** 793-805.

Kim, J. B., Kim, K. H., Yun, S.-T. & Bae, G.-N. 2016. Detection of Carbonaceous Aerosols Released in CNT Workplaces Using an Aethalometer. *Annals of Occupational Hygiene*.

Kumar, P., Martani, C., Morawska, L., Norford, L., Choudhary, R., Bell, M. & Leach, M. 2016. Indoor air quality and energy management through real-time sensing in commercial buildings. *Energy and Buildings,* 111**,** 145-153.

Lai, H. K., Bayer-Oglesby, L., Colvile, R., Götschi, T., Jantunen, M. J., Künzli, N., Kulinskaya, E., Schweizer, C. & Nieuwenhuijsen, M. J. 2006. Determinants of indoor air concentrations of PM2.5, black smoke and NO2 in six European cities (EXPOLIS study). *Atmospheric Environment,* 40**,** 1299-1313.

Lappalainen, S., Salonen, H., Salmi, K. & Reijula, K. 2013. Indoor air particles in office buildings with suspected indoor air problems in the Helsinki area.

International Journal of Occupational Medicine and Environmental Health, 26**,** 155-164.

Lee, J. H., Hopke, P. K., Holsen, T. M. & Polissar, A. V. 2005. Evaluation of Continuous and Filter-Based Methods for Measuring PM2.5 Mass Concentration. *Aerosol Science and Technology,* 39**,** 290-303.

Levy, J. I., Clougherty, J. E., Baxter, L. K., Houseman, E. A. & Paciorek, C. J. 2010. Evaluating heterogeneity in indoor and outdoor air pollution using land-use regression and constrained factor analysis. *Res Rep Health Eff Inst***,** 5-80; discussion 81-91.

Lin, C., Gillespie, J., Schuder, M. D., Duberstein, W., Beverland, I. J. & Heal, M. R. 2015. Evaluation and calibration of Aeroqual series 500 portable gas sensors for accurate measurement of ambient ozone and nitrogen dioxide. *Atmospheric Environment,* 100**,** 111-116.

Mohammadyan, M., Ashmore, M. & Shabankhani, B. 2010. Indoor PM2.5 Concentrations in the Office, Café, and Home. *International Journal of Occupational Hygiene* 2**,** 57-62.

Mohammed, M. O. A., Song, W. W., Ma, W. L., Li, W. L., Ambuchi, J. J., Thabit, M. & Li, Y. F. 2015. Trends in indoor-outdoor PM2.5 research: A systematic review of studies conducted during the last decade (2003-2013). *Atmospheric Pollution Research,* 6**,** 893-903.

Quang, T. N., He, C., Morawska, L., Knibbs, L. D. & Falk, M. 2012. Vertical particle concentration profiles around urban office buildings. *Atmos. Chem. Phys.,* 12**,** 5017-5030.

Rim, D., Wallace, L. A. & Persily, A. K. 2013. Indoor Ultrafine Particles of Outdoor Origin: Importance of Window Opening Area and Fan Operation Condition. *Environmental Science & Technology,* 47**,** 1922-1929.

Schembari, A., Triguero-Mas, M., de Nazelle, A., Dadvand, P., Vrijheid, M., Cirach, M., Martinez, D., Figueras, F., Querol, X., Basagaña, X., Eeftens, M., Meliefste, K. & Nieuwenhuijsen, M. J. 2013. Personal, indoor and outdoor air

pollution levels among pregnant women. *Atmospheric Environment,* 64**,** 287-295.

Semple, S., Apsley, A. & MacCalman, L. 2013. An inexpensive particle monitor for smoker behaviour modification in homes. *Tobacco Control,* 22**,** 295-298.

Semple, S., Garden, C., Coggins, M., Galea, K. S., Whelan, P., Cowie, H., Sánchez-Jimenéz, A., Thorne, P. S., Hurley, J. F. & Ayres, J. G. 2012. Contribution of solid fuel, gas combustion or tobacco smoke to indoor air pollutant concentrations in Irish and Scottish homes. *Indoor air,* 22**,** 212-223.

Steinle, S., Reis, S., Sabel, C. E., Semple, S., Twigg, M. M., Braban, C. F., Leeson, S. R., Heal, M. R., Harrison, D., Lin, C. & Wu, H. 2015. Personal exposure monitoring of PM2.5 in indoor and outdoor microenvironments. *Science of The Total Environment,* 508**,** 383-394.

Tasić, V., Jovašević-Stojanović, M., Vardoulakis, S., Milošević, N., Kovačević, R. & Petrović, J. 2012. Comparative assessment of a real-time particle monitor against the reference gravimetric method for PM10 and PM2.5 in indoor air. *Atmospheric Environment,* 54**,** 358-364.

Underhill, J. L., Bose, S., Williams, L. D. A., Romero, M. K., Malpartida, G., Breysse, N. P., Klasen, M. E., Combe, M. J., Checkley, W. & Hansel, N. N. 2015. Association of Roadway Proximity with Indoor Air Pollution in a Peri-Urban Community in Lima, Peru. *International Journal of Environmental Research and Public Health,* 12.

Viana, M., Díez, S. & Reche, C. 2011. Indoor and outdoor sources and infiltration processes of PM1 and black carbon in an urban environment. *Atmospheric Environment,* 45**,** 6359-6367.

WHO 2002. Indoor Air Pollution, Health and the Burden Diseases. Geneva, Switzerland: World Health Organization.

WHO. 2005. *WHO Air Quality Guidelines for Particulate Matter, Ozone, Nitrogen Dioxide and Sulphur Dioxide* [Online]. Available: http://apps.who.int/iris/bitstream/10665/69477/1/WHO_SDE_PHE_OEH_06.02_eng.pdf [Accessed 20 October 2014].

Yahya, N. 2014. *Indoor Air Quality in Refurbished University Offices.* MSc, University of Strathclyde.

7 URBAN OUTDOOR MEASUREMENTS

7.0 Background

Spatial and temporal variations in individual exposure to combustion-related air pollutants can be substantial in urban areas. Kaur *et al.* (2007) categorised some of the determinants of traffic-related air pollution exposures in urban microenvironments, including: mode of transport; meteorological conditions; proximity to traffic; and individual factors. Concentrations of air pollutants may also vary with vertical distance from ground level to human breathing height. For example, Buzzard *et al.* (2009) found that short-term human exposure to airborne particulates emitted from traffic varied with vertical height. As increased urban pollution has been shown to negatively influence the respiratory health of people living near main roads (Bayer-Oglesby *et al.*, 2005) it is important to understand how the exposures of adults and children may differ in both horizontal and vertical dimensions during travel alongside urban roads.

This chapter discusses field-monitoring exercises in Glasgow city centre in two studies using mobile and static monitors to characterise individual exposure to combustion-related air pollutants, including particulate matter (PM), black carbon

(BC) and nitrogen dioxide (NO_2). The use of GPS data to generate maps of BC and NO_2 exposures are described. In addition, this chapter applies the reflectometer and office scanner measurement techniques outlined in Chapter 4 to estimate outdoor BC concentrations.

7.1 Mobile and static measurements of combustion-related pollutants at two heights

7.1.1 Monitoring locations

This study used a mobile pollution monitoring platform ('traffic trolley') designed by Ricardo Energy and Environment. The traffic trolley was equipped with instruments set up to sample air at heights of 0.8 m (approximate inhalation heights of child seated in a pram) and 1.68 m (approximate inhalation heights of a Scottish adult) (Figure 7.1). $PM_{2.5}$ specimens and passive diffusion tubes (PDTs) were collected from the trolley. The traffic trolley was pushed around a designated sampling route in Glasgow city centre. The route was approximately 4 km in length and took more than 1 hour to complete one circuit. During measurement days, the trolley was pushed for up to 10 hours (~8:00 – 18:00).

Passive samplers were deployed at the same 2 heights at 8 fixed locations in street canyon and pedestrian zones along the route to measure NO_2 concentrations (Figures 7.2 & 7.3). PDT site locations were categorised by the distance of the lamppost to the roadside and type of street (Figure 7.3 & Table 7.1). Four sections of Hope St. were studied. Two of these sections (with 3 sites) were separated from roadway areas with vehicles with running engines by official and unofficial parking areas. Two pedestrianised sections of Sauchiehall Street and Buchanan Street were included. Another sampling site in George Street was next to the road connecting the City Centre section to University of Strathclyde campus.

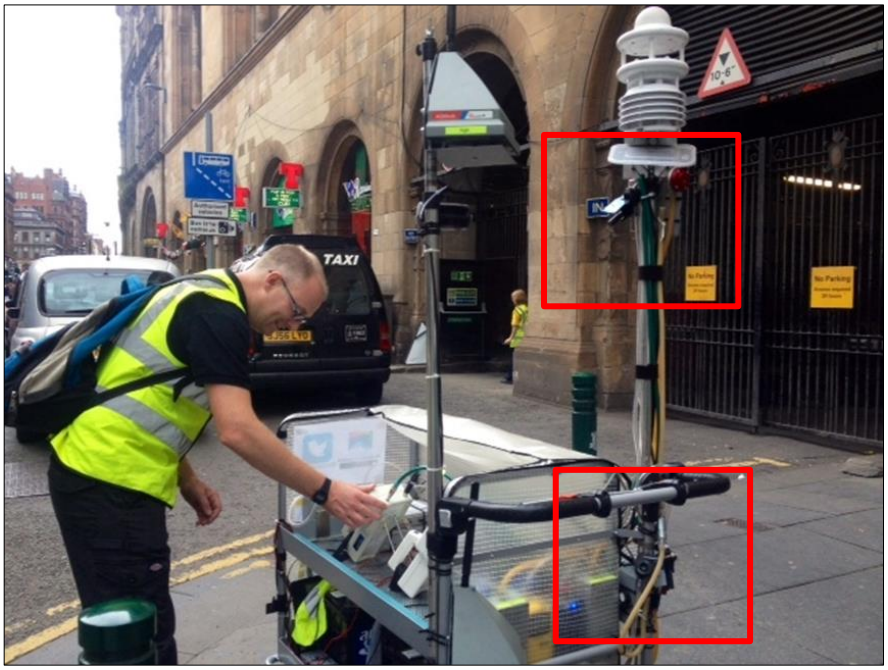

Figure 7.1: Traffic trolley with air pollution equipment (red boxes show $PM_{2.5}$ cyclones at upper 1.68 m and lower 0.8 m heights).

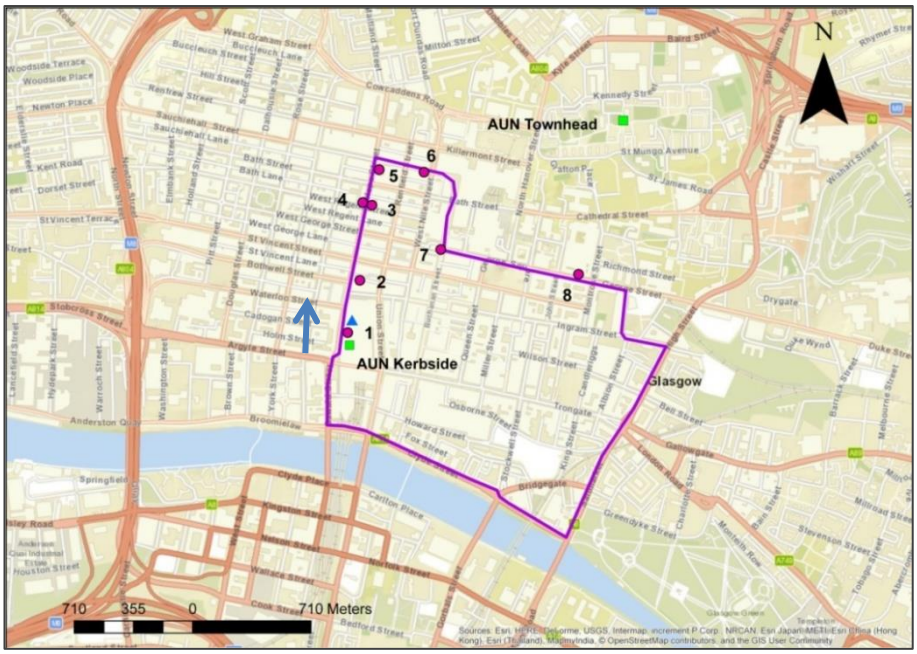

Figure 7.2: Study area within Glasgow city centre. The purple line shows the route that the mobile trolley was pushed along. The points (pink circles) on the map show the locations and names of the static monitoring sites, where NO_2 PDT measurements were made at dual heights. The 'blue' arrow shows the direction that the traffic trolley along the kerbside.

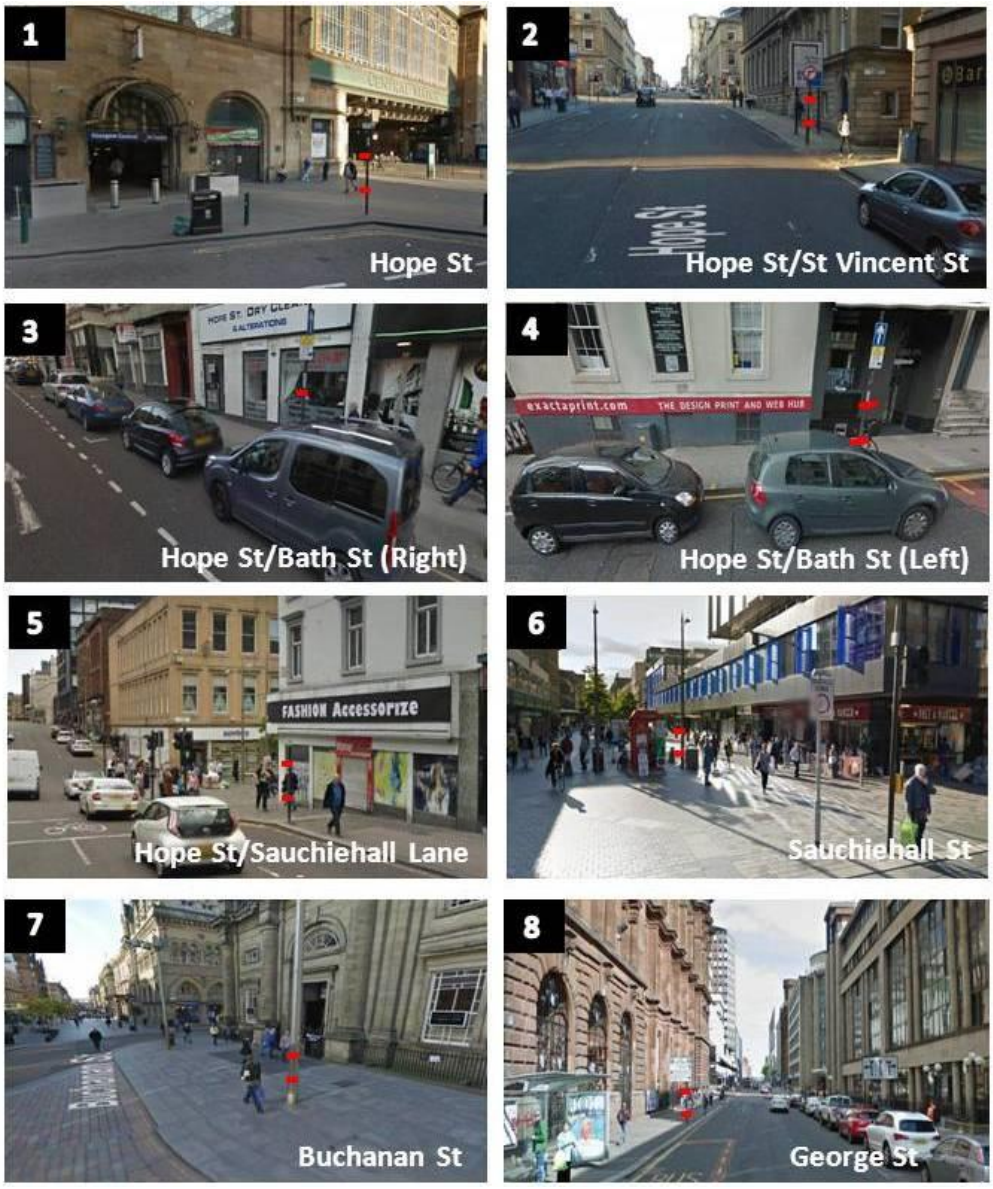

Figure 7.3: Locations where passive samplers were deployed in Glasgow City Centre. Two red markers show lamp posts where PDTs were attached at lower (0.8 m) and upper (1.68 m) heights. Photographs show that sites 3 & 5 were separated from roadway areas with vehicles with running engines by parking bays. Site 4 was also observed most of the time to be some distance from areas of road with running engines as a result of the road layout and unofficial parking (Photo 4).

Images were taken from Google street view (https://www.google.co.uk/intl/en-GB/streetview/).

Table 7.1: Description of PDT monitoring sites. The distance categories were matched to those specified by Kenagy *et al.* (2016).

Monitoring Site	Distance from roadside (m)	Distance category	Sub-group
1. Hope St	0.76	0.7 -0.9 m	Active taxi rank/Urban Canyon
2. Hope St/St Vincent St	0.50	0.5 m	Urban Canyon
3. Hope St/Bath St (Right)	0.66 + 2.5*	2.5 - 3.0 m	Roadside parking/Urban Canyon
4. Hope St/Bath St (Left)	0.68 + 2.5**	2.5 - 3.0 m	Roadside parking/Urban Canyon
5. Hope St/Sauchiehall Lane	0.50 + 2.5*	2.5 - 3.0 m	Roadside parking/Urban Canyon
6. Sauchiehall St	9.0	9.0 m	City centre district/Pedestrianised Lane
7. Buchanan St	2.75	2.5 - 3.0 m	City centre district/Pedestrianised Junction
8. George St	0.74	0.7 -0.9 m	Urban canyon

*Sites 3 & 5 were separated from roadway areas with vehicles with running engines by parking bays. **Site 4 was also noted to be some distance from areas of road with running engines as a result of the road layout and unofficial parking (Figure 6.3(4)). For safety reasons the width of these parking areas were estimated as 2.5 m (https://en.wikipedia.org/wiki/Parking_space)

7.1.2 Experimental design

7.1.2.1 Mobile measurements

Field experiments were conducted over 4 separate periods in July & August 2014 using the traffic trolley with duplicate personal air sampling pumps (BGI, U.S.A) and passive samplers (Gradko Ltd, UK) (section 4.2.1). Pre-weighed 37-mm PTFE filters within respirable dust cyclones were used to collect particle specimens. A rotameter was used to set the flow rate of the personal sampling pumps (section 4.1.1.1) to 3.65 L min^{-1} to approximate $PM_{2.5}$ sampling (MesaLabs, 2016). The cyclones were secured with cable ties at 0.8 m and 1.68 m heights. The times when the pumps were switched on/off, and the PDTs were uncapped/retrieved, were recorded.

7.1.2.2 Static measurements

Static PDT sampling was conducted in two monitoring campaigns. The first campaign involved four sets of measurement in May, July and August 2014. A second campaign with 4 additional sets of measurements was conducted in July 2015. The PDTs were exposed for 3-5 days during each study period. Foam pads were attached to the PDTs using electrical tape prior to attaching the PDTS on the lampposts with cable ties to reduce the risk of vandalism. Over 95% of duplicate tubes deployed were retrieved for inclusion in the data analyses.

7.1.3 Health & safety

Precautions were taken when working outdoors (refer to appendix for appropriate Risk Assessment forms (appendix 10B (3)).

7.1.4 Data analyses

Collected filter and PDT specimens were transferred to the University of Strathclyde (UoS) laboratories to measure $PM_{2.5}$ mass concentration, $PM_{2.5}$ absorption coefficient and NO_2 concentrations (as described in sections 4.1.3.4, 4.1.3.1 & 4.2.1.2). Paired t-tests (two-tailed) were used to determine if the differences in pollutant concentration at 0.8 m and 1.68 m were significant.

7.2 Results

7.2.1 Traffic trolley measurements

Table 7.2 summarises average $PM_{2.5}$ mass, $PM_{2.5}$ absorption coefficient, and NO_2 concentrations. Bioaerosol concentrations measured by Sykes (2014) at the two heights on the trolley during three experiments are shown for comparison. Particle mass concentrations and absorption coefficient were consistently greater at the lower height (0.8 m) compared to those at upper height (1.68 m) (13.6% and 19.2% higher respectively – Table 7.2). Paired t-tests demonstrated a significant difference in $PM_{2.5}$ mass concentrations at 0.8 m and 1.68 m ($p = 0.016$).

This is similar to the differences in $PM_{2.5}$ absorption coefficient, which significant in the paired t-test ($p = 0.017$). There were inconsistent and non-significant patterns in NO_2 and bioaerosol concentration differences between lower and upper heights (Table 7.2). The average measurements at two heights from traffic trolley data were compared with $PM_{2.5}$ and NO_2 concentrations measured at the AUN sites (Kerbside and Background) during the same monitoring day (Table 7.3). NO_2 concentrations measured by PDTs on the traffic trolley were higher than concurrent AUN measurement at Kerbside (Hope St) and Background (Townhead). The average $PM_{2.5}$ concentrations measured at upper and lower heights from the traffic trolley were of similar magnitude to AUN Kerbside. $PM_{2.5}$ urban background concentrations recorded from AUN Background were lower than measured by the traffic trolley.

Table 7.2: The average concentration of $PM_{2.5}$ and NO_2 measured at 0.8 m and 1.68 m on traffic trolley between 8 July – 15 August 2014. Duplicate measurements were made at each height.

Pollutant	Date	Lower ($\mu g/m^3$)	±	SD	Upper ($\mu g/m^3$)	±	SD	Average[a] ($\mu g/m^3$)	±	SD	Average[b] (%)	±	SD	p value	Significant?
$PM_{2.5}$ mass	8/7/2014	14.7	±	1.5	12.5	±	0.4								
	14/7/2014	7.8	±	0.3	7.1	±	0.3								
($\mu g/m^3$)	9/8/2014	12.9	±	0.2	11.3	±	1.0	-1.6	±	0.6	-13.6	±	3.2	0.004	Yes
	15/8/2014	15.2	±	0.3	13.5	±	0.6								
	8/7/2014	5.5	±	0.1	3.9	±	0.1								
$PM_{2.5}$ abs.coeff.	14/7/2014	1.9	±	0.3	1.8	±	0.1								
($10^{-5}m^{-1}$)	9/8/2014	2.1	±	0.1	1.8	±	0.1	-0.6	±	0.7	-19.2	±	15.3	0.017	Yes
	15/8/2014	4.2	±	1.8	3.7	±	0.1								
NO_2	8/7/2014	Nil*													
	14/7/2014	86.6	±	1.9	74.8	±	0.0								
($\mu g/m^3$)	9/8/2014	101.9	±	20.6	106.8	±	5.6	-0.9	±	9.4	-3.1	±	11.1	0.677	No
	15/8/2014	213.1	±	11.9	217.3	±	6.6								
Bioaerosols	8/7/2014	2494	±	97	1951	±	286								
PCA	14/7/2014	2118	±	942	2547	±	1267								
(Sykes, 2014)	9/8/2014	Nil*						-129.3	±	501.9	-10.0	±	23.6	0.542	No
	15/8/2014	1726	±	506	1452	±	265								

[a]average difference between upper & lower heights ($\mu g/m^3$). [b]percentage difference between upper & lower heights (%).

Table 7.3: Summary of $PM_{2.5}$ and NO_2 concentrations ($\mu g/m^3$) from AUN sites and traffic trolley.

Monitoring Sites	Pollutant	Pollutant Concentration ($\mu g/m^3$)			
		8 July 2014	14 July 2014	9 Aug 2014	15 Aug 2014
Traffic trolley	$PM_{2.5}$	14.0	7.0	12.0	14.0
High St (kerbside)		17.0	7.0	19.0	12.0
Townhead (background)		6.0	2.0	6.0	-
Traffic trolley	NO_2	-	80.7	104.4	215.2
High St (kerbside)		72.0	26.0	47.0	61.0
Townhead (background)		23.0	12.0	20.0	28.0

7.2.2 Static measurements using PDTs

128 replicates of passive tubes collected during the 2014 & 2015 monitoring campaigns, with 3 pairs tubes loss due to theft. PDT data from Sauchiehall St collected between 11 – 14th July 2014 were excluded because of laboratory analysis error. NO_2 concentrations measured by duplicate PDTs at both heights at each monitoring site are shown in Figures 7.4 & 7.5.

NO_2 concentrations at the lower and upper heights ranged from 30.3 - 183.5 and 31.1 - 182.3 $\mu g/m^3$ respectively. Highest NO_2 concentrations were observed in Hope Street/Vincent Street. Lowest NO_2 concentrations were observed in George St and Sauchiehall Street in 2014 and 2015 respectively. NO_2 concentrations measured during the monitoring study generally exceeded the UK annual air quality standard of 40 $\mu g/m^3$ (DEFRA, 2004).

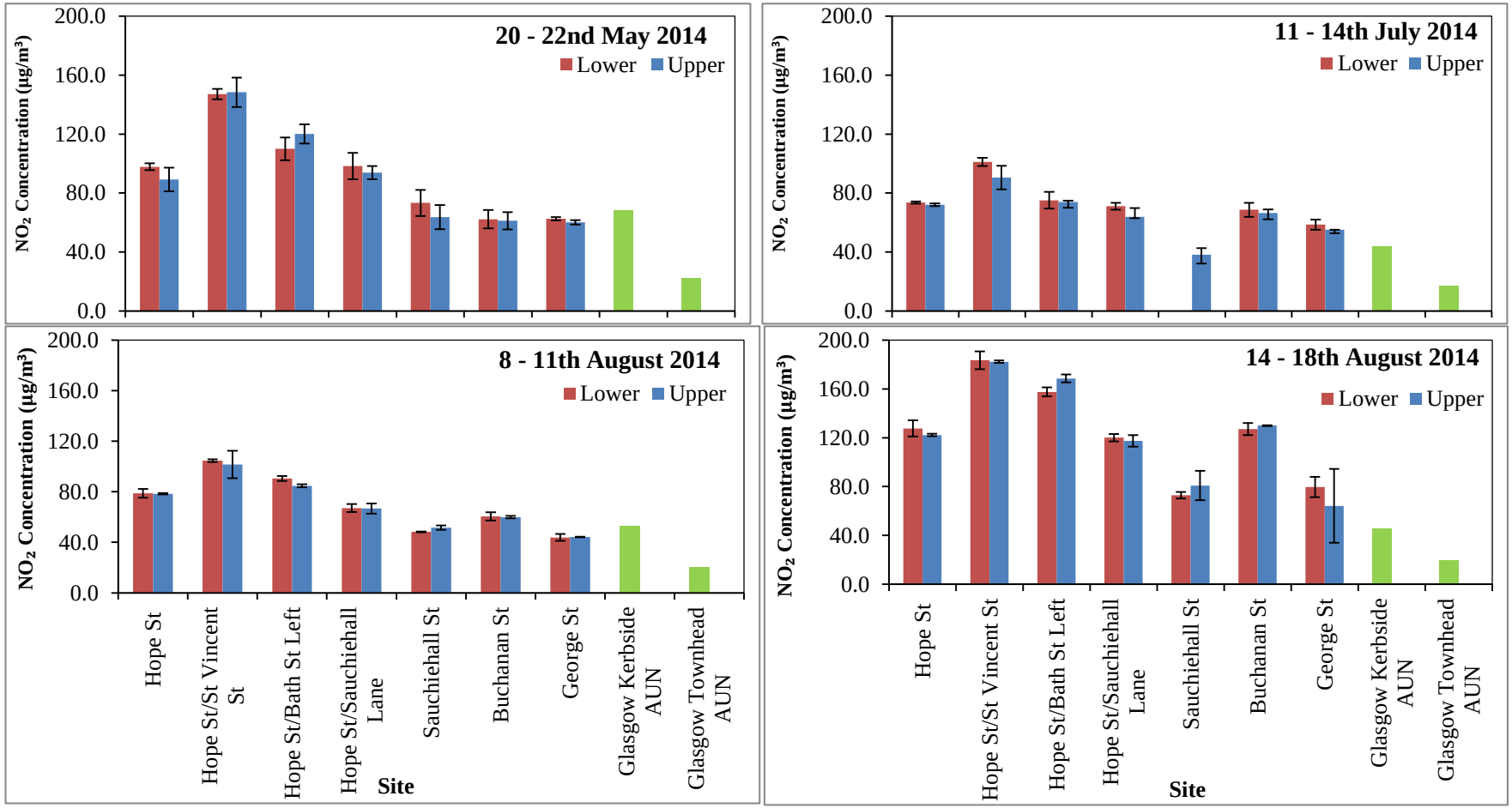

Figure 7.4: Average concentrations of NO_2 measured by PDTs at 1.68 m and 0.8 m during 2014. Green bars show concentrations measured at the AUN sites during the same periods. Error bars represent the standard deviation of duplicate measurements.

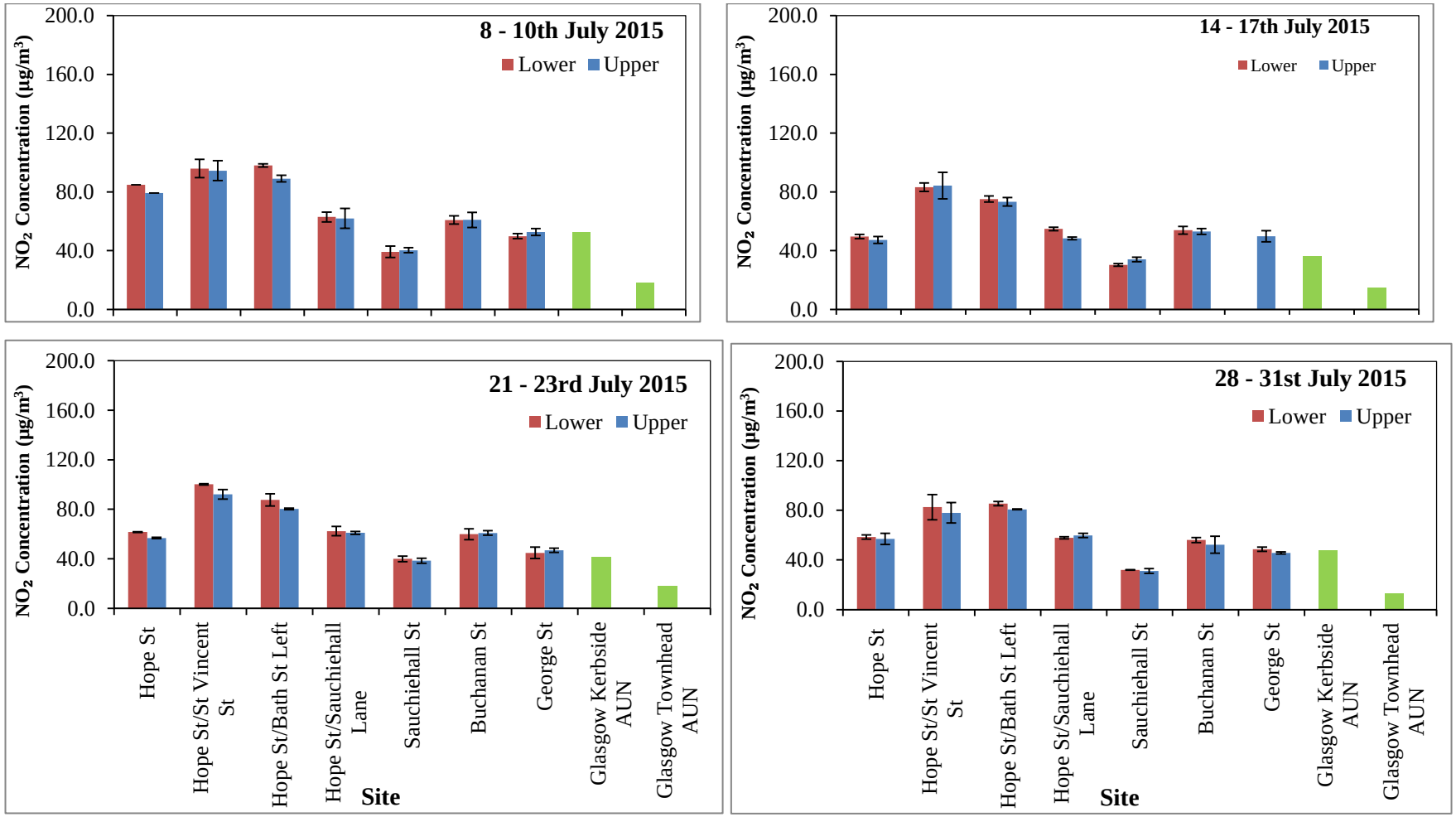

Figure 7.5: Average concentrations of NO_2 measured by PDTs at 1.68 m and 0.8 m during 2015. Green bars show concentrations measured at the AUN sites during the same periods. Error bars represent the standard deviation of duplicate measurements.

Table 7.4 shows average NO_2 concentrations measured at 0.8 m and 1.68 m heights at 7 monitoring sites. The site at Hope St/Bath St (right) site was excluded from the analyses because of incompleteness resulting from lost samples. The data were grouped based on distance from road sections with moving vehicles (allowing for separation of some of the monitoring sites from moving traffic by the presence of roadside parking bays).

Consistently higher NO_2 concentrations were observed at 0.8 m compared to 1.68 m above the ground for most of study sites, with the exception of sites in pedestrian precincts in Sauchiehall St (site 6) and Buchanan St (site 7). The clearest evidence of difference in NO_2 concentration between the two heights occurred at Hope St with mean percentage difference of 4.9% ($p = 0.002$). This suggests that the active service taxis parked near the sampling site contributed to greater combustion-related NO_2 exposures at lower height. A pooled analysis of locations within 2.5 m of moving traffic observed that concentrations were on average 6.5% greater at the lower height ($p = 0.01$, $n = 23$). A paired t-test on locations greater than 2.5 m from the road showed no significant evidence measurements at upper and lower heights ($p = 0.30$, $n = 31$).

Table 7.4: Summary of differences in NO_2 concentrations measured by PDTs at upper and lower heights during 2014 and 2015 monitoring exercises.

Descriptions	N	Lower ± SD ($\mu g/m^3$)	Upper ± SD ($\mu g/m^3$)	Average[a] ± SD ($\mu g/m^3$)	Average[b] ± SD (%)	p value	Significant?
Site number & monitoring site*							
1. Hope St	8	79.0 ± 25.0	75.3 ± 23.6	-3.8 ± 2.8	-4.9 ± 3.2	**0.002**	**Yes**
2. Hope St/St Vincent St	8	112.3 ± 35.1	105.4 ± 39.8	-6.9 ± 12.6	-9.8 ± 19.9	0.120	No
4. Hope St/Bath St Left	8	97.4 ± 26.9	96.3 ± 32.8	-1.1 ± 7.6	-2.6 ± 6.8	0.468	No
5. Hope St/Sauchiehall Lane	8	74.3 ± 22.8	71.6 ± 22.6	-2.7 ± 3.1	-4.1 ± 5.5	**0.018**	**Yes**
6. Sauchiehall St	7	48.0 ± 18.1	48.6 ± 18.1	0.8 ± 5.5	2.0 ± 9.0	0.860	No
7.Buchanan St	8	68.6 ± 24.1	68.1 ± 25.4	0.4 ± 2.0	0.5 ± 3.3	0.070	No
8.George St	7	55.4 ± 12.7	52.7 ± 7.6	-2.7 ± 6.2	-6.9 ± 12.6	0.160	No
Distance from roadside							
0.5 – 0.9 m from road (sites 1,2, 8)	23	83.4 ± 34.5	78.9 ± 34.3	-4.5 ± 8.2	-6.5 ± 12.7	**0.010**	**Yes**
> 2.5 m from road	31	70.6 ± 30.7	71.9 ± 29.6	-1.0 ± 4.9	-1.8 ± 6.4	0.30	No

[a]average difference between upper & lower heights ($\mu g/m^3$). [b]percentage difference between upper & lower heights (%).

* site 3 at Hope St/Bath St Right was excluded.

7.3 Discussion

Both mobile and static measurements from urban Glasgow city centre show evidence to suggest that there are increased concentrations of $PM_{2.5}$ mass, $PM_{2.5}$ absorption coefficient (BC) and NO_2 closer to the ground (Table 7.2 and Table 7.4). This is consistent with recent studies conducted on PM and NO_2 in Edinburgh (Kenagy *et al.*, 2016) and Barcelona (Garcia-Algar *et al.*, 2015), showing greater pollutant concentrations at lower height compared to upper height.

In mobile trolley study, the average $PM_{2.5}$ mass and $PM_{2.5}$ absorption coefficient were 13.6% and 19.2% respectively higher at the lower height. This result agrees well with what have been observed by Sykes (2014) and Stratton (2014) with 10% increase of bioaerosols concentrations and particulate number at the lower height using the same traffic trolley. In a study evaluating fungal spores at adult breathing height and roof building height, Khattab and Levetin (2008) reported that fungal aeroallergens concentrations were higher at the ground level.

However, the findings are contrary with Galea *et al.* (2015), where their study found that adults were highly exposed to air pollutants compared to children. Although the two studies design was similar using a mobile platform, there were differences in the methods that may have influenced the difference in results. This study encompassed a full day of measurements during both weekdays and weekends compared to Galea *et al.* (2015), whose measurements were made during a weekday morning. Additionally, this study utilised filters to collect the particle specimens, which provide a single concentration for the duration of the study period whereas the Galea work used real-time device recording $PM_{2.5}$ concentrations in 10 seconds time-based. The advantage of this direct reading instruments is that clear peak in concentration can be observed and compared for the different heights. Other important influential factors that were not discussed in this study include traffic density and meteorological conditions.

All instrument were consistently allocated at the lower (as 0.8m – children) and upper heights (as 1.68 m –adult) during the course of the monitoring period. The devices being calibrated and maintained the airflow, therefore this should be considered that the findings were not influenced by the instrument effect. However, to try to understand the instrument effect to the two height measurements, it would be ideal to conduct additional co-location comparison using similar instrument (Galea *et al.*, 2015). It is also recommended that paired pumps be used at upper and lower heights, which would give duplicate samples (Sykes, 2014).

It is suggested that the changes to the sampling routes during the Team Scotland Athletes' Parade on 15 August 2014 were responsible for the higher $PM_{2.5}$ mass, $PM_{2.5}$ absorption coefficient, and NO_2 concentrations compared to other monitoring periods. The number of samples collected upon traffic trolley was limited due to the duration of sampling campaign and the availability of the trolley to conduct the mobile monitoring exercises depended on the weather condition. Micallef and Colls (1999) suggested that moving platforms can stir pollution from mechanical turbulence. This may explain why the PDTs measured on the mobile platform were not significantly different from two heights compared to the fixed sites where the PDTs were deployed. The mobile PDTs always measured greater concentrations of NO_2 when compared to the AUN site. This may be attributed to the short exposure time, where the mobile measurements captured only daylight hours.

The static measurements of NO_2 provide an indication of longer-term measurements compared to the limited number of mobile studies carried out by the trolley. Analysis of paired t-tests showed that there was a significant difference between the average NO_2 in the upper and lower heights at monitoring sites located near the urban street canyon for the category of 0.5 – 0.9 m from the road. This finding is similar to a study in Slovenia reporting the significant decrease of NO_2 with increasing height at urban canyon street-like (Vintar and Ogrin, 2015). Regardless of the distance of the lamppost and the PDTs were mounted onto the road along the street canyon (Hope St), no difference in the NO_2 levels were observed at the upper

and lower heights near the roadside parking. The turbulent mixing could result in a homogeneous pollutant concentration at a given height range along urban canyon streets (Vardoulakis *et al.*, 2003).

The over predicted PDTs compared with the automatic analysers could be due to the duration of sampling, where PDTs were exposed for 2 - 4 days compared to the measurement for AUN, which took from an hourly snapshot. The difference also could be because of the distant location between the sampler and the monitor inlet. There was no difference between adult and children's exposure to NO_2 concentrations in pedestrian streets (Sauchiehall St. and Buchanan St.). This is similar to what have been observed in Edinburgh study, where there was no statistical difference found at two heights sites that were located more than 3.0 m from the main road (Kenagy *et al.*, 2016). The effect of wind direction and wind speed would be considerable to stir the gaseous concentrations from road traffic emissions. The enclosed sides were observed from commercial buildings at the pedestrian sites on Sauchiehall St and this is likely to decrease the rate and extent of NO_2 dilution. This observation suggests that the variation in NO_2 sampling at two different heights is affected by the street geometry and wind direction.

It was not the focus of this study to assess the difference between children and adult breathing rate or personal factor. However, the explorative technique of monitoring personal exposure using static and moving platform at two heights represented children and adult's breathing height provide an indication of the combustion-related pollutant concentrations at the urban environment differ with height. As the first approach to systematically evaluate the capability and illustrate the potential applications of the developed techniques, the field tests have been extended using wearable real-time instruments and described in section 7.4.

7.4 Monitoring spatio-temporal variability of BC and NO_2

The spatial-temporal variability of BC and NO_2 concentrations were measured while walking on a pre-defined route in Glasgow Central in two separated field campaigns (Table 7.6). This will assess and characterise BC and NO_2 concentrations where the individuals are exposed during commuting in the urban Glasgow city centre. The first campaign was conducted from 29 June – 24 July 2015 during commutes in central Glasgow, namely the city centre route (details are described in section 7.4.1.1).

To elicit the spatial variability of BC and NO_2, the walking route was segmented into four walking zones where primarily higher traffic volumes and other diesel sources from lower gradient pollutions to higher pollution areas of traffic-related activities. This will contrast the pollution concentrations and give a wide range of exposure measurements in the urban environment. The data was also presented in a concentration map to demonstrate the spatial-temporal variability during walking on each monitoring zone in Glasgow city centre.

The second campaign involved walking on a designated route namely the campus network route (details are described in section 7.4.1.2). Personal exposures to BC and NO_2 were measured during the rush hour period to understand the temporal variations in a smaller scale walking area near the UoS avenue. The measurements were conducted on six separate days (between 27 October & 8 December 2015 – Table 7.5) during the morning, mid-day and afternoon rush hour.

Table 7.5: Date of mobile sampling of BC and NO_2 at city centre and campus network routes. Each monitoring period for morning, mid-day and afternoon during campus network campaign was shown.

Date of Study	
City centre route	Campus network route (monitoring period)
30/6/2015	27/10/2015 (morning, mid-day, afternoon)
6/7/2015	3/11/2015 (morning, mid-day, afternoon)
9/7/2015	7/11/2015 (morning, mid-day, afternoon)
14/7/2015	24/11/2015 (morning, afternoon)
15/7/2015	1/12/2015 (mid-day, afternoon)
22/7/2015	8/12/2015 (morning, mid-day, afternoon)
23/7/2015	
24/7/2015	

7.4.1 Sampling site

7.4.1.1 The city centre route

The sampling exercise started and ended at Cathedral St. along with four sections of walking routes; Campus (C – 3.4 km), Pedestrianised precinct (P – 0.5 km) , Hope St. (H - 0.7 km) and Union St. (U – 1.3 km). Each trip took about 72 minutes to complete. The same route was followed each day for 8 trips along 5.9 km of total walking distance.

Total time taken to complete the whole set of route depended on weather condition and the walking pace. The outward journey was taken from C, along the eastern side of Cathedral St. to campus network, residential areas in Townhead and commercial areas in George St. The journey continued to P, at pedestrian zones from Buchanan St to Sauchiehall St and towards the northern side of street canyon at Hope St. The

return journey (U) being made from Argyle St to Union St and passing George St back to Cathedral St. Details of the walking zones are shown in Figure 6.6.

7.4.1.2 The campus network route

The UoS air pollution sources were dominated by high levels of traffic in Cathedral St. It was estimated that 500 – 1000 of vehicles travel on this road during morning rush hour (08:00 – 09:00) (GlasgowCityCouncil, 2015). Overall, the walking route (see below Figure 7.7) was approximately 2.4 km long starting from Cathedral St. to UoS campus street in North Portland St., passing commercial buildings along George St. to the west and towards the steep gradient in Montrose St. and ended at residential area in Townhead. Three trips were carried out in the morning (~8.00 – 9:30 a.m.), mid-day peak (~1.00 – 2:30 p.m.) and afternoon (~4:00 – 5:30 p.m.) during each sampling day depending on the weather conditions.

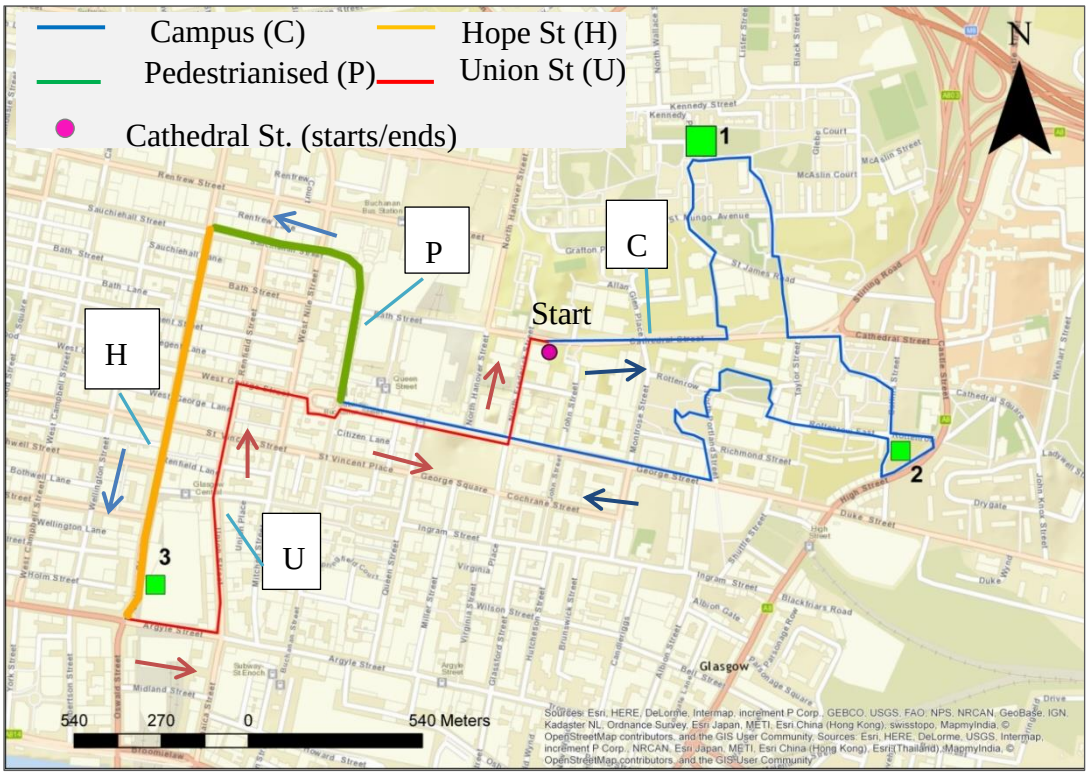

Figure 7.6: Location of the monitoring site and walking routes in the study area. The walking route started at the starting point (blue arrow) and returned to the same point on Cathedral St from Union St. (red arrow). The AUN sites are as follow; (1) Townhead, (2) High St. (3) Hope St.

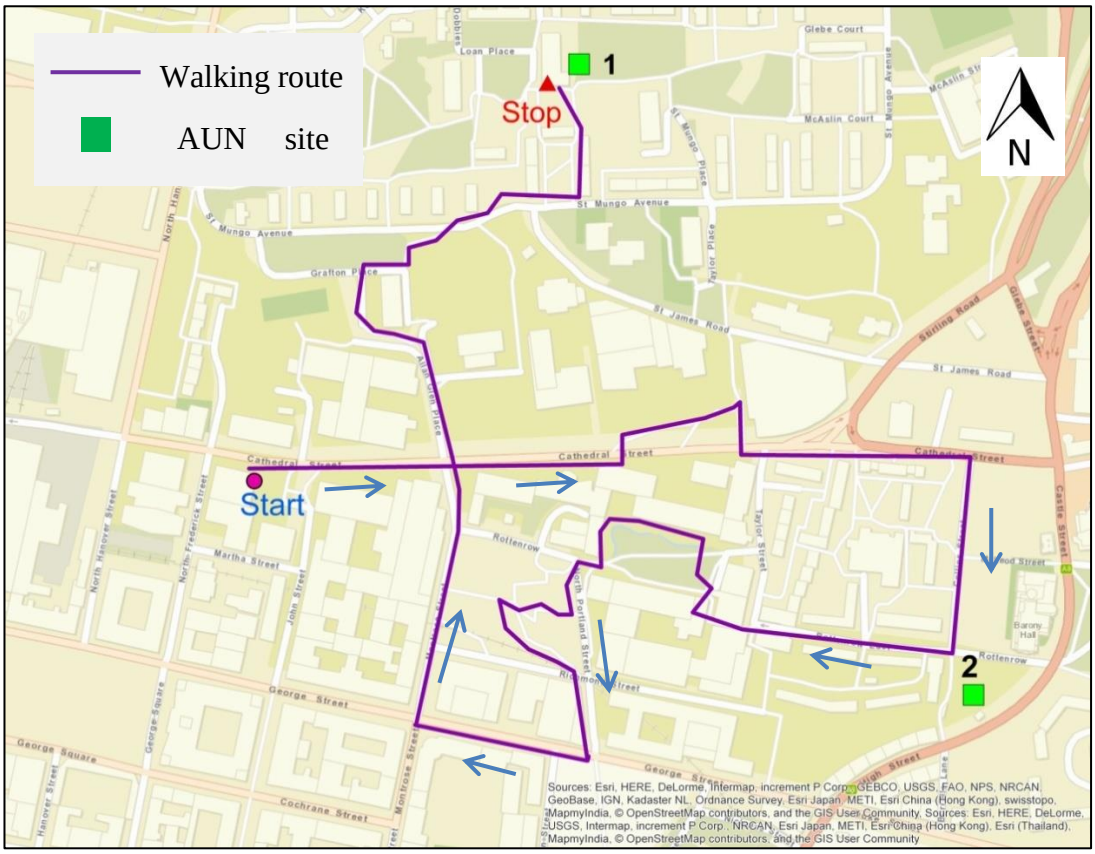

Figure 7.7: The sampling route for the campus campaign from the start point to the north of Cathedral St. until the end of sampling point at Townhead residential area. The AUN sites are as follows: (1) Townhead & (2) High St.

7.4.2 Sampling methods

BC was monitored using AE51 Aethalometer (Model AE51 Aethlabs, San Francisco, CA, USA) at 150 ml min^{-1} at 1 sec measurement time-base (as described in section 4.1.4.1). This was done to allow better resolution at the walking speeds when capturing the instantaneous data during mobile monitoring. Duplicate BC devices were used to investigate the inter-comparison of BC measurements during mobile sampling. One set of NO_2 and O_3 Aeroqual (Aeroqual Ltd., Auckland, New Zealand) were used to monitor NO_2 concentrations at 1-min time resolution (section 4.2.2). These instruments were carried in a backpack with AE51 Aethalometer's sampling tubes attached at the breathing zone of the walker. The Aeroquals were fitted at the mesh pocket of the same backpack. The time and location were

manually recorded in the diary to log details of temporal resolutions. The time was pencilled during start, stop and at designated sampling routes.

BC and NO_2 data were also downloaded from the nearest site to the sampling route (AUN Townhead, High St and Hope St – section 4.3) concurrent with the same period that both measurements were obtained. Note that, all measurements were taken during weekdays, thus higher concentrations of traffic emissions were expected to capture during the sampling exercises.

Additional Global Positioning Systems (GPS) data were included during the measurement period using a Garmin Forerunner 110 GPS-Enabled Sports Watch (Garmin Ltd., Switzerland) to check the accuracy of manually logged diaries. Further in-comparison of BC device were carried out after the campus network campaign finished on separated 9 walks from January to April 2016 on the same walking route. Meteorological data were obtained from Glasgow Airport during the sampling campaigns:

(http://mesonet.agron.iastate.edu/request/download.phtml?network=GB__ASOS).

The average temperature during the city centre campaign (section 7.4.1.1) was 16.4°C, ranging from 14.3 – 19°C. The average temperature during campus network campaign (section 7.4.1.2) was 7.9 °C, ranging from 3.0 – 13.8 °C

In addition, the personal sampling pump (model Apex Pro Pump, Casella, UK) was used during the campus network walk to collect the loaded carbonaceous particles on 25-mm Teflon filter at 1.0 L min^{-1} (as described in section 5.1.1). The filter specimen was checked for accumulated darkness for each sampling session using reflectance and scanner measurements (section 5.5.1 & 5.5.2). Each value was transformed into BC concentrations using derived equation from previous field evaluation (as described in section 5.1.1). These estimated values were compared with collocated aethalometer and reference site of BC measurements.

7.4.3 Health & safety

Precautions were taken when working outdoors (refer to appendix 10B (4) for appropriate Risk Assessment forms).

7.4.4 Data analyses

Data were mainly analysed using Excel 2010 for descriptive statistics. The inter-comparison between duplicate AE51 Aethalometer instruments were investigated using RMA line computed by Excel 2010. Warton et al. (2006) suggested that major axis (MA) regression can be applied to test the similarity of the replicate instruments. Raw BC data obtained had a high incidence of noise from 1 sec time resolution, therefore the values were corrected (as described in section 4.1.4) and averaged in 1-min time-stamp to compare with corrected NO_2 data. The Aeroqual NO_2 measurements were corrected based on the nearest field calibration exercise in AUN Townhead (as described in section 5.2). The equations used to correct the NO_2 values were shown in Table 7.6.

Table 7.6: The derived equation from the field calibration of Aeroqual system NO_2-O_3 in AUN Townhead to account for their cross-sensitivity with ozone.

Sampling period	Correction equation
30 June 2015	$0.74*O_3 - 31.5$
6 - 9 July 2015	$1.1*O_3 - 53.4$
14 - 24 July 2015	$0.8*O_3 - 43.2$
27 October 2015	$0.98*O_3 - 59.70$
3 - 24 November 2015	$1.60*O_3 - 66.11$
1 - 8 December 2015	$1.45*O_3 - 61.26$

The spatiotemporal data on 24 July 2015 was further analysed using GIS tool, ArcGIS v.10.2.2 (Esri, USA). Gillespie (2015) developed a script from R-Studio to interpolate the GPS data fitted to the steady walking speeds of one-second intervals

(refer to appendix C for the script used in R software). The 1-min time-stamp for each measurement of BC and NO_2 were matched with the GPS data using the database management called ArcCatalogue, before exported to the ArcMap in the ArcGIS. The output predictions of BC and NO_2 were exported into JPEG format. The matrices plots were illustrated using R software (RCoreTeam, 2012) to investigate the correlation between measured pollutants from the real-time sensors and ambient concentrations recorded from AUN monitoring sites. BC and NO_2 analyses during campus network campaign were provided by Nicola Masey (*personal communication* – details in Appendix 10A (3)).

7.4.5 Quality control-quality assurance

Both MicroAeth (BC) and Aeroqual (NO_2) instruments were manufacturer calibrated. The ATN values for MicroAeth were inspected prior to start any sampling session, where the values cannot be more than 45, otherwise the filter tape will be changed (as described in section 4.1.4). For the GPS data, data-cleaning process was applied to reduce the invalid points on the concentration map.

7.5 Results

7.5.1 BC inter-comparison during mobile sampling

Figure 7.8 (a) & (b) show the inter-comparison of duplicate BC device AE51 Aethalometer (referred as MicroAeth 1204 and MicroAeth 1303 –based on S/N) during two separated mobile sampling campaigns on city centre route and campus network route. An average 1-min time resolution and one-day of sampling exercise was also shown in each monitoring route. MicroAeth 1303 gave higher concentrations than 1204 in the city centre and campus network campaigns (13% and 9% higher respectively).

The MicroAeth 1303 and 1204 were highly correlated in 1-min time-stamp during city centre campaign (R^2 = 0.71). A moderate correlation was observed for both instruments for 8 days of completed measurement trips on the same route (R^2 =

0.65). A small number of outliers on the regression slope were observed with a wider scatter across the BC concentration range, resulted in moderate association. The city centre campaign encompassed walking trips on different street topography, which depicted gradient of pollutant concentrations from the urban traffic emissions. An excellent correlation was observed for the duplicate MicroAeth during campus network campaign in average 1-min time-based and measurement day ($R^2 \geq 0.99$).

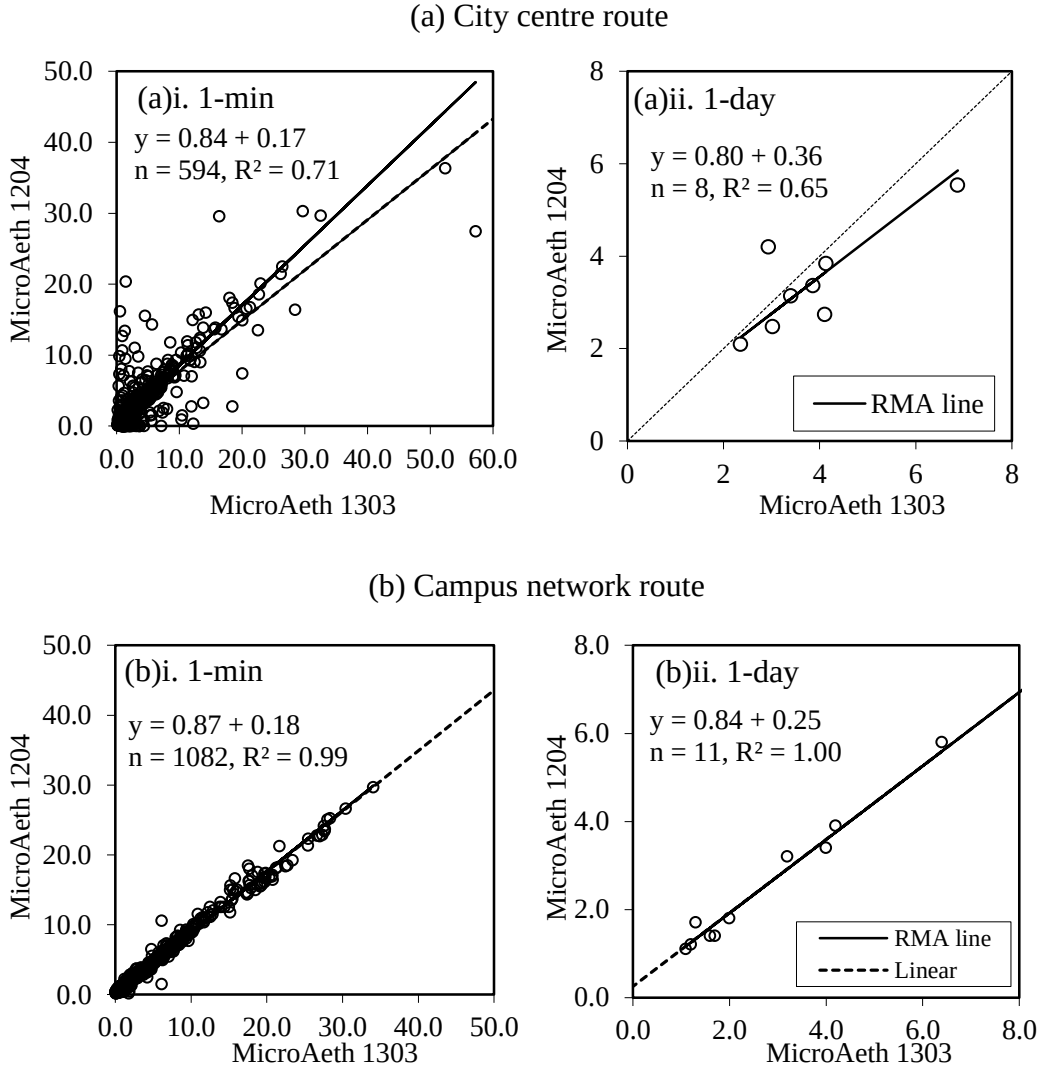

Figure 7.8: Comparison between MicroAeth 1303 and MicroAeth 1204 BC concentration measurements (μg/m^3) on: (a) city centre route; and (b) campus network route for (i) 1-min and (ii) 1-day average periods. The BC data were corrected to account for changes in attenuation value of AE51 (Apte *et al*., 2011).

7.5.2 Spatio-temporal variability of BC and NO_2 in the city centre route

7.5.2.1 BC and NO_2 measurements on each sampling period

Table 7.7 shows statistical summary of the BC and NO_2 concentrations measured on each sampling day. All measurements were in 1-min time resolutions. The highest average BC concentrations were recorded on 30 June 2015 (min = 1.1 & max = 44.4 $\mu g/m^3$ respectively). Meanwhile, the highest average NO_2 values were measured on 6 July 2015 (60.7 ± 21.8 $\mu g/m^3$). The lowest average concentrations of BC and NO_2 were observed on 9 July 2015. This finding coincides with the lower average background concentrations measured in the AUN Townhead (0.4 and 13.3 $\mu g/m^3$ for BC and NO_2 respectively) during the same period when the measurements took place.

Table 7.7: Summary of descriptive statistics for BC and NO_2 concentrations ($\mu g/m^3$) measured from 30 June – 24 July 2015.

Sampling day	BC conc. ($\mu g/m^3$)					NO_2 conc. ($\mu g/m^3$)				
	Min	Max	Mean	±	SD	Min	Max	Mean	±	SD
30-Jun-15	1.1	44.4	6.2	±	6.9	31.5	136.7	60.7	±	21.8
6-Jul-15	0.4	42.4	3.5	±	6.2	34.5	280.6	76.5	±	38.8
9-Jul-15	0.2	19.0	2.7	±	3.6	-11.8	126.5	22.7	±	28.8
14-Jul-15	0.4	13.9	3.3	±	2.8	13.3	122.7	55.4	±	28.2
15-Jul-15	0.1	30.0	3.8	±	4.7	13.3	116.6	55.6	±	20.7
22-Jul-15	0.7	31.1	4.0	±	4.9	15.0	156.9	56.8	±	31.9
23-Jul-15	0.2	10.5	2.2	±	2.0	8.4	155.3	54.2	±	27.6
24-Jul-15	0.3	24.5	3.6	±	4.5	-1.6	144.3	42.9	±	31.0

7.5.2.2 BC and NO_2 measurements on each sampling zone

For a meaningful comparison of BC and NO_2 results, these concentrations were presented at each walking zone Figure 7.9 (a) – (d). A higher range of BC and NO_2

concentrations were observed at Hope Stand Union St walking zones. Overall, the BC and NO_2 measurements followed the same trend against each other during the measurement periods. The spatio-temporal variability for BC and NO_2 measurements were suggest reflected by the difference in street topographies during each measurement trip (details of time series during each sampling day are described in the appendix).

The distribution of BC and NO_2 variations at each walking zone during measurement periods (n = 8) were illustrated from the interquartile range (IQR) in Figure 7.10. The mean BC concentrations vary on different zones of the routes with elevated values observed on streets nearer to the local traffic sources in the city centre and higher average BC concentrations were observed along Hope St. with IQR = 7.5 (min = 0.5 $\mu g/m^3$; min = 42.4 $\mu g/m^3$). Similarly, the IQR for NO_2 concentrations measured at this walking segment were the highest (47.7) (min = -12.5 $\mu g/m^3$; max = 118.9 $\mu g/m^3$).

The average BC concentrations were the lowest at the campus walking segment with concentrations ranged from 0.1 – 31.1 $\mu g/m^3$ (IQR = 1.5). The average concentrations of NO_2 measured at Campus, Pedestrianised and Union St. are exceeded the NO_2 annual standard (> 40 $\mu g/m^3$) (DEFRA, 2004). Two walking segments of Pedestrianised and Hope St. are physically close to each other. Both of Hope St. and Union St. are predominately-street canyons type. The negative values shown from the lower whiskers implied that the large range of outliers exists in the NO_2 distributions, therefore further research should be conducted to ascertain the calibration use of Aeroqual in the mobile sampling exercises.

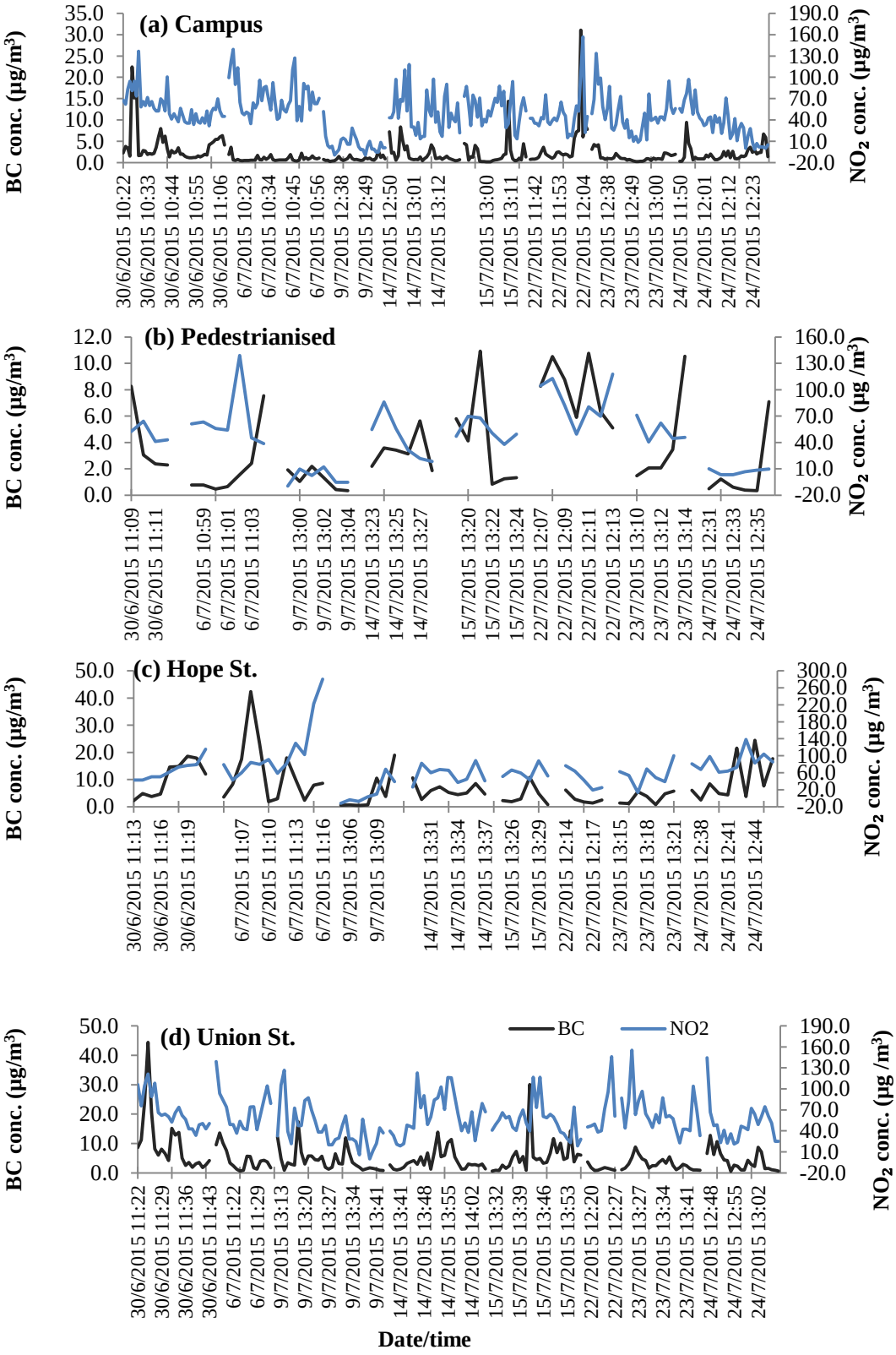

Figure 7.9: (a) – (d) BC and NO_2 concentrations (µg/m^3) measured at designated monitoring zones on city centre walking route.

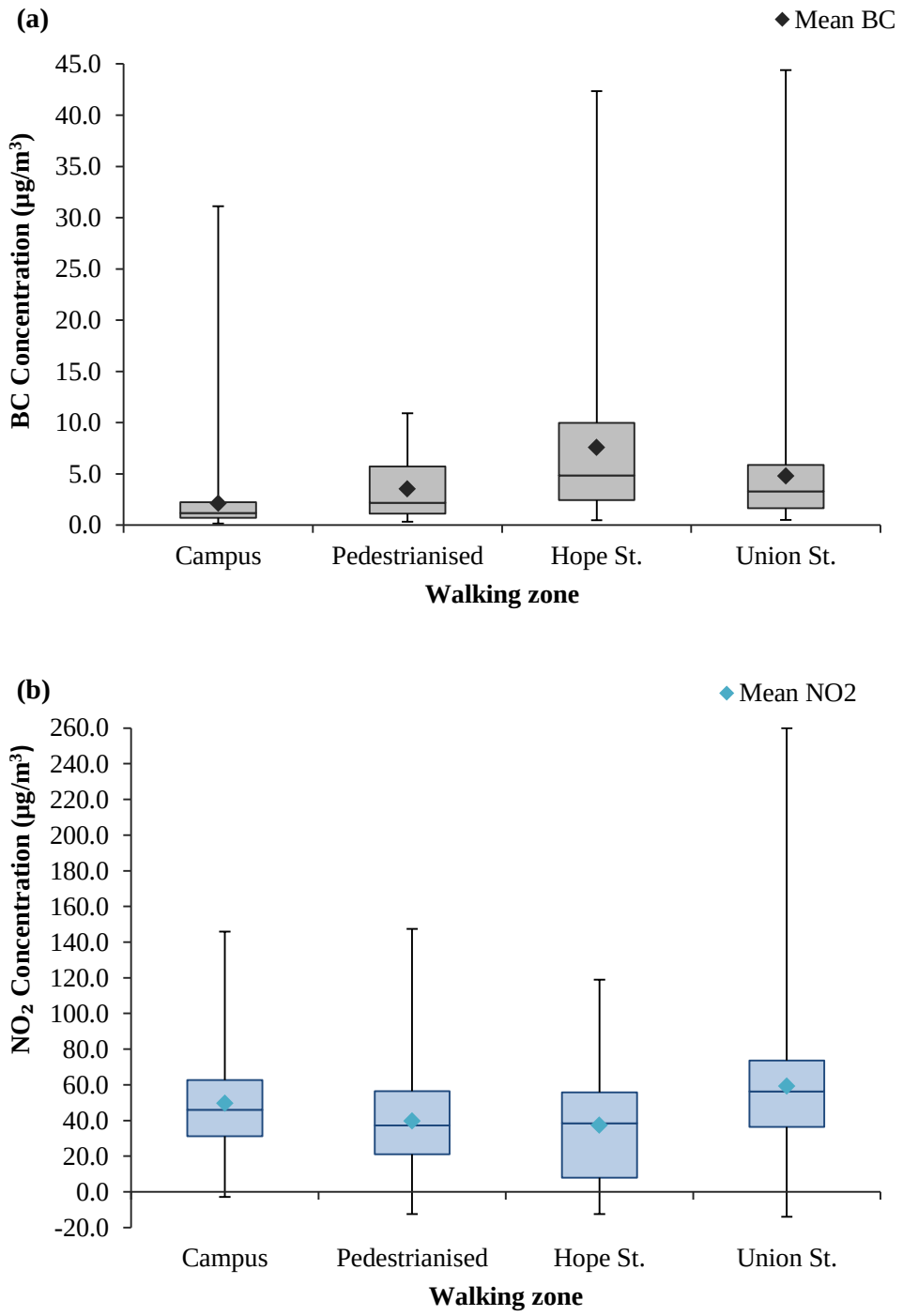

Figure 7.10: (a) BC and (b) NO_2 values calculated for each walking zone from 30 June – 24 July 2015 on city centre route. The whisker plot shows the 3rd quartile at the upper end of box and the lower end shows the 1st quartile. The diamond points represents the mean of each measurements at the designated walking zones.

7.5.3 Temporal-variations of BC and NO_2 concentrations on the campus network route

7.5.3.1 BC and NO_2 concentrations measured during morning, mid-day and afternoon

The average BC and NO_2 concentrations in three measurement sessions of morning, mid-day and afternoon were shown in Figure 7.11 (a). Measurement results indicate that the BC and NO_2 concentrations varied in different measurement days. The BC values were highest on 3/11/2015 morning session. The wind speed recorded during the period of observation was very low (1.2 m/s^1). Meanwhile, the lowest BC concentrations were recorded during evening measurements on 3 December (1.6 $\mu g/m^3$) with high wind speeds at 10.5 m/s^1.

A higher increase of BC and NO_2 concentrations were observed on 24 November 2015 during morning and afternoon sampling period. The average temperature and wind speed on the same day were 6.8°C and 14.5 m/s^1 respectively. Although, it was drizzling during the afternoon session, the BC levels were 1.4 times higher than the morning session. This indicates that the observed higher BC concentrations originated from the local traffic emissions.

The BC and NO_2 concentrations were statistically analysed with distribution variations and presented in the plot box (Figure 7.11 (b) (i) – (ii)). The BC and NO_2 concentrations observed during mid-day measurements were 22% higher than the average morning and afternoon. This may indicate that the temporal variability of BC and NO_2 reflected the influence of traffic emissions during mid-day peak hour. Larger error bars were obtained during morning and afternoon BC measurement indicates larger variability of the BC values during both monitoring sessions.

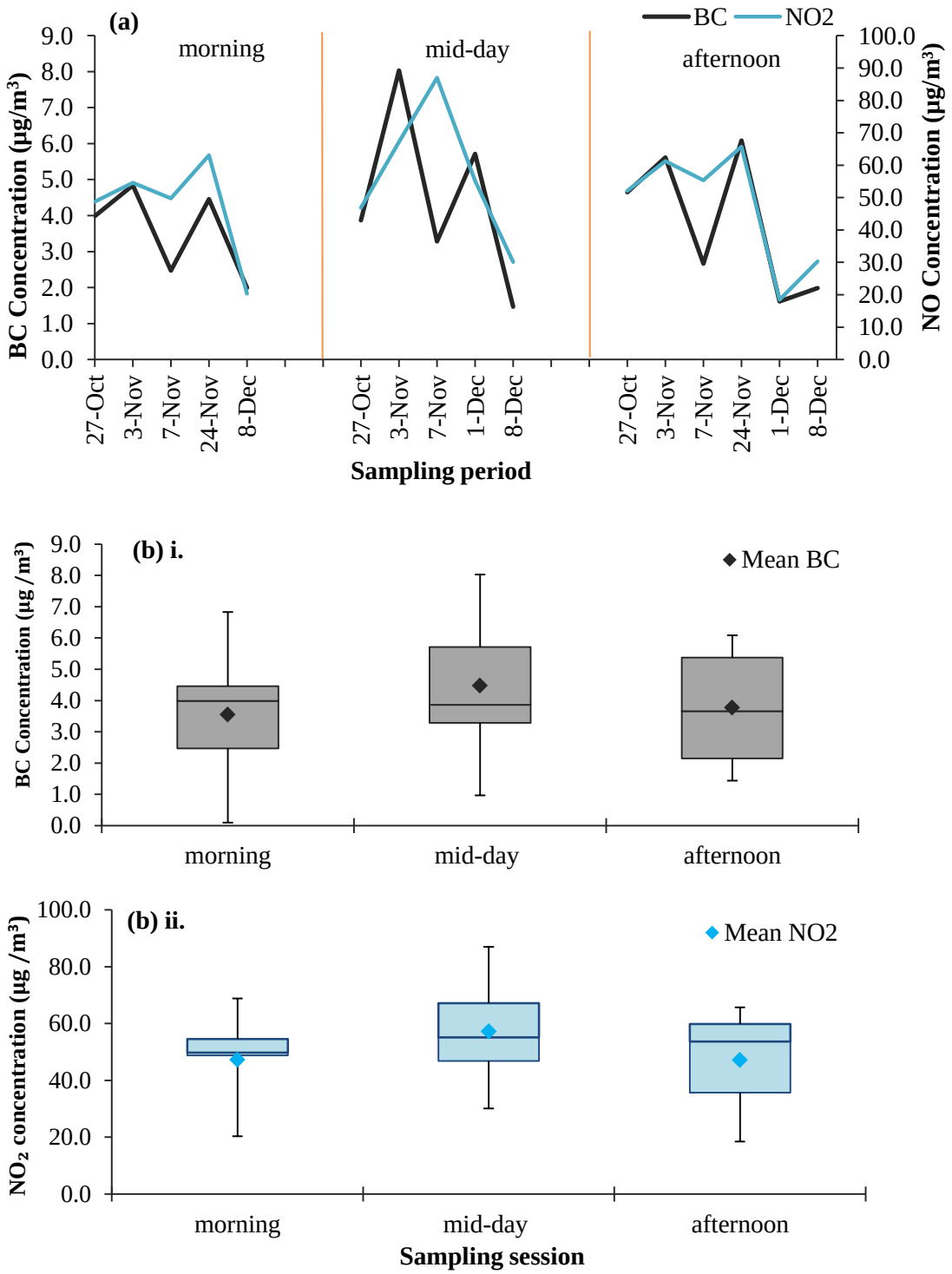

Figure 7.11: (a) The time-series of BC and NO_2 values measured in the morning, mid-day and afternoon from 27 October – 8 December 2015. Distributions of (b) i. BC and (b) ii. NO_2 measured on each sampling session are shown. The box demarcated by the interquartile range with the diamond point shows the mean for each pollutant concentration.

7.5.4 Short-term BC and NO_2 personal exposures from mobile monitoring in the city centre and campus network routes

7.5.4.1 Correlations of BC and NO_2

The BC and NO_2 boxplots were illustrated to investigate correlation between these pollutants in different average of time-based in the city centre (re described in section 8.4.2 & Figure 8.6) and campus network routes (Figure 7.12). The 1-min time resolutions were averaged to 5 min and 15 min. Overall, there were higher correlation in mean of BC and NO_2 at 5-min & 15-min time-based during city centre sampling campaign. However, BC and NO_2 measurement on 6/7/2015 & 15/7/2015 showed poorer correlations in all time-based average. A similar observation was also noted for campus network sampling routes, where the mean of BC and NO_2 were highly correlated at the average of 5-min & 15-min time resolutions. The afternoon measurement of BC and NO_2 showed the highest correlation in different time-based.

7.5.4.2 NO_2 and BC variations in 5-min average time resolutions

In order to assess the short duration of personal exposures of NO_2 and BC, average of 5-min NO_2 and BC were used using reduced major axis (RMA) statistics (Gillespie *et al.*, 2017). As shown in Table 7.8, NO_2 *vs.* BC measurements in 5-min average of time resolutions were calculated under RMA slopes for both sampling campaigns on city centre and campus network routes. Both measurements on 6/7/2015 & 15/7/2015 showed the smallest variations were excluded. This may explains the poorer correlation observed on these dates. Interestingly, 5-min NO_2 and BC measurements explained 38% variations of spatial and temporal variations for both campaigns conducted in city centre and campus network routes. Overall, 5-min NO_2 and BC measurements in city centre route explained 0 - 64% variations and for campus network route explained 31 - 48% variations measured in the morning, mid-day and afternoon.

Study name/measurement date	1-min	5-min	15-min
City centre (30/6/2015)	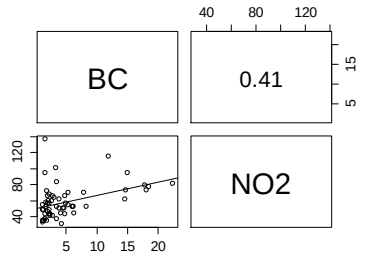	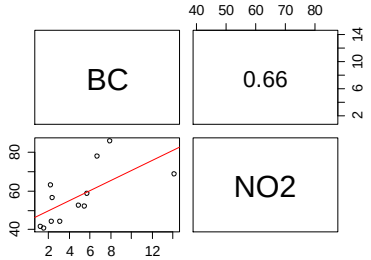	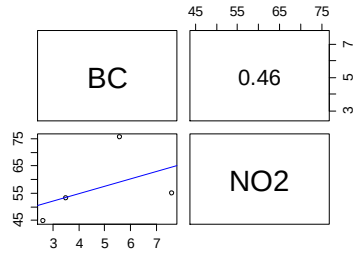
City centre (6 /7/2015)	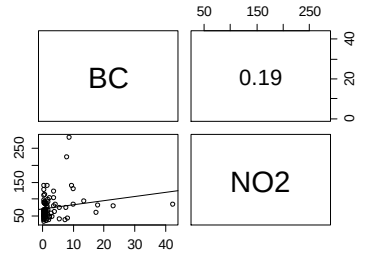	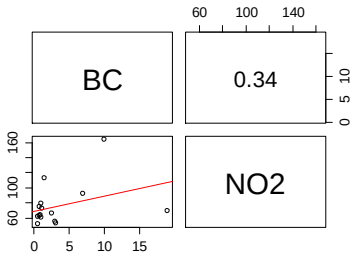	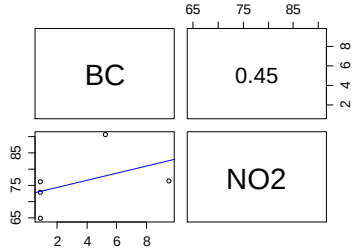
City centre (9/7/2015)	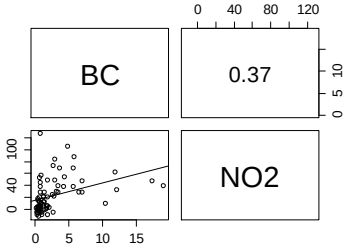	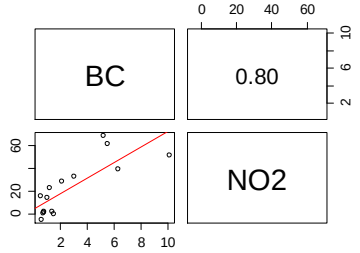	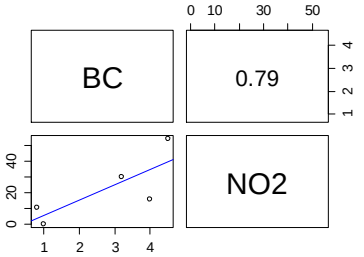

City centre (14 /7/2015)	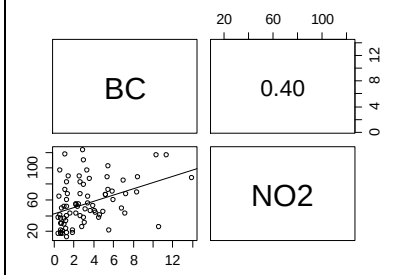	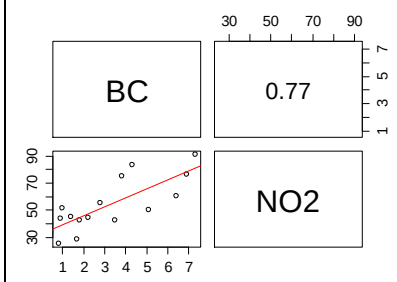	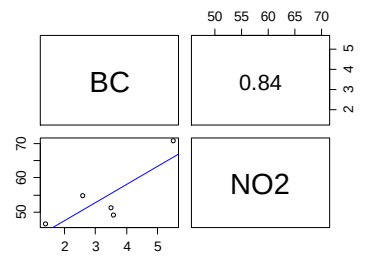
City centre (15/7/2015)	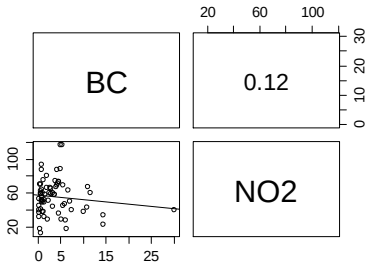	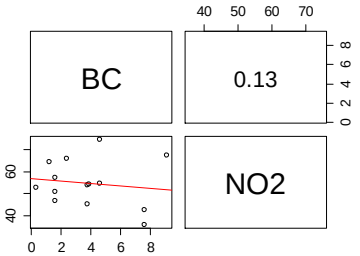	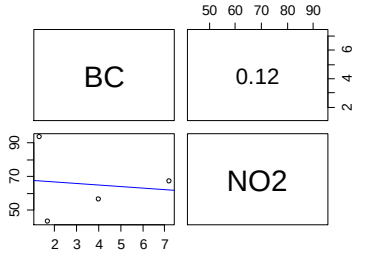
City centre (22/7/2015)	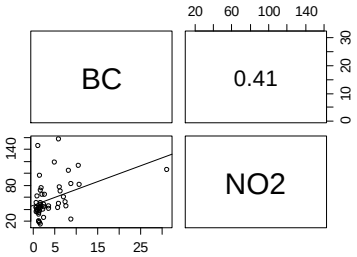	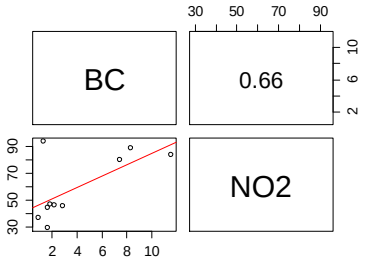	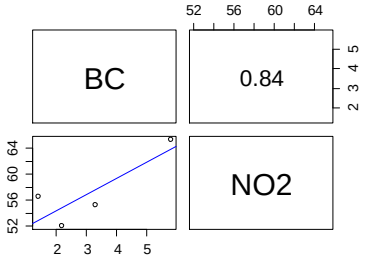

City centre (23/7/2015)	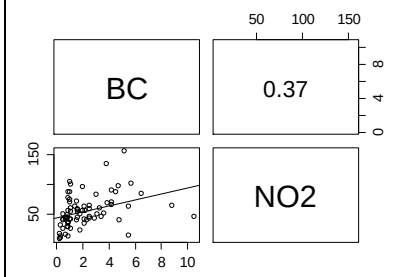	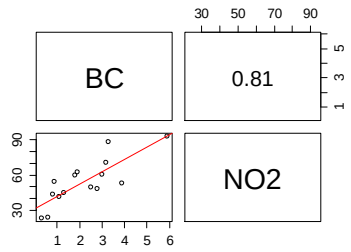	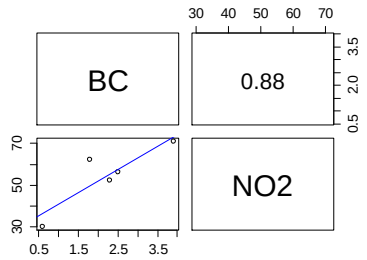
City centre (24 /7/2015)	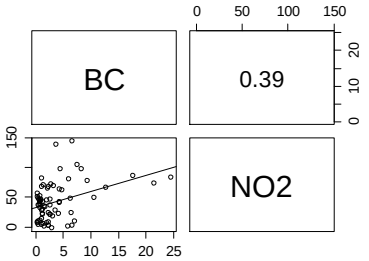	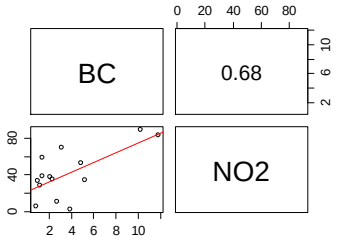	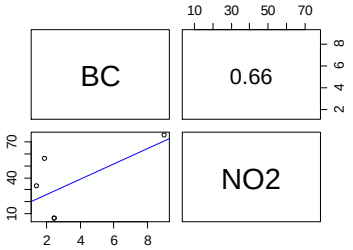
Campus morning (27/10/2015, 3/11/2015,7/11/2015, 24/11/2015 & 8/12/2015)	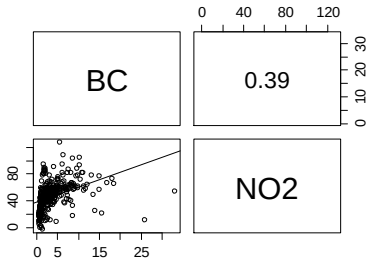	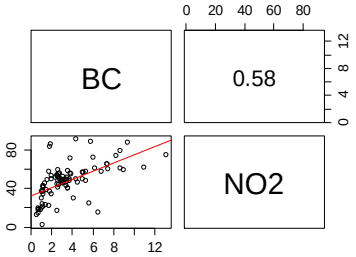	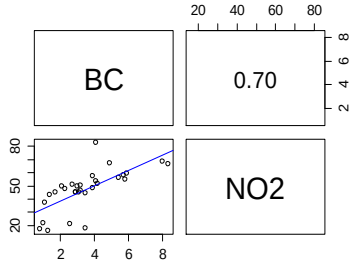

Campus mid-day (27/10/2015, 3/11/2015,7/11/2015, 1/12/2015 & 8/12/2015)	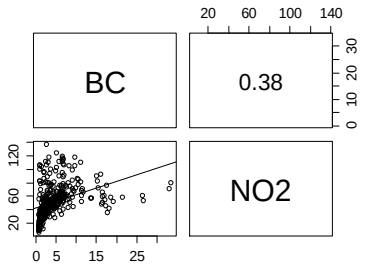	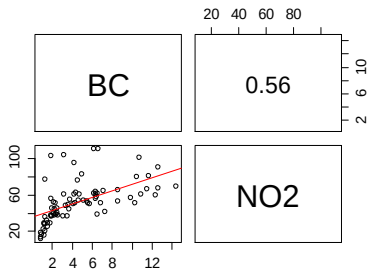	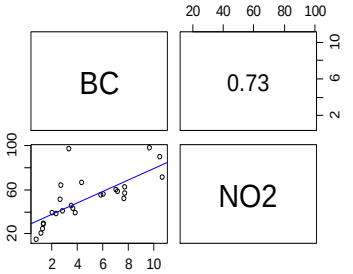
Campusafternoon (27/10/2015,3/11/2015, 7/11/2015,24/11/2015, 1/12/2015 & 8/12/2015)	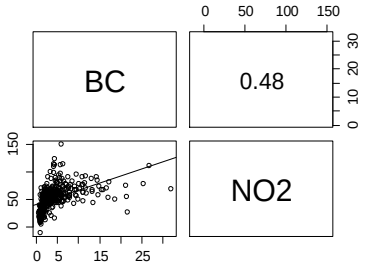	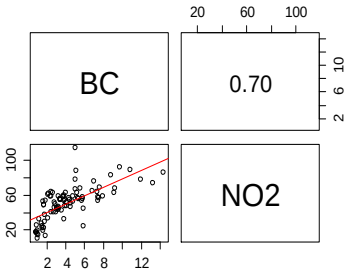	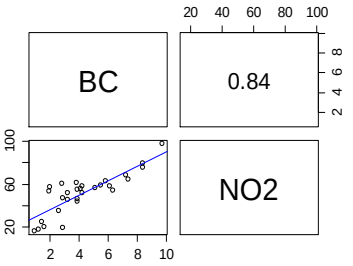

Figure 7.12: BC and NO_2 correlations in different time averaged 1-min, 5-min and 15-min during city centre and campus network sampling campaigns.

Table 7.8: Summary of RMA statistics of NO_2 *vs.* BC in average 5-min time-based measured on city centre (as can be seen in Table 8.6) and campus network walking routes.

Study period	n	R^2	slope	intercept
Glasgow city centre				
30/6/2015	12	0.43	0.25	-9.5
6/7/2015	15	0.12	0.17	-9.7
9/7/2015	15	0.64	0.12	0.1
14/7/2015	15	0.59	0.12	-3.0
15/7/2015	14	0.02	0.25	-10.1
22/7/2015	10	0.43	0.15	-5.2
23/7/2015	15	0.65	0.08	-2.0
24/7/2015	14	0.46	0.07	0.9
All	110	0.22	0.12	-3.0
All (exc. 6/7/2015 & 15/7/2015)	81	0.38	0.12	-2.2
Campus network				
Morning	90	0.34	0.27	-8.9
Mid-day	78	0.31	0.20	-6.0
Evening	90	0.48	0.15	-3.4
All	258	0.38	0.15	-3.2

7.5.5 Application of GIS to the pollutants measured at the city centre route

The concentration map (re described in section 8.4.2 & Figure 8.3) for each BC and NO_2 of the study area on city centre route are shown in Figure 7.13 & Figure 7.14.

The spatial and temporal distributions were based on the BC and NO_2 measurements made on 24 July 2015. The total journey duration was 72 minutes. The average wind speed was lower (3.5 m/s^1) with wind direction blown mainly west-southwest during the sampling day.

Each circle point with different sizes and colour spectrum represented a specific range of BC and NO_2 observed at the designated walking route. Both of concentrations varied in each segmented road due to the contrast of traffic flow and street topography. From C, both pollutants values were distributed higher at Cathedral St. and High St. The NO_2 concentrations were 4 times lower than the average values recorded along Cathedral St. and High St. when walking from UoS Architecture Garden to George St.

Lower BC and NO_2 concentrations were measured when walking at the pedestrianised precinct (P) along Buchanan St and Sauchiehall St. The highest concentrations were spotted at the street canyon along Hope St. (H) with highest BC and NO_2 concentrations of 24.5 and 138.3 $\mu g/m^3$ respectively. This was also observed when returning to the UoS along Union St. towards North Frederick St. The NO_2 concentrations recorded along Cathedral St., Hope St., and Union St. (C, H and U) were breaching the standard annual values of 40 $\mu g/m^3$.

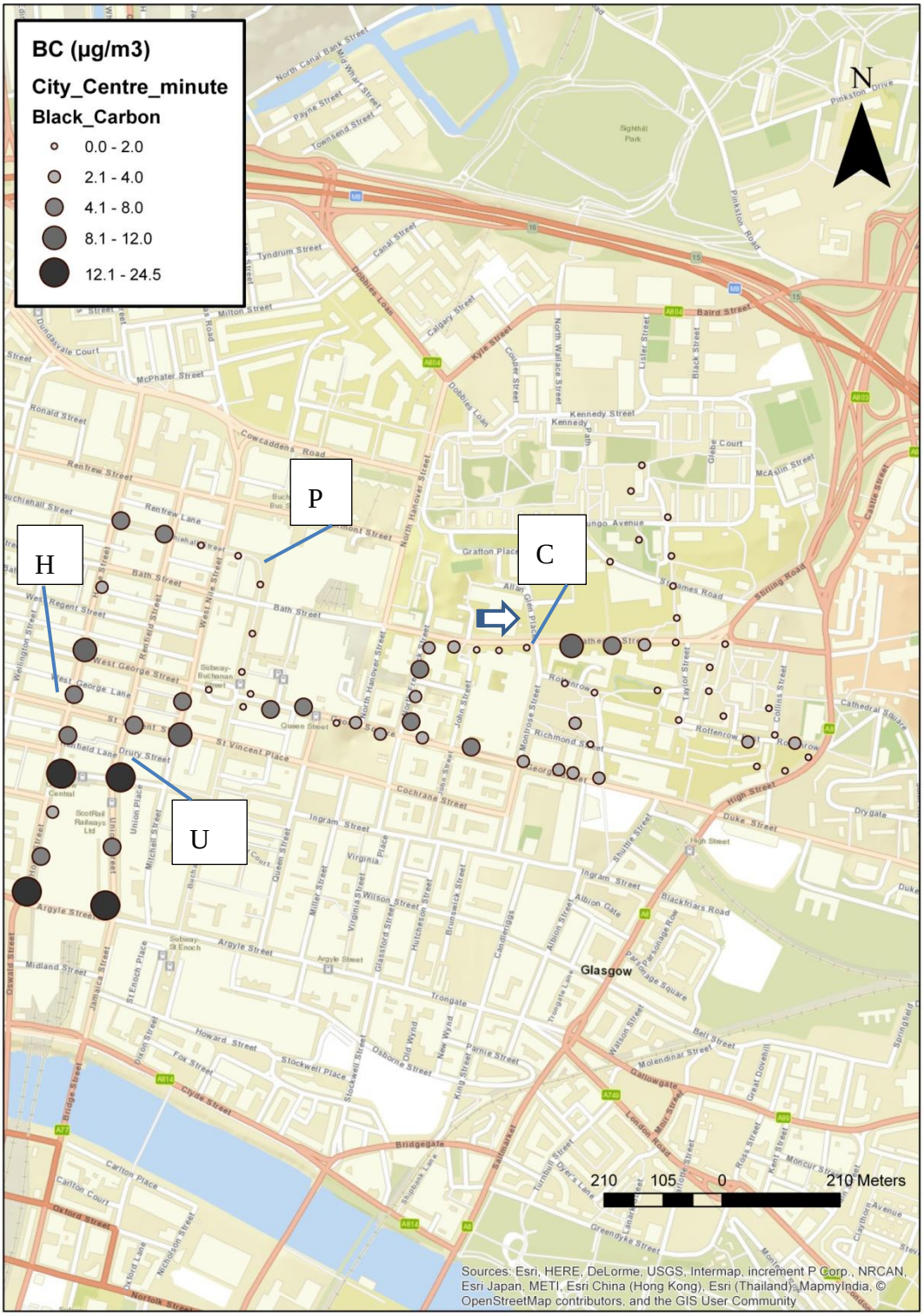

Figure 7.13: Spatial and temporal distribution of BC concentrations when walking from UoS to Glasgow Central and returned to the UoS along 4 walking zones (from C,P, H and U) (as can be seen in Figure 8.4).

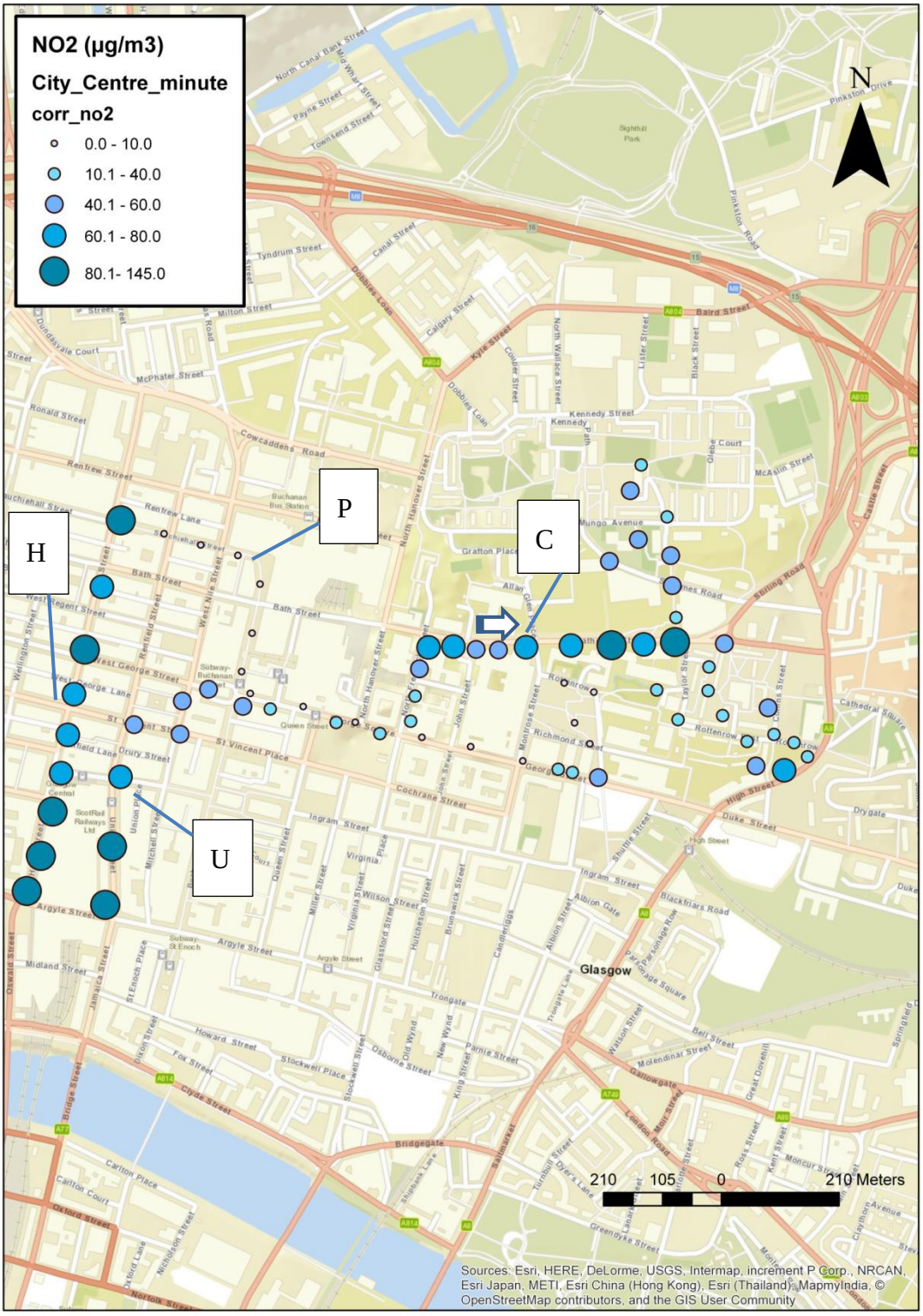

Figure 7.14: Spatial and temporal distribution of NO_2 concentrations when walking from UoS to Glasgow Central and returned to the UoS along 4 walking zones (from C,P,H and U) (as can be seen in Figure 8.4).

Table 7.9 shows the average concentrations of BC, NO_2, O_3, $PM_{2.5}$ and PM_{10} during the same period of sampling day measured at the AUN sites. NO_2 measurement recorded at traffic background site in High St. and Kerbside were higher compared to the urban background values.

Table 7.9: Summary of average pollutants recorded at the AUN sites on 24 July 2015.

Pollutants ($\mu g/m^3$)	Towhead	High St	Kerbside
NO_2	17.0	36.3	50.3
O_3	41.3	N.A*	N.A
BC	0.6	1.4	N.A
$PM_{2.5}$	4.3	6.7	N.A
PM_{10}	7.3	9.3	N.A

*data were not available.

7.5.6 Relationship between measured BC and NO_2 with ambient concentrations measured by the reference site

Figure 7.15 (a) shows correlation matrix plots between average BC and NO_2 measured during walking trips at city centre route and compared with measurements recorded by AUN monitoring sites. BC measured during walking were highly correlated with NO_2 measured at Townhead and Hope St. sites ($r = 0.47$ & $r = 0.79$). Similar results were also observed, where BC measured at Townhead were highly correlated with NO_2 measured at Hope St. ($r = 0.75$). This may suggest that the trend in BC concentrations closer to urban sources was being followed by NO_2 regardless of the monitoring location. There was weak correlation between BC and NO_2 measured during mobile measurements compared with measurements recorded at High St. Note that the location of the AUN Townhead site is closer to the major walking zones compared to AUN High St. fixed site.

Figure 7.15 (b) shows correlation matrix plots between BC and NO_2 measured during walking on campus route between 27 October and 8 December 2015. Measured concentrations at each monitoring period were averaged by day. Both BC and NO_2 levels recorded at High St were excluded due to incomplete number of data. BC and NO_2 measured during walking around campus route were highly correlated with reference site recorded in Townhead. This indicates that this site has common sources of BC and NO_2 during rush hour period from the direct traffic emissions. There was weak correlation of BC measured during mobile measurements and from Townhead compared to Hope St. The Hope St. site was located far from the sampling route.

(a) City centre route

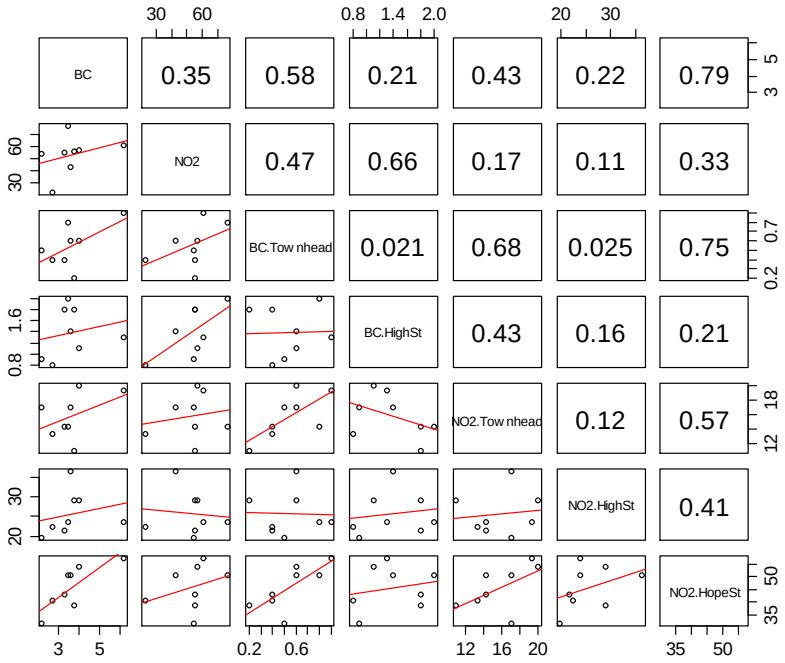

(b) Campus network route

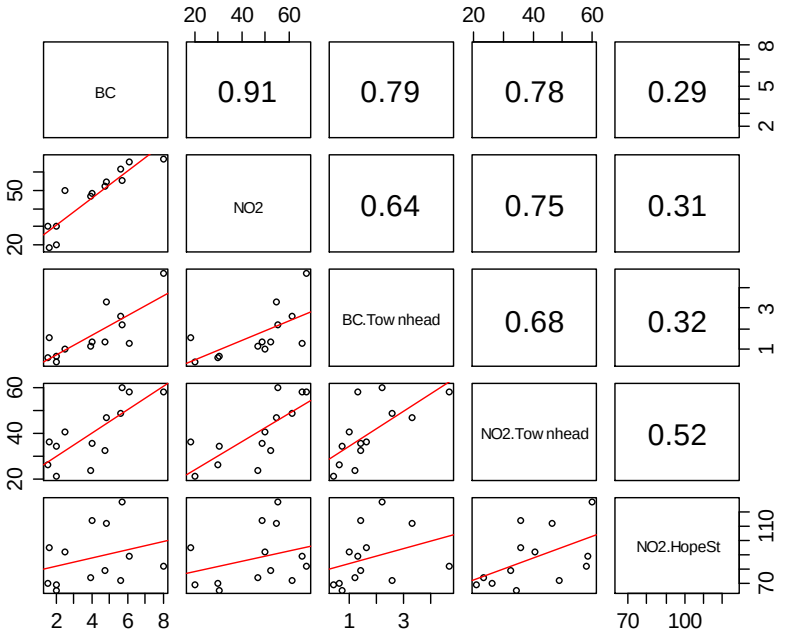

Figure 7.15: Scatter plots of average BC and NO_2 measured at (a) city centre and (b) campus network routes during each sampling period and compared to other pollutants measured at the three AUN sites (Townhead, High St. and Hope St).

7.5.7 Relationship between BC estimated by reflectometer, scanner, and AUN reference aethalometer

Figure 7.16 shows the correlation matrix plots between BC concentrations estimated by the reflectometer and scanner system (as described in section 5.1) and compared with collocated AE51 Aethalometer and AUN Townhead measurements. The estimated BC concentrations by reflectometer showed a stronger relationship with the side-by-side real time and AUN measurements ($r > 0.69$). BC levels estimated by the scanner system had a good relationship with collocated AE51 microaethalometer.

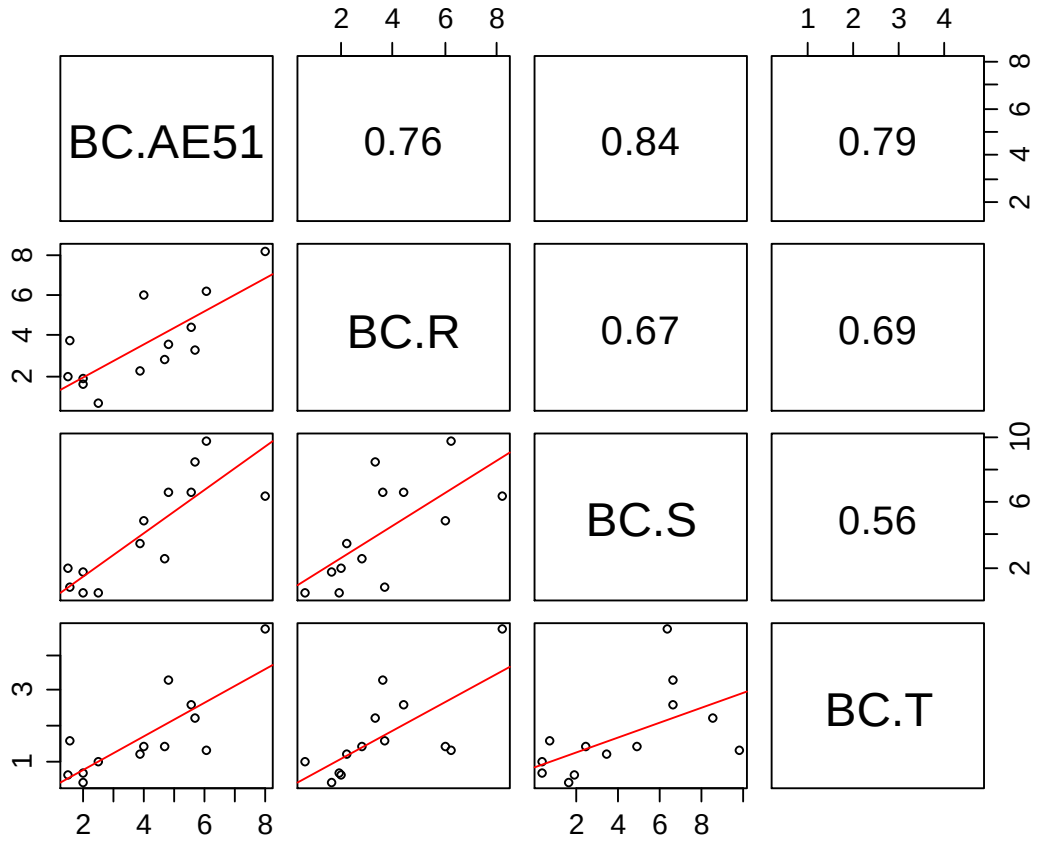

Figure 7.16: Estimated BC concentrations from reflectometer and scanner systems compared with BC measured by AE51 Aethalometer (BC.AE51) and AUN site (BC.T – Townhead). Measurements were made on campus network route (27 October – 8 December 2015).

7.6 Discussion

7.6.1 Validation of AE51 Aethalometer

More insight into the performance of the BC real-time sensor during mobile air quality monitoring was demonstrated from two campaigns conducted in the city centre and campus network walking routes. Several studies presented the evaluation and critical issues encountered from the AE51 Aethalometer uses (Hagler *et al.*, 2011, Cai *et al.*, 2013, Cai *et al.*, 2014). The physical movement and rapid changes of ambient temperature and relative humidity can disrupt the operation of MicroAeth, therefore will affect the high temporal readings from the sensor unit. The inspection of ATN values prior to conducting any measurement trip during two campaigns tends to favour the functioning of the device to generate consistency of measurement data. Note that, both of AE51 Aethalometer units were extensively used for more than 6 months.

Accurate BC exposure assessments by focusing on a similar walking segment and with more datasets are one method to reduce exposure misclassification during inter-comparison of mobile sampling study. AE51 Aethalometer had proved its operation to capture short-term outdoor BC exposure from mobile and stationary field evaluation. Kondo *et al.* (2014) found a high agreement between duplicate AE51 Aethalometer used in their study from static measurements near the fixed sampling sites. This is also in line with what has been found by Viana *et al.* (2015) from their evaluation study on replicates BC measurements in Barcelona.

7.6.2 Validation of reflectometer and scanner methods to estimate BC

The estimated BC concentrations from reflectometer and scanner methods showed high correlation with the real-time sensor used during the second measurement campaign. This indicates this is the cost-effective approach and using filter-based measurements and optical analysis can demonstrate their functions to measure BC values in the outdoor environment. The relationship between the estimated BC reflectometer and the reference measurements (AE51 Aethalometer and AUN site) were observed higher compared to BC estimated by the office scanner. This is likely

due to particle light scattering formed under different measurement technique. The reflectometer method had been extensively studied as the proxy to the BC exposure (Cyrys *et al.*, 2003, Janssen *et al.*, 2011) and to the author's knowledge, this is the first study reporting estimated values calculated from the scanned filter samples compared to AUN measurements. Analyses with more data would aid interpretation and improve the feasibility of the proposed low-cost techniques.

7.6.3 Factors influencing BC and NO_2 in the urban environment

The results show the spatial and temporal variability from high time resolution of BC and NO_2 measurements near urban roads and during rush hour trips for both sampling campaigns on different monitoring routes. This is agreed with those found by Wu *et al.* (2015). Their study observed high spatial variability, which BC concentrations had 2.3 times higher values in the urban street compared to the near urban background site.

Traffic intensity is also the main consideration for BC and NO_2 exposure, unfortunately, the traffic counts were not carried out during the sampling measurement campaigns. Since our data were collected during rush hour, it was expected that the measured pollutants were higher during high traffic flows. This was confirmed by the average increment of BC and NO_2 measured at the urban and high agreement for traffic background AUN sites (Townhead and Kerbside respectively) obtained during the city centre campaign ($r = 0.75$). This is also consistent with measurements recorded at the AUN sites during the campus campaign, where there was a good agreement between BC and PM_{10} at the Towhead and High St. sites ($r = 0.69$).

The distribution variation in BC and NO_2 values were substantially higher near the street canyons along Hope St and Union St during the city centre campaign. The NO_2 IQR during the measurement along Hope St. in this campaign was two-fold higher than reported by Jiménez *et al.* (2012). Note that, their results were obtained from the static reference AUN site, thus reflected the lower NO_2 concentrations. For

BC, the concentration peaks were found prominent when passed by the bus stop along the walking segments at Cathedral St, Hope St, Union St and North Frederick St. The diesel exhausts emissions from buses are the major contributor of high BC and NO_2 concentrations (Ning *et al.*, 2012).

Due to the congestion of buses along the street canyon of Hope St. and Union St. (GlasgowCityCouncil, 2015), it would be useful in more extensive studies to determine the dominant vehicle fleets and private cars along with traffic flows moving along these streets. The findings from Mumovic *et al.* (2006) suggested a diurnal variation of carbon monoxide concentrations near Union St result from poor ventilation. Exposure to BC and NO_2 will, therefore, be higher within the enclosed nature of street canyons that produced poorer dilution coupled with high traffic intensities.

Besides, the wind direction and wind speed are considered to influence the major variation of pollutant measurements along this type of street (Zhang *et al.*, 2015). The highest BC concentrations were recorded when the wind speeds were low and vice versa (Husain *et al.*, 2007). Both wind speed and wind directions were recorded from a distant station in Glasgow Airport from the monitoring locations. Therefore, the observed contrast between different streets in the city centre remains uncertain in these data. It would be useful to measure wind speed at the street level using a portable instrument along with the pollutant measurements in the future study.

A further look at the average concentrations of BC and NO_2 along the pedestrianisation street (P) shows both of the values were higher than the urban background measurements recorded at the AUN Townhead during the period of monitoring (6 and 3 times higher respectively). These findings perhaps indicated that the near vehicle emissions sources from traffic density at different sections from Bath St., Reinfield St. and Hope St. have influenced the pollutant concentrations at the pedestrian precinct.

The impact of traffic rush hour exposure was also explored during campus campaign. Rakowska *et al.* (2014) found the BC and NO_x values higher in the morning compared to the noon measurements in the urban area in Hong Kong. This is contrast to what we found from our study, where the mid-day measurement exceeds morning observations for BC and NO_2 levels. This might be because the study conducted by Rakowska *et al.* (2014) had only presented measurements timing on Monday, therefore the traffic flows during the first day in the weekdays are expected to be higher especially during morning rush hour.

Similar observations were found from Garcia-Algar *et al.* (2014) and Gidhagen *et al.* (2005) in the urban cities in Barcelona and Stockholm, where higher levels of fine particulates were measured on working days compared to the non-working days. Additionally, the correlations observed for both combustion-pollutants of BC and NO_2 in different time-resolution were higher during afternoon rush hour. This suggests concentrations of BC and NO_2 were influenced by increases in vehicle emissions from road traffic. The changes in traffic-related emissions in peak hour measurements had greatly influenced the concentrations of combustion-related pollutants, further indicating that these pollutants could be temporally homogeneous.

The difference in particles concentrations measured during rush hour observation period can be influenced by additional sources from the external sampling region or number of traffic flows (Kaur *et al.*, 2007). It should be noted that campus network study was conducted during winter, therefore further investigation of the relationship between three rush hour periods (morning, mid-day and afternoon) in weekdays and weekend would provide beneficial information to confirm the results in other seasons and day-to-day variations.

7.6.4 Short-term exposure of combustion-related air pollutants to urban pedestrians

Short-term variations in BC and NO_2 concentrations have addressed the relationship between general traffic and diesel exhaust indicators from personal monitoring study

at both city centre and campus walking routes in the Glasgow central. Two sampling campaigns in the city centre and campus network walking routes showed BC and NO_2 were correlated with each other.

Overall, BC and NO_2 correlations from campus network campaign conducted in the winter season showed higher values than the city centre study, which was carried out during summer in the same year. It should be noted that the walking routes and street topography were different in both studies. Gillespie *et al.* (2017) observed similar results where BC and NO_2 were highly correlated with their winter measurements. In contrast, Levy *et al.* (2014) found that correlation between BC and NO_2 in a Canadian urban area were higher in the summer than the winter. However, the sampling techniques employed for the two sampling campaigns, Gillespie et al. and Levy et al. were different.

5-min average of NO_2 and BC showed 38% variations in the two mobile sampling campaigns. This highlights the importance to characterise the spatial and temporal patterns in the urban environments. Given the high level of personal exposures to the pedestrians commuting in the centre of Glasgow, it is important that more research is conducted focusing on the unknown frequency and duration of personal exposure.

7.6.5 Personal BC and NO_2 concentrations map

The application of the GPS-derived location to illustrate the spatial variability along the city centre walking segments has found several drawbacks, which hamper the data measured to be linked to the monitoring zones. Issues addressed in the GPS data analysis include the mismatched of the sampling location due to the inaccuracy of the GPS signal hindered by the nearby buildings particularly in the urban environment (Dons *et al.*, 2013). A small number of GPS points was trimmed down after the data cleaning process (Dias and Tchepel, 2014). Generally, this approach does not affect the concentrations map produced by the author, however, it may not clearly explain the intra- and inter-variability of the personal total exposure levels.

7.7 Summary

Duplicate real-time BC monitors examined in this study showed relatively high inter-instrument precision and a similar spatial-temporal pattern for simultaneous measurements of NO_2. The short time resolution of these types of portable instruments can help to characterise spatial and temporal variations in occupational and environmental exposure to combustion-related air pollutants through mobile measurements.

The reflectometer and office scanner measurements enabled the transformation of filter darkness into BC concentrations, demonstrating good potential as alternative methods to quantify BC in the outdoor environment. Relatively high correlations were noted between real-time measurements of NO_2 and BC suggesting a common dominant source for both pollutants in the city centre environment studied. Collectively these observations suggest that it may be possible to develop simple methods based on filter darkening to better characterise the main characteristics of temporal and spatial variations in traffic-related air pollution.

Filter-based samplers, passive samplers, and real-time sensors were applied in stationary and mobile measurements to enable novel assessment of personal exposure to combustion-related air pollutants at 2 vertical heights at high spatial and temporal resolution in Glasgow city centre. This study suggests that children may have greater exposure than adults to airborne particles closer to roads. Static measurements of NO_2 also observed a difference between PDTs sampling at different heights at locations within 2.5 m of moving traffic. NO_2 concentration differences were not identified on the traffic trolley, perhaps as a result of the relatively short PDT exposure times on the trolley. These findings are consistent with children's breathing zones being closer to the height at which car exhaust systems discharge. Therefore, health effects in children may be greater than in adults because of both higher exposures and differences in pulmonary physiology (Schwartz, 2004).

Air pollution in Glasgow city centre varies substantially in space and time. Very high BC and NO_2 concentrations were measured in street canyons in Hope St. (max BC = 42.4 µg/m^3; max NO_2 = 118.9 µg/m^3) and Union St. (max BC = 44.4 µg/m^3; max NO2 = 260.0 µg/m^3). Concentrations exhibited high temporal variability during measurements. 5-min average of NO_2 and BC explained 38% variations measured from the city centre and campus network routes. The use of GIS-based concentration maps from GPS data enabled additional interpretation of personal exposures. The high temporal resolution demonstrated by the portable real-time sensors have opened new possibilities to measure BC and NO_2 at the personal exposure level in the real world environment. This will be discussed in the next chapter.

7.8 References

Bayer-Oglesby, L., Grize, L., Gassner, M., Takken-Sahli, K., Sennhauser, F. H., Neu, U., Schindler, C. & Braun-Fahrländer, C. 2005. Decline of Ambient Air Pollution Levels and Improved Respiratory Health in Swiss Children. *Environmental Health Perspectives,* 113**,** 1632-1637.

Buzzard, N. A., Clark, N. N. & Guffey, S. E. 2009. Investigation into pedestrian exposure to near-vehicle exhaust emissions. *Environmental Health,* 8**,** 13-13.

Cai, J., Yan, B., Kinney, P. L., Perzanowski, M. S., Jung, K.-H., Li, T., Xiu, G., Zhang, D., Olivo, C., Ross, J., Miller, R. L. & Chillrud, S. N. 2013. Optimization approaches to ameliorate humidity and vibration related issues using the microAeth black carbon monitor for personal exposure measurement. *Aerosol science and technology : the journal of the American Association for Aerosol Research,* 47**,** 1196-1204.

Cai, J., Yan, B., Ross, J., Zhang, D., Kinney, P. L., Perzanowski, M. S., Jung, K., Miller, R. & Chillrud, S. N. 2014. Validation of MicroAeth® as a Black Carbon Monitor for Fixed-Site Measurement and Optimization for Personal Exposure Characterization. *Aerosol and air quality research,* 14**,** 1-9.

Cyrys, J., Heinrich, J., Hoek, G., Meliefste, K., Lewne, M., Gehring, U., Bellander, T., Fischer, P., van Vliet, P., Brauer, M., Wichmann, H. E. & Brunekreef, B. 2003. Comparison between different traffic-related particle indicators: elemental carbon (EC), PM2.5 mass, and absorbance. *J Expo Anal Environ Epidemiol,* 13**,** 134-43.

DEFRA. 2004. *Nitrogen Dioxide in the United Kingdom Summary* [Online]. London. Available: https://uk-air.defra.gov.uk/assets/documents/reports/aqeg/nd-summary.pdf [Accessed 15 October 2015].

Dias, D. & Tchepel, O. 2014. Modelling of human exposure to air pollution in the urban environment: a GPS-based approach. *Environ Sci Pollut Res Int,* 21**,** 3558-71.

Dons, E., Temmerman, P., Van Poppel, M., Bellemans, T., Wets, G. & Int Panis, L. 2013. Street characteristics and traffic factors determining road users' exposure to black carbon. *Science of The Total Environment,* 447**,** 72-79.

Galea, K. S., MacCalman, L., Jones, K., Cocker, J., Teedon, P., Cherrie, J. W. & van Tongeren, M. 2015. Comparison of residents' pesticide exposure with predictions obtained using the UK regulatory exposure assessment approach. *Regul Toxicol Pharmacol,* 73**,** 634-43.

Garcia-Algar, O., Canchucaja, L., d'Orazzio, V., Manich, A., Joya, X. & Vall, O. 2015. Different exposure of infants and adults to ultrafine particles in the urban area of Barcelona. *Environ Monit Assess,* 187**,** 4196.

Garcia-Algar, O., Canchucaja, L., d'Orazzio, V., Manich, A., Joya, X. & Vall, O. 2014. Different exposure of infants and adults to ultrafine particles in the urban area of Barcelona. *Environmental Monitoring and Assessment,* 187**,** 1-10.

Gidhagen, L., Johansson, C., Langner, J. & Foltescu, V. L. 2005. Urban scale modeling of particle number concentration in Stockholm. *Atmospheric Environment,* 39**,** 1711-1725.

Gillespie, J. 2015. *RE: Script Used for GPS Interpolation.*

Gillespie, J., Masey, N., Heal, M. R., Hamilton, S. & Beverland, I. J. 2017. Estimation of spatial patterns of urban air pollution over a 4-week period from repeated 5-min measurements. *Atmospheric Environment,* 150**,** 295-302.

GlasgowCityCouncil. 2015. *Glasgow City Centre Transport Strategy 2014-2015* [Online]. Available: https://www.glasgow.gov.uk/CHttpHandler.ashx?id=27887&p=0 [Accessed 18 August 2016].

Hagler, G. S. W., Yelverton, T. L. B., Vedantham, R., Hansen, A. D. A. & Turner, J. R. 2011. Post-processing Method to Reduce Noise while Preserving High Time Resolution in Aethalometer Real-time Black Carbon Data. *Aerosol Air Qual Res,* 11**,** 539–54.

Husain, L., Dutkiewicz, V. A., Khan, A. J. & Ghauri, B. M. 2007. Characterization of carbonaceous aerosols in urban air. *Atmospheric Environment,* 41**,** 6872-6883.

Janssen, N. A., Hoek, G., Simic-Lawson, M., Fischer, P., van Bree, L., ten Brink, H., Keuken, M., Atkinson, R. W., Anderson, H. R., Brunekreef, B. & Cassee, F. R. 2011. Black carbon as an additional indicator of the adverse health effects of airborne particles compared with PM10 and PM2.5. *Environ Health Perspect,* 119**,** 1691-9.

Jiménez, S. A., Heal, M. R. & Beverland, I. J. 2012. Correlations of particle number concentrations and metals with nitrogen oxides and other traffic-related air pollutants in Glasgow and London. *Atmospheric Environment,* 54**,** 667-678.

Kaur, S., Nieuwenhuijsen, M. J. & Colvile, R. N. 2007. Fine particulate matter and carbon monoxide exposure concentrations in urban street transport microenvironments. *Atmospheric Environment,* 41**,** 4781-4810.

Kenagy, H. S., Lin, C., Wu, H. & Heal, M. R. 2016. Greater nitrogen dioxide concentrations at child versus adult breathing heights close to urban main road kerbside. *Air Quality, Atmosphere & Health,* 9**,** 589-595.

Khattab, A. & Levetin, E. 2008. Effect of sampling height on the concentration of airborne fungal spores. *Ann Allergy Asthma Immunol,* 101**,** 529-34.

Kondo, M. C., Mizes, C., Lee, J. & Burstyn, I. 2014. Black carbon concentrations in a goods-movement neighborhood of Philadelphia, PA. *Environmental monitoring and assessment,* 186**,** 4605-4618.

Levy, I., Mihele, C., Lu, G., Narayan, J. & Brook, J. R. 2014. Evaluating multipollutant exposure and urban air quality: pollutant interrelationships, neighborhood variability, and nitrogen dioxide as a proxy pollutant. *Environ Health Perspect,* 122.

MesaLabs. 2016. *Personal sampling cyclones* [Online]. Available: http://bgi.mesalabs.com/personal-sampling-cyclones [Accessed 20 November 2016].

Micallef, A. & Colls, J. J. 1999. Measuring and modelling the airborne particulate matter mass concentration field in the street environment: model overview and evaluation. *Science of The Total Environment,* 235**,** 199-210.

Mumovic, D., Crowther, J. M. & Stevanovic, Z. 2006. Integrated air quality modelling for a designated air quality management area in Glasgow. *Building and Environment,* 41**,** 1703-1712.

Ning, Z., Wubulihairen, M. & Yang, F. 2012. PM, NOx and butane emissions from on-road vehicle fleets in Hong Kong and their implications on emission control policy. *Atmospheric Environment,* 61**,** 265-274.

Rakowska, A., Wong, K. C., Townsend, T., Chan, K. L., Westerdahl, D., Ng, S., Močnik, G., Drinovec, L. & Ning, Z. 2014. Impact of traffic volume and composition on the air quality and pedestrian exposure in urban street canyon. *Atmospheric Environment,* 98**,** 260-270.

RCoreTeam. 2012. *R: A Language and Environment for Statistical Computing* [Online]. Vienna, Austria. Available: https://www.r-project.org/ [Accessed 20 June 2016].

Schwartz, J. 2004. Air pollution and children's health. *Pediatrics,* 113**,** 1037-43.

Stratton, S. 2014. *Unpublished and unverified results from the moving platform studies.*

Sykes, D. 2014. *Height Differential of Roadside Bioaerosols. Are Children at a Greater Risk?* MSc Environmental Engineering, University of Strathclyde.

Vardoulakis, S., Fisher, B. E. A., Pericleous, K. & Gonzalez-Flesca, N. 2003. Modelling air quality in street canyons: a review. *Atmospheric Environment,* 37**,** 155-182.

Viana, M., Rivas, I., Reche, C., Fonseca, A. S., Pérez, N., Querol, X., Alastuey, A., Álvarez-Pedrerol, M. & Sunyer, J. 2015. Field comparison of portable and stationary instruments for outdoor urban air exposure assessments. *Atmospheric Environment,* 123, Part A**,** 220-228.

Vintar, M. & Ogrin, M. 2015. Spatial variations in nitrogen dioxide concentrations in urban Ljubljana, Slovenia. *Moravian Geographical Reports.*

Warton, D. I., Wright, I. J., Falster, D. S. & Westoby, M. 2006. Bivariate line-fitting methods for allometry. *Biol Rev Camb Philos Soc,* 81**,** 259-91.

Wu, H., Reis, S., Lin, C., Beverland, I. J. & Heal, M. R. 2015. Identifying drivers for the intra-urban spatial variability of airborne particulate matter components and their interrelationships. *Atmospheric Environment,* 112**,** 306-316.

Zhang, H., Xu, T., Zong, Y., Tang, H., Liu, X. & Wang, Y. 2015. Influence of Meteorological Conditions on Pollutant Dispersion in Street Canyon. *Procedia Engineering,* 121**,** 899-905.

8 ASSESSMENT OF AIR POLLUTION EXPOSURE AT AN EXPERIMENTAL UNCONVENTIONAL NATURAL GAS (UNG) OPERATIONS SITE

8.0 Background

This chapter will be submitted for publication in Atmospheric Environment Journal. Eliani Ezani (E.E) and Iain Beverland (I.B) designed the study, E.E collated data and conducted data analyses. E.E. wrote the first draft of the manuscript. The first draft of the manuscript was written by E.E and all other authors contributed to discussions on data analysis and revisions of the paper. All authors have given approval to the final version of the manuscript.

The chapter discusses the sampling approach in the context of its application to an advanced field-based evaluation of air monitoring in UNG experimental site, using previous sensor calibration in the field evaluation study (as described in section 5.2). The chapter then looks at the schematic map of the operation site to visualize the location of monitoring area during the fieldwork with sampling trajectories over the wind directions. The chapter also studies the comparison of black carbon (BC) devices and the spatio-temporal pattern of simultaneous measurements from a nitrogen dioxide (NO_2) sensor. This chapter also presents an additional analysis of the individual exposures to BC and NO_2 emissions in the urban Glasgow (as described in section 7.4.1.1).

8.1 Title page information

Assessment of air pollution exposure at an experimental unconventional natural gas operations site

Eliani Ezani[12], Nicola Masey[1], Jonathan Gillespie[1],

Tara K. Beattie[1], Robert Kalin[1], Zoe K. Shipton, Iain J. Beverland[1]*

[1]Department of Civil and Environmental Engineering, University of Strathclyde, James Weir Building, 75 Montrose Street, Glasgow, G1 1XJ, UK

[2]Department of Environmental and Occupational Health, Faculty of Medicine and Health Science, Universiti Putra Malaysia, 43400 Serdang, Selangor, MALAYSIA

*****CORRESPONDING AUTHOR: Dr Iain J. Beverland, Department of Civil and Environmental Engineering, University of Strathclyde, 505F James Weir Building, 75 Montrose Street, Glasgow, G1 1XJ, UK; email: iain.beverland@strath.ac.uk; Tel: +44 141 548 3202

Graphical abstract:

Research highlights:

- Mobile and static measurements made with BC, O_3 and NO_2 sensors.
- Average BC concentrations downwind of fracking pumps = 14 µg/m³

- Average NO_2 concentrations downwind of fracking pumps = 113 µg/m³
- Average downwind concentrations for BC & NO_2 were ~20x & 4x higher than upwind
- BC and NO_2 concentrations were relatively correlated in time and space.

8.2 Abstract

Background & aim: Unconventional natural gas (UNG) extraction activities have considerable potential to affect air quality. However, there are very limited quantitative observations of the magnitude of such impacts. To provide context, we compared exposures to diesel engine exhaust from industrial fracking equipment at UNG training simulation site in Łowicz, Poland to pedestrian exposures to traffic-related air pollution in the city centre of Glasgow, UK.

Methods: We made mobile and static measurements at varying distances from sources in both of the above locations with Aethlabs microAeth AE51 portable Aethalometer (AE51 Aethalometer) for black carbon (BC) and Aeroqual series-500 monitors for nitrogen dioxide (NO_2) and ozone (O_3). Duplicate BC measurements were compared with NO_2 observations, after correction of the sensor response for the latter for O_3 interference effects.

Results: Duplicate BC instruments provided similar real-time measurements (r = 0.92), which in turn were relatively highly correlated with NO_2 observations at 5-minute temporal resolution at the UNG experimental site (r = 0.75) and on the central Glasgow walking route (r = 0.68). Average BC and NO2 concentrations measured approximately 10 m downwind of diesel powered fracking pumps were 14 and 113 µg/m³ respectively. These concentrations were approximately 35 times and 4 times higher than the upwind background BC and NO_2 concentrations at the site, and approximately 3 times higher than average BC and NO_2 concentrations measured in traffic influenced areas in Glasgow city centre.

Conclusions: Marked elevations of BC and NO_2 concentrations were observed in downwind proximity to industrial fracking equipment and traffic sources. This suggests that exposure to diesel engine exhaust emissions from fracking equipment may present a significant risk to people working on UNG sites over extended time periods. The short time resolution of the portable instruments used enabled identification of sources of occupational and environmental exposure to combustion-related air pollutants.

Keywords: Unconventional Natural Gas (UNG), Air Monitoring, Black Carbon (BC), Nitrogen Dioxide (NO_2), Ozone (O_3), AE51 Aethalometer.

8.3 Introduction

Unconventional natural gas (UNG), e.g. tight gas and shale gas, is gas that trapped within low permeability material, originating from rock formations that have a permeability of less than 1 millidarcy (Wang *et al.*, 2014). Extraction of UNG as a substitute for conventional hydrocarbon sources has transformed natural gas production worldwide, especially in the USA.

The development of UNG in countries outside the USA, including the UK, has been constrained as a result of concerns over possible impacts on the environment and human health. Current evidence regarding possible public health risks associated with UNG development is limited in detail and quality, resulting in intense debate around potential public health issues (Adgate *et al.*, 2014, Hays *et al.*, 2015, Kovats *et al.*, Werner *et al.*, 2015). Controversy of this nature is often a direct consequence of uncertainties in scientific assessment (NPL, 2015), which in turn hampers policy decisions, and can result in high levels of anxiety within local communities (Larock and Baxter, 2013) and even produce adverse health effects (Chapman *et al.*, 2013). For example, in Scotland this anxiety has culminated with the announcement of a moratorium on shale gas and coal bed methane extraction until a full health impact assessment is completed (Scottish-Government, 2015, SEPA, 2015).

Air quality is one of several health concerns related to UNG developments (Field *et al.*, 2014). There are analogies between the challenges of assessing potential public health risks from air pollution from UNG development and existing areas of environmental health research including traffic-related (HEI, 2010) and waste management-related environmental pollution (Mohan *et al.*, 2009, UK-Committee-on-Toxicity, 2010, Vrijheid, 2009). UNG operations, including well construction/operation and transportation of gas/other materials from the site, release a range of air pollutants including oxides of nitrogen (which include nitrogen dioxide (NO_2)) (NOx), ozone (O_3), particulate matter (PM), carbon monoxide (CO), sulphur dioxide (SO_2) and benzo(a)pyrene (BaP) (Field *et al.*, 2014). These air pollutants have recommended guideline values specified by the World Health Organization (Table 8.1). Another pollutant of concern associated with diesel combustion is black carbon (BC), which is mostly found within fine particle fractions (Viidanoja *et al.*, 2002). Currently, there are no legislative air quality standards for BC (EEA, 2013) despite its increasingly clear association with negative health outcomes (Englert, 2004, Heal and Quincey, 2012, WHO, 2012) and its recognition as a simple marker of local combustion emissions.

Table 8.1: Guidelines for ambient air pollutants (Krzyzanowski and Cohen, 2008)

Air Pollutants	Averaging Time	Guideline Values
NO_2	1 hour	200 μg/m^3
	1 year	40 μg/m^3
O_3	1 hour	120 μg/m^3

A small number of recent studies have highlighted the risk of adverse health effects in communities exposed to atmospheric emissions from nearby UNG facilities. McKenzie *et al.* (2012) (Elliott *et al.*, 2017, Islam *et al.*, 2016, Elsner and Hoelzer, 2016, Paulik *et al.*, 2016) used the air samples of volatile organic compounds (VOCs) collected on-site and off-site and conducted health risk assessments in two groups living near UNG developments in Colorado. Their study observed that

residents living less than 0.8 km from UNG sites have a higher risk of developing cancer and non-cancer diseases. McKenzie *et al.* (2014) observed that maternal residence within 16 km from a gas well was associated with a raised of 30% greater prevalence of congenital heart defects and two times of neural tube defects in offspring. Rabinowitz *et al.* (2015); (McKenzie *et al.*, 2016, Rasmussen *et al.*, 2016) observed frequent respiratory symptoms were experienced by people living less than 1 km close to the natural gas wells. In common with other areas of environmental health, there are crucial limitations in characterisation of exposure to potential hazards (Lioy, 2015), which prevent reliable confirmation or refutation of causal linkage between potential environmental influences on human health through misclassification bias (Armstrong, 1998).

In addition to uncertainties about environmental exposures affecting local communities, there is relatively limited published information on assessment of occupational exposures of people working in UNG operations. The most common sources of occupational exposure are likely to include: (1) direct and fugitive emissions of hydrocarbons from the well and associated infrastructure; (2) deliberate venting and flaring of gas and related petroleum products; (3) diesel exhaust emissions from hydraulic fracturing equipment, trucks and generators (Adgate *et al.*, 2014). These air pollutants have recommended guideline values specified by the World Health Organization (Table 1). Another pollutant of concern associated with diesel combustion is black carbon (BC), which is mostly found within fine particle fractions (Viidanoja *et al.*, 2002). Currently, there are no legislative air quality standards for BC (EEA, 2013) despite its increasingly clear association with negative health outcomes (Englert, 2004, Heal and Quincey, 2012, WHO, 2012) and its recognition as a simple marker of local combustion emissions.

The implementation of adequate air pollution monitoring is vital for effective management of risks to human health from UNG operations. This includes the collection of information on spatial and temporal patterns of air pollution from measurements and/or modelling (McKenzie *et al.*, 2014) to estimate human exposure

at specific locations (Werner *et al.*, 2015). For example, Zielinska *et al.* (2014) observed variations in benzene, NO_2 and VOCs concentrations from preliminary surveys and continuous measurements at several distances from the operation of UNG and within residential areas. Their study indicates that the main source of air pollutants emissions is generated from the gas production facilities.

Our study investigated short-term exposure to BC, NO_2 and O_3 in different locations at a simulated hydraulic fracturing site in Poland. We also made measurements of BC, NO_2 and O_3 within Glasgow city-centre to provide context to the concentrations measured at the UNG site. Knowledge about air pollution from UNG operations can be substantially improved through the deployment autonomy of portable measurement systems. We deployed miniature low power (hence portable and readily deployable (Snyder *et al.*, 2013)) sensor-based systems to measure exposures upwind, within and downwind of operation of hydraulic fracturing equipment. The results of this study have implications for best practice in protecting workers in close proximity to hydraulic fracturing equipment and begin to address some of the exposure assessment challenges associated with UNG development.

8.4 Methods

8.4.1 Monitoring Site

Field measurements were made on 22 June 2015 during a field visit to an UNG service company's logistics and storage site in Łowicz county (52.087°N, 19.916°E), 80 km west of Warsaw, Poland (Figure 8.1). This service company provided drilling, hydraulic fracturing, well testing services and seismic data acquisition services to the onshore oil and gas industry. The site was of similar scale to an active UNG site (area = 8862 m^2) and consisted of: an administrative and laboratory building; open storage area for heavy equipment; indoor storage warehouses; and a paved yard. The company set up a simulated hydraulic fracturing array in the yard consisting of a control cabin, three diesel-powered truck-mounted pumps, a blender and manifold truck (Figure 8.2 (a)).

Such simulated hydraulic fracturing procedures are part of the training for the company's operators. The equipment was not connected to a wellhead, but was run under equivalent pressures and loads to an active site. This experimental setup allowed us to assess the air quality effects of the diesel engines which used to power the hydraulic fracturing pumps (Josifovic *et al.*, 2016) in absence of pollution from natural gas, flowback water (which can degass), and gas infrastructure such as compressors and flarestacks.

8.4.2 Sampling strategy

We selected air sampling points (Figure 8.2 (b)) based on a site survey and assessment of wind direction. Wind direction was estimated using a compass and visual observation from the movement of nearby vegetation, and the direction in which visible exhaust smoke from machinery travelled. The wind was generally north to north-easterly for the duration of the visit. We made both mobile and static measurements. Mobile measurements were made while walking with the air monitors in background, upwind and downwind areas across the site (Figure 8.2 (b)). Static measurements were made at single upwind/downwind locations where the researcher stood with the monitors for 2 minutes to characterise emissions of air pollutants near the fracking pumps.

Monitoring locations are shown in Figure 8.2 (b) and described in Table 8.2. All monitoring locations were located within 10 m of diesel fracking pumps, to characterise exposure to combustion-related pollutants of the personnel who work in close proximity to this machinery. We also made indoor measurements in an office in the administrative building situated to the north-west of the fracking simulation site. This provided continuous monitoring of concentrations of pollutants alternately in different microenvironments at the experimental UNG facilities over a one-day visit.

We measured BC, NO_2 and O_3 concentrations during four time periods between 11:00 and 16:00 around the UNG facility. This included: mobile background measurements (between 11:00 and 12:00); indoor measurements in the office (between 13:00 to 14:30); and mobile and static measurements in the vicinity of operating hydraulic fracturing equipment (12:00 to 12:45 and 15:00 to 16:00).

We monitored BC, NO_2 and O_3 during the first sampling period (12.00-12.45), however we could only monitor BC during the second period (15:00 and 16:00) because of rain (the handheld NO_2 and O_3 instruments were not weather-proof). We made upwind and downwind BC measurements during the second period, but static measurements could not be made in the centre of the site during the operation of the high pressure pumps due to safety procedures. A summary of measurement locations and durations are presented in Table 8.3.

Both static and mobile measurements of upwind background concentrations were made (Figure 8.2(b)) to allow the cross-site gradient of air pollution concentrations to be compared to the nearest local authority air monitoring station (Figure 8.1). Additional mobile background measurements were made while walking from the administrative building towards to the east side of the heavy equipment open storage area (Figure 8.2(a)).

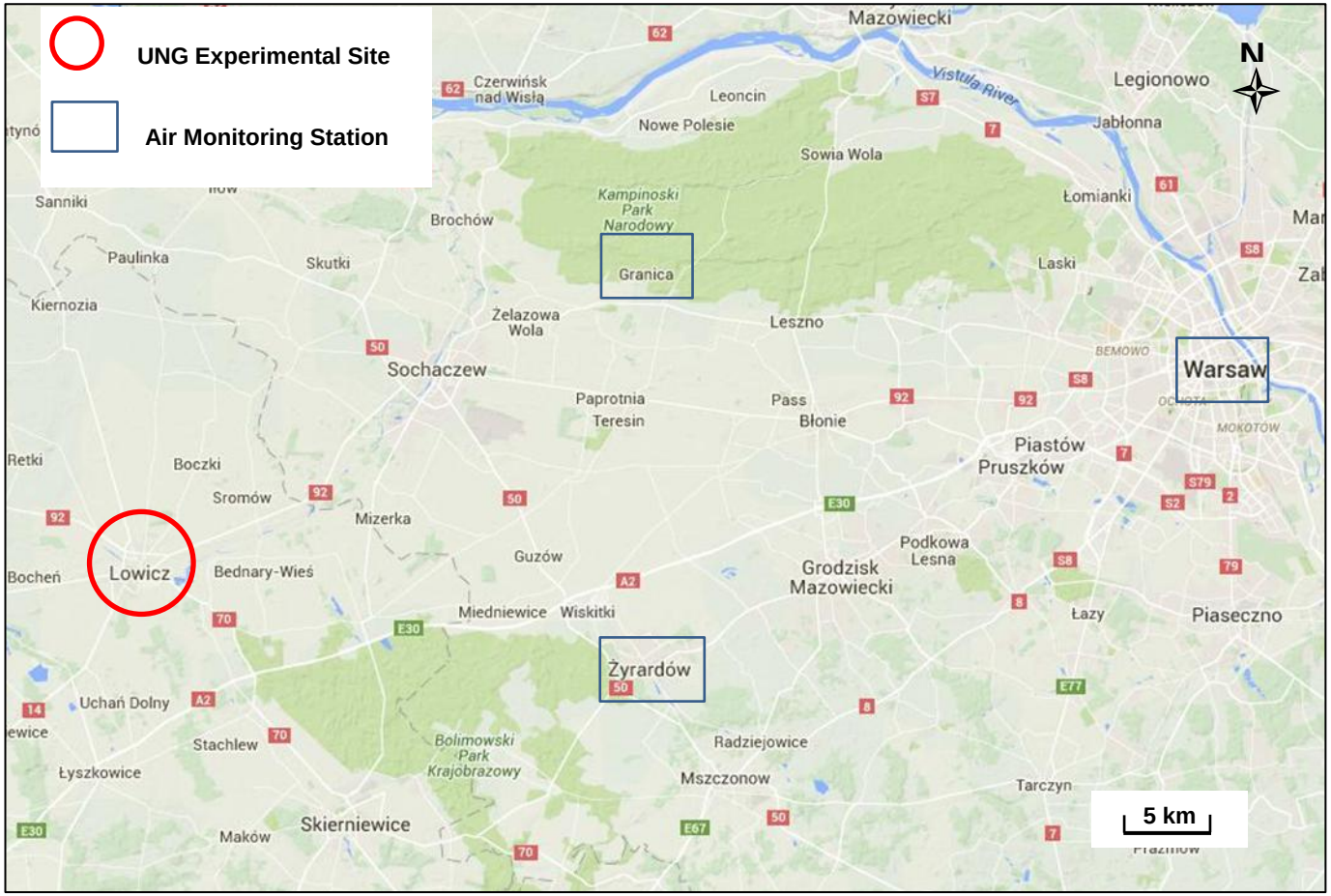

Figure 8.1: Location of UNG test site in Łowicz, Poland in relation to local air monitoring stations located in Granica (rural background), Zyrardow-Roosevelta (urban background), and Warszawa-Komunikacyjna (traffic site).

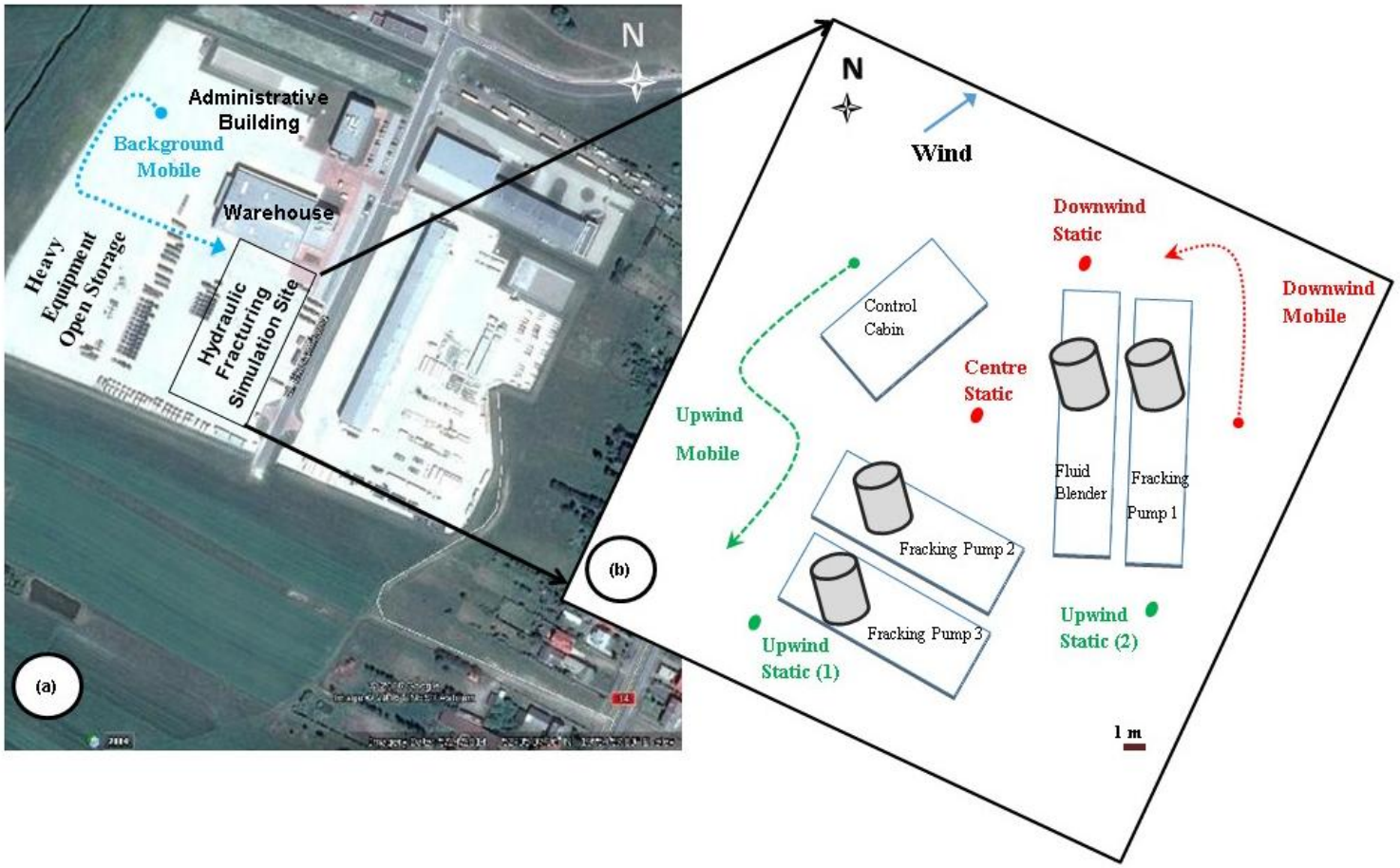

Figure 8.2: (a). The experimental UNG facility based in Łowicz county, Poland. The blue line represents the path of the mobile background measurements; (b) Schematic diagram of hydraulic fracturing simulation site, with locations of mobile and static measurements were taken; centre of site, downwind and upwind. The cylinder symbols represent locations of diesel exhaust stacks. The mobile measurements started from '●' and finished at the arrow tip.

Table 8.2: Location of mobile and static sampling points across the experimental hydraulic fracturing site.

Sample location name (& code)	Details of sample location (Figure 8.2b)
Upwind Static (1) - US(1)	2.5 metres from fracking pump 2 and 3
Upwind Static (2) - US(2)	2 metres from fracking pump 1
Downwind Static	1.5 metres from fluid blender and fracking pump 1
Centre Static (CS)	Between control cabin, fracking pump 2 & fluid blender
Background Mobile	While walking from the administrative building to the east side of heavy equipment open storage area (Fig. 8.2a)
Upwind Mobile (UM)	While walking from control cabin control to fracking pump 3
Downwind Mobile (DM)	While walking from east side to north side of fracking pump 1
Indoor	Static sample collected from an office in the administrative building

Table 8.3: Summary of black carbon (BC), nitrogen dioxide (NO_2) and ozone (O_3) measurements at different sampling sites.

Air Monitoring	Measurement duration (min)	Air Pollutant
Background	60	BC, NO_2 and O_3
Indoor[1]	90	BC, NO_2 and O_3
First Monitoring Period	45	BC, NO_2 and O_3
Second Monitoring Period	45	BC only

[1] the office room at the administrative building.

8.4.3 Black Carbon (BC) concentrations

We measured BC with two Aethlabs microAeth AE51 portable Aethalometer (AE51 Aethalometer; AethLabs, San Francisco, CA, USA). This instrument has been widely used to measure personal exposure to BC in different microenvironments (Dons *et al.*, 2014, Dons *et al.*, 2013, Dons *et al.*, 2012). AE51 Aethalometer samples air through a PTFE coated glass fibre (T60) filter strip, and quantify BC by attenuation of laser light. A 1 m length of conductive tubing was fitted to the BC instrument, the open end of which was fitted with a plastic rain hood to prevent water ingress to the instrument.

In this paper, we refer to the BC instruments according to their serial number (AE51 Aethalometer 1204 and 1303). BC instruments were calibrated by the manufacturer and new filters were fitted prior to conducting the measurements. The instruments were set to record data every second, with a flow rate of 100 ml min^{-1}. BC data was downloaded using MicroAethCOM software v2.2.4.0, and processed using an optimised noise adjustment (ONA) method ($\Delta ATN = 0.01$) to retain the highest possible temporal resolution (Hagler *et al.*, 2011). We averaged 1-seconds BC data to 1-minute intervals, to allow comparison with measurements recorded at 1-minute intervals from the NO_2 and O_3 monitors.

8.4.4 Nitrogen dioxide (NO_2) and ozone (O_3) concentrations

We measured NO_2 and O_3 with Aeroqual series 500 sensor-based monitors (Aeroqual Ltd, Auckland, New Zealand). In these monitors NO_2 was quantified using an electrochemical sensor (GSE 0–1 ppm) and ozone was quantified with a gas sensitive metal oxide semiconductor sensor (OZU 0–0.15 ppm). The Aeroqual NO_2 and O_3 monitors were set to record data at the highest resolution interval of 1-minute.

The Aeroqual NO_2 sensor has previously been shown to be affected by cross sensitivity to O_3, and consequently we corrected the concentrations measured by the Aeroqual NO_2 sensor prior to use following the method described in Lin et al. (2015). Briefly, the Aeroqual NO_2 and Aeroqual O_3 sensors were deployed at the

UK government Automatic Urban and Rural Network urban background monitoring station at Townhead, Glasgow (55.866 ºN, 4.244 ºW), which contains a chemiluminescence analyser measuring real-time NO_2 concentrations (referred to as the reference analyser). The concentrations measured by the reference analyser are subject to national QA and QC procedures (DEFRA, 2010) The co-location of the sensors at Townhead was from 17:00 (12 May 2015) to 08:00 (18 May 2015), 35-days prior to the measurements at the UNG site. A linear regression equation was calculated to describe the relationship between the difference in NO_2 concentration measured by the Aeroqual sensor and the reference analyser at the site, and the concurrent concentrations measured by the Aeroqual O_3 sensor (*Aeroqual O_3)*(µg/m^3) ((Masey *et al.*, 2017)*in preparation*):

$$NO_2 \text{ difference} = 0.97 * \text{Aeroqual } O_3 - 32.46 \qquad (8.1)$$

where:

NO_2 difference (µg/m^3) = observed difference between NO_2 concentration measured by the Aeroqual NO_2 monitor and the reference NO_2 analyser.

Equation 1 allows the concentrations measured by the Aeroqual NO_2 sensor to be corrected using concurrent measurements from the Aeroqual O_3 sensor to account for the Aeroqual NO_2 instrument cross-sensitivity to O_3:

$$NO_2 \text{ corrected} = NO_2 \text{ Aeroqual} - NO_2 \text{ difference} \qquad (8.2)$$

where:

NO_2 corrected (µg/m^3) = corrected Aeroqual NO_2 concentrations

NO_2 Aeroqual (µg/m^3) = unadjusted Aeroqual NO_2 concentrations

8.4.5 Field deployment procedure

The duplicate BC instruments were carried separately in two backpacks carried by 2 researchers. We fitted the NO_2 and O_3 monitors securely in the external mesh pockets of one of the backpacks. The internal clocks of all instruments were synchronised with internet time servers. All monitors were switched on at the same time and the sampling duration was recorded. We recorded a time-activity diary by hand during measurement periods.

8.4.6 Fixed air monitoring station

Local air pollution and meteorological data was obtained from monitoring stations on the Warsaw Regional Inspectorate of Environmental Protection internet site (http://sojp.wios.warszawa.pl/?par=90). These air quality measuring stations are operated by local government in Mazowieckie province. The nearest fixed monitoring sites were a rural background site (Granica-KPN; 50 km North East), a city background site (Zyrardow-Roosevelta; 45 km East North East), and a traffic site (Warszawa-Komunikacyjna; 85 km East) (Figure 8.1).

8.4.7 Additional BC and NO_2 measurements in Glasgow city centre

To provide context to the BC and NO_2 exposure measurements at the UNG site we made additional measurements of the same pollutants on a pre-defined walking route in Glasgow city centre using the portable real-time monitors (AE51 Aethalometer & Aeroqual) during 8 repeat walks over a four week period (30 June 2015 - 24 July 2015). To better understand the influence of nearby traffic on the BC and NO_2 concentrations measured by the instruments in Glasgow, we examined detailed spatiotemporal patterns for an example study period on 24 July 2015 using ArcGIS v.10.2.2 (Esri, USA). We also examined bivariate relationships between observed BC and NO_2 concentrations for the different study periods in Poland and Glasgow using reduced major axis regression (Ayers, 2001).

8.5 Results and discussion

8.5.1 Exposure assessment of BC, NO_2 and O_3 at hydraulic fracking test site

The concentrations of all pollutants measured at the hydraulic fracking test site increased as a result of fracking pump operation (Figure 8.3). As shown in Table 8.4, mobile background measurements reported a mean BC concentration of 0.008 µg/m^3, a mean NO_2 concentration of 19.1 µg/m^3 and a mean O_3 concentration of 39.9 µg/m$^{3.}$ Figure 8.3 (a) shows the time series for each sampling location for BC, NO_2 and O_3 measurements between 11:00 and 16:00 across all sampling sites. Changes in peak concentrations of BC and NO_2 were observed from the time series during the operation of the fracking pumps and gradually declined after the fracking pumps were switched off, during both the first and second monitoring periods.

Overall, spikes in BC and NO_2 accounted for the existence of local exhaust plumes emitted from the near-source of the fracking pumps. This characterises the short-term exposure that a site operator may experience working closely around the active pumps in comparison to the degree of pollutant concentrations travelling to the nearby vicinity. A similar observation was reported in Korea, where a higher levels of exposure was found in municipal household waste collectors working closer to the trash truck engines than the drivers of those trucks (Lee *et al.*, 2015).

We expanded the results into two discrete time-series based graphs to assess the BC, NO_2 and O_3 measurements during the first (Figure 8.3 (b)) and second (Figure 8.3 (c)) monitoring period for 45 minute sampling frames when the fracking pumps were operational. Observed concentrations of BC, NO_2 and O_3 varied substantially between the upwind and downwind sampling locations. During the first monitoring period, the maximum BC (51.2 µg/m^3) and NO_2 (287.5 µg/m^3) concentrations were highest at the downwind static and downwind mobile monitoring sites respectively. In contrast, the highest O_3 concentrations were recorded at the mobile upwind site (max = 53.0 µg/m^3). Fluctuating trends of all air pollutant concentration can be observed in the time series during downwind mobile measurements in Figure 8.3 (b).

Peaks for BC and NO_2 coincided with each other at centre static, downwind mobile and downwind static monitoring locations. Concentrations of O_3 appear more pronounced at the static upwind site. BC concentrations measured during the second monitoring period are also shown in Figure 8.3 (c). The BC concentrations were lower during this sampling event compared to the first monitoring period with several peaks observed at mobile and static monitoring downwind sites. This is resulted either from one of the fracking pumps being switched off or due to the weather's condition during this session. A sharp fall was observed from transition downwind mobile to downwind static sampling site. The magnitude and extent of these pollutant peaks were likely to be influenced by the on-site diesel machinery and wind direction. Zhu et al. (2002) reported significant discrepancies of combustion-related pollutants from motor vehicles monitored upwind and downwind of major highways. This variation indicates that the wind direction effects (upwind/downwind) play a major role in estimations of pollutant concentrations with the proximity to the nearby sources.

We compared the average of selected air pollutant metrics and metrological data from the nearest fixed monitoring station to Łowicz; city background, rural background and traffic (Table 8.5). The averaged air temperature and relative humidity recorded for the three monitoring stations were 19.5^0C and 42.4% correspondingly. The work was only carried out on one day, however the metrological conditions on this day were typical of the time of year 2015. Generally, the average of NO_2 concentrations measured from the rural background monitoring station (2.6 $\mu g/m^3$) were lower compared to averaged one-hour of background monitoring at the experimental site (19.1 $\mu g/m^3$). However, the maximum 1-minute of NO_2 measurements (287.5 $\mu g/m^3$) at the experimental site was nearly three times higher than the maximum 1-hour of the traffic measurement (101.4 $\mu g/m^3$). Violante et al. (2006) found personal exposure levels measured at the roadside environment were higher compared to measurements made by air monitoring station. The difference in the comparison of observed concentrations was directed to the major separation distance between the portable operated personal sensors and reference analyser.

Table 8.4: Summary statistics of black carbon (BC), nitrogen dioxide (NO_2) and ozone (O_3) concentrations of measurements at different sampling locations during operation of hydraulic fracturing pumps.

Site	**Start Time**	**End Time**	**Black Carbon (µg/m³)**			**Nitrogen dioxide (µg/m³)**			**Ozone (µg/m³)**		
			Mean	Max	Min	Mean	Max	Min	Mean	Max	Min
Background Mobile	11:00:00	12:00:00	0.0	0.0	0.0	19.1	33.6	-8.3	39.9	57.0	10.0
Fracking Test Site - First monitoring period											
Upwind Mobile	12:01:00	12:13:00	0.1	0.3	0.0	35.8	52.5	-5.2	7.8	49.0	0.0
Centre Static	12:14:00	12:16:00	16.9	27.5	9.7	192.8	256.5	124.5	0.0	0.0	0.0
Downwind Mobile	12:17:00	12:32:00	8.1	22.9	0.7	110.4	287.5	32.1	7.7	34.0	0.0
Downwind Static	12:33:00	12:35:00	46.2	51.2	42.1	128.9	172.5	87.6	24.7	37.0	0.0
Upwind Static (1)	12:37:00	12:39:00	0.1	0.1	0.1	49.4	69.5	34.8	30.3	46.0	0.0
Upwind Mobile	12:40:00	12:45:00	0.2	0.3	0.1	10.7	44.8	-8.6	53.0	64.0	45.0
Administrative Building	13:00:00	14:30:00	0.8	1.9	0.4	40.9	59.5	15.6	4.4	40.0	0.0
Fracking Test Site - Second monitoring period											
Upwind Static (2)	15:00:00	15:26:00	0.4	0.9	0.3	*					
Downwind Mobile	15:27:00	15:31:00	2.4	8.1	0.5	*					
Downwind Static	15:32:00	15:34:00	7.8	10.9	5.1	*					
Upwind Static (1)	15:36:00	15:38:00	0.3	0.4	0.3	*					
Upwind Mobile	15:39:00	15:45:00	0.5	0.6	0.3	*					

* NO_2 and O_3 concentrations were not measured during this period because of rainfall.

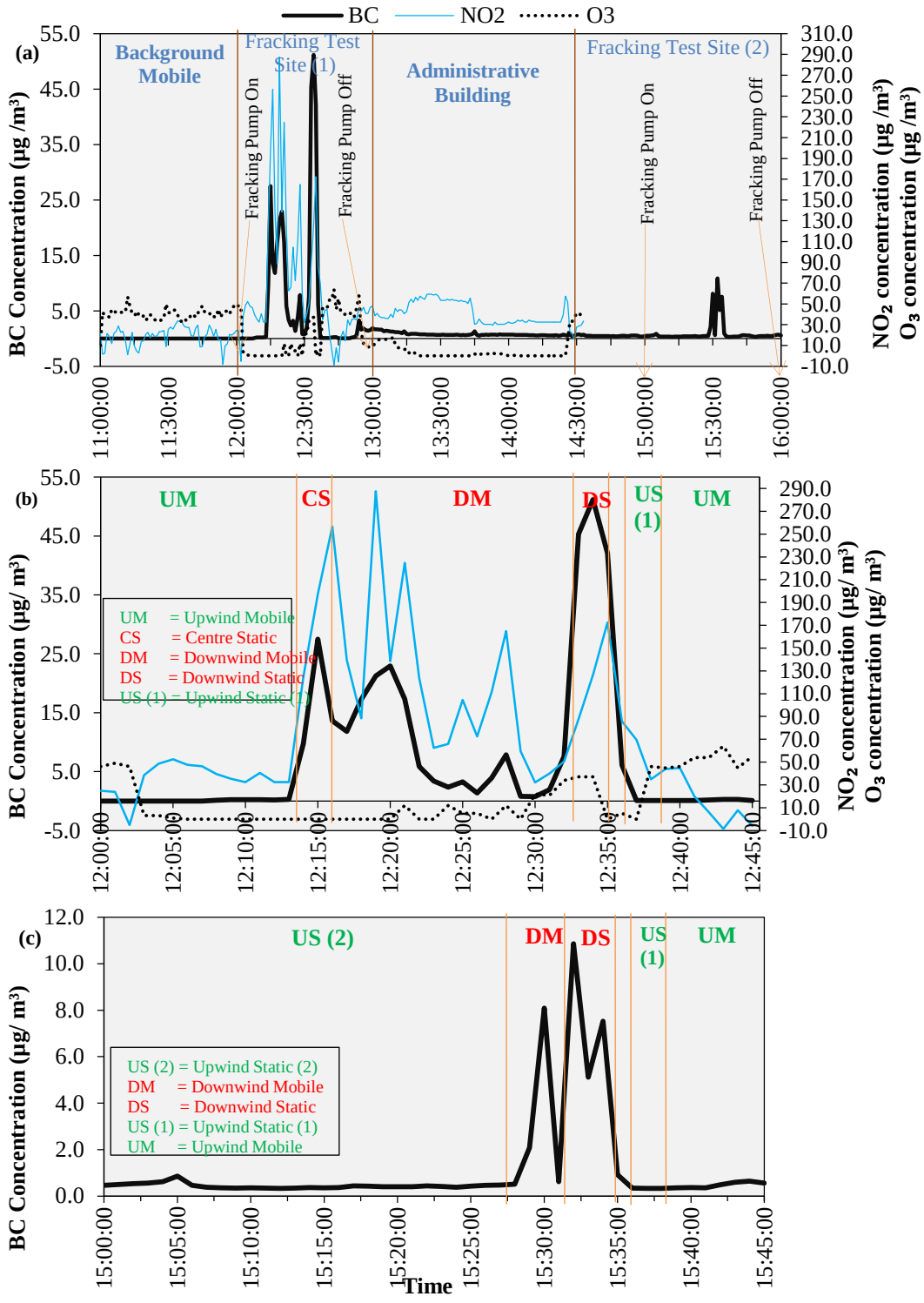

Figure 8.3: (a) Air pollutant concentrations measured at different locations within UNG site over full monitoring period. (b) BC, NO_2 and O_3 concentrations at the fracking test site during the first monitoring period, from 12:00 to 12:45. (c) BC concentrations measured.

Table 8.5: Meteorological and air pollution data obtained from monitoring stations near the sampling location (Figure 8.1). All data were obtained from the Warsaw Regional Inspectorate of Environmental Protection's website. 1-hour resolution data was selected to match the monitoring period on 22 June 2015 between 11:00 to 16:00.

Date and Time	**Granica-KPN (Rural Background)**				**Zyrardow-Roosevelta (City Background)**					**Warszawa-Komunikacyjna (Traffic)**				
	Temp (^{0}C)	RH (%)	Wind Speed (m/s^1)	NO_2 (µg/m^3)	Temp (^{0}C)	RH (%)	Wind Speed (m/s^1)	$PM_{2.5}$ (µg/m^3)	PM_{10} (µg/m^3)	Temp (^{0}C)	RH (%)	$PM_{2.5}$ (µg/m^3)	PM_{10} (µg/m^3)	NO_2 (µg/m^3)
22/6/2015 11:00	n/a[a]				18.1	47	0.89	4.7	8.5	18.5	46	11.2	30.3	79.2
22/6/2015 12:00	19.3	44	2.12	1.9	18.9	44	1.02	4.1	5.6	19.7	40	8.3	19.8	61.4
22/6/2015 13:00	19.7	42	2.02	3.5	19.8	42	1.06	2.8	4.2	20.2	38	9.4	24.7	81.3
22/6/2015 14:00	19.9	42	1.97	2.3	20.0	41	0.97	6.4	18.3	20.2	38	9.1	22.8	69.7
22/6/2015 15:00	19.2	44	1.78	2.4	19.2	42	0.99	9.1	22.6	20.5	37	10.0	28.1	93.9
22/6/2015 16:00	19.2	46	2.19	2.8	18.9	49	0.80	11.5	24.0	20.7	37	10.6	24.4	101.4

[a]data was not available.

8.5.2 Contrasting personal exposure to BC and NO_2 in urban traffic and industrial fracking environments

Figure 8.4 illustrates a concentration map of personal BC and NO_2 exposures in Glasgow city centre. Marked pollution gradients in both BC and NO_2 were observed on the walking routes depending on proximity to local traffic. The spatial pattern was relatively consistent between pollutant metrics and designated walking route. For a meaningful comparison in contrasting industrial and urban traffic environments, results for BC and NO_2 were presented in Figure 8.5.

The average concentrations of BC and NO_2 measured downwind of the hydraulic fracturing simulation site (11.2 and 111.3 $\mu g/m^3$ respectively) were approximately 3 times higher than walking in Glasgow city centre (3.7 and 42.3 $\mu g/m^3$). These concentrations were approximately 35 times and 4 times higher than the upwind background BC and NO_2 concentrations at the fracking site (0.3 and 20.8 $\mu g/m^3$ respectively). The BC measurements made at the hydraulic fracking simulation site (downwind) were found to be higher (mean = 11.2 $\mu g/m^3$) than the observation made in typical urban traffic area in Glasgow city centre (mean = 3.7 $\mu g/m^3$). The measurement is also higher compared to other observations in New York city reported by Kinney *et al.* (2000), that ranged between 1.5 to 6.2 $\mu g/m^3$.

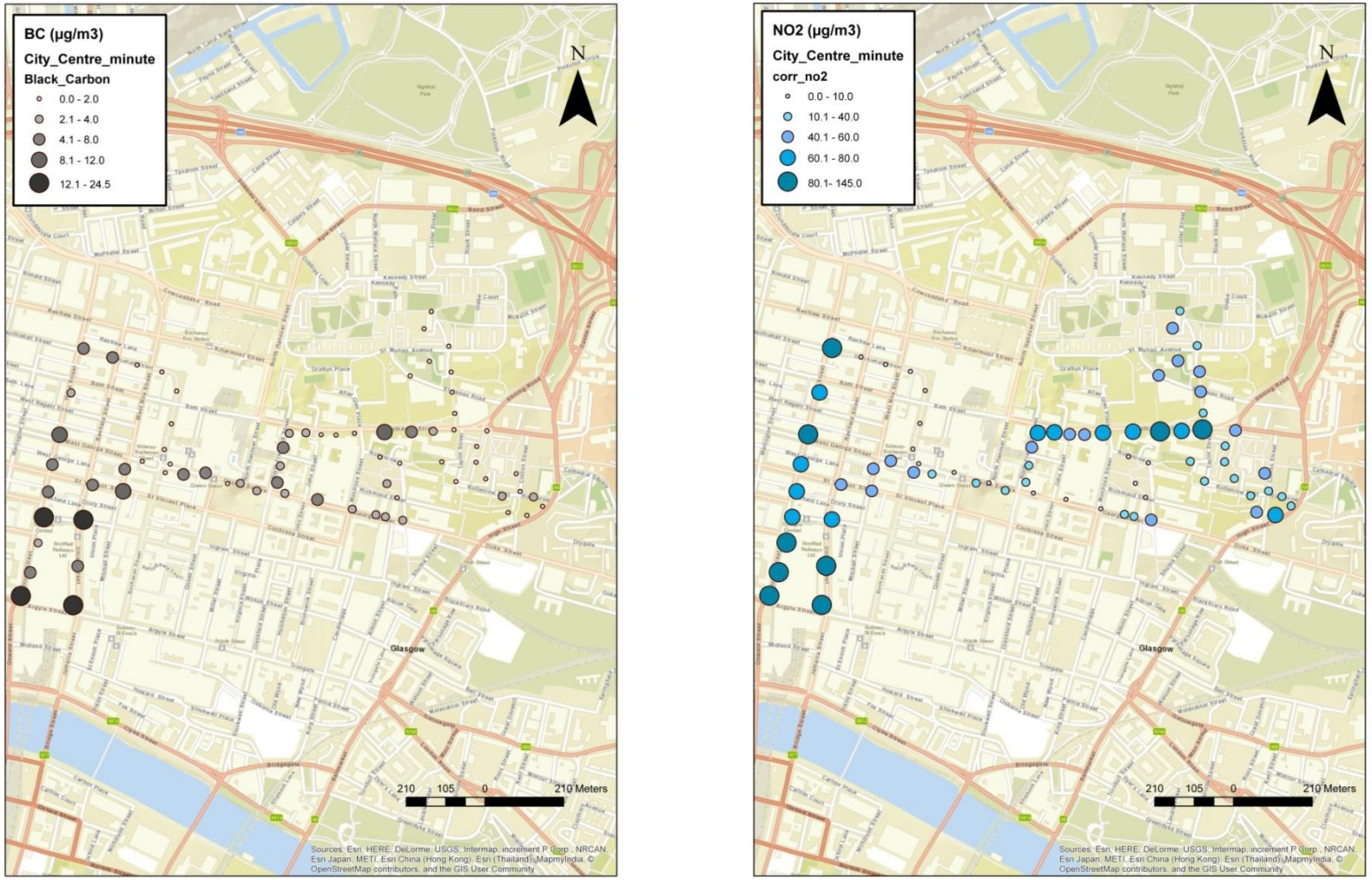

Figure 8.4: Examples of mobile measurements of BC (left hand map) and NO_2 (right hand map) made in Glasgow city centre on 24 July 2015.

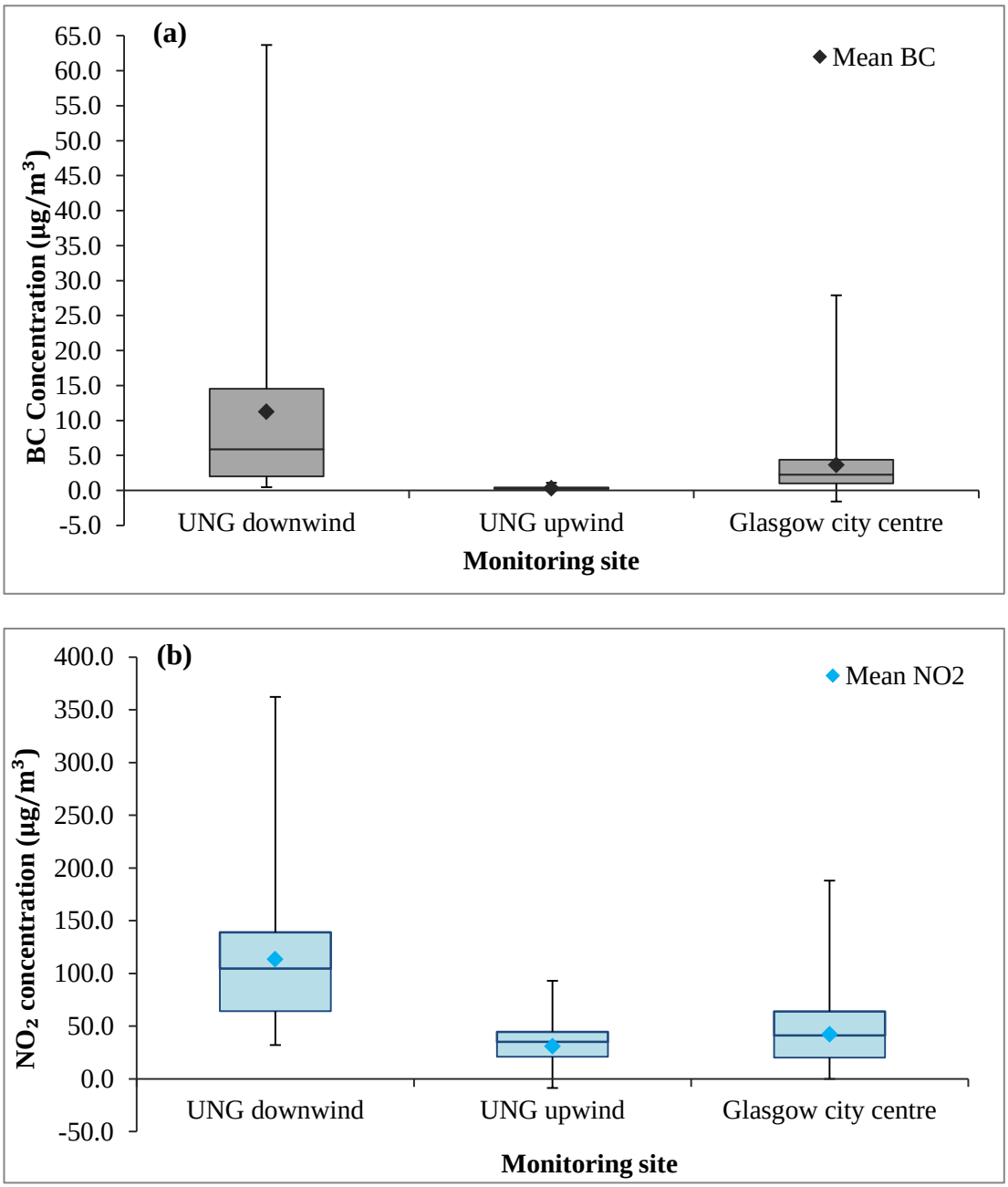

Figure 8.5: BC (a) and NO_2 (b) concentrations (µg/m^3) measured for each sampling site at UNG downwind (n = 23), UNG upwind (n = 53) and walking route in Glasgow city centre (n = 72). All measurements were shown in 1-minute intervals. The whisker plot shows the 3rd quartile at the upper end of box and the lower end shows the 1st quartile. The diamond points represent the average for BC and NO_2 measurements.

The correlation between BC, NO_2 and O_3 concentrations in different time-based intervals at hydraulic fracking test site and Glasgow city centre is shown in the correlation matrix (Figure 8.6 (a) – Figure 6 8.(c)). Our study shows that BC and NO_2 were correlated over different time resolutions and microenvironments. This shows that the increase of BC concentrations was followed by an increasing amount of NO_2. Similarly, there was a high correlation in mean BC and NO_2 reported by Riley *et al.* (2016) in their large scale campaigns in Baltimore, USA. Their study found BC and NO_2 were highly correlated (r = 0.85) during summer season.

Other studies also reported higher correlations between BC and NO_2 during winter season (Penttinen *et al.*, 2000) and at different types of road; roadside (Gillespie *et al.*, 2017) and highway (Beckerman *et al.*, 2008). Lower correlation between mean concentrations of BC and NO_2 measured in 1-minute compared to 5-minute and 15-minute time based, suggests that average 1-minute mobile measurements are poorly estimating extended spatial contrasts in both pollutants. In contrast, BC and NO_2 observations were highly correlated at 5-minute temporal resolution at the HF experimental site (r = 0.75) and the central Glasgow walking route (r = 0.68).

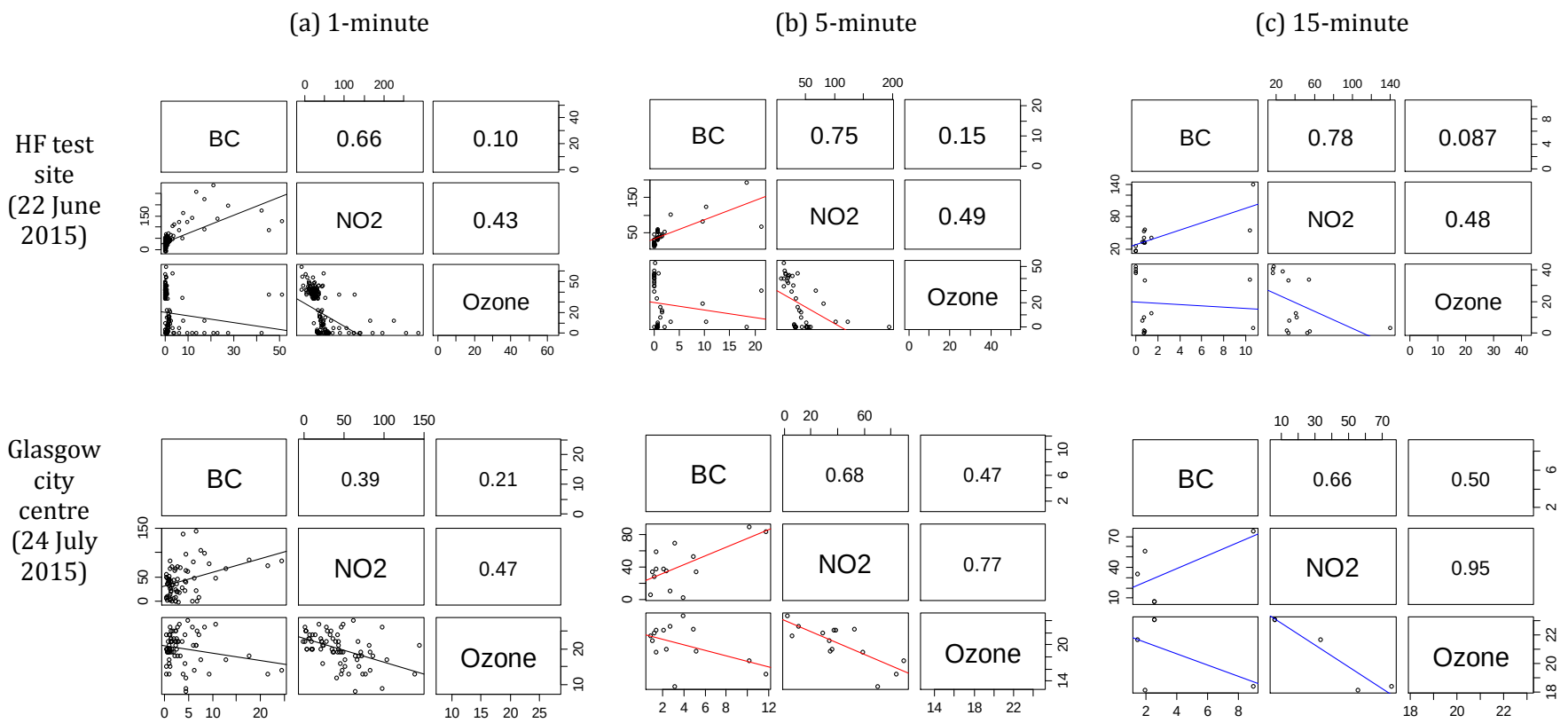

Figure 8.6: Black carbon, nitrogen dioxide and ozone correlation matrices measured at hydraulic fracking test site in Poland, and walking route in Glasgow city centre, UK for: (a). 1-minute resolution; (b). 5-minute resolution; and (c). 15-minute resolution.

We further investigated the bivariate relationship between NO_2 and BC for 5-minute average time resolutions (Table 8.6). Measurements made on 6/7/2015 & 15/7/2015 in Glasgow city centre were excluded due to the lower correlation between BC and NO_2 observed on these dates. Five minute average NO_2 concentrations explained 57% variation in measured BC concentrations at the HF site (n = 42). In contrast, the NO_2 measurements made in Glasgow city centre explained 38% of variance in BC concentrations (n =110). All measurements for walking study in Glasgow city centre explained 0 to 64% variations of 5-minute NO_2 and BC. The measurements made in the city centre were anticipated to have varying pollution concentrations due to the emissions from passing vehicles, compared to the UNG site which was anticipated to have more consistent emissions, and therefore the higher correlation between BC and NO_2 measurements a the UNG site was anticipated. The correlation between short-duration BC concentrations, measured using AE51 instrument, and weekly NO_2 concentrations, measured using passive sampler devices, have previously been shown to be improved with repeated measurements (R^2 = 0.28 for single measurements compared to R^2 = 0.75 for study-average concentrations) (Gillespie et al., 2017). The improved correlation observed between BC and NO_2 concentrations in this work compared to that reported by Gillespie et al. (2017) could be attributed to our concentrations being measured simultaneously over a shorter period of time.

A negative correlation between NO_2 and O_3 can be observed from the correlation matrix measured at HF test site and Glasgow city centre. This explains O_3 concentrations decreased with increasing NO_2 concentrations when the fracking pumps operate. Our study found ozone levels declined 60% on average after the operation of fracking pumps due to reaction with nitric oxide from NO_2 compounds. We would expect that NO_2 and O_3 concentrations to be correlated since we used O_3 to correct the NO_2 concentrations. This is similar to observations made by Durant et al. (2010) in vehicle emissions during a short exposure study; NO_2 concentrations were found to be higher than O_3 levels measured near the highway.

Table 8.6: Summary of Reduced Major Axis (RMA) Regression statistics for NO_2 vs. BC for 5-minute averaging periods for mobile measurements in Poland and Glasgow city centre (as can be seen in Table 7.8). Equivalent RMA statistics for static 'spot' measurements reported by Gillespie et al. (2017) are given for comparison.

Study name	n	R^2	slope	intercept
UNG test site Poland	42	0.57	0.14	-3.81
Glasgow city centre (exc. 6/7/2015 & 15/7/2015)	81	0.38	0.12	-2.2
Gillespie et al. (2017)	70	0.28	10.7	24.1
Individual study days for Glasgow city centre				
30/6/2015	12	0.43	0.25	-9.54
6/7/2015	15	0.12	0.17	-9.7
9/7/2015	15	0.64	0.12	0.10
14/7/2015	15	0.59	0.12	-2.96
15/7/2015	14	0.02	0.25	-10.12
22/7/2015	10	0.43	0.15	-5.22
23/7/2015	15	0.65	0.08	-1.99
24/7/2015	14	0.46	0.07	0.87

8.5.3 Comparing real time instruments

In this study, we demonstrated the feasibility of successful application of portable real-time air monitoring systems at a hydraulic fracking simulation site. The BC concentrations measured by the two BC devices at the hydraulic fracking test site were plotted against each other and the result is presented in Fig.6. The in-comparison of duplicate AE51 Aethalometer showed a good agreement ($R^2 > 0.90$). This demonstrates the on-line validation of AE51 Aethalometer monitors to measure BC concentrations consistently with short time resolutions. The average measurements made by AE51 Aethalometer 1204 (1.5 $\mu g/m^3$) were slightly higher than AE51 Aethalometer 1303 (1.7 $\mu g/m^3$), but consistent trends between both measurements was shown. Differences between the two monitors may have resulted from small spatial discrepancy as two individuals carried the monitors in separate

backpacks. The differences in BC readings can be associated with changes in humidity and temperature conditions especially during outdoor measurements (Cai *et al.*, 2014). Our findings only reported the use of duplicate BC sensors, therefore further research is needed for real-time NO_2 and O_3 instruments. This will give a clear understanding on instrument validations (Lewis and Edwards, 2016) as a proxy for mobile personal air sampling to meet relevant occupational and environmental measurement standards.

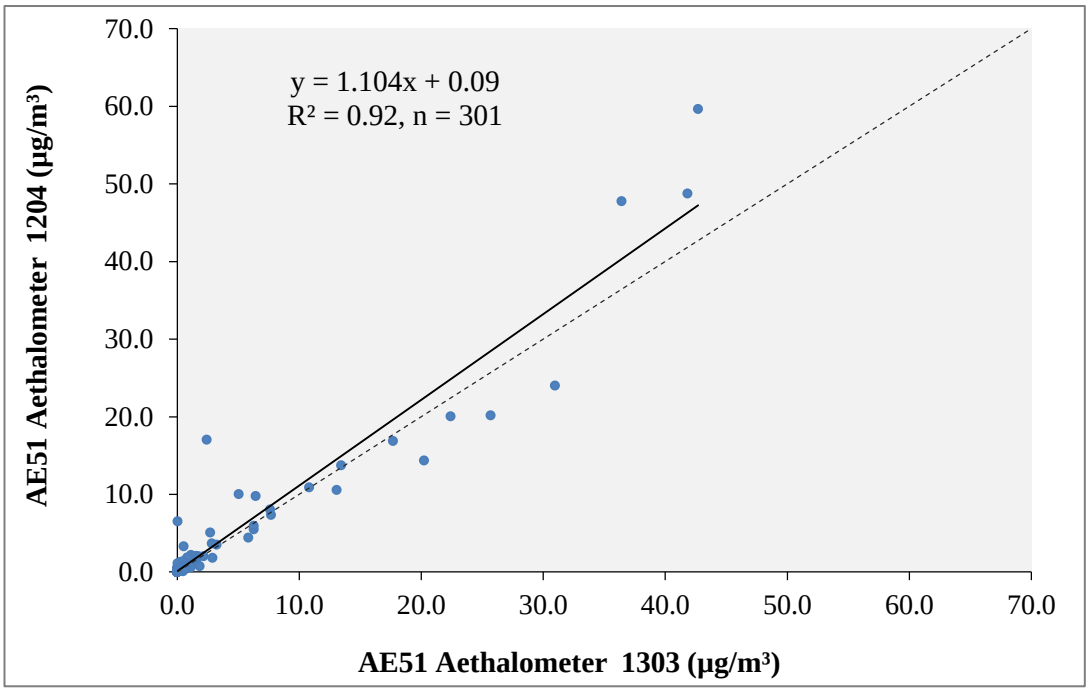

Figure 8.7: Simultaneous 1-minute average measurements made by AE51 Aethalometer 1303 and AE51 Aethalometer 1204 for monitoring at UNG site between 11:00 and 16:00.

8.6 Conclusions and recommendations

Through deployment of duplicate BC monitors and one set of NO_2 and O_3 sensors in a rural hydraulic fracking test site in Poland we have shown that site operators are exposed to levels of pollutants 2-3 times higher than pedestrians in the city centre of Glasgow. We observed high BC and NO_2 concentrations in close proximity to the diesel-powered machinery during the running of three fracking pumps. These high levels occur in locations on the site that are downwind of the diesel-powered pumps. Locations measured upwind of the pumps have pollutant concentrations ten times lower than the city centre, equivalent to typical rural levels. Measurements of the background levels at the study area and found no other significant source of air pollution.

These observations have significant implications for best practice in site design: control cabins should always, where practical be situated in the predominantly upwind direction. In addition, for measuring site exposure, these techniques should be used to quantify personal exposures to emissions to air pollutants generated during fracking operations, and to quantify exposures in nearby communities. The site that we worked at was running two to three pumps under simulated ideal operating conditions. Real sites often run up to 20 pumps which typically each of the pump designed to generate maximum pressure of 1000 bar (King, 2012), and under real operating conditions, the pumps often run under non-optimal loads due to for instance pump failure, complex geotechnical feedback. Further provisional assessment may require monitoring the occasional emissions from arrays of fracking pumps in real-world operating conditions.

Such information will be beneficial to potentially reduce diesel engines on site through, for example power from gas turbines, electric pumps and measure to reduce power consumption by pumps (Josifovic *et al.*, 2016). Exposure characterisation will be advantageous to UNG extraction operators by enabling quantitative assessment of the benefits and costs of implementing engineering controls and/or personal protective equipment (PPE) to reduce employee exposure to diesel engine emissions

(HSE, 2012). Further work into personal exposure required to asses most appropriate respirator (Penconek *et al.*, 2013) under the condition of exposure to diesel exhaust emissions at UNG operations site.

8.7 Acknowledgement

Eliani Ezani is funded by the Ministry of Higher Education Malaysia (KPT(BS)860126295394). Nicola Masey is funded through a UK Natural Environment Research Council CASE PhD studentship (NE/K007319/1), with support from Ricardo Energy and Environment. Jonathan Gillespie is funded through an Engineering and Physical Sciences Research Council Doctoral Training Grant (EPSRC DTG EP/L505080/1 and EP/K503174/1) studentship, with support from the University of Strathclyde and Ricardo Energy and Environment. We acknowledge the late Dr. David Cunningham of Department of Design Manufacture & Engineering Management, University of Strathclyde for organising the site visit to Poland. We also thanks to Megan Tailford for her assistance during fieldwork.

8.8 Summary

This study case study has offered an evaluative technique on monitoring air pollutants and conducted by means of notable real-time instruments of BC and NO_2 near the UNG operations. This study also encountered a number of limitations such as the monitoring was performed for only one day due to restrict access to the field site. The operation of the wearable real-time monitors in Glasgow urban outdoor areas also demonstrates practicability of deploying the instrument in the real world situation. The personal exposure to BC and NO_2 measured in Glasgow and Poland was compared using dedicated high temporal resolutions of MicroAeth and Aeroqual sensors. Average of BC and NO_2 concentrations at the downwind of hydraulic fracturing test site were approximately 2-3 times higher respectively than the urban Glasgow central. Despite the differences in measurement techniques and environmental settings, the personal exposure to combustion-related air pollutants can still be characterised. The application of the real-time sensors demonstrates their adaptability and precision measurements in the real world environment.

8.9 References

Adgate, J. L., Goldstein, B. D. & McKenzie, L. M. 2014. Potential Public Health Hazards, Exposures and Health Effects from Unconventional Natural Gas Development. *Environmental Science & Technology,* 48**,** 8307-8320.

Armstrong, B. G. 1998. Effect of measurement error on epidemiological studies of environmental and occupational exposures. *Occupational and Environmental Medicine,* 55**,** 651-656.

Ayers, G. P. 2001. Comment on regression analysis of air quality data. *Atmospheric Environment,* 35**,** 2423-2425.

Beckerman, B., Jerrett, M., Brook, J. R., Verma, D. K., Arain, M. A. & Finkelstein, M. M. 2008. Correlation of nitrogen dioxide with other traffic pollutants near a major expressway. *Atmospheric Environment,* 42**,** 275-290.

Cai, J., Yan, B., Ross, J., Zhang, D., Kinney, P. L., Perzanowski, M. S., Jung, K., Miller, R. & Chillrud, S. N. 2014. Validation of MicroAeth® as a Black Carbon Monitor for Fixed-Site Measurement and Optimization for Personal Exposure Characterization. *Aerosol and air quality research,* 14**,** 1-9.

Chapman, S., St George, A., Waller, K. & Cakic, V. 2013. The pattern of complaints about Australian wind farms does not match the establishment and distribution of turbines: support for the psychogenic, 'communicated disease' hypothesis. *PLoS One,* 8**,** e76584.

DEFRA. 2010. *The Data Verification and Ratification Process* [Online]. Available: https://ukair.defra.gov.uk/assets/documents/The_Data_Verification_and_Ratification_Process.pdf [Accessed 16 March 2017].

Dons, E., Int Panis, L., Van Poppel, M., Theunis, J. & Wets, G. 2012. Personal exposure to Black Carbon in transport microenvironments. *Atmospheric Environment,* 55**,** 392-398.

Dons, E., Temmerman, P., Van Poppel, M., Bellemans, T., Wets, G. & Int Panis, L. 2013. Street characteristics and traffic factors determining road users' exposure to black carbon. *Science of The Total Environment,* 447**,** 72-79.

Dons, E., Van Poppel, M., Kochan, B., Wets, G. & Panis, L. I. 2014. Implementation and validation of a modeling framework to assess personal exposure to black carbon. *Environment International,* 62**,** 64-71.

EEA, E. E. A. 2013. *Air Quality in Europe - 2013 report* [Online]. Denmark. Available: http://www.eea.europa.eu/publications/air-quality-in-europe-2013 [Accessed 17 October 2015 9].

Elliott, E. G., Trinh, P., Ma, X. M., Leaderer, B. P., Ward, M. H. & Deziel, N. C. 2017. Unconventional oil and gas development and risk of childhood leukemia: Assessing the evidence. *Science of the Total Environment,* 576**,** 138-147.

Elsner, M. & Hoelzer, K. 2016. Quantitative Survey and Structural Classification of Hydraulic Fracturing Chemicals Reported in Unconventional Gas Production. *Environmental Science & Technology,* 50**,** 3290-3314.

Englert, N. 2004. Fine particles and human health—a review of epidemiological studies. *Toxicology Letters,* 149**,** 235-242.

Field, R. A., Soltis, J. & Murphy, S. 2014. Air quality concerns of unconventional oil and natural gas production. *Environmental Science: Processes & Impacts,* 16**,** 954-969.

Gillespie, J., Masey, N., Heal, M. R., Hamilton, S. & Beverland, I. J. 2017. Estimation of spatial patterns of urban air pollution over a 4-week period from repeated 5-min measurements. *Atmospheric Environment,* 150**,** 295-302.

Hagler, G. S. W., Yelverton, T. L. B., Vedantham, R., Hansen, A. D. A. & Turner, J. R. 2011. Post-processing Method to Reduce Noise while Preserving High Time Resolution in Aethalometer Real-time Black Carbon Data *Aerosol and Air Quality Research,* 11**,** 546.

Hays, J., Finkel, M. L., Depledge, M., Law, A. & Shonkoff, S. B. C. 2015. Considerations for the development of shale gas in the United Kingdom. *Science of The Total Environment,* 512–513**,** 36-42.

Heal, M. R. & Quincey, P. 2012. The relationship between black carbon concentration and black smoke: A more general approach. *Atmospheric Environment,* 54**,** 538-544.

HEI. 2010. *Traffic-Related Air Pollution: A Critical Review of the Literature on Emissions, Exposure, and Health Effects. Health Effects Institute, Special Report 17* [Online]. Available: http://pubs.healtheffects.org/view.php?id=334 [Accessed 17 March 2017].

HSE 2012. Control of diesel engine exhaust emissions in the workplace. 2 ed.

Islam, S. M. N., Jackson, P. L. & Aherne, J. 2016. Ambient nitrogen dioxide and sulfur dioxide concentrations over a region of natural gas production, Northeastern British Columbia, Canada. *Atmospheric Environment,* 143**,** 139-151.

Josifovic, A., Roberts, J. J., Corney, J., Davies, B. & Shipton, Z. K. 2016. Reducing the environmental impact of hydraulic fracturing through design optimisation of positive displacement pumps. *Energy,* 115, Part 1**,** 1216-1233.

King, G. E. 2012. *Hydraulic fracturing 101: what every representative environmentalist regulator reporter investor university researcher neighbor and engineer should know about estimating frac risk and improving frac performance in unconventional gas and oil wells* [Online]. Available: http://www.kgs.ku.edu/PRS/Fracturing/Frac_Paper_SPE_152596.pdf [Accessed 21 March 2017].

Kinney, P. L., Aggarwal, M., Northridge, M. E., Janssen, N. A. & Shepard, P. 2000. Airborne concentrations of PM(2.5) and diesel exhaust particles on Harlem sidewalks: a community-based pilot study. *Environmental Health Perspectives,* 108**,** 213-218.

Kovats, S., Depledge, M., Haines, A., Fleming, L. E., Wilkinson, P., Shonkoff, S. B. & Scovronick, N. The health implications of fracking. *The Lancet,* 383**,** 757-758.

Krzyzanowski, M. & Cohen, A. 2008. Update of WHO air quality guideline. *Air Qual Atmos Health,* 1**,** 13.

Larock, S. & Baxter, J. 2013. Local facility hazard risk controversy and non-local hazard risk perception. *Journal of Risk Research,* 16**,** 713-732.

Lee, K.-H., Jung, H.-J., Park, D.-U., Ryu, S.-H., Kim, B., Ha, K.-C., Kim, S., Yi, G. & Yoon, C. 2015. Occupational Exposure to Diesel Particulate Matter in Municipal Household Waste Workers. *PLoS ONE,* 10**,** e0135229.

Lewis, A. & Edwards, P. 2016. Validate personal air-pollution sensors. *Nature,* 535**,** 29-31.

Lin, C., Gillespie, J., Schuder, M. D., Duberstein, W., Beverland, I. J. & Heal, M. R. 2015. Evaluation and calibration of Aeroqual series 500 portable gas sensors for accurate measurement of ambient ozone and nitrogen dioxide. *Atmospheric Environment,* 100**,** 111-116.

Lioy, P. J. 2015. Exposure science and its places in environmental health sciences and risk assessment: why is its application still an ongoing struggle in 2014? *Journal of Exposure Science and Environmental Epidemiology,* 25**,** 1-3.

Masey, N., Gillespie, J., Ezani, E., Lin, C., Hao, W., Heal, M. R., Ferguson, N., Hamilton, S. & Beverland, I. J. 2017. Temporal changes in field calibration relationships for Aeroqual S500 NO_2 and O_3 sensors.(*in preparation*)

McKenzie, L. M., Allshouse, W. B., Burke, T., Blair, B. D. & Adgate, J. L. 2016. Population Size, Growth, and Environmental Justice Near Oil and Gas Wells in Colorado. *Environmental Science & Technology,* 50**,** 11471-11480.

McKenzie, L. M., Guo, R., Witter, R. Z., Savitz, D. A., Newman, L. S. & Adgate, J. L. 2014. Birth outcomes and maternal residential proximity to natural gas development in rural Colorado. *Environ Health Perspect,* 122**,** 412-7.

McKenzie, L. M., Witter, R. Z., Newman, L. S. & Adgate, J. L. 2012. Human health risk assessment of air emissions from development of unconventional natural gas resources. *Science of The Total Environment,* 424**,** 79-87.

Mohan, R., Leonardi, G. S., Robins, A., Jefferis, S., Coy, J., Wight, J. & Murray, V. 2009. Evaluation of Methodologies for Exposure Assessment to Atmospheric Pollutants from a Landfill Site. *Journal of the Air & Waste Management Association,* 59**,** 490-501.

NPL. 2015. *Facts on fracking needed to make responsible decisions about UK energy* [Online]. Available: http://www.npl.co.uk/news/facts-on-fracking-needed-to-make-responsible-decisions-about-uk-energy. [Accessed 17 March 2017].

Paulik, L. B., Donald, C. E., Smith, B. W., Tidwell, L. G., Hobbie, K. A., Kincl, L., Haynes, E. N. & Anderson, K. A. 2016. Emissions of Polycyclic Aromatic Hydrocarbons from Natural Gas Extraction into Air. *Environmental Science & Technology,* 50**,** 7921-7929.

Penconek, A., Drążyk, P. & Moskal, A. 2013. Penetration of Diesel Exhaust Particles Through Commercially Available Dust Half Masks. *The Annals of Occupational Hygiene,* 57**,** 360-373.

Penttinen, P., Alm, S., Ruuskanen, J. & Pekkanen, J. 2000. Measuring reflectance of TSP-filters for retrospective health studies. *Atmospheric Environment,* 34**,** 2581-2586.

Rabinowitz, P. M., Slizovskiy, I. B., Lamers, V., Trufan, S. J., Holford, T. R., Dziura, J. D., Peduzzi, P. N., Kane, M. J., Reif, J. S., Weiss, T. R. & Stowe, M. H. 2015. Proximity to natural gas wells and reported health status: results of a household survey in Washington County, Pennsylvania. *Environ Health Perspect,* 123**,** 21-6.

Rasmussen, S. G., Ogburn, E. L., McCormack, M., Casey, J. A., Bandeen-Roche, K., Mercer, D. G. & Schwartz, B. S. 2016. Association Between Unconventional Natural Gas Development in the Marcellus Shale and Asthma Exacerbations. *Jama Internal Medicine,* 176**,** 1334-1343.

Riley, E. A., Schaal, L., Sasakura, M., Crampton, R., Gould, T. R., Hartin, K., Sheppard, L., Larson, T., Simpson, C. D. & Yost, M. G. 2016. Correlations between short-term mobile monitoring and long-term passive sampler measurements of traffic-related air pollution. *Atmospheric Environment,* 132**,** 229-239.

Scottish-Government. 2015. *Moratorium called on fracking* [Online]. Available: http://news.scotland.gov.uk/News/Moratorium-called-on-fracking-1555.aspx. [Accessed 17 March 2017].

SEPA. 2015. *Shale gas and coal bed methane* [Online]. Available: http://www.sepa.org.uk/environment/energy/non-renewable/shale-gas-and-coal-bed-methane/. [Accessed 17 March 2017].

Snyder, E. G., Watkins, T. H., Solomon, P. A., Thoma, E. D., Williams, R. W., Hagler, G. S. W., Shelow, D., Hindin, D. A., Kilaru, V. J. & Preuss, P. W. 2013. The Changing Paradigm of Air Pollution Monitoring. *Environmental Science & Technology,* 47**,** 11369-11377.

UK-Committee-on-Toxicity. 2010. *COT second statement on landfill sites. UK Committee on Toxicity (Food Standards Agency)* [Online]. Available: http://cot.food.gov.uk/cotstatements/cotstatementsyrs/cotstatements2010/cot201001 [Accessed 17 March 2017].

Viidanoja, J., Sillanpää, M., Laakia, J., Kerminen, V.-M., Hillamo, R., Aarnio, P. & Koskentalo, T. 2002. Organic and black carbon in PM2.5 and PM10: 1 year of data from an urban site in Helsinki, Finland. *Atmospheric Environment,* 36**,** 3183-3193.

Vrijheid, M. 2009. Landfill sites and congenital anomalies - have we moved forward? *Occupational and Environmental Medicine,* 66**,** 71-71.

Wang, Q., Chen, X., Jha, A. N. & Rogers, H. 2014. Natural gas from shale formation – The evolution, evidences and challenges of shale gas revolution in United States. *Renewable and Sustainable Energy Reviews,* 30**,** 1-28.

Werner, A. K., Vink, S., Watt, K. & Jagals, P. 2015. Environmental health impacts of unconventional natural gas development: A review of the current strength of evidence. *Science of The Total Environment,* 505**,** 1127-1141.

WHO. 2012. *Health Effects of Black Carbon* [Online]. Denmark. Available: http://www.euro.who.int/__data/assets/pdf_file/0004/162535/e96541.pdf [Accessed 20 January 2015].

Zielinska, B., Campbell, D. & Samburova, V. 2014. Impact of emissions from natural gas production facilities on ambient air quality in the Barnett Shale area: a pilot study. *J Air Waste Manag Assoc,* 64**,** 1369-83.

9 CONCLUSIONS

9.0 Overall aims of this study

This research has successfully developed state-of-art methods for assessing exposure to combustion-related air pollutant in indoor and outdoor locations. The following objectives were achieved:

(i) Innovative sampling and analysis techniques were developed using a simple and relatively low-cost portable, low power sampler for particulate matter (PM), black carbon (BC), Ozone (O_3), nitrogen dioxide (NO_2**)** and particulate-bound polycyclic aromatic hydrocarbons (pPAHs). This system was developed for personal and environmental monitoring with a focus on the simplest metric of exposure - colour analysis of particle darkness, alongside measurements using passive NO_2 samplers, and portable real-time monitors. The portability of these measurement systems simplified exposure assessment procedures. More complex and expensive analytical laboratory techniques using GC-MS for pPAHs compounds were also examined.

(ii) The systems identified and developed for cost-effective, portable low power monitoring were evaluated by comparison against reference PM, BC, O_3 and NO_2 measurements. Simple methods for non-destructive and low-cost optical analysis of sequentially loaded filter air samples were used to estimate BC from filter reflectance

and scanned images by calibration against co-located micro-aethalometer observations. Real-time micro-aethalometer BC and Aeroqual sensors were evaluated by comparison against reference BC and NO_2 measurements at a UK government Automatic Urban and Rural Network (AURN) monitoring site.

(iii) Combustion related air pollutants, including PM, BC and NO_2 were assessed in indoor and urban outdoor locations. Indoor PM, BC and NO_2 concentrations measured in the university offices were generally low compared to the outdoor pollution objectives specified in the UK National Air Quality Strategy and associated EU directives. In contrast, outdoor NO_2 concentrations (> 40 $\mu g/m^3$) measured in the Glasgow city centre had exceeded the guideline value.

(iv) The main determinants of PM, BC and NO_2 concentrations in different locations and personal exposures were examined. Exposure to combustion-related air pollutants were influenced by the ventilation systems in indoor office locations. Commuters were exposed to high BC and NO_2 concentrations when walking along busy street canyons. There were consistently higher $PM_{2.5}$ mass and BC concentrations, closer to the height of traffic exhaust emissions along walking routes in Glasgow city centre. Therefore, children may have greater exposure than adults to airborne particles close to the urban roadsides. Marked elevations of BC and NO_2 concentrations were also observed in proximity to industrial fracking operations.

(v) PM, BC and NO_2 were identified as useful proxies for combustion-related air pollutants from urban traffic and industrial diesel exhaust emissions. These pollutant metrics were consistently highly correlated with each other despite differences in absolute concentrations resulting from different pollutant source-receptor characteristics in different locations.

9.1 Summary of specific findings

The novel methods developed for measurement of combustion-related air pollutants address specific requirements for improved exposure assessment (Jantunen *et al.*, 2002, Koehler and Peters, 2015). Within the above broad context, this thesis identifies pressing requirements for reliable measurement techniques to quantify personal exposure to combustion-related pollutants. Correspondingly, the specific findings in the thesis are divided between development of novel exposure assessment methods and application of those methods to quantify exposure to combustion-related air pollutants in indoor and outdoor locations.

9.1.1 The state-of-art methods of sampling and analysis of combustion-related air pollutants

(a) In chapter 4, the development of methods was described for combustion-related air pollutants including PM, BC, NO_2 and pPAHs. The techniques were developed to collect and analyse the air pollutant samples from simple, and low-cost systems over a range of exposure time intervals. The performance of personal air sampling pumps, passive diffusion samplers, and the real-time sensors were evaluated in pilot experiments. The application of a relatively low flow rate (1.0 L min^{-1}) using Casella Apex personal air sampling pumps provided stable operation over extended periods required to collect PM specimens in environmental exposure assessment.

(b) In chapter 5, the field evaluation of collocated portable low power equipment of BC and NO_2 against reference analysers, demonstrated that these monitors could be calibrated to enable subsequent application in mobile and peripatetic monitoring of combustion-related air pollutants.

(c) The use of simple methods for non-destructive and low-cost optical analysis of sequentially loaded filter air samples are described in Chapter 5 & 7. These have demonstrated how BC can be estimated from filter reflectance and scanned filter images calibrated against co-located micro-aethalometer observations. Quadratic functional relationships between filter darkness and accumulated BC density (BC

mass/filter area) explained more than 97% of the variation in the latter, from normalised reflectance and scanner measurements.

(d) In chapter 6 & 7, filter-based gravimetric and reflectometer measurements provided reliable estimates of PM mass and darkness of carbonaceous particles (BC) in indoor and outdoor locations. In chapter 6, PM_1, $PM_{2.5}$, PM_{10}, BC, NO_2 and O_3 were measured using real-time instruments (Osiris, MicroPEM, micro-aethalometer, Aeroqual and LEO respectively). Passive NO_2 samplers were evaluated at the AURN monitoring sites and used in outdoor and indoor measurements.

(e) In chapter 8, the operation of the wearable real-time sensors demonstrates practicability of deploying the instrument in the industrial fracking test site in Poland.

9.1.2 Measurement of PM, BC and NO_2 exposure in indoor and outdoor locations

(a) Indoor pollution exposure was measured in refurbished (Department of Civil & Environmental Engineering) and existing office (International Study Centre) in the University of Strathclyde buildings during summer 2014 & 2016 respectively. Indoor measurements of PM, BC and NO_2 were influenced by the outdoor sources through natural and mechanical ventilation of buildings near roads in Glasgow city centre. The use of office equipment including printers and photocopiers was found to be a determinant of PM and BC concentrations in the office areas.

(b) Generally, the mean personal exposure levels of PM, BC and NO_2 are lower seen for indoor measurements. The mean exposures of $PM_{2.5}$ at both offices were ranged between 2.8 – 6.6 $\mu g/m^3$ respectively (48-hour measurements). This concentration is similar to that reported by Semple *et al.* (2013), Semple *et al.* (2012) in Scottish non-smoking households and Steinle *et al.* (2015) in Scottish office and public buildings (3.0 – 6.3 $\mu g/m^3$). These concentrations are however lower than those another studies reported in homes and school building of low- and middle-income countries

(LMICs). For example, concentrations of $PM_{2.5}$ reported in urban schools in Malaysia (11.3 – 32.9 µg/m^3) (Zainal Abidin *et al.*, 2014), rural and urban Nepalese households (29 – 2610 µg/m^3) (Kurmi *et al.*, 2008), and Malawian homes ranging between 30 – 856 µg/m^3 (Fullerton *et al.*, 2009).

(c) The methods employed using filter-based sampling, passive samplers, and real-time monitors were used to assess PM, BC and NO_2 exposure while walking on a pre-defined route in Glasgow city centre during summer 2014 & 2015 and winter 2015. Measurements were made at two heights to investigate whether the combustion-related air pollutant concentrations at child pushchair and adult inhalation heights were different from lower to upper heights at roadside locations. Consistent increased $PM_{2.5}$ mass concentrations (13.6% increases in mean) and reflectance (19.2% increase in mean) were observed at the lower height (0.8 m) compared to upper height (1.68 m). NO_2 concentrations were also generally greater at the lower height.

(d) Another set of BC and NO_2 measurements were made using micro-aethalometer and Aeroqual instruments on different walking routes in Glasgow. Variations of BC and NO_2 measured on these routes were mainly determined by time of day and street topography. BC and NO_2 concentrations measured at near roadsides were substantially higher than the measurements recorded at the AURN background monitoring site. Highest BC and NO_2 concentrations were recorded in the Hope St. street canyon (24.5 µg/m^3 and 138.3 µg/m^3 respectively). Average BC and NO_2 concentrations during mid-day observations were 22% higher than morning and mid-afternoon measurements along walking routes close to the University of Strathclyde campus.

(e) Mobile measurements at varying distances from sources of diesel exhaust emissions were made at an experimental fracking site in Poland (Chapter 7). Marked elevations of BC and NO_2 concentrations were observed downwind of industrial fracking equipment sources. Average concentrations of BC and NO_2 in these

locations were three times higher than measured during walking at the urban Glasgow city centre. However, the average NO_2 concentrations recorded at the fracking test site (113.3 µg/m^3) were 2.6 times higher than average NO_2 concentrations measured in Glasgow city centre (42.3 µg/m^3). The BC measurements made at the hydraulic fracking test site were found to be higher (mean =11.2 µg/m^3) than the observation made in urban traffic area in Glasgow city centre (mean = 3.7 µg/m^3).

9.2 Summary of research impacts

This research developed novel measurement methods to provide additional insight on personal exposure to combustion related air pollutants. The main research impacts of this study are:

(a) Provision of new methods to improve strategies to assess personal exposure to combustion-related air pollutants. The key development here was to improve flexibility and effectiveness of sample collection and analysis systems for combustion-related air pollutants. Simple sample collection methods, were combined with portable real-time sensors and GPS technologies to enable improved characterisation of spatial and temporal variability of pollution exposure in the urban environment. This approach was extended to a study of pollution concentration at two vertical heights using mobile and stationary measurement systems to estimate differences in pollutant exposure to adults and children.

(b) Provision of cost-effective exposure measurement techniques. In chapter 5, a simple and low-cost method to estimate BC concentrations was introduced using a smoke stain reflectometer and an office scanner. The results reported in Chapter 5 & 7 demonstrate that these approaches can be used to approximate BC values and estimate exposures to combustion-related air pollutants in studies of the effects of air pollution on human health. The cost of the AE51 aethalometer monitoring system

was approximately 5 times higher than the total cost of the personal sampling pump and office scanner sampling and analytical technique.

(c) Characterisation of combustion-related sources. The short time resolution of the some of the portable instruments used in this study can help identify the sources of occupational and environmental exposure to combustion-related air pollutants. This should help to characterise exposures in vulnerable groups, e.g. children. This research has also identified markers of combustion-related air pollutants, which can be used to provide more extensive assessments of health effects associated with short-term exposure.

(d) *Novel development of methods for assessment of occupational and environmental exposure in proximity to industrial fracking sites.* Population-base studies evaluating health effects from unconventional natural gas (UNG) development have highlighted the need to provide exposure monitoring close proximity to the sources (McKenzie *et al.*, 2012, McKenzie *et al.*, 2014, Rabinowitz *et al.*, 2015). The results in Chapter 8, illustrate how combustion-related air pollutants (BC and NO_2) can be measured at short time resolution using portable monitors during the operation of fracking diesel machinery. These preliminary observations are beneficial for initial estimation of health risks before, during, and after UNG activities.

(e) Social and policy impacts. The indoor air quality study in chapter 6 provided information that can inform university policy regarding ventilation of office buildings to improve comfort and well-being of staff. The urban outdoor air pollution study provided information on personal exposure during walking in Glasgow city centre. Some of this information has been made available on the internet (http://www.cerc.co.uk/environmental-research/smart-cities/glasgow-platform.html), this allows individuals to make choices to reduce their exposure to combustion-related air pollutants by selection of walking route. Currently there is no regulation for BC; therefore the findings in this study have potential benefits to inform the setting of regulatory standards in relation to the potential health effects of BC exposure.

9.3 Study limitations

(i) The commercially available, advanced real-time monitors used in this study have limitations. The Aeroqual gas sensors were unable to measure very low NO_2 concentrations resolutions particularly in indoor measurements. Additionally, the Aeroqual sensors are difficult to waterproof, this makes measuring in inclement weather more challenging.

(ii) The use of single filter to measure BC concentrations from sequential sampling may have introduced shadowing/saturation effects from the deposited particles on the filter surface. However, the BC surface density loading collected from the sampling system in this study was generally lower compared to other studies. The relatively narrow range of measured BC concentrations during the calibration experiments may have affected the evaluation of these field calibrations (i.e. more variation in BC concentrations may be anticipated to be explained by filter darkness measurements when BC concentrations vary more widely).

(iii) The extended measurements for indoor and urban outdoor settings were conducted mostly in the summer. Similar measurements in other seasons would have been beneficial. The two indoor air quality measurement experiments used different monitoring techniques, therefore the results cannot be directly compared.

9.4 Recommendations for future work

The range of methods developed, tested and validated in this research demonstrates clearly that the quantification of combustion-related air pollutants in different location is complex. Future research needs to focus to expand amount of measurements in order to produce robust data and more comprehensive understanding in characterising personal exposure to PM, BC and NO_2.

As future work, it would be useful to improve analysis, which including:

(i) Particle-bound polycyclic aromatic hydrocarbon (pPAH) concentrations (including BaP) can be measured using a GC-MS system. As a result of laboratory charges for the use of such systems this was beyond the scope of this thesis. More studies would be required to develop reliable methods for quantification of pPAHs in low mass airborne specimens. This would help to determine whether if BaP can be used as a proxy marker for other pPAHs from combustion-related sources, and for health risk assessment in individual and population-based studies.

(ii) The range of BC concentrations and BC loading on filters could be expanded to ascertain the reliability of this type of measurement of BC over a wider concentration range. BC measurement from calibrated sequential filter reflectance and scanned values could be tested against other calibrated methods including thermal-optical analysis (Ramanathan *et al.*, 2011).

(iii) The use of simpler lower-cost measurement systems (office scanner) to estimate BC concentrations opens new possibilities to research other metrics of particle emissions, including particle mass and particle number. Further research in this area should be beneficial to validate whether another model of office scanner can estimate exposures to combustion-related air pollutants. The novel low-cost approach can complement the more sophisticated measurement technique to characterise combustion-related air pollutant exposure concentrations and very useful in resource-constrained situations, particularly in LMICs. This would further benefit the improvement regarding the proposed technique in greater concentrations range in these countries. This also would provide necessary background information for policy-maker responding to air quality data and standards, which has significant implications for health.

(iv) Further investigation of the relationship between indoor and outdoor pollution concentrations would help to determine the roles of air exchange resulting from window opening behaviour and frequency of printer/copier use in office environments. Exposure assessment could be expanded by combining time activity

patterns and field evaluation of spatial-temporal exposures to study the health effects on people exposed to high levels of combustion-related air pollution, including professional drivers, vehicle maintenance personnel and traffic wardens. This type of study could also be extended to children and other vulnerable groups. Other determinants including traffic density within defined areas, traffic counts on nearest road, and seasonal factors should be taken into account in future studies.

(v) Simultaneous measurements with wearable real-time sensors and GPS systems in different microenvironments would help to fully characterise the effects of short and long-term exposure to combustion related air pollutants. The use of wearable heart rate variability and blood pressure devices would provide health status data that could be linked in time and space to identification of peak exposures in indoor and outdoor locations. This would enable advancement of knowledge of the effects of acute and chronic exposures to inform science and engineering approaches to manage environmental and occupational risks in innovative ways.

9.5 References

Fullerton, D. G., Semple, S., Kalambo, F., Suseno, A., Malamba, R., Henderson, G., Ayres, J. G. & Gordon, S. B. 2009. Biomass fuel use and indoor air pollution in homes in Malawi. *Occupational and Environmental Medicine,* 66**,** 777-783.

Jantunen, M., Hänninen, O., Koistinen, K. & Hashim, J. H. 2002. Fine PM measurements: personal and indoor air monitoring. *Chemosphere,* 49**,** 993-1007.

Koehler, K. A. & Peters, T. M. 2015. New Methods for Personal Exposure Monitoring for Airborne Particles. *Curr Environ Health Rep,* 2**,** 399-411.

Kurmi, O. P., Semple, S., Steiner, M., Henderson, G. D. & Ayres, J. G. 2008. Particulate Matter Exposure during Domestic Work in Nepal. *The Annals of Occupational Hygiene,* 52**,** 509-517.

McKenzie, L. M., Guo, R., Witter, R. Z., Savitz, D. A., Newman, L. S. & Adgate, J. L. 2014. Birth outcomes and maternal residential proximity to natural gas development in rural Colorado. *Environ Health Perspect,* 122**,** 412-7.

McKenzie, L. M., Witter, R. Z., Newman, L. S. & Adgate, J. L. 2012. Human health risk assessment of air emissions from development of unconventional natural gas resources. *Science of The Total Environment,* 424**,** 79-87.

Rabinowitz, P. M., Slizovskiy, I. B., Lamers, V., Trufan, S. J., Holford, T. R., Dziura, J. D., Peduzzi, P. N., Kane, M. J., Reif, J. S., Weiss, T. R. & Stowe, M. H. 2015. Proximity to natural gas wells and reported health status: results of a household survey in Washington County, Pennsylvania. *Environ Health Perspect,* 123**,** 21-6.

Ramanathan, N., Lukac, M., Ahmed, T., Kar, A., Praveen, P. S., Honles, T., Leong, I., Rehman, I. H., Schauer, J. J. & Ramanathan, V. 2011. A cellphone based system for large-scale monitoring of black carbon. *Atmospheric Environment,* 45**,** 4481-4487.

Semple, S., Garden, C., Coggins, M., Galea, K. S., Whelan, P., Cowie, H., Sánchez-Jimenéz, A., Thorne, P. S., Hurley, J. F. & Ayres, J. G. 2012. Contribution of

solid fuel, gas combustion or tobacco smoke to indoor air pollutant concentrations in Irish and Scottish homes. *Indoor air*, 22**,** 212-223.

Semple, S., Ibrahim, A. E., Apsley, A., Steiner, M. & Turner, S. 2013. Using a new, low-cost air quality sensor to quantify second-hand smoke (SHS) levels in homes. *Tobacco Control*.

Steinle, S., Reis, S., Sabel, C. E., Semple, S., Twigg, M. M., Braban, C. F., Leeson, S. R., Heal, M. R., Harrison, D., Lin, C. & Wu, H. 2015. Personal exposure monitoring of PM2.5 in indoor and outdoor microenvironments. *Science of The Total Environment*, 508**,** 383-394.

Zainal Abidin, E., Semple, S., Rasdi, I., Ismail, S. N. S. & Ayres, J. G. 2014. The relationship between air pollution and asthma in Malaysian schoolchildren. *Air Quality, Atmosphere & Health*, 7**,** 421-432.

10 APPENDICES

APPENDIX A: LIST OF AUTHOR'S CONTRIBUTIONS

A (1): Impact of filter shadowing correction algorithms on agreement of portable AE51 micro-aethalometer and reference AE33 aethalometer black carbon measurements.

A (2): Temporal changes in field calibration relationships for Aeroqual S500 NO_2 and O_3 sensors.

A (3): Temporal variation of peripatetic real time pollution measurements and their ability to estimate longer term concentrations.

A (4): Conferences

A (5): Image of Research Competition

The manuscript is will be submitted to Atmospheric Environment and approved by the author.

Impact of filter shadowing correction algorithms on agreement of portable AE51 micro-aethalometer and reference AE33 aethalometer black carbon measurements

Nicola Masey[1], Eliani Ezani[14], Jonathan Gillespie[1], Chun Lin[2],

Mathew R. Heal[2], Scott Hamilton[3], Iain J. Beverland[1]*

[1]Department of Civil and Environmental Engineering, University of Strathclyde, James Weir Building, 75 Montrose Street, Glasgow, G1 1XJ, UK

[2]School of Chemistry, Joseph Black Building, University of Edinburgh, David Brewster Road, Edinburgh, EH9 3FJ, UK

[3]Ricardo Energy and Environment, 18 Blythswood Square, Glasgow, G2 4BG, UK

[4]Department of Environmental and Occupational Health, Faculty of Medicine and Health Science, Universiti Putra Malaysia, 43400 Serdang, Selangor, MALAYSIA

*CORRESPONDING AUTHOR: Dr Iain J. Beverland, email: iain.beverland@strath.ac.uk; Tel: +44 141 548 3202

Research Highlights

- High precision (R^2 > 0.90) between duplicate AE51 instruments
- Average R^2 = 0.78 between hourly reference AE33 and AE51 concentrations
- Scattered data and reduced agreement at BC concentrations below 1 µg/m^3
- Correcting AE51 for filter darkening overestimated analyser concentrations
- AE51 less accurate when filter attenuation values exceed 50

Abstract

We deployed duplicate micro-aethalometers at an urban background automatic monitoring station in Glasgow, UK for 4 periods between April and August 2016, to collect over 1000 hours of co-located micro-aethalometer (AE51) and reference aethalometer (AE22) black carbon (BC) measurements (measurements from the latter adjusted for filter darkening using a standard procedure employed in the UK BC monitoring network). We observed high correlations between duplicate AE51 measurements at hourly-averaging periods (R^2 > 0.90). We also observed high correlations between unadjusted AE51 and reference AE22 concentrations for 3 of the 4 deployment periods (R^2 ≥ 0.75), generally with the AE51 underestimating the AE22 concentrations. During one deployment period, at concentrations below 1 µg/m^3 the data were more scattered with lower correlations between unadjusted AE51 and reference AE22 concentrations (R^2 between 0.58 – 0.70). We compared equations reported in other publications for correction of underestimation of ambient concentrations by the AE51 micro-aethalometer associated with filter darkening effects. We observed that the corrected AE51 concentrations generally overestimated reference AE22 concentrations. This suggests that environments with low concentrations, resulting in slow filter loading, may not require correction for filter loading. We observed that unadjusted AE51 measurements started to underestimate AE22 concentrations at attenuation values of 50 and above.

Keywords: air pollution; black carbon; micro-aethalometer; attenuation; filter loading

1. Introduction

Black carbon (BC) is a constituent of particulate matter which is produced during combustion processes. The health effects associated with particulate matter, including BC, include respiratory and cardiovascular diseases (Janssen et al., 2012, 2011). In the UK, BC is monitored at 14 stations which are part of the Automatic Urban and Rural Network (https://uk-air.defra.gov.uk). These real-time sites are limited in number due to their high installation, equipment and maintenance costs combined with the lack of reporting for compliance monitoring.

Lower-cost, hand-held instruments have been developed to measure real-time BC, whose small-size and light-weight make them suitable for use in a variety of applications including: static locations in a network (Gillespie et al., 2017; Montagne et al., 2015; Weichenthal et al., 2014), mobile monitoring (Apte et al., 2011; Hankey and Marshall, 2015; Van den Bossche et al., 2015) and/or personal monitoring (Dons et al., 2014, 2013, 2012; Williams and Knibbs, 2016).

The real-time instrument used in this work is an Aethelometer and as such we focus our discussion on this instrument. The Aethelometer measures the concentration of black carbon using optical scattering techniques: air is drawn through a filter where particles are deposited, and the concentration of these particles is derived by comparing the attenuation of a light passed through the loaded filter to an unloaded reference point on the same filter. The concentrations measured using these filter-based instruments have been shown to suffer from three main sources of errors: noise introduction from mechanical shock, rapid temperature and/or relative humidity changes, and filter shadowing effects. Noise (large spurious positive and negative peaks) has been shown to be introduced to high resolution data during mobile monitoring, e.g. Apte et al. (2011). Cushioning the instruments, e.g. using foam padding, has been used to minimise the vibrations experienced by the instrument during mobile measurements (Hankey and Marshall, 2015) and correction algorithms have been developed to remove these erroneous concentration peaks (Apte et al., 2011; Hagler et al., 2011). Rapid changes in temperature and relative humidity, such as those experienced during personal monitoring, can also lead to large positive and negative peaks in the Aethelometer BC concentrations due to condensation of moisture on the instrument filters or optics (Cai et al., 2013). The impact of these changes were reduced in Cai et al. (2013) through use of a drying filter on the inlet, however the efficiency of this drier was improved when the instruments were used as personal monitors which was attributed to thermal heating. The accumulation of particles on the filter, leading to filter darkening (the attenuation), is related to the concentration of BC, however this relationship is not linear for high attenuation values. Several studies have proposed correction equations to be applied to the Aethelometer data to account for these filter loading effects (Kirchstetter and Novakov, 2007; Virkkula et al., 2007). However, few studies have comparatively evaluated these correction algorithms to determine which should be adopted as standard procedure (Good et al., 2016).

This study aims to compare BC data collected using a real-time hand-held Aethelometer, both before and after correction using some of the commonly adopted methods in the literature, to determine the accuracy of each method and suggest a standard method to be adopted. The instruments were deployed statically, minimising the impact of any mechanical vibrations, and the outdoor exposure was anticipated not to suffer from any rapid temperature or relative humidity changes. We deployed duplicate instruments at an urban background automatic monitoring station in Glasgow, UK, approximately 50 days of co-located measurements over a 5 month period.

2. Methods

2.1. Site description

The work was carried out at Townhead monitoring station, an urban background automatic analyser located in the north of Glasgow (55.866 ºN, 4.244 ºW). This site is part of the UK governments Automatic Urban and Rural Network (AURN) and undergoes regular quality control (Butterfield et al., 2015). Black carbon concentrations at the automatic analyser are measured using an AE22 Magee aethelometer (https://uk-air.defra.gov.uk/networks/network-info?view=ukbsn) and hourly concentration data are available to download from https://uk-air.defra.gov.uk/data/data_selector. Additionally, 5-minute black carbon data was available for the site from Kings College London which allowed the accuracy of the micro-aethalometers to be evaluated under higher temporal resolutions. The hourly-concentration data was supplied corrected for filter darkening effects using the correction procedure described in Virkkula et al. (Butterfield et al., 2015; Virkkula et al., 2007), however the raw 5-minute concentration data obtained required similar correction prior to use (see Supplementary Information and Figure S1 for details).

2.2. Instrument set up

We evaluated two identical micro-aethalometer AE51 instruments (https://aethlabs.com/) in this work (referred to as 'BC1204' and 'BC1303'). We deployed the AE51 instruments in waterproof boxes on the roof of the automatic monitoring station and sampled ambient air through a 1 m length of tubing supplied by the manufacturer. The inlet to the tubing was protected using a conductive plastic asbestos sampling inlet (SKC Ltd, UK) to prevent water ingress into the instrument. The flow rate of the micro-aethalometers was set to 50 ml/min and data was recorded every minute.

The evaluation of the micro-aethalometers occurred over 4 study periods: April (94 hours – BC1303 only), May (726 hours), July (68 hours) and August (334 hours) (Table 1). During each study the site was visited approximately every 5 days to allow the micro-aethalometer data to be downloaded and the filters to be changed. This meant that the filter attenuation (ATN) did not exceed a value of 65.

2.3. Correction of black carbon data

Three different correction procedures that can be applied to black carbon data collected using the micro-aethalometer have been evaluated in this work:

a) The Optimized Noise Algorithm (ONA) can be applied to the raw micro-aethalometer black carbon data to smooth the data and minimise the number of negative values in the dataset (Hagler et al., 2011). The change in the attenuation value used to average the black carbon concentration in this method was set to 0.05. Software available on the AethLabs website (https://aethlabs.com/dashboard) was used to process the microAeth data using the ONA algorithm.
b) A correction has been previously derived to account for instrument underestimation of black carbon concentration as the darkness of the filter in the micro-aethalometer increases. The correction equation published in Kirchstetter and Novak (2007) was applied to the ONA-corrected black carbon concentrations measured by the microAeth.
c) Virkkula et al. (2007) also developed a simple method to correct the black carbon concentrations measured using the microAeth for the effects of increased filter darkness. This requires the calculation of a constant k based on field measurements

using the AE51's and reference analyser black carbon concentrations and the attenuation values from the micro-aethalometers. The value of k for each micro-aethalometers was calculated following the method in Cheng and Lin (2013) and was found to be 0.0015 and 0.0035 for 1 hour, and 0.0082 and -0.0019 for 5 minute averaging, for BC1204 and BC1303 respectively, when all available data was included in the dataset used to calculate k.

The 1 minute data collected by the micro-aethalometer was averaged to produce a concentration every 5 minutes and every hour for comparison with the black carbon concentrations available from the reference analyser at the site.

3. Results & Discussion

3.1. Precision and accuracy of micro-aethalometers

Time series of hourly-average unadjusted concentrations measured by the two duplicate micro-aethalometers and the reference AE22 showed very similar temporal patterns between instruments (Figure 1a). The overall correlation between the two micro-aethalometers was high (R^2 = 0.93) with both instruments measuring similar concentrations (slope = 1.05, intercept = 0.00) (Figure 1b). Similarly high correlations between duplicate micro-aethalometers has been reported in other studies, e.g. Dons et. al (2012) found R^2 values > 0.95 between 13 identical micro-aethalometers.

The agreement between the hourly-average reference and unadjusted micro-aethalometer concentrations was good, with R^2 > 0.75 for the studies in April, May and August (Figure 2). Previous evaluation of a micro-aethalometer at a different AURN station found a high agreement between the micro-aethalometers and reference analyser (R^2 = 90), which was a similar magnitude to our studies which exhibited a similar range of reference analyser concentrations as the published work (0 – 5 μg/m^3, as observed in May and August studies) (Delgado-Saborit, 2012). The relationship was poorer during the July study, which was anticipate was due to the very low range of BC concentrations during the deployment (< 1 μg/m^3) (Table 1). The regression lines show that at concentrations < 3 μg/m^3 the relationship between the reference and micro-aethalometers falls very close to the 1:1 line, while above this concentration the micro-aethalometers appear to underestimate the reference concentrations. The mean bias (MB) values show the overestimation of analyser concentrations during the April study, while the other studies show small deviations (-0.05 to 0.04 μg/m^3) (Table 2). The normalised mean bias (NMB) values show the August study to have micro-aethalometer concentrations most similar to those measured by the reference analyser, while the largest deviation was observed during the April study (Table 2).

When 5-minute average concentrations were analysed, the agreement between the methods was poorer (R^2 0.08 – 0.52), with the underestimation above 3 μg/m^3 being more pronounced (Figure 2). There is a lot more scatter in the 5-minute measurements for both reference and micro-aethalometer measurements, leading to a more scattered data set with consequently lower R^2 values. The increased noise and scatter in data collected at 5 minute resolution has been highlighted previously by Cheng and Lin (2013) who also noted this scatter was greater at concentrations below 2 μg/m^3. Viana et al. (2015) found higher agreement (R^2 > 0.75) between micro-aethalometers and reference analysers, at 10 minute resolution, than our study, however the concentration range in that work was from 1.5 to 3.5 μg/m^3 whereas our study had concentrations below this. The regression statistics are given in Table 3. The more scattered 5-minute concentration data, compared to the 1-hour concentrations, leads to higher Root Mean Square Error (RMSE) values (Table 3). The MB and NMB values are similar between the 1-hour and 5-minute concentrations showing that, despite the lower R^2 values, the instruments still show reasonable agreement with the analyser concentrations.

The above highlight the ability of the micro-aethalometers to represent concentrations measured by the analyser at hourly-concentrations. At the higher (5-minute) resolution, the data measured by both the reference analyser and micro-aethalometer is more scattered leading to poorer correlations between the instruments, but despite this the error values remain relatively consistent between the two temporal resolutions tested. At the lower concentrations (below approximately 1.5 μg/m^3) the micro-aethalometer concentrations have more scatter and show larger deviations from the 1:1 line than those higher concentrations. This suggests that the ability of the micro-aethalometer to measured very low concentrations, such as those experienced in personal indoor monitoring (e.g. 0.5 μg/m^3 reported by Williams and Knibbs (2016)), is poorer than its ability to measure the higher concentrations outdoor ambient conditions (4-6 μg/m^3 reported by Dons et al. (2012) for commuting measurements), and consequently the error in these lower concentration environments is anticipated to be higher. Therefore the representativeness of 'true' indoor concentrations by the AE51's should be used with caution. Additionally, this work deployed the instruments statically at a monitoring station therefore there are no artefacts in the measurements associated with mechanical shock, such as experienced when the instrument is used as a personal monitor. The addition of noise through shock we anticipate would worsen the agreement between the instruments and the reference analyser at high temporal resolution and low concentrations.

3.2. Impact of filter shadowing correction algorithms

The hourly and 5-minute average concentrations measured by the reference analyser were plotted against the raw micro-aethalometer concentrations, and the micro-aethalometer concentrations after correction using the methods described in Section 2.3, for all deployment periods combined (Figure 3). As previously discussed, the agreement between the raw and reference concentrations was higher for the hourly-averaging compared to the 5-minute averaging, with the latter method showing the micro-aethalometers to underestimate the reference concentrations and the hourly-average concentrations being closer to the 1:1 line (Figure 3a).

The ONA-correction had very little impact on the regression lines for either resolution; however it led to small increases in R^2 value compared to the raw measurements (Figure 3b). The ONA-algorithm is designed to remove noise in the micro-aethalometer data, which can be introduced through vibrations such as those when walking. In this work the instruments were deployed in a static manner, therefore no vibrations were expected, and the low impact of the ONA-algorithm is not unexpected. A similar finding has been published by Cheng and Lin (2013) for a static BC deployment at a roadside location with higher concentrations than in this present work. We anticipate that, if the instruments were to be used in mobile monitoring, this correction would have more of an impact on micro-aethalometer concentrations.

The Kirchstetter-corrected micro-aethalometer data leads to increases in the slope values for both temporal resolutions, however for the hourly-data this leads to the micro-aethalometers overestimating those concentrations measured by the reference analyser (Figure 3c). For the 5-minute data the concentrations after Kirchstetter correction show less underestimation of the reference analyser than the raw data. The increase in micro-aethalometer concentrations after correction is expected as this correction takes into account filter darkening. After correction, the agreement between the reference and micro-aethalometer concentrations is slightly poorer for the hourly-average concentrations (R^2 = 0.83 vs. 0.81) while for the 5-minute concentrations there is a slight improvements (R^2 = 0.51 vs. 0.53). Correction using the Kirchstetter formula has previously been shown to underestimate the filter loading

effects when a clean filter was used, but overestimate the loading effects when pre-loaded filters were used, under controlled chamber-experiments (Good et al., 2016).

Similarly, the Virkkula correction increases the concentrations measured by the micro-aethalometer to account for filter shadowing effects, leading to an increase in the regression slope between the micro-aethalometer and reference analyser (Figure 3d). The corrected regression slopes are closer to the 1:1 line than the Kirchstetter correction for the hourly-corrected data, however for the 5-minute concentrations the Kirchstetter correction produces a slope closer to the 1:1 line than the Virkkula correction, with the latter underestimating the analyser concentration. The underestimation of BC using the Virkkula correction has been previously reported in a chamber-type experiment comparing BC concentrations measured using a loaded and unloaded filter (Good et al., 2016). Despite the improved slope for the Virkkula corrected vs. raw micro-aethalometer concentrations, there is no impact on the R^2 values after correction.

The root mean square error (RMSE), mean bias (MB) and normalised mean bias (NMB) values show the Kirchstetter-corrected hourly micro-aethalometer data have the largest bias for both hourly and 5-minute concentrations, while the raw or ONA-corrected data have the lowest values (Tables 4 & 5). The Kirchstetter correction overcorrects the micro-aethalometer concentrations for filter darkening effects (larger positive MB and NMB) while the Virkkula correction overcorrects the concentrations by a lesser amount but still shows poorer agreement with the analyser concentrations than the raw or ONA-corrected data. For static calibration studies, such as in this work, the micro-aethalometer data can be used directly from the instrument. This work was based at an urban background site with relatively low black carbon concentrations, and consequently relatively slow filter darkening occurs. At a site with higher black carbon concentrations thus faster changes in attenuation, the impact of filter darkening on instrument accuracy may be more pronounced.

3.3. Impact of ATN values on micro-aethalometer corrections

The ATN value at which the filter in the micro-aethalometer should be changed is variable, with different studies identifying different ATN values at which to change the filters which range from ATN = 40 to ATN = 80 (Cheng, 2013; Dons et al., 2013; Virkkula et al., 2007). We investigated the ratio between the micro-aethalometer and reference analyser concentrations as a function of ATN to establish the range of ATN values at which the micro-aethalometer can reproduce the analyser concentrations at and if there is a limit to the ATN range under which the correction investigated can be successfully applied. Above ATN values of approximately 50 there is a larger amount of scatter in the ratio values for the raw and ONA-corrected data (Figure 4a & 4b). The Virkkula corrected BC data showed more variation in the ratio between micro-aethalometer and reference concentrations which appeared at a lower ATN value (approximately 40) (Figure 4d). The ratio values for the Kirchstetter correction show the overestimation in micro-aethalometer concentrations observed in the scatterplots and highlight that this overestimation increases with increasing filter ATN value (Figure 4c). This suggests that at the lower concentrations in this study or under static monitoring the Kirchstetter correction is not fit for purpose and should be avoided. Good et al. (2016) showed that an ATN value of 80 should not be exceeded in order to maintain accurate BC measurements using the micro-aethalometer, however they noted some divergence in the measurements above ATN values of 60. Our work suggests that changing the filter at a value of 60 could still lead to poorer accuracy measurements at this higher attenuation value, and that the filters should be changed before an ATN value of 50 in order to ensure filter darkening effects do not adversely affect the micro-aethalometer instrument performance.

4. Conclusions

Two micro-aethalometers were deployed at an urban background monitoring station in Glasgow, UK, for over 1000 hours of measurements spread over 4 deployment periods. There was high precision between the duplicate BC instruments (R^2 > 0.90) during these measurements. Concurrent reference analyser concentrations of BC were available at hourly and 5-minute resolutions for each deployment.

The agreement between the micro-aethalometer and reference analyser BC concentrations was good (R^2 > 0.75 (hourly) and R^2 > 0.42 (5-minute)) for 3 of the 4 studies, with a linear relationship close to the 1:1 line between the methods. The micro-aethalometers can estimate the hourly concentrations relatively well, with some slight underestimation at concentrations > 2 μg/m^3, while the 5-minute concentrations showed larger underestimation in the regression lines above these values. The 5-minute micro-aethalometer and reference analyser concentrations had much more scatter than the corresponding hourly concentrations and as a result the agreement was lower for the higher temporal resolution analysis. Concentrations of BC below 1 μg/m^3 showed more scatter in the measurements, which lead to poorer agreement with the analyser concentrations such as those observed during our July study when all concentrations fell below 1 μg/m^3 (R^2 > 0.58 for hourly measurements, R^2 < 0.10 for 5-minute concentrations)). This suggests the accuracy of the micro-aethalometers in very low pollution environments, such as indoor monitoring, may be subject to larger errors than measurements made in more polluted environments and this should be taken into consideration in e.g. personal monitoring epidemiology studies.

The performance of 3 post-processing methods to account for noise in high resolution data and filter darkening effects were compared. Correcting for noise had little impact on the micro-aethalometer performance, which was unsurprising due to the static deployments used in this work. The concentrations corrected for filter darkening generally overestimated the reference analyser concentrations, and had larger error values, than the raw micro-aethalometer data. The impact of filter attenuation on the ratio between micro-aethalometer and reference analyser measurements showed deviations from the optimal value of 1 above ATN values of 50, and we suggest that filters should not be allowed to exceed this value in order to obtain most accurate BC concentration estimates.

a)

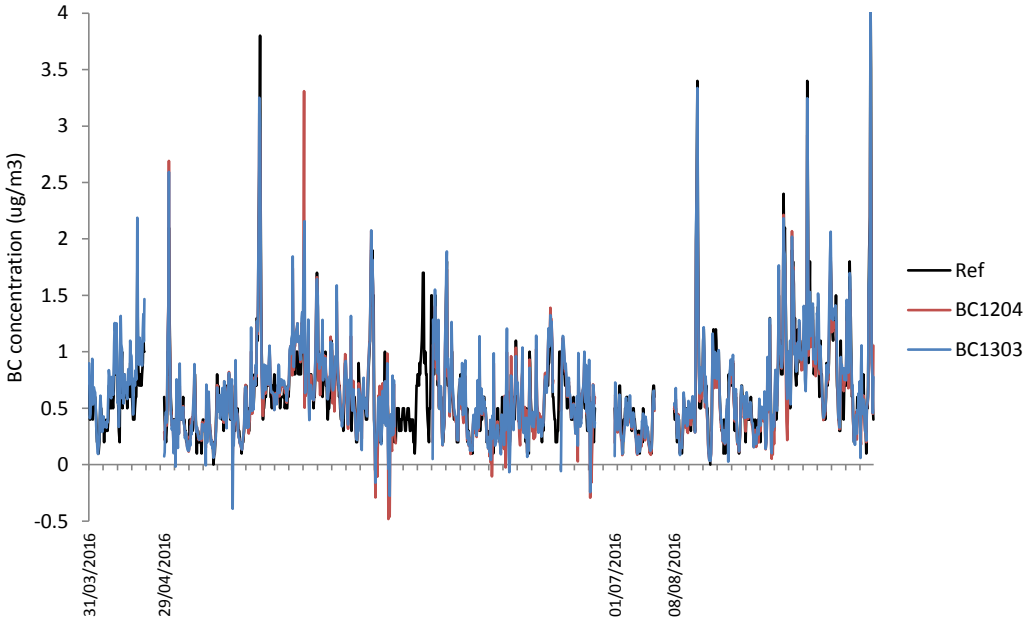

b)

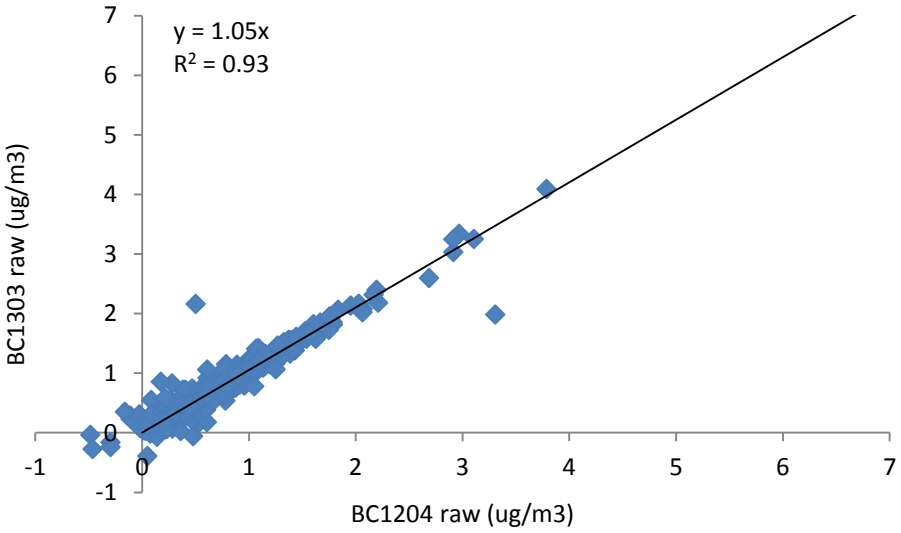

Figure 1: (a) time series showing hourly-average black carbon concentrations measured by the Townhead reference analyser and the raw concentrations measured by the two BC instruments (BC1204 and BC1303). Non-consecutive time series are shown with a gap between them. (b) Agreement between hourly-average concentrations measured by the duplicate BC instruments. The Reduced Major Axis (RMA) regression line is shown on this plot.

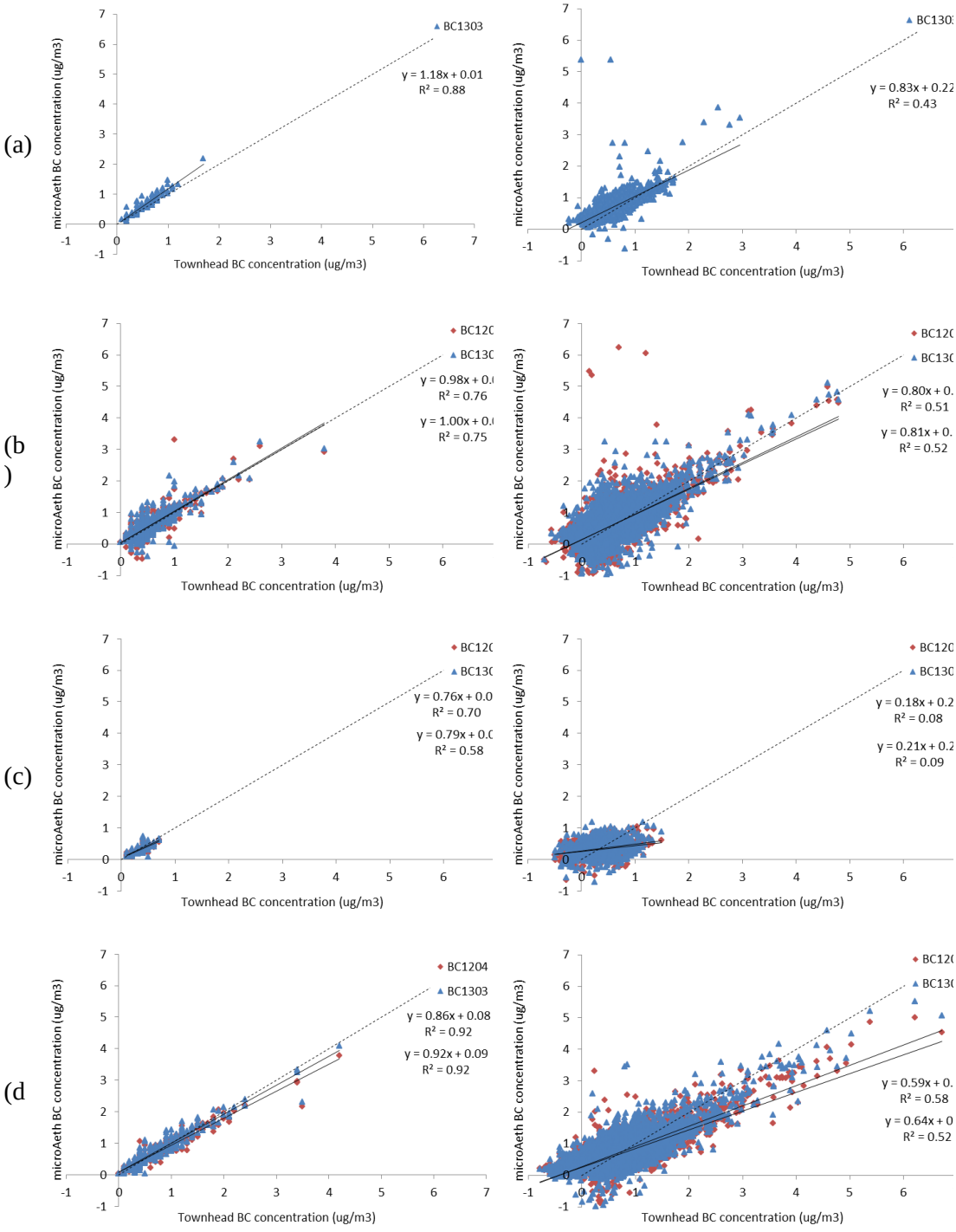

Figure 2: Scatter plots showing hourly-average BC concentrations measured by the reference analyser vs. the raw BC instruments (left) and 5-minute average concentrations (right). This is shown for each individual study: (a) April; (b) May; (c) July; and (d) August. Ordinary Least Squares (OLS) regression lines are shown for each graph, and the dashed line denotes the 1:1 concentrations.

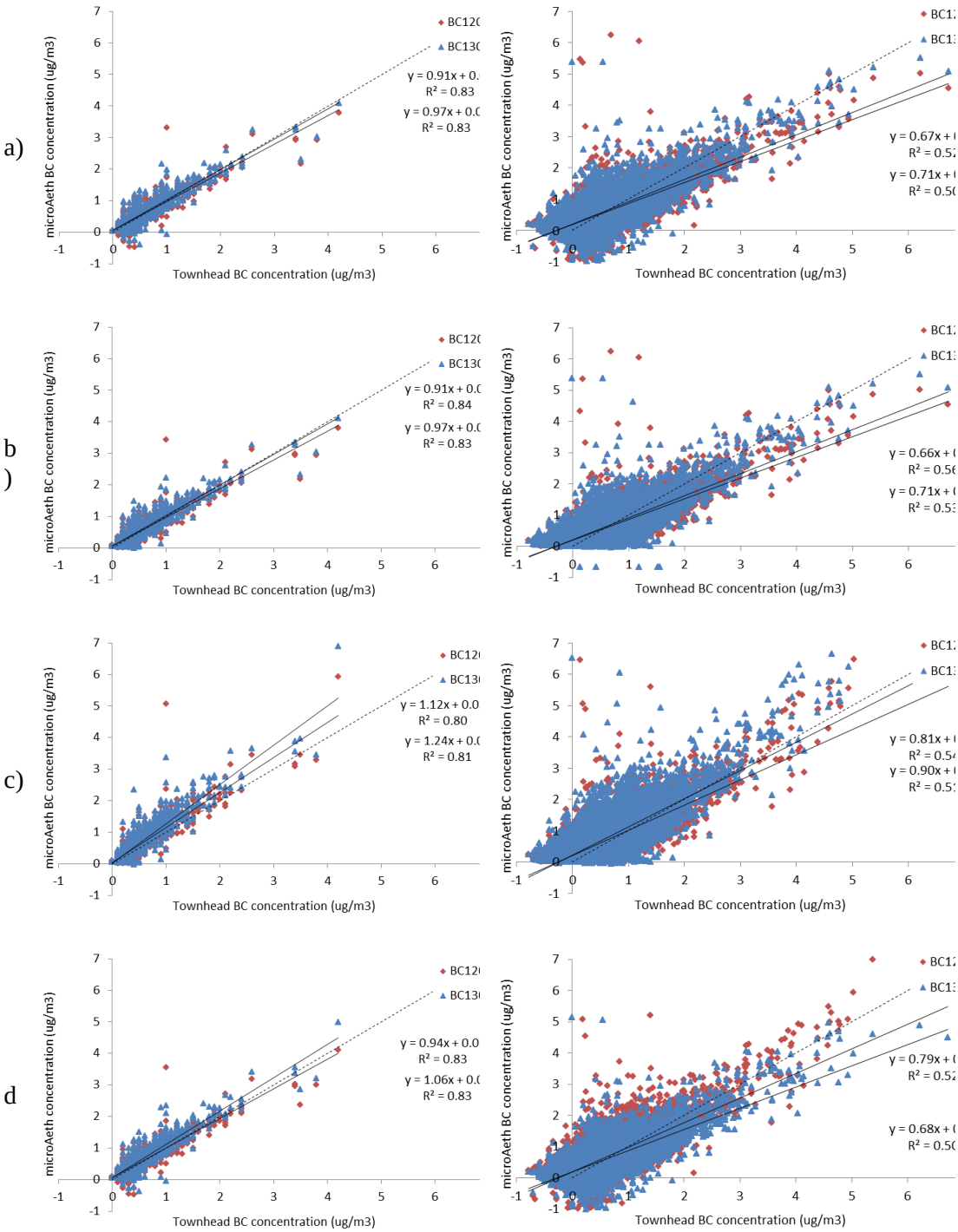

Figure 3: Scatter plots showing the hourly-average (left) and 5-minute average (right) BC concentrations measured by the reference analyser and the concentrations measured using the BC instruments for different correction methods: (a) raw concentrations, (b) noise corrected using ONA (c) Kirchstetter-corrected and (d) Virkkula-corrected (using k value derived from all studies hourly or 5 minute measurements). The data for all deployments combined is shown.

(a)

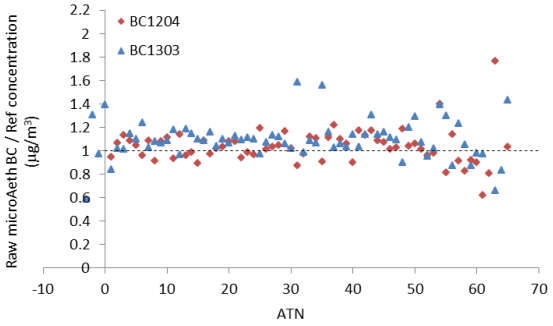

(b)

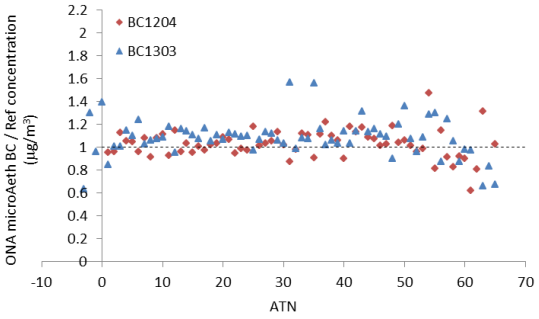

(c)

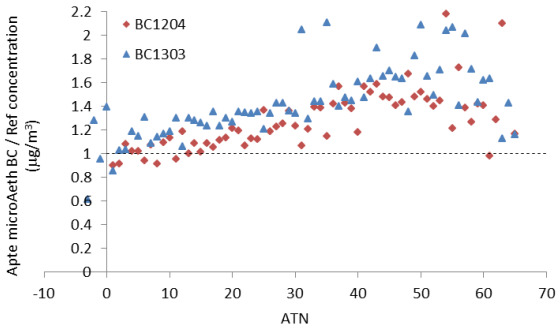

(d)

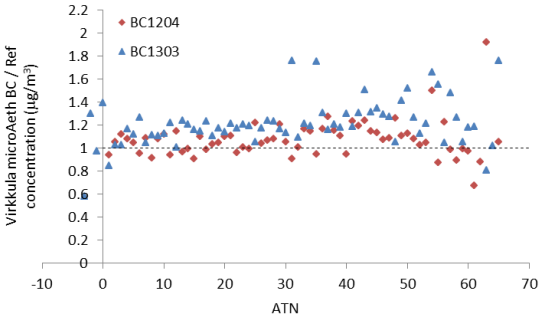

Figure 4: Scatter plots showing the ratio between the hourly concentrations measured using the micro-aethalometers and the reference analyser and the ATN values measured by the micro-aethalometers. Plots are shown for: (a) raw, (b) ONA-corrected, (c) Kirchstetter-corrected and (d) Virkkula-corrected micro-aethalometer concentrations, with all study data included. The average ratio for each ATN integer value is shown to ease the visualisation of the graph. The dashed line represents the ideal ratio value of 1.

Table 1: Dates and durations of BC instrument deployments. Also shown are the minimum, maximum, average and median hourly BC concentrations measured by the reference analyser during each deployment period.

Study Name	Start date	Duration (hours)	Analyser min hourly concentration (µg/m^3)	Analyser max hourly concentration (µg/m^3)	Analyser mean hourly concentration (µg/m^3)	Analyser median hourly concentration (µg/m^3)
April	31/03/2016	94	0.10	1.70	0.61	0.60
May	29/04/2016	651	0.00	3.80	0.57	0.50
July	01/07/2016	68	0.10	0.70	0.37	0.40
August	08/08/2016	318	0.00	4.20	0.75	0.60

Table 2: OLS regression equations (95 % confidence intervals) between the hourly BC concentrations measured by the reference analyser and the BC instruments (raw) for each individual deployment period. Also provided are statistics about the relationship: coefficient of determination (R^2), root mean square error (RMSE), mean bias (MB), normalised mean bias (NMB) and the number of hourly observations (n). BC1204 was not deployed in April 2016.

BC	Study	Slope [95 % C.I.]	Intercept [95 % C.I.] / µg m^{-3}	R^2	RMSE / µg m^{-3}	MB / µg m^{-3}	NMB	n
1204	April	-	-	-	-	-	-	-
	May	0.98 [0.94, 1.03]	0.04 [0.01, 0.06]	0.76	0.19	0.03	0.05	651
	July	0.76 [0.64, 0.88]	0.04 [-0.01, 0.09]	0.70	0.10	-0.05	-0.14	68
	August	0.86 [0.83, 0.88]	0.08 [0.05, 0.10]	0.92	0.16	-0.03	-0.04	318
1303	April	1.18 [1.09, 1.27]	0.01 [-0.05, 0.07]	0.88	0.17	0.12	0.19	94
	May	1.00 [0.96, 1.05]	0.04 [0.01, 0.07]	0.75	0.21	0.04	0.08	648
	July	0.79 [0.63, 0.97]	0.06 [-0.01, 0.12]	0.58	0.11	-0.02	-0.05	68
	August	0.92 [0.89, 0.95]	0.09 [0.06, 0.12]	0.91	0.16	0.03	0.04	318

Table 3: OLS regression equations (95 % confidence intervals) between the 5-minute BC concentrations measured by the reference analyser and the BC instruments (raw) for each individual deployment period. Also provided are statistics about the relationship: coefficient of determination (R^2), root mean square error (RMSE), mean bias (MB), normalised mean bias (NMB) and the number of hourly observations (n). BC1204 was not deployed in April 2016.

BC	Study	Slope [95 % C.I.]	Intercept [95 % C.I.] / µg m^{-3}	R^2	RMSE / µg m^{-3}	MB / µg m^{-3}	NMB	n
1204	April	-	-	-	-	-	-	-
	May	0.80 [0.78, 0.82]	0.14 [0.13, 0.15]	0.51	0.34	0.02	0.04	7642
	July	0.18 [0.14, 0.23]	0.25 [0.23, 0.27]	0.08	0.38	-0.06	-0.15	791
	August	0.59 [0.58, 0.61]	0.26 [0.25, 0.28]	0.58	0.46	-0.04	-0.06	3934
1303	April	0.83 [0.78, 0.89]	0.22 [0.18, 0.26]	0.43	0.37	0.12	0.19	1105
	May	0.81 [0.79, 0.83]	0.14 [0.13, 0.16]	0.51	0.34	0.04	0.07	7588
	July	0.21 [0.16, 0.26]	0.27 [0.25, 0.30]	0.09	0.38	-0.03	-0.07	791
	August	0.64 [0.62, 0.66]	0.29 [0.27, 0.31]	0.52	0.50	0.02	0.02	3934

Table 4: OLS regression equations (95 % confidence intervals) between the hourly BC concentrations measured by the reference analyser and the BC instruments when the different correction methods are tested. Data is shown when all studies were combined into a single data set. Also provided are statistics about the relationship: coefficient of determination (R^2), root mean square error (RMSE), mean bias (MB), normalised mean bias (NMB) and the number of hourly observations (n).

BC	Correction	Slope [95 % C.I.]	Intercept [95 % C.I.] / µg m^{-3}	%R^2	RMSE / µg m^{-3}	MB / µg m^{-3}	NMB	n
1204	Raw	0.91 [0.88, 0.93]	0.06 [0.04, 0.08]	0.83	0.18	0.002	0.003	1038
	ONA	0.91 [0.89, 0.93]	0.06 [0.04, 0.08]	0.84	0.17	0.002	0.003	1038
	Kirchstetter	1.12 [1.08, 1.15]	0.03 [0.00, 0.05]	0.80	0.26	0.10	0.16	1038
	Virkkula	0.94 [0.91, 0.97]	0.05 [0.04, 0.07]	0.83	0.18	0.02	0.03	1038
1303	Raw	0.97 [0.94, 0.99]	0.06 [0.04, 0.08]	0.83	0.19	0.04	0.07	1129
	ONA	0.97 [0.94, 0.99]	0.06 [0.04, 0.08]	0.83	0.18	0.04	0.07	1129
	Kirchstetter	1.24 [1.21, 1.28]	0.02 [0.00, 0.05]	0.81	0.32	0.17	0.28	1129
	Virkkula	1.06 [1.03, 1.09]	0.05 [0.03, 0.07]	0.83	0.22	0.09	0.14	1129

Table 5: OLS regression equations (95 % confidence intervals) between the 5-minute BC concentrations measured by the reference analyser and the BC instruments when the different correction methods are tested. Data is shown when all studies were combined into a single data set. Also provided are statistics about the relationship: coefficient of determination (R^2), root mean square error (RMSE), mean bias (MB), normalised mean bias (NMB) and the number of hourly observations (n).

BC	Correction	Slope [95 C.I.]	%	Intercept [95 C.I.] / µg m^{-3}	%	R^2	RMSE / µg m^{-3}	MB / µg m^{-3}	NMB	n
1204	Raw	0.67 [0.66, 0.68]		0.20 [0.19, 0.21]		0.52	0.38	-0.002	-0.003	12367
	ONA	0.66 [0.65, 0.67]		0.20 [0.20, 0.21]		0.56	0.36	-0.002	-0.003	12367
	Kirchstetter	0.81 [0.79, 0.82]		0.21 [0.20, 0.22]		0.54	0.42	0.09	0.15	12367
	Virkkula	0.79 [0.77, 0.80]		0.21 [0.20, 0.22]		0.52	0.43	0.08	0.13	12367
1303	Raw	0.71 [0.70, 0.72]		0.21 [0.20, 0.22]		0.50	0.40	0.03	0.06	13417
	ONA	0.71 [0.69, 0.72]		0.22 [0.21, 0.22]		0.53	0.38	0.04	0.06	13417
	Kirchstetter	0.90 [0.88, 0.91]		0.23 [0.22, 0.24]		0.51	0.49	0.17	0.27	13417
	Virkkula	0.68 [0.67, 0.69]		0.21 [0.20, 0.22]		0.50	0.39	0.01	0.02	13417

Acknowledgements

Nicola Masey is funded through a UK Natural Environment Research Council CASE PhD studentship (NE/K007319/1), with support from Ricardo Energy and Environment. Eliani Ezani is funded by the Malaysian Government (**grant number**). Chun Lin is funded through **XXXXXX**. We acknowledge access to the AURN measurement data, which were obtained from uk-air.defra.gov.uk and are subject to Crown 2014 copyright, Defra, licenced under the Open Government Licence (OGL). We thank Kings College London for providing access to the 5-minute temporal resolution black carbon concentrations. The research data associated with this paper are available at: http://dx.doi.org/XXXXX (*doi to be provided at time of publishing*).

References

Apte, J.S., Kirchstetter, T.W., Reich, A.H., Deshpande, S.J., Kaushik, G., Chel, A., Marshall, J.D., Nazaroff, W.W., 2011. Concentrations of fine, ultrafine, and black carbon particles in auto-rickshaws in New Delhi, India. Atmos. Environ. 45, 4470–4480.

Butterfield, D., Beccaceci, S., Quincey, P., Sweeney, B., Lilley, A., Bradshaw, C., Fuller, G., Green, D., Font Font, A., 2015. 2014 Annual Report for the UK Black Carbon Network (No. NPL Report AS 97).

Cai, J., Yan, B., Kinney, P.L., Perzanowski, M.S., Jung, K.-H., Li, T., Xiu, G., Zhang, D., Olivo, C., Ross, J., Miller, R.L., Chillrud, S.N., 2013. Optimization Approaches to Ameliorate Humidity and Vibration Related Issues Using the MicroAeth Black Carbon Monitor for Personal Exposure Measurement. Aerosol Sci. Technol. 47, 1196–1204. doi:10.1080/02786826.2013.829551

Cheng, Y.-H., 2013. Real-Time Performance of the microAeth® AE51 and the Effects of Aerosol Loading on Its Measurement Results at a Traffic Site. Aerosol Air Qual. Res. doi:10.4209/aaqr.2012.12.0371

Delgado-Saborit, J.M., 2012. Use of real-time sensors to characterise human exposures to combustion related pollutants. J. Environ. Monit. 14, 1824. doi:10.1039/c2em10996d

Dons, E., Int Panis, L., Van Poppel, M., Theunis, J., Wets, G., 2012. Personal exposure to Black Carbon in transport microenvironments. Atmos. Environ. 55, 392–398. doi:10.1016/j.atmosenv.2012.03.020

Dons, E., Temmerman, P., Van Poppel, M., Bellemans, T., Wets, G., Int Panis, L., 2013. Street characteristics and traffic factors determining road users' exposure to black carbon. Sci. Total Environ. 447, 72–79.

Dons, E., Van Poppel, M., Kochan, B., Wets, G., Int Panis, L., 2014. Implementation and validation of a modeling framework to assess personal exposure to black carbon. Environ. Int. 62, 64–71.

Gillespie, J., Masey, N., Heal, M.R., Hamilton, S., Beverland, I.J., 2017. Estimation of spatial patterns of urban air pollution over a 4-week period from repeated 5-min measurements. Atmos. Environ. 150, 295–302. doi:10.1016/j.atmosenv.2016.11.035

Good, N., Mölter, A., Peel, J.L., Volckens, J., 2016. An accurate filter loading correction is essential for assessing personal exposure to black carbon using an Aethalometer. J. Expo. Sci. Environ. Epidemiol. doi:10.1038/jes.2016.71

Hagler, G.S.W., Yelverton, T.L.B., Vedantham, R., Hansen, A.D.A., Turner, J.R., 2011. Post-processing Method to Reduce Noise while Preserving High Time Resolution in Aethalometer Real-time Black Carbon Data. Aerosol Air Qual. Res. 11, 539–546. doi:10.4209/aaqr.2011.05.0055

Hankey, S., Marshall, J.D., 2015. On-bicycle exposure to particulate air pollution: Particle number, black carbon, PM2.5, and particle size. Atmos. Environ. 122, 65–73. doi:10.1016/j.atmosenv.2015.09.025

Janssen, N., Gerlofs-Nijland, M., Lanki, T., Salonen, R., Cassee, F., Hoek, G., Fischer, P., Brunekreef, B., Krzyzanowski, M., 2012. Health effects of black carbon. World Health Organisation.

Janssen, N., Hoek, G., Simic-Lawson, M., Fischer, P., van Bree, L., ten Brink, H., Keuken, M., Atkinson, R., Anderson, H., Brunekreef, B., Cassee, F., 2011. Black carbon as an additional indicator of the Adverse Health Effects of Airborne Particles Compared with PM10 and PM2. 5. Environ. Health Perspect. 119, 1691–1699. doi:10.1289/ehp.1003369

Kirchstetter, T.W., Novakov, T., 2007. Controlled generation of black carbon particles from a diffusion flame and applications in evaluating black carbon measurement methods. Atmos. Environ. 41, 1874–1888. doi:10.1016/j.atmosenv.2006.10.067

Montagne, D.R., Hoek, G., Klompmaker, J.O., Wang, M., Meliefste, K., Brunekreef, B., 2015. Land Use Regression Models for Ultrafine Particles and Black Carbon Based on Short-Term Monitoring Predict Past Spatial Variation. Environ. Sci. Technol. 49, 8712–8720. doi:10.1021/es505791g

Van den Bossche, J., Peters, J., Verwaeren, J., Botteldooren, D., Theunis, J., De Baets, B., 2015. Mobile monitoring for mapping spatial variation in urban air quality: Development and validation of a methodology based on an extensive dataset. Atmos. Environ. 105, 148–161. doi:10.1016/j.atmosenv.2015.01.017

Viana, M., Rivas, I., Reche, C., Fonseca, A.S., Pérez, N., Querol, X., Alastuey, A., Álvarez-Pedrerol, M., Sunyer, J., 2015. Field comparison of portable and stationary instruments for outdoor urban air exposure assessments. Atmos. Environ. 123, Part A, 220–228. doi:10.1016/j.atmosenv.2015.10.076

Virkkula, A., Mäkelä, T., Hillamo, R., Yli-Tuomi, T., Hirsikko, A., Hämeri, K., Koponen, I.K., 2007. A Simple Procedure for Correcting Loading Effects of Aethalometer Data. J. Air Waste Manag. Assoc. 57, 1214–1222. doi:10.3155/1047-3289.57.10.1214

Weichenthal, S., Farrell, W., Goldberg, M., Joseph, L., Hatzopoulou, M., 2014. Characterizing the impact of traffic and the built environment on near-road ultrafine particle and black carbon concentrations. Environ. Res. 132, 305–310. doi:10.1016/j.envres.2014.04.007

Williams, R.D., Knibbs, L.D., 2016. Daily personal exposure to black carbon: A pilot study. Atmos. Environ. 132, 296–299. doi:10.1016/j.atmosenv.2016.03.023

The manuscript will be submitted to Environmental Science & Technology and approved by the author.

Temporal changes in field calibration relationships for Aeroqual S500 NO_2 and O_3 sensors

Nicola Masey[1], Jonathan Gillespie[1], Eliani Ezani[14], Chun Lin[2], Hao Wu [2],

Mathew R. Heal[2], Neil S Ferguson[1], Scott Hamilton[3], Iain J. Beverland[1*]

[1]Department of Civil and Environmental Engineering, University of Strathclyde, James Weir Building, 75 Montrose Street, Glasgow, G1 1XJ, UK

[2]School of Chemistry, Joseph Black Building, University of Edinburgh, David Brewster Road, Edinburgh, EH9 3FJ, UK

[3]Ricardo Energy and Environment, 18 Blythswood Square, Glasgow, G2 4BG, UK

[4]Department of Environmental and Occupational Health, Faculty of Medicine and Health Science, Universiti Putra Malaysia, 43400 Serdang, Selangor, MALAYSIA

Research highlights

- Aeroqual sensors were repeatedly compared to reference analysers over a 6-month period
- Clear linear relationships identified between *Aeroqual O_3 vs. Reference O_3*
- Clear linear relationships identified between *(Aeroqual NO_2 – Reference NO_2) vs. Aeroqual O_3*
- Calibration relationships changed over time
- Temporal changes appeared to result partly from reduction in sensitivity of Aeroqual O_3 sensors
- Accuracy of calibrated estimates was improved by repeated calibration

Abstract:

We made intermittent comparisons (6 times over a 6-month period) of gas concentrations measured by Aeroqual gas sensitive semiconductor ozone (O_3) and electrochemical nitrogen dioxide (NO_2) sensors (two of each) to reference gas analysers in the UK Automatic Urban and Rural Network (AURN). We observed significant linear relationships between *Aeroqual O_3 vs. Reference O_3* concentrations, and *(Aeroqual NO_2 – Reference NO_2) vs. Aeroqual O_3* concentrations allowing the Aeroqual sensors to be calibrated against the reference analysers. The calibration relationships changed over time, primarily as a result of gradual reduction in the sensitivity of the Aeroqual O_3 sensors. The accuracy of calibrated estimates of gas concentrations was improved by repeated intermittent calibration over time, and application of the most recent calibration relationships to test data.

Keywords: Air pollution; sensors, gas sensitive semiconductor; electrochemical, nitrogen dioxide, ozone, field calibration

1. Introduction

The concentrations of gaseous air pollutants, including nitrogen dioxide (NO_2) and ozone (O_3), are monitored to assess compliance with legislation and guidelines. Monitoring is usually conducted at static, automatic monitoring stations that record concentrations at high temporal resolution. However, the cost of these stations, together with practical considerations regarding suitable sites, invariably limits the spatial coverage of automatic networks. Wider geographical networks of passive diffusion samplers (PDS) can mitigate some of these restrictions on spatial coverage (Gillespie et al., 2017, 2016); however PDS provide limited temporal information, and are subject to measurement inaccuracies associated with changing meteorological (Masey et al., Submitted) and atmospheric chemistry conditions (Heal et al., 1999).

Battery-powered real-time hand-held sensors for air pollutants are continually being developed, which have potential to supplement data from existing monitoring networks. Hand-held sensors usually have lower capital costs than automatic analysers, meaning more instruments could be made available for deployment, potentially increasing the spatial resolution of measurement networks with high temporal resolution concentration measurements (Heimann et al., 2015; Mead et al., 2013; Wang et al., 2016). The use of such sensors in mobile and personal monitoring has been reported (Deville Cavellin et al., 2016; Mead et al., 2013).

An important potential limitation of gas sensors is cross-sensitivity of the response of the sensor to other pollutants and/or meteorological variables (Lewis and Edwards, 2016; Lewis et al., 2015). For example, the response of some electrochemical sensors have been shown to be susceptible to changes in temperature or relative humidity (Masson et al., 2015; Mead et al., 2013; Pang et al., 2017; Spinelle et al., 2015). Sensors for NO_2 have been shown to be cross-sensitive to O_3, meaning that both pollutants must be measured simultaneously to allow correction of the NO_2 sensor response (Lin et al., 2015; Mead et al., 2013). Consequently, for accurate estimation of ambient concentrations, sensor-based instruments require to be calibrated for use in field studies making appropriate allowance for known cross-sensitivities.

Previously, we evaluated two pairs of Aeroqual S500 ozone and nitrogen dioxide sensors at an urban background site including detailed study of the effects of accidental damage and subsequent repair to one of the sensors (Gillespie et al., In preparation). This paper extends our investigations of the same Aeroqual instruments/sensors over an extended time period subsequent to the above sensor repair to assess if the instrument responses change as the sensors age over time and repeated exposure to outdoor conditions. The deployments referred to in this paper reflect real-world calibrations, whereby the instruments were removed from the site, used in other field measurements at different locations, and returned to the site between each calibration deployment. Additionally, we investigated if it was possible to optimise the method (including timing) of field calibration of the sensors. Our analyses provide context to important research challenges associated with subsequent refinement and use of field calibration relationships for these Aeroqual instruments in mobile measurements across geographical areas with widely varying pollution microclimates (*Lin et al., in preparation*).

2. Methods

We evaluated two pairs of Aeroqual (www.aeroqual.com) O_3 and NO_2 sensors at the Townhead urban background site located in the north part of Glasgow city centre (55.866 ºN, 4.244 ºW). This site is part of the UK government Automatic Urban and Rural Network (AURN). Hourly-average concentration data from the reference analysers (API200A

chemiluminescence analyser for NO_2 and Thermo 49i photometric analyser for O_3) at this site was downloaded from www.scottishairquality.co.uk. All AURN measurements are subject to documented national quality control and assurance procedures (DEFRA, 2017).

We deployed the Aeroqual instruments within the ventilated waterproof enclosures provided by Aeroqual affixed to the galvanised steel safety railings surrounding the roof of the AURN monitoring cabin (Figure 1). The O_3 instruments contained gas sensitive semiconductor sensors (OZU2, range 0 – 0.15 ppm). The NO_2 instruments contained electrochemical sensors (ENW2, range 0 – 1 ppm). These were the same instruments/sensor combinations reported in our previous study (Gillespie et al., In preparation) and are referred to as *NO_2_1*, *NO_2_2*, *O_3_3* and *O_3_4*. *O_3_3* was the sensor that was damaged and repaired as examined in our previous study. *NO_2_1* and *O_3_3* were located next to one another on the eastern railing while *NO_2_2* and *O_3_4* were located on the western railing. Mains power was available on the roof of the site allowing the instruments to run continuously. We set the instruments to record gravimetric concentrations ($\mu g/m^3$) at 1-minute intervals, prior to computation of hourly-average concentrations for comparison with the analysers.

This paper focuses on six separate instrument co-location deployment periods (of different durations) made intermittently over 6 months (November 2015 – May 2016). In the first part of our analyses we truncated each deployment period to the first 96 hours of field deployment to simplify comparison between periods (Table 1). In subsequent analyses we examined temporal changes over the longest continuous deployment period (duration of 10 days).

3. Results and discussion

3.1. Calibration of Aeroqual O_3 instruments

Aeroqual O_3 concentration measurements closely followed temporal trends in the O_3 reference analyser concentrations, with *O_3_3* generally over-predicting and *O_3_4* generally under-predicting the analyser concentrations (Figure 2). The observations from the two Aeroqual instruments were highly correlated (R^2 > 0.90) but with *O_3_4* reporting concentrations approximately half the magnitude of those measured by *O_3_3* and with a significant positive offset (Figure 2).

We calibrated the response of the O_3 instruments by calculating Ordinary Least Squares (OLS) regression equations between unadjusted Aeroqual O_3 concentration measurements and O_3 concentrations measured by the reference analyser. We compared three methods of calibration - in each method the first 96 hours of data for each deployment period was split in half, with the first 48 hours of 'training' data used to generate calibration equations, and the second 48 hours of 'test' data used to evaluate the accuracy of the calibrated predictions. The first calibration method used the training data [0-48 h] for each deployment period to correct the test data [48-96 h] for the same deployment period i.e. a *unique* calibration for each deployment period (referred to as '*Aq_corr_u'*, Figures 3a & 3b). This method represented calibrations computed at close time intervals to the measurements being corrected. The second calibration method used a combination of training data from *all* deployment periods to derive a single global calibration equation, which was then applied to the training data for each period (referred to as *'Aq_corr_a',* Figure 3c). This method of calibration involving interspersed intervals during the extended set of deployments had a larger number of data points in the calibration, spread over a longer time period, thus represented a larger range of pollution conditions. The third calibration method used the calibration equation derived from the training data from the first study period (*November*) to correct the test data from all of the subsequent studies (referred to as *'Aq_corr_N',* Figure 3d). This method represented a calibration derived at the start of an extended field trial, and

was included to assess how the accuracy/precision of a '1-off pre-measurement campaign' calibration might deteriorate during extended field measurements.

The OLS calibration equations calculated for each of the three methods (as displayed in Figure 3 and summarised in Table S1) were used to adjust the test data, resulting in similar overall temporal patterns in the time series of adjusted Aeroqual and reference analyser O_3 concentrations (adjusted concentration estimates shown for both *training* and *test* data in Figure S1). O_3 concentrations measured by the reference analyser and the corrected Aeroqual deviated for a short period at the end of the December deployment, when the reference analyser measured very low O_3 concentrations and the corrected Aeroqual instruments were slightly negative. This period corresponded to a winter pollution episode with elevated NO_2 concentrations (Figure 6). None of the three calibration methods accurately corrected the Aeroqual measurements at these very low O_3 concentrations, presumably as a result of the marked change in pollution concentrations between the training and test data. This highlights the importance of [when possible] calibrating the Aeroqual systems using pollution concentrations similar to those anticipated during intended applications of the Aeroqual systems.

We calculated high correlation coefficients ($R^2 > 0.90$) and slopes close to 1 (slope: 0.91 – 1.07) for scatter plots of all the adjusted test data for combined deployment periods *vs.* analyser-measured O_3 concentrations for all three calibration methods (Figures 4 and S2). However, the scatter plot for the *Aq_corr_N* calibration (for both Aeroqual units) had relatively large negative intercept compared with the scatter plots for the other two calibration methods, resulting from underestimation of reference analyser O_3. The root mean square error (RMSE), mean bias (MB) and normalised mean bias (NMB) for *Aq_corr_N* were correspondingly larger than the other two calibration methods (Table 2, Figure S2).

These evaluation statistics indicate that calibrations derived from test data interspersed regularly throughout the deployment periods provide a more accurate estimate of the test analyser concentrations than a single calibration at the start of the deployment periods. There were only small differences in R^2, RMSE, MB, and NMB statistics between *Aq_corr_u* and *Aq_corr_a* methods, which were partly instrument dependent. For *O_3_3*, all four statistics for the *Aq_corr_u* method indicated a slightly better fit between adjusted sensor and analyser data. There was a less consistent pattern for the statistics for *O_3_4* although the differences involved were negligible. Hence we concluded that both *Aq_corr_u* and *Aq_corr_a* methods enabled useful adjustment to improve the agreement between sensor and analyser data, with some marginal additional benefits from the former method.

3.2. Calibration of Aeroqual NO_2 instruments

We corrected known cross-sensitivity of the Aeroqual NO_2 sensors to O_3 concentrations using a procedure described by Lin et al. (2015). Briefly, for each pair of Aeroqual sensors, we calculated the OLS regression line between the difference in NO_2 concentration measured by the Aeroqual sensor and the reference analyser (*NO_2_difference*) *vs. Aeroqual O_3*, and used the regression line to adjust the measured Aeroqual NO_2 concentration. The Aeroqual instruments were arbitrarily paired in this correction (reflecting the arbitrary pairing that occurs when a pair of instruments is used for field measurements), with *NO_2_1* corrected using *O_3_3* and *NO_2_2* corrected using *O_3_4*. The three different calibration methods described in Section 3.1 were used, leading to NO_2 concentrations adjusted using the *Aq_corr_u*, *Aq_corr_a* and *Aq_corr_N* selections of training data (Figure 5). The OLS regression calibration equations computed for each method are also summarised in Table S1.

The time series of reference analyser and adjusted Aeroqual NO_2 concentrations had similar temporal trends (Figure 6). A pronounced feature of the time series was a pollution episode

with elevated NO_2 concentrations (up to 90 µg/m^3) that occurred at the end of the December 2015 deployment period. All three calibration methods resulted in clearly defined linear relationships between adjusted Aeroqual and reference analyser NO_2 concentrations with R^2 values ranging from 0.80 to 0.90 (Figure 7 & Table 2). The slope and intercept values were closest to 1 and 0, respectively, R^2 values highest, and RMSE values lowest for the *Aq_corr_u* selection of training data for both of the Aeroqual NO_2 instruments (Figure 5 & Table 2). The NMB values were less variable over individual deployment periods for the *Aq_corr_u* selection of training data (Figure S2). The elevated NMB values in the May2 study probably resulted from the different response of the instruments during calibration for this period, as evident by the change in the NO_2 calibration equations (Table S1 and Figure S2).

The evaluation statistics for both Aeroqual NO_2 instruments suggested that using calibrations derived closer in time to the periods that the calibrations were applied (*Aq_corr_u* training data selection) resulted in closer agreement between the adjusted Aeroqual NO_2 and reference analyser concentrations. This highlights the importance of regular calibration as close as possible in time to the period when measurements are to be corrected. Our observations suggested that a single calibration study e.g. at the start of a monitoring campaign, is unlikely to be adequate to correct the NO_2 concentrations collected during extended monitoring. Instead, several shorter calibrations appear to be beneficial within field measurement campaigns.

3.3. Temporal changes in Aeroqual O_3 and NO_2 instrument responses

We calculated the ratio of Aeroqual:analyser concentrations over the 6 months of this study using unadjusted Aeroqual O_3 concentrations to further investigate the NO_2 calibration, such as is occasions of poorer NO_2 calibration a result of poorer performance of the Aeroqual O_3 instrument (Figure 8a). Large deviations (i.e. large ratio values) between the Aeroqual and reference O_3 concentrations occurred at the end of the December deployment period, when the NO_2 pollution episode (presumably as result of concurrently elevated NO) coincided with lower than usual reference analyser O_3 concentrations at the site. These low O_3 concentrations were not accurately estimated by the Aeroqual instruments (Section 3.1). The ratio between the O_3 concentrations measured by the Aeroqual and the analyser generally declined over the 6 month duration of this study (Figure 8a). This decline may have resulted from deterioration in the sensitivity of the O_3 instruments as the sensors age. However, the calibration procedures in Section 3.1 overcome these effects to enable reasonably accurate representation of variations in analyser concentrations. The sensors used in this work were over 2 years old, which is the working lifetime of the sensors specified by the manufacturer (Aeroqual, 2015 personal communication). Assuming the sensor deterioration only affects the magnitude of the signal from the O_3 sensor, and not the existence of a response to temporal variations in gas concentration, frequent calibrations as discussed previously would appear to allow the sensors to remain useable beyond this specified lifetime.

We plotted also the ratio of Aeroqual:analyser concentrations for Aeroqual NO_2 concentrations adjusted using *Aq_corr_u* and *Aq_corr_a* training data selections (Figures 8b and 8c). These ratios had less temporal drift than the equivalent ratios for O_3 because the calibration procedures for the Aeroqual NO_2 sensors will have partly corrected the temporal drift of the Aeroqual O_3 sensors. The Aeroqual:analyser NO_2 ratio varied more using the *Aq_corr_a* calibration method, compared to the *Aq_corr_u* method, with an increase in the ratio within some of the individual deployment periods, and a large increase in ratio during the final deployment period.

Daily averages of the hourly residuals for the Aeroqual O_3 and NO_2 measurements adjusted using the first set of training data (*Aq_corr_N*) were calculated for all of the available study

data (including data for deployments > 96 hours in length) (Figure 9). The daily O_3 residuals became more negative during each deployment period; however at the start of each deployment the residuals appeared to revert to close to zero, as measured for the first residual values in the *Aq_corr_N* calibration period in November 2015. This may be indicative of changes in the O_3 sensor response after the instrument has been turned on, and that this effect occurred repeatedly for all of the individual deployment periods. The Aeroqual NO_2 sensors exhibit a general increase in the daily residual plots during each deployment period that is likely to have resulted from the use of the Aeroqual O_3 data in the calibration of the Aeroqual NO_2 sensor.

The above suggests that it may be beneficial to make calibration and field measurements after consistent time periods following instrument start-up (as has been done in this evaluation exercise). Alternatively, future work could investigate the change in calibration equations over time since the instrument switch on to address the drift in instrument response over time.

3.4. Daily NO_2 and O_3 calibrations derived using alternate days

We investigated the effect of short-term (< 2 weeks) temporal drift on the calibration of the Aeroqual instruments by applying 24-hour calibration procedures in the first of the deployment periods in May 2016. This deployment period, which extended over 10 days of measurements, was the longest deployment period in the study. The 24-hour calibration calculations located test and training data close in time to one another, minimising the extent of drift in instrument responses over time, to establish if calibrations improved when the smallest, practical length of time between calibration and measurements is used. However the smaller number of data points (24) and reduced concentration ranges may limit the performance of the calibration and consequently result in poorer corrected data.

The observations were split into training and test datasets, with alternative days assigned to each category (training data = 5, 7, 9, 11, and 13 May; test data = 6, 8, 10, 12 and 14 May). Three calibration methods were investigated: (a) individual test days adjusted using calibrations computed from the preceding training day i.e. alternative day correction (*Aq_corr_alt*); (b) all test days adjusted using calibrations computed from training data from all training days combined (*Aq_corr_all_alt*); and (c) all test days adjusted using calibrations computed from the first day of training data [5 May 2016] (*Aq_corr_first*). The OLS regression equations calculated for each of these calibration procedures (Figure S3 and Table S1) were different from the 48 hour calibrations for the first deployment period in May 2016 (Figures 3 and 5 and Table S1), with the 24-hour calibrations generally having lower slope and R^2 values.

We noted similar temporal variations in adjusted Aeroqual and analyser O_3 concentrations for all three calibration methods (Figures S4 and S5). However there were periods when the adjusted Aeroqual O_3 concentrations deviated from the reference analyser concentration. These deviations were most apparent when the O_3 data was adjusted using the *Aq_corr_alt* training data selection method (Figure S4). The time series for adjusted Aeroqual NO_2 concentrations were also generally similar to the reference analyser; however there were also periods where temporal trends for the sensor and analyser deviated for all calibration methods, which corresponded to periods with poorer calibration equations (*e.g.* on 8-9 May 2016) (Figure S5, Table S1).

The highest R^2 values for the comparisons of *adjusted Aeroqual O_3 vs. reference O_3* concentrations occurred for the *Aq_corr_all_alt* and *Aq_corr_first* calibration methods (Figure 10, Table 3). The *Aq_corr_all_alt* method resulted in adjusted Aeroqual O_3 concentrations that underestimated analyser concentrations at low concentrations (Figure 10)

with a regression slope and intercept significantly different from 1 and 0 respectively (Table 3). The *Aq_corr_first* method produced a regression line closer to 1:1 and the smallest RMSE values (Figure 10, Table 3). The potential benefit of using shorter (*Aq_corr_alt*) calibrations to address the issue of instrument drift appeared to have been outweighed by fewer data and narrower concentration ranges, which hampered interpretation of the overall patterns in these data.

The scatter plots of *adjusted NO_2* test data *vs. reference analyser NO_2* appeared generally more consistent (than for O_3) between the three calibration methods (Figure 10). The slopes of all three regression lines were less than 1 as the adjusted Aeroqual NO_2 concentrations tended to underestimate the reference analyser concentrations at concentrations > 20 µg/m^3. The RMSE values for the three calibration methods were similar to one another (range: 5.26 – 6.88 µg/m^3 (Table 3)).

It would be laborious to make calibration measurements the day before every set of field measurements, especially for a long-term trial, and our observations suggest that, for a 10-day study such as this, there may be limited benefit to making and applying calibrations on every alternate day. However, the combination of several calibration periods interspersed within the overall measurement period (as outlined in section 3.1) would appear to mitigate the risk of only relying on calibration data from a short period when the range of concentrations may be limited or otherwise unrepresentative.

It was difficult to discern trends in the ratio of Aeroqual to reference analyser concentrations for O_3 and NO_2, (Figure S6) and daily average residual plots (Figure S7) indicating that on the short time scales of a single deployment period the apparent drift of the sensor response may sometimes be less evident.

4. Conclusions

We deployed two pairs of Aeroqual S500 NO_2 and O_3 sensors next to the inlets of reference gas analysers at an urban background monitoring station in Glasgow. We investigated different calibration methods and changes in the relative agreement between sensors and analyser measurements as the Aeroqual sensors reached the manufacturer's specified 2-year lifetime. The Aeroqual O_3 instruments were calibrated directly using linear relationships between concentrations measured by the sensors and reference analyser. The Aeroqual NO_2 instruments were calibrated allowing for cross-sensitivity to O_3 determined from Aeroqual O_3 measurements.

All of the methods tested in this study substantially improved the agreement between adjusted Aeroqual and analyser concentrations, emphasising the importance of field calibration of these real-time sensors. The calibrations should be collected in a similar pollution environment to that expected to be measured during the field measurements to avoid inaccuracies associated with extrapolation. We found some temporal drift of the instruments over time, and we suggest it may be beneficial to make calibration and field measurements after consistent time periods following instrument start-up (as has been done in this evaluation exercise). Calibrations in this 6-month duration study were more effective when interspersed at intervals throughout the study period and data corrected using calibrations close in time to measurements. The sensors used in this study exceeded their specified life time of 2 years. However we have demonstrated that appropriate calibration procedures allow the sensors to provide useful estimates of ambient pollution concentrations.

References

DEFRA, 2017. The Data Verification and Ratification Process [WWW Document]. URL https://uk-air.defra.gov.uk/assets/documents/The_Data_Verification_and_Ratification_Process.pdf (accessed 4.1.17).

Deville Cavellin, L., Weichenthal, S., Tack, R., Ragettli, M.S., Smargiassi, A., Hatzopoulou, M., 2016. Investigating the Use Of Portable Air Pollution Sensors to Capture the Spatial Variability Of Traffic-Related Air Pollution. Environ. Sci. Technol. 50, 313–320. doi:10.1021/acs.est.5b04235

Gillespie, J., Beverland, I.J., Hamilton, S., Padmanabhan, S., 2016. Development, Evaluation, and Comparison of Land Use Regression Modeling Methods to Estimate Residential Exposure to Nitrogen Dioxide in a Cohort Study. Environ. Sci. Technol. 50, 11085–11093. doi:10.1021/acs.est.6b02089

Gillespie, J., Masey, N., Beverland, I., Heal, M., Lin, C., Wu, H., Hamilton, S., In preparation. Field evaluation of Aeroqual S500 O3 and NO2 sensors at an air quality station over 1 year.

Gillespie, J., Masey, N., Heal, M.R., Hamilton, S., Beverland, I.J., 2017. Estimation of spatial patterns of urban air pollution over a 4-week period from repeated 5-min measurements. Atmos. Environ. 150, 295–302. doi:10.1016/j.atmosenv.2016.11.035

Heal, M.R., O'Donoghue, M.A., Cape, J.N., 1999. Overestimation of urban nitrogen dioxide by passive diffusion tubes: a comparative exposure and model study. Atmos. Environ. 33, 513–524. doi:10.1016/S1352-2310(98)00290-8

Heimann, I., Bright, V.B., McLeod, M.W., Mead, M.I., Popoola, O.A.M., Stewart, G.B., Jones, R.L., 2015. Source attribution of air pollution by spatial scale separation using high spatial density networks of low cost air quality sensors. Atmos. Environ. 113, 10–19. doi:10.1016/j.atmosenv.2015.04.057

Lewis, A., Edwards, P., 2016. Validate personal air-pollution sensors. Nature 535, 29–31. doi:10.1038/535029a

Lewis, A.C., Lee, J., Edwards, P.M., Shaw, M.D., Evans, M.J., Moller, S.J., Smith, K., Ellis, M., Gillott, S., White, A., Buckley, J.W., 2015. Evaluating the performance of low cost chemical sensors for air pollution research. Faraday Discuss. doi:10.1039/C5FD00201J

Lin, C., Gillespie, J., Schuder, M.D., Duberstein, W., Beverland, I.J., Heal, M.R., 2015. Evaluation and calibration of Aeroqual series 500 portable gas sensors for accurate measurement of ambient ozone and nitrogen dioxide. Atmos. Environ. 100, 111–116.

Masey, N., Gillespie, J., Heal, M.R., Hamilton, S., Beverland, I.J., Submitted. Influence of wind-speed on short duration NO2 measurements using Palmes and Ogawa passive diffusion samplers.

Masson, N., Piedrahita, R., Hannigan, M., 2015. Quantification Method for Electrolytic Sensors in Long-Term Monitoring of Ambient Air Quality. Sensors 15, 27283–27302. doi:10.3390/s151027283

Mead, M.I., Popoola, O.A.M., Stewart, G.B., Landshoff, P., Calleja, M., Hayes, M., Baldovi, J.J., McLeod, M.W., Hodgson, T.F., Dicks, J., Lewis, A., Cohen, J., Baron, R., Saffell, J.R., Jones, R.L., 2013. The use of electrochemical sensors for monitoring

urban air quality in low-cost, high-density networks. Atmos. Environ. 70, 186–203. doi:10.1016/j.atmosenv.2012.11.060

Pang, X., Shaw, M.D., Lewis, A.C., Carpenter, L.J., Batchellier, T., 2017. Electrochemical ozone sensors: A miniaturised alternative for ozone measurements in laboratory experiments and air-quality monitoring. Sens. Actuators B Chem. 240, 829–837. doi:10.1016/j.snb.2016.09.020

Spinelle, L., Gerboles, M., Villani, M.G., Aleixandre, M., Bonavitacola, F., 2015. Field calibration of a cluster of low-cost available sensors for air quality monitoring. Part A: Ozone and nitrogen dioxide. Sens. Actuators B Chem. 215, 249–257. doi:10.1016/j.snb.2015.03.031

Wang, A., Fallah-Shorshani, M., Xu, J., Hatzopoulou, M., 2016. Characterizing near-road air pollution using local-scale emission and dispersion models and validation against in-situ measurements. Atmos. Environ. 142, 452–464. doi:10.1016/j.atmosenv.2016.08.020

Figures and Tables:

Figure 1: Deployment of the Aeroqual sensors on the roof of the Defra Automatic Urban Network monitoring station at Townhead, Glasgow. *NO_2_1* and *O_3_3* were located in the enclosures on the right hand (eastern) side of the roof. *NO_2_2* and *O_3_4* were located in the enclosures on the left hand (western) side of the roof. Temperature and relative humidity measurements were made at the north-east corner of the roof under a solar radiation shelter.

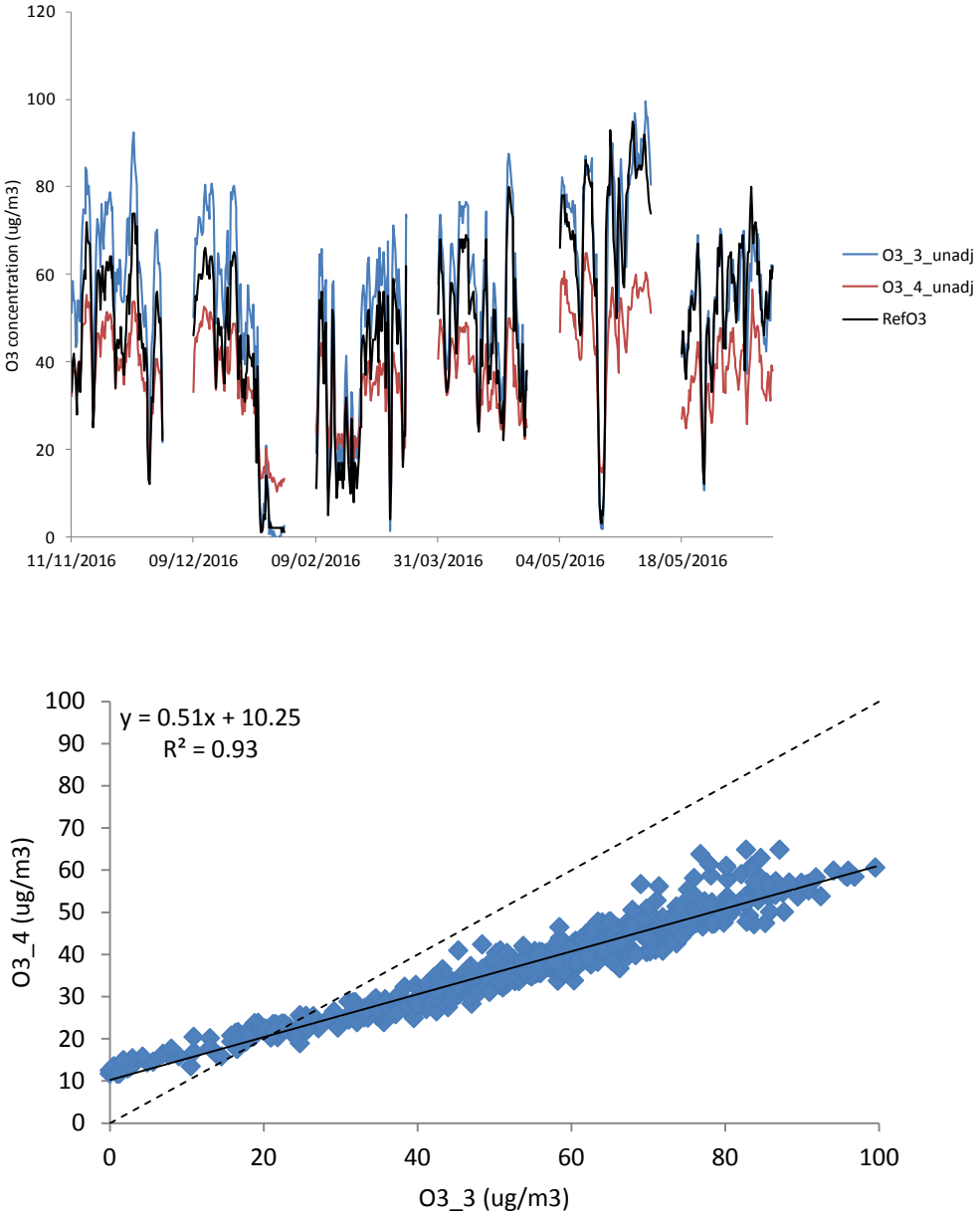

Figure 2: (a) Time series of unadjusted hourly-averaged O_3 concentrations measured by the two O_3 Aeroqual instruments and by the reference analyser for the full duration of each deployment period. Different deployment periods are separated by gaps in time series. (b) Scatter plot of unadjusted hourly data from the two O_3 Aeroqual instruments.

(a)

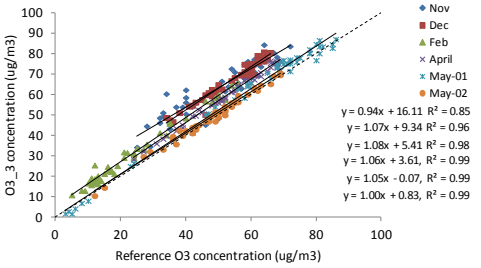

(b)

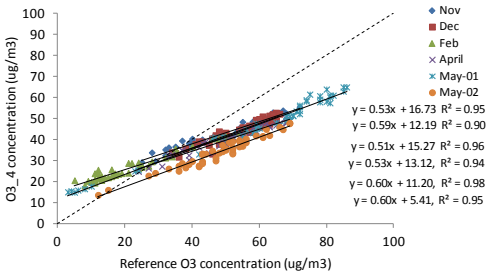

(c)

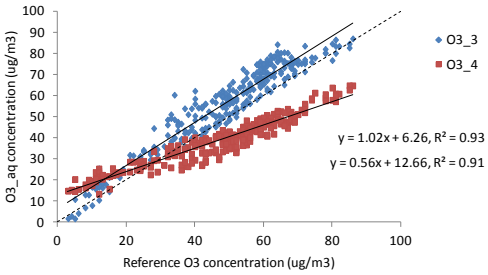

(d)

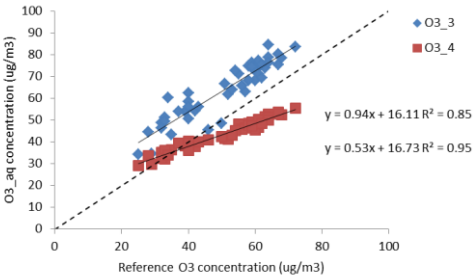

Figure 3: Scatter plots of hourly Aeroqual O_3 vs. reference analyser O_3, using the first 48 hours of data in each deployment period only (training data). These scatter plots were used to estimate different sets of calibration lines: (a) and (b) calibrations using training data in each unique deployment period (*O_3_aq_corr_u*) (panels (a) and (b) show data for Aeroqual O_3 units #3 and #4 separately); (c) calibrations using training data combined from all deployment periods (*O_3_aq_corr_a*), for O_3 units #3 and #4 separately; (d) calibrations using the first deployment period (November) only (*O_3_aq_corr_N*), for O_3 units #3 and #4 separately.

(a)

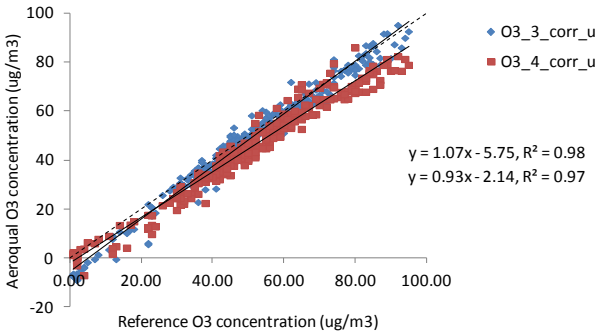

(b)

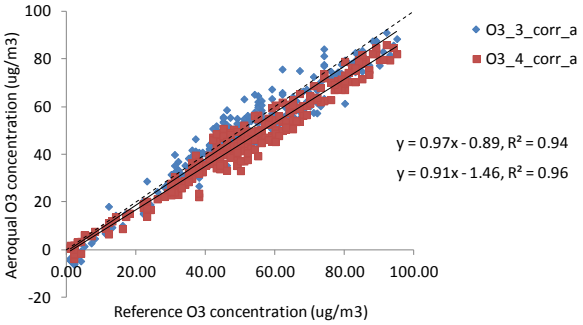

(c)

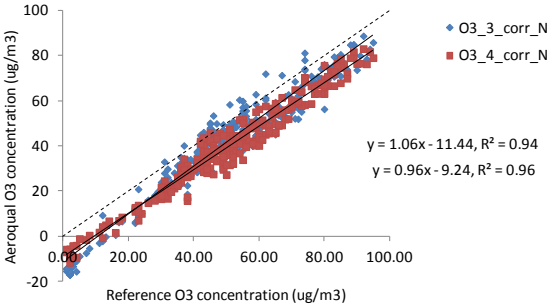

Figure 4: Scatter plots of adjusted hourly Aeroqual O_3 concentration estimates *vs.* reference analyser concentrations for the test data (i.e. 2nd half of deployment periods only). (a) *O_3_aq* adjusted using calibration derived from training data in each unique deployment period (*O_3_aq_corr_u*). (b) *O_3_aq* adjusted using calibration derived from training data combined from all deployment periods (*O_3_aq_corr_a*). (c) *O_3_aq* adjusted using calibration derived from the first deployment period (November) only (*O_3_aq_corr_N*).

(a)

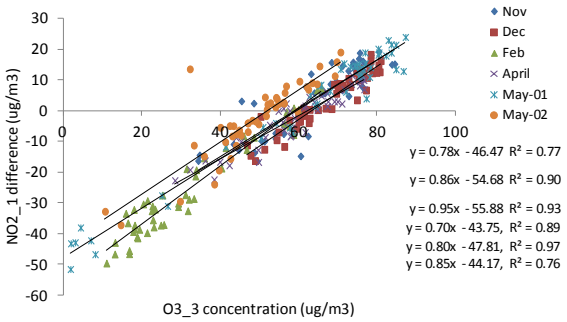

(b)

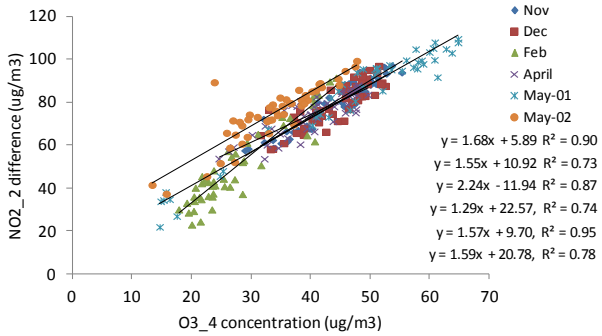

(c)

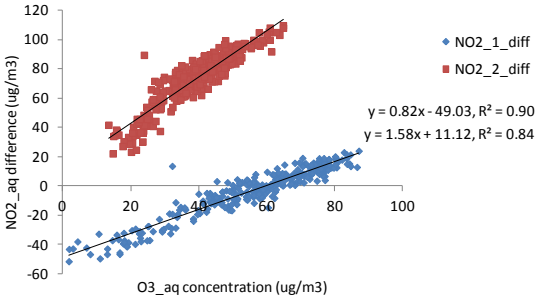

(d)

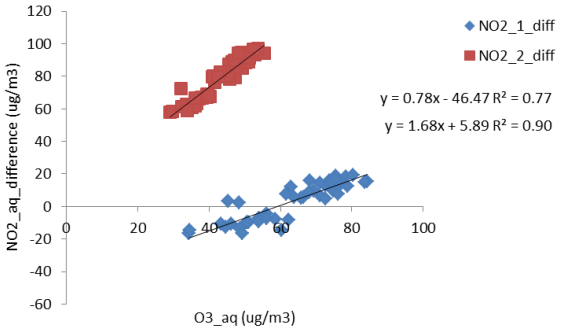

Figure 5: Scatter plots of hourly *Aeroqual NO_2 – Ref NO_2 (NO2_aq_difference) vs. Aeroqual O_3* using the first 48 hours of training data of each deployment period only. These scatter plots were used to estimate different sets of calibration lines (a) calibration using training data in each unique deployment period (*aq_corr_u*) for NO_2_1 vs. O_3_3; (b) calibration using training data in each unique deployment period (*aq_corr_u*) for NO_2_2 vs. O_3_4; (c) calibration using training data from all deployment periods combined (*aq_corr_a*), for NO_2_1 vs. O_3_3 and for NO_2_2 vs. O_3_4, separately; (d) calibration using the first deployment period (November) only (*aq_corr_N*), for NO_2_1 vs. O_3_3 and for NO_2_2 vs. O_3_4, separately.

(a)

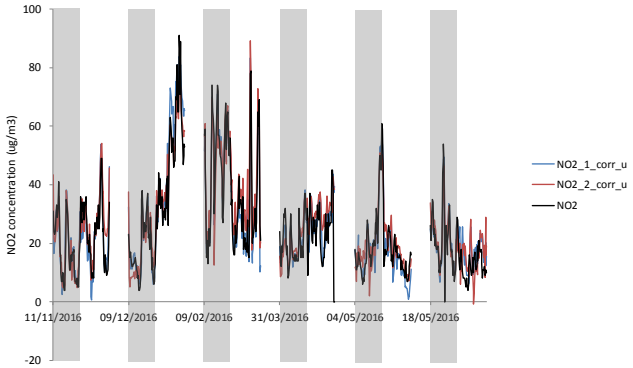

(b)

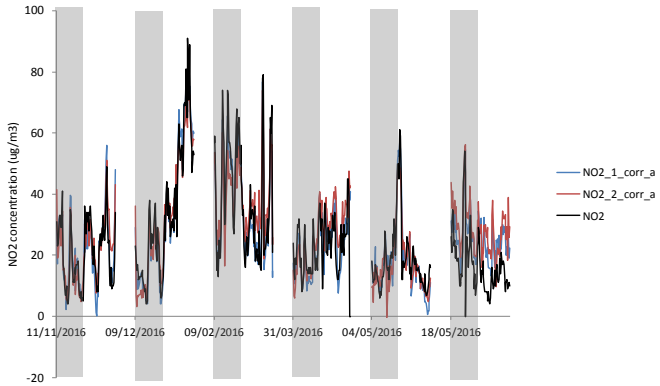

(c)

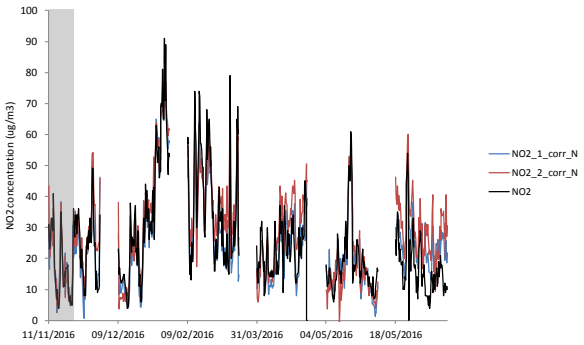

Figure 6: Time series of adjusted hourly Aeroqual NO_2 concentrations and reference analyser NO_2 concentrations using the following calibrations: (a) training data from each unique deployment period (*aq_corr_u*); (b) training data from all deployment periods (*aq_corr_a*); (c) training data from first (November) deployment period (*aq_corr_N*). Both training and test data sets are included (training data indicated by grey boxes). Different deployment periods are separated by gaps in time series.

(a)

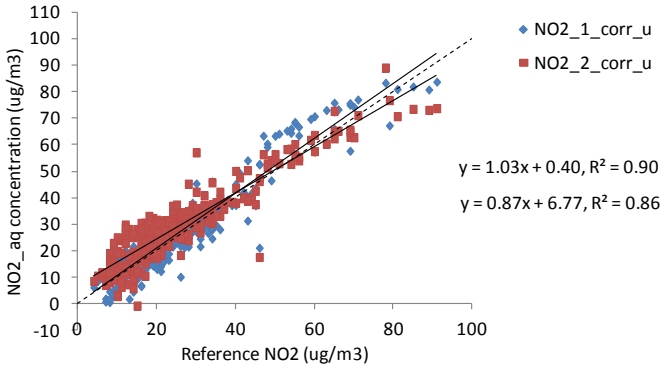

(b)

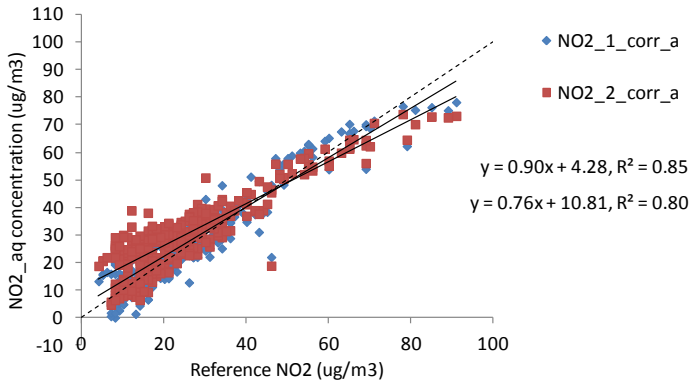

(c)

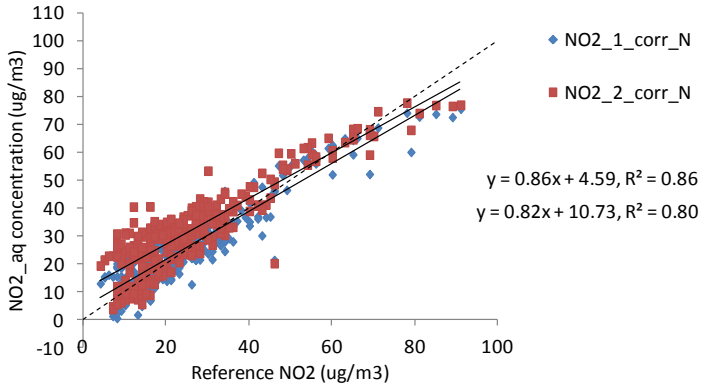

Figure 7: Scatter plots of adjusted hourly Aeroqual NO_2 concentration estimates *vs.* reference analyser concentrations for the test data (i.e. 2nd half of deployment periods only). (a) Aeroqual data adjusted using calibration derived from training data in each unique deployment period (*aq_corr_u*). (b) Aeroqual data adjusted using calibration derived from training data combined from all deployment periods (*aq_corr_a*). (c) Aeroqual data adjusted using calibration derived from the first deployment period (November) only (*aq_corr_N*).

(a)

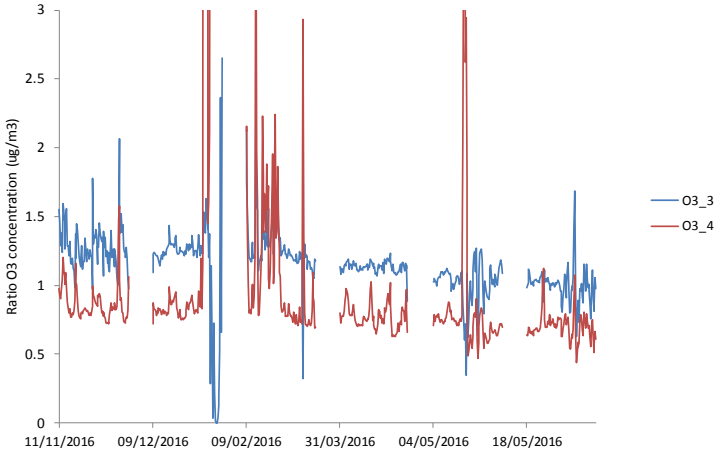

(b)

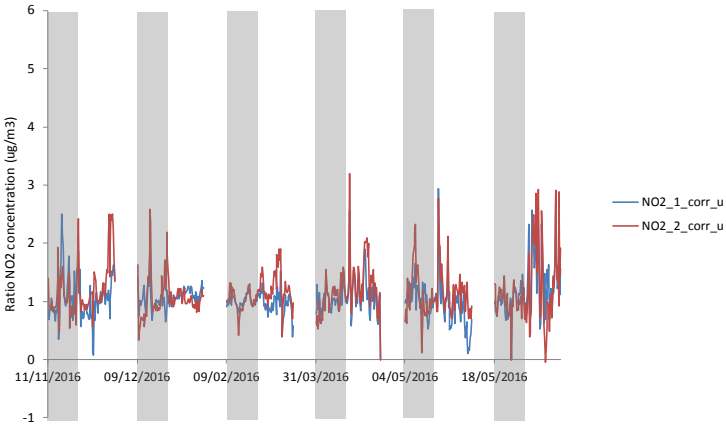

(c)

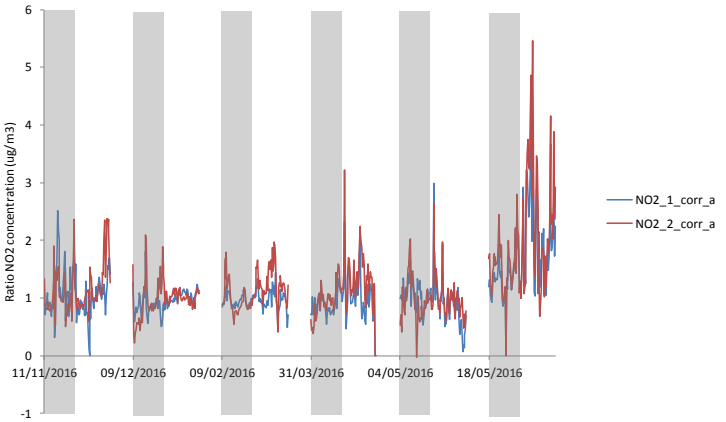

Figure 8: (a) Ratio of unadjusted Aeroqual *O_3_aq* to reference O_3. (b) Ratio of *NO_2_aq_corr_u* to reference NO_2. (c) Ratio of *NO_2_aq_corr_a* to reference analyser NO_2. Training periods for NO_2 are indicated by grey boxes, and the dashed line shows ratio value of 1. All concentration data are hourly averages.

(a)

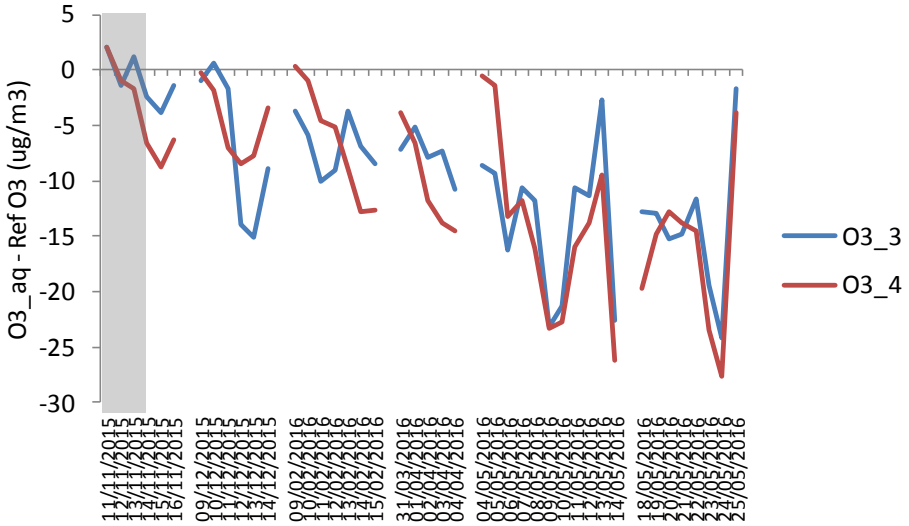

(b)

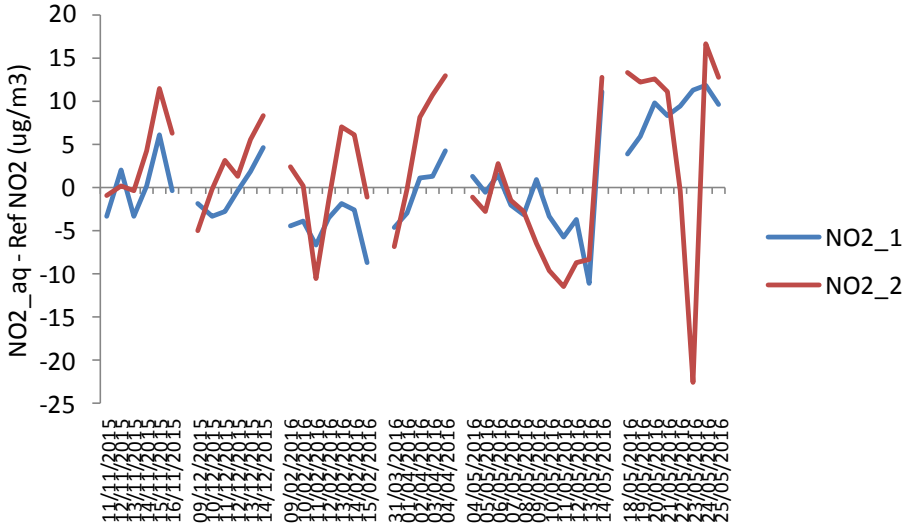

Figure 9: Daily average difference between hourly *Aq_corr_N* adjusted Aeroqual and analyser concentrations for each measurement day for (a) O_3 and (b) NO_2. The *Aq_corr_N* calibration period (November) is indicated by grey boxes. All data measured for each deployment period, before truncation to the first 96 hours, are shown. Different deployment periods are separated by gaps in time series.

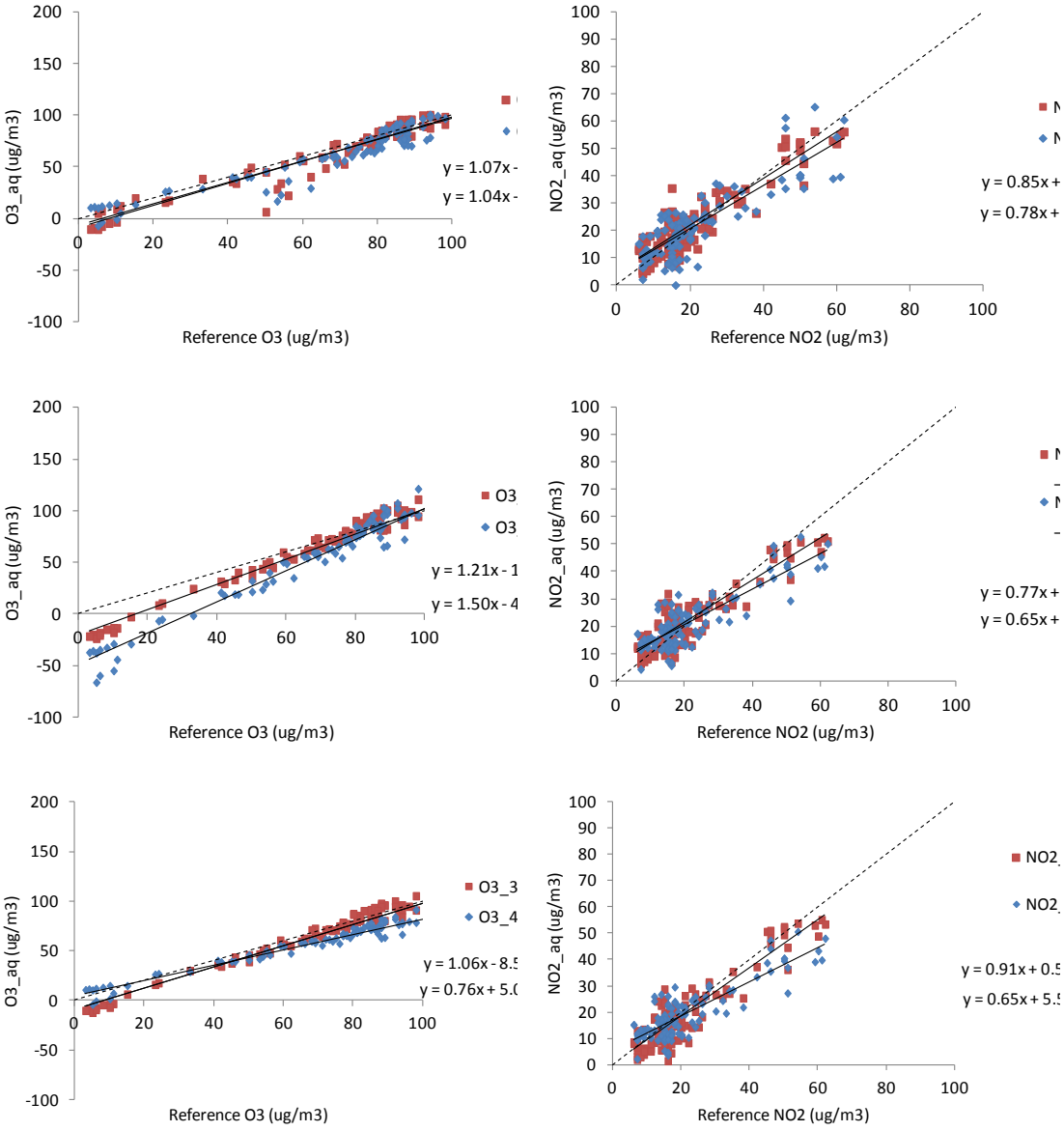

Figure 10: Scatter plots for short-term adjusted *Aeroqual O_3 vs. reference analyser O_3* concentrations (left) and adjusted *Aeroqual NO_2 vs. reference analyser NO_2* concentrations (right) using three calibration procedures (*aq_corr_alt*, *aq_corr_all_alt*, *aq_corr_first*). Only the test data (for 6, 8, 10, 12 and 14 May 2016) is shown in these Figures.

Table 1: Dates of 96-hour deployments of Aeroqual instruments at Townhead AURN site.

Study Name	Dates of Study
November	11/11/2015 – 15/11/2015
December	09/12/2015 – 13/12/2015
February	09/02/2016 - 15/02/2016
April	31/03/2016 – 04/04/2016
May1	04/05/2016 – 08/05/2016
May2	18/05/2016 – 22/05/2016

Table 2: OLS linear regression parameters (and 95% confidence intervals), coefficient of determination and summary statistics for adjusted Aeroqual NO_2 and O_3 concentrations compared to analyser measured concentrations. The calibration adjustments applied were: the second 48 hours of each deployment period corrected using the unique calibration derived using the first 48 hours of that deployment period (*Aq_corr_u*); the second 48 hours of each deployment period corrected using the calibration derived when the first 48 hours of data from all studies were combined (*Aq_corr_a*); and the second 48 hours of each deployment period corrected using the calibration derived from the first 48 hours in the first (November) study only (*Aq_corr_N*).

Instrument	**Correction**	**Slope [95 % C.I.]**	**Intercept [95 % C.I.] / μg m^{-3}**	R^2	**RMSE / μg m^{-3}**	**MB / μg m^{-3}**	**NMB**	**n**
O_3_3	O_3_corr_u	1.07 [1.06, 1.09]	-5.75 [-6.77, -4.72]	0.98	4.59	-2.10	-0.04	286
	O_3_corr_a	0.97 [0.94, 1.00]	-0.89 [-2.50, 0.72]	0.94	6.25	-2.17	-2.17	286
	O_3_corr_N	1.06 [1.03, 1.09]	-11.44 [-13.19, -9.68]	0.94	10.72	-8.54	-8.54	286
O_3_4	O_3_corr_u	0.93 [0.91, 0.95]	-2.14 [-3.20, -1.07]	0.97	6.94	-5.56	-0.11	286
	O_3_corr_a	0.91 [0.89, 0.93]	-1.46 [-2.57, -0.35]	0.96	7.22	-5.68	-0.12	286
	O_3_corr_N	0.96 [0.94, 0.99]	-9.24 [-10.41, -8.07]	0.96	11.80	-10.99	-0.23	286
NO_2_1	NO_2_corr_u	1.03 [0.99, 1.07]	0.40 [-0.82, 1.62]	0.90	5.79	1.25	0.05	286
	NO_2_corr_a	0.90 [0.85, 0.94]	4.28 [2.94, 5.62]	0.85	6.60	1.55	0.06	286
	NO_2_corr_N	0.86 [0.81, 0.90]	4.59 [3.33, 5.85]	0.86	6.34	0.82	0.03	286
NO_2_2	NO_2_corr_u	0.87 [0.83, 0.91]	6.77 [5.50, 8.03]	0.86	7.08	3.45	0.13	286
	NO_2_corr_a	0.76 [0.72, 0.80]	10.81 [9.45, 12.17]	0.80	8.70	4.55	0.17	286
	NO_2_corr_N	0.82 [0.77, 0.87]	10.73 [9.24, 12.22]	0.80	9.60	6.02	0.23	286

Table 3: OLS linear regression parameters (and 95% confidence intervals), coefficient of determination and summary statistics for corrected NO_2 concentrations compared to the analyser measured NO_2 concentrations. The corrections considered for each study were: alternate 24 hour periods used to correct the next 24 hours (*Aq_corr_alt*); all of the alternate 24 hour periods combined into a single data set and used to correct all of the remaining 24 hour periods (*Aq_corr_all_alt*); and the first 24 hour period used to correct all of the remaining alternate 24 hour periods (*Aq_corr_first*). These analyses were restricted to the first deployment period in May 2016.

Instrument	Correction	Slope [95 % C.I.]	Intercept [95 % C.I.] / μg m^{-3}	R^2	RMSE / μg m^{-3}	MB / μg m^{-3}	NMBn	
O_3_3	O_3_corr_alt	1.07 [1.01, 1.12]	-8.93 [-13.47, 4.39]	0.939	9.99	-3.26	-0.04	117
	O_3_corr_all_alt	1.21 [1.16, 1.27]	-19.59 [-23.82, 15.36]	0.951	0.64	-3.55	-0.05	117
	O_3_corr_first	1.06 [1.01, 1.10]	-8.55 [-12.24, 4.86]	0.958	.17	-4.21	-0.05	117
O_3_4	O_3_corr_alt	1.04 [0.98, 1.10]	-7.05 [-12.19, 1.92]	0.911	0.77	-4.05	-0.05	117
	O_3_corr_all_alt	1.50 [1.44, 1.56]	-48.04 [-53.03, 43.04]	0.962	4.24	-11.04	-0.14	117
	O_3_corr_first	0.76 [0.73, 0.80]	5.06 [2.52, 7.60]	0.961	5.50	-12.93	-0.17	117
NO_2_1	NO_2_corr_alt	0.85 [0.77, 0.92]	4.97 [3.02, 6.93]	0.81	5.95	2.02	0.09	117
	NO_2_corr_all_alt	0.77 [0.70, 0.84]	6.03 [4.21, 7.85]	0.81	5.78	1.40	0.07	117
	NO_2_corr_first	0.91 [0.83, 0.99]	0.53 [-1.45, 2.51]	0.83	5.26	-1.07	-0.05	117
NO_2_2	NO_2_corr_alt	0.78 [0.69, 0.88]	5.09 [2.73, 7.75]	0.726	.81	1.12	0.05	117
	NO_2_corr_all_alt	0.65 [0.58, 0.72]	7.53 [5.66, 9.40]	0.746	.72	0.50	0.02	117
	NO_2_corr_first	0.65 [0.57, 0.72]	5.54 [3.68, 7.41]	0.746	.88	-1.53	-0.07	117

The manuscript will be submitted to Atmospheric Environment and approved by the author.

Temporal variation of peripatetic real time pollution measurements and their ability to estimate longer term concentrations

Nicola Masey[1], Eliani Ezani[14], Jonathan Gillespie[1], Mathew R. Heal[2], Scott Hamilton[3], Iain J Beverland[1*]

[1]Department of Civil and Environmental Engineering, University of Strathclyde, James Weir Building, 75 Montrose Street, Glasgow, G1 1XJ, UK

[2]School of Chemistry, Joseph Black Building, University of Edinburgh, David Brewster Road, Edinburgh, EH9 3FJ, UK

[3]Ricardo Energy and Environment, 18 Blythswood Square, Glasgow, G2 4BG, UK

[4]Department of Environmental and Occupational Health, Faculty of Medicine and Health Science, Universiti Putra Malaysia, 43400 Serdang, Selangor, MALAYSIA

*CORRESPONDING AUTHOR: Dr Iain J. Beverland, Department of Civil and Environmental Engineering, University of Strathclyde, 505F James Weir Building, 75 Montrose Street, Glasgow, G1 1XJ, UK; email: iain.beverland@strath.ac.uk; Tel: +44 141 548 3202

Research highlights:

- Similar spatial trends estimated by 1-week NO_2 and 6-minute peripatetic monitoring of NO_2, BC and PN
- High correlation between peripatetic BC and PN and NO_2 concentrations
- Better correlation between peripatetic measurements during peak times
- Peripatetic BC and weekly NO_2 concentrations highly correlated ($R^2 > 0.68$)
- Higher correlations with greater number of repeat measurements per site

Abstract

Peripatetic measurements can be used to supplement monitoring networks. Using hand-held sensors we made 6-minute measurements, three-times a day (AM, Noon and PM), once per week over 7 weeks at 10 sites in Glasgow, UK. Additionally, we deployed passive samplers to measure weekly nitrogen dioxide (NO_2) concentrations simultaneously at each site. The spatial trends measured by the passive samplers were in agreement with those predicted from the peripatetic black carbon (BC), particle number (PN) and NO_2 measurements, while the peripatetic ozone (O_3) measurements predicted the opposite trends.

The relationship between the peripatetic measurements for all weeks was variable, with some (e.g. BC-PN) showing reasonable correlation (R^2 0.46 – 0.84) while others had a poorer relationship (e.g PN-O_3 R^2 0.06 – 0.29). Using the study-average peripatetic concentrations at each site improved the correlation coefficients between the hand-held instruments, highlighting the importance of repeat measurements. The study-average concentrations at each site showed high correlation between the two particle metrics, and the particle measurements and NO_2, which were greatest during the morning peak period (R^2 = 0.92 (BC-PN), 0.70 (BC-NO_2), 0.56 (PN-NO_2)), suggesting these could be used to estimate NO_2 concentrations in the absence of measurements. BC was also highly correlated with the longer-term passive sampler measurements ($R^2 > 0.68$ for all times of day) suggesting that mobile BC measurements could be used as a reliable estimator for longer-term NO_2. Peripatetic PN provides some estimate of longer-term concentrations ($R^2 > 0.5$), while NO_2 suffered from outliers as a result of atypical pollution concentrations observed during some

of the peripatetic measurements, which is a limitation of this monitoring approach, leading to poorer than anticipated relationship. Peripatetic O_3 could not be used to estimate the longer term trends ($R^2 < 0.25$).

This work highlights the ability of peripatetic measurements to provide an indicator of the spatial trends associated with traffic-related air pollution. Estimates of the longer-term NO_2 concentrations can be made using the particle metrics, however in order to obtain the best estimates many repeats should be undertaken at each monitoring location.

Keywords: air pollution; hand-held instruments; mobile measurements; passive samplers: peripatetic monitoring

1. Introduction

Monitoring of air pollution is important in order to assess compliance with legislation, which is in place in response to the detrimental health effects associated with exposure to air pollution (World Health Organization, 2013). Historically, monitoring has taken place at government funded automatic monitoring stations, which provide real-time but spatially limited pollutant concentrations, supplemented using passive monitoring, which can be deployed in higher density networks due to their low cost and simple deployment (Gillespie et al., 2017, 2016) but provide time-averaged concentrations. Estimates of population exposure to pollution are obtained using the nearest monitor as an estimate or through pollution modelling, however the spatial and temporal information these methods provided is limited.

Hand-held real-time instruments are continually being developed to help address the need for high spatially and temporally resolved monitoring networks. These type of instruments have been used to measure pollution concentrations continuously via platforms on bicycles or vehicles (Hankey and Marshall, 2015; Van den Bossche et al., 2015) or through short, static measurements at sites throughout the study area (Deville Cavellin et al., 2016; Norris and Larson, 1999). The results of mobile monitoring have been used to model concentrations over an extended study area (Montagne et al., 2015) or personal exposures (Delgado-Saborit, 2012; Dons et al., 2013). Limited work into the relationship between hand-held sensor measuring different pollutants or the representativeness of these mobile measurements of longer-term concentrations has been reported (Beckerman et al., 2008; Durant et al., 2014; Gillespie et al., 2017; Klompmaker et al., 2015; Riley et al., 2016).

In our previous study we investigated the relationship between short peripatetic measurements of black carbon and particle number, and longer-term average nitrogen dioxide concentrations (Gillespie et al., 2017). This work extends upon our previous study through use of a different study area, to identify the transferability of our previous findings, inclusion of peripatetic gaseous (as well as particle) measurements, and additionally we investigate if the time of day (peak or off-peak) has an influence on the relationships identified.

2. Methods

2.1. Study Design

Measurements were made during six consecutive 1-week study periods between 27th October 2015 and 8th December 2015. During these studies passive diffusion tubes (PDTs) were located at 10 sites anticipated to have different pollution environments (Figure 1). Site 10 was located within 10 m of the Townhead Automatic Monitoring Station which contains automatic analysers measuring hourly average concentrations of NO_2, O_3 and BC. On the Tuesday of each monitoring week, mobile measurements of BC, PN, O_3 and NO_2 were made during morning (AM), lunchtime (Noon) and afternoons (PM), with a static, 6-minute 'spot' measurements being made at each PDT site, giving 7 days of peripatetic monitoring. Six minute measurements were selected as the Aeroqual instruments make instantaneous measurements every minute, meaning that 5 instantaneous values would be included in each spot measurement. Tuesday was selected as it was expected to represent 'typical' traffic flows during the week while being uninfluenced by any holidays during the study period. The AM and PM measurements took place during peak times with anticipated higher traffic flows (0800 – 0930 and 1600 – 1730), while Noon measurements were off-peak (1300 – 1430). The measurements made on each of the 7 spot measurement days will be referred to using '*w/c X*' where *X* corresponds to the week number of the study.

Sites were visited in numerical order on each measurement occasion, and the times at each site were accurately recorded. Hand-held instruments were used to measure NO_2 (using an Aeroqual S500 electrochemical sensor ENW2, range 0 – 1 ppm), O_3 (using an Aeroqual S500 gas sensitive semi-conductor OZU2, range 0 – 0.15 ppm), BC (using an Aethlabs AE51 microAethelometer) and PN (using a TSI Condensation Particle Counter (CPC) 3007).

2.2. Preparation, deployment and analysis of passive samplers

Static measurements of nitrogen dioxide were measured at each site using Palmes-style PDTs. The tubes were prepared in-house, using the dipping method to coat the stainless steel collection meshes with 1:1 TEA:acetone solution (Heal, 2008), for each week of the study. Duplicate PDTs were deployed on a lamppost at each site, using foam to provide a gap between the post and the PDTs and secured using cable ties. This set up was selected to minimise the likelihood of theft of the PDTs as the sites in this work are located on busy streets. The PDTs were exposed for 1 week, giving 6 weeks of measurements. Two laboratory blank PDTs were prepared with the field samples, stored in the fridge unexposed for the duration of each study, then analysed with the field samplers. The Limit of Detection was found to be below the concentrations of field samplers for all study weeks (study-average limit of detection (concentration of blank + 3*standard deviation of blanks) = 6.9 $\mu g/m^3$).

Analysis of the PDT was carried out in the University of Strathclyde by UV-Vis spectrophotometry following guidelines provided by DEFRA (2008). Analysis was carried out for each week of PDTs to minimise the length of time between retrieval and analysis. The concentration of NO_2 measured using spectrophotometry was determined using the equation below:

$$C_0 = \frac{QL}{DAt}$$

where: C_0 is the average NO_2 concentration during the PDT exposure ($\mu g/m^3$), Q is the nitrite mass measured in each PDT by UV-Vis (ng cm^{-3}), L is the length of the PDT (7.1 cm), D is the diffusion coefficient of NO_2 (0.151 $cm^2 s^{-1}$), A is the area of the PDT (0.916 cm^2) and t is the time the PDT was exposed for (s).

2.3. Measurements using hand-held sensors

The BC instrument was carried inside a backpack and sampled air through 1 m conductive tubing inlets attached to the shoulder strap of the backpack. The instrument recorded data every second at a flow rate of 150 ml/min. Filters within the aethelometers were changed when ATN values reached 75, which resulted in the filter being changed each week. The BC data was downloaded and post processed using the Optimised Noise-Reduction Algorithm (ONA) on the Aethlabs website (https://www.aethlabs.com/dashboard) using ΔATN = 0.01. This data was further processed following the equation stated by Apte et al. (2011) to account for changes in filter attenuation value as the filter becomes darker:

$$BC = BC_0(0.88Tr + 0.12)^{-1}$$

where $Tr = \exp(-\frac{ATN}{100})$, BC_0 is the Black Carbon concentration measured by the instrument after smoothing by ONA, and *ATN* is the attenuation value.

The CPC, which measured data every second, was carried in by hand as it must be held horizontal to prevent solvent running into the detector, resulting in an error message and the instrument stopping recording for a short duration. The solvent cartridge was replenished after each use. The PN data was downloaded from the instruments and this data did not require any post processing prior to use.

The two Aeroqual instruments were located in external mesh pockets on either side of the backpack, thus sampled air at approximately chest height. They recorded data at the highest resolution interval, which was 1 minute, which provided instantaneous concentrations and not an average of concentrations measured throughout the minute. The O_3 data did not require any post processing prior to use. Previous work has shown that the NO_2 measurements made by the Aeroqual systems are cross-sensitive to O_3 concentrations, meaning the NO_2 data needs to be corrected prior to analysis (Lin et al., 2015; Masey et al., In preparation). Following the procedure detailed in Lin et al. (2015) calibration equations were derived from 5-day collocation studies at Townhead (Table 1). The October correction was used to correct the October measurements, the November correction for the November studies and the December correction for the December studies.

None of these instruments are waterproof, meaning additional precautions had to be taken during wet weather. In practice this meant for several of the measurement periods the backpack was worn on the front of the participant and this was shielded from the rain using an umbrella. The CPC was also held in the shelter of the umbrella to prevent water being sampled.

The concentrations measured during consecutive days of peripatetic measurement were averaged to provide a single concentration for each site and week, referred to as '*Week X*', where *X* corresponds to the number of the start of the week (e.g. Week 1 refers to the average concentrations from w/c 1 and w/c 2).

3. Results and Discussion

3.1. Agreement between Townhead spot measurements and analyser concentrations

The agreement between the PDT concentrations measured at site 10 and the analyser NO_2 concentrations was very good (R^2 > 0.75), however the PDTs overestimate the concentrations measured at the site (Figure 2). The agreement between the PDT and analyser concentrations are higher than previously reported for the site, which may be attributed to longer exposures and higher NO_2 concentrations (Masey et al., Submitted). The spot measurements made during each study period (AM, Noon and PM) were compared to the analyser concentrations measured during the two-hour period in which the spot measurements were made, and these showed linear agreement with R^2 values of 0.72, 0.51

and 0.83 for BC, NO_2 and O_3 respectively (Figure 2). No measure of particle number is available from Townhead to assess the PN measurements. The agreement between the mobile and reference BC concentrations is of similar magnitude to previously published co-location studies of longer durations, such as Viana et al. (R^2 > 0.75 for 2 - 4 day exposures) (2015) or Delgado-Saborit (2012) and Cheng and Lin (2013) (R^2 >0.90 for 16 - 25 hour exposures). The performance of the Aeroqual sensor was slightly poorer than previously published results for longer exposures, which have R^2 values > 0.6 for NO_2 and R^2 > 0.90 for O_3 (Delgado-Saborit, 2012; Lin et al., 2015; Masey et al., In preparation). The good agreement between the analyser and short-duration instrument concentrations gives confidence that the instruments provide a reasonable estimate of the background concentrations during the study and thus are expected to also provide a reasonable indication of the concentrations at the other sites.

In order to take into account temporal variations in background pollution concentrations between the study periods, the spot measurement at site 10 for each study was subtracted from the concentration measurements at the remaining site. Subtracting a single spot measurement to correct for background was thought to be appropriate due to the good agreement between the analyser concentrations shown above and the short time over which each measurement period occurred (approximately 1.5 hours) was anticipated to have little change in background values. During w/c 5 the NO_2 and O_3 instrument failed and no data was available for site 10, therefore the regression line from Figure 2 was used to estimate the spot concentrations based on the concentrations measured at Townhead and this estimated spot was subtracted from the other site spot measurements.

3.2. Temporal variations in pollution concentrations

3.2.1. Weekly variations in pollution concentrations

Similar spatial trends and generally close concentrations are noted at the sites each week, with roadside sites having higher NO_2, BC and PN concentrations and lower O_3 concentrations than those sites located further from the road (Supplementary Information Figure S1). Similar spatial trends in NO_2 and O_3 concentrations over relatively small study areas have been previous published (Lin et al., 2016). The concentrations of O_3 are often negative which is due to higher O_3 concentrations measured at the background site than the roadside site since O_3 is depleted by photochemical reaction with nitric oxides from vehicle exhausts.

To assess the ability of the spot measurements to predict longer concentrations, the concentrations measured each week were regressed against the average concentration for all the measurements at each site (Table S1). The measurements of BC each week are able to represent the longer term concentrations well, regardless of the time of day the measurements were made (R^2 > 0.6), while the PN measurements were able to estimate rush hour concentrations well but were less able to represent those measurements made during Noon (Table 2). The average correlation between weekly O_3 and study O_3 got poorer as the day went on while the opposite was true for NO_2 (Table 2). For all hand-held measurements, the concentrations that were the average of the three periods throughout the day showed best agreement with the study-averaged concentrations (Table 2), which is as expected from the more similar daily-average concentrations compared to each unique time period for each study shown in Figure S1. A similar procedure was carried out for the PDT measurements which showed the weekly PDT measurements were highly correlated with the study average concentrations measured by the PDTs at each site (R^2 > 0.7 for all weeks) (Table S1).

The slopes and intercepts from the regressions vary between weeks for each pollutant despite the high R^2 values (Table S1). The high R^2 values show that the trends in pollution concentrations estimated by the short-term measurements are consistent with those average

concentrations from the whole study period. However, the variation in the regression equations suggest the absolute values of the concentrations vary between weeks, despite the background subtraction which aimed to minimise temporal variation between weeks (Table S1).

This suggests that short static spot measurements can be used to give an indication of the pollution environment in an area and generally provide representative information about the spatial trends; however the concentrations recorded by the instruments should only be used as an indication as there are large variations between the concentrations each week. The hand-held instruments could be used to help identify monitoring sites for longer–term measurements, which could provide better indications of the 'true' pollution concentrations at the sites.

3.2.2. Daily variations in pollution concentrations

The study-average pollutant concentrations for each site show similar spatial trends regardless of the time of day the measurement was made at (Figure 3). The spatial trends of BC, PN and NO_2 are broadly similar to those measured by the PDTs, with higher concentrations present at roadside sites (e.g. site 2) and lower concentrations at sites further from roads (e.g. site 6). The measurements made during the lunchtime period generally had the lowest concentrations at each site for the pollutants directly related to traffic (NO_2, BC and PN) which was expected as there is anticipated to be fewer vehicles on the road during midweek lunchtimes. Consequently, the opposite is true for O_3 which had the highest concentrations during the lunchtime periods where there was less nitric oxides present for it to react photochemically with. BC and NO_2 concentrations are highest during the afternoon measurements for the sites 1 to 3, which are located in close proximity to a busy road, while for the remaining sites the afternoon and morning measurements are more similar to one another. For PN the morning measurements are higher than the afternoon measurements for the early sites (Figure 3). This could suggest an additional source of PN compared to the BC and NO_2 measurements in the morning, such as a greater number of buses on the road during the morning. The similar spatial trends between the different times of day when the measurements were made suggest that, providing enough measurements are made, spatial information about pollution concentrations can be accurately gathered independent of the time the measurements were made.

The ratio of within site to between site variance was calculated for each of AM, Noon, PM and daily-average measurements and compared to previously published values (Table 3) (Gillespie et al., 2017; Klompmaker et al., 2015). Our ratios of BC (all times) and PN (AM, PM and Average) measurements are lower than previously published results, including those from our previous study using the same instruments (Gillespie et al., 2017). The Noon measurements for PN show much larger ratios which could, in part, be attributed to the very low concentrations of PN recorded during week 6 (Figure S1). Those measurements made during peak times show lower ratios for the particle measurements than the Noon measurements. The gaseous spot measurements, however, show the smallest ratios for those Noon measurements. For all spot measurements, however, the ratios for the daily-average concentrations have the lowest ratio values, suggesting that in order to get the best estimate of long-term pollution concentrations from spot measurements, measurements should be made at a variety of times throughout the day and a daily-average calculated. For a large number of sites this may not be practical due to time restraints, in which case particle measurements are more representative of longer-term concentrations when made during rush-hour periods while the opposite is true for gaseous pollutants. Our previous study also observed lower than anticipated variance ratios , based on the short-duration of the spot measurements, which we suggested could be due to the small size of the study area and short

measurement period (Gillespie et al., 2017). However, the measurements in the current study were made at a different location to our previous work and over a slightly longer duration suggesting the temporal-stability of the pollutants at these short-time scales may be greater than those measurements made over longer durations.

3.3. Agreement between hand-held instruments

The 1-minute and 5-minute average concentrations for the hand-held instruments for the whole study (i.e. including time when walking between sites) showed reasonable agreement between the particle metrics for the two averaging times, with the 5 minute averaging period having a greater coefficient of determination for the relationship (Figure S2). However there is a lot of scatter in the data which is not entirely unexpected due to the rapidly changing concentrations that occur in a short space and time combined with the possibility of turbulence effects while walking. This is similar to results published by Hankey and Marshall (2015) who found that mobile BC and PN measurements made on a bicycle were more correlated the longer the averaging time used. The gas samplers also show agreement with each other which is due to the NO_2 sensor being corrected using the O_3 sensor. The gas and particle metrics show no significant relationship with one another in these mobile measurements (Figure S2). In most instances the highest agreement between the mobile measurements of different pollutants occurs in the afternoon 5-minute average measurements.

The relationship between the weekly-average spot measurements for the sites (i.e. average of 2 repeat static spot measurements) for the different pollutant at each site was greater than the mobile measurements, presumably due to the static nature of the measurements (Figure 4). The relationship between PN and BC and NO_2 and O_3 remained high for all time periods. Additionally a relationship between the particle metrics and the gas measurements is now apparent, with a good relationship between BC and NO_2. This relationship is strongest in the morning and is much lower during lunchtime and afternoon (R^2 = 0.50 and 0.16 for AM and Noon/PM respectively). Similarly, the other pollutant relationships are lowest during Noon (with the exception of that between PN and O_3). The R^2 value for the relationship between BC and O_3 has been reported to be 0.29 (Riley et al., 2016), which is similar to our AM measurements, however our correlations are much lower during Noon and PM.

When a study-average pollutant concentration from all measurement periods is calculated for each site, the regression lines are more linear and the R^2 values between the pollutants are higher (Figure 5). The relationship between BC and PN is consistently high (R^2 > 0.65) for all times of day and suggests that the concentration of BC could provide an estimate of the particle number at a location. The BC concentration also could provide an estimate of NO_2 concentrations, which is especially pronounced for the morning measurements (R^2 = 0.70). The lunchtime and afternoon measurements have a single outlier which leads to a poorer correlation than expected - excluding this outlier leads to R^2 value of > 0.90 (data not shown). The R^2 values from our AM measurements are of similar magnitude to those reported by Beckerman et al. (2008) for 10 minute pooled measurements at peak time for BC-PN and BC-O_3; lower for BC-NO_2, PN-O_3, and PN-NO_2; and better for NO_2-O_3; which could be down to the different nature of the measurements (Beckerman used non hand-held instruments mounted in a vehicle), or a greater number of sites over a larger study area used in this work. The BC-O_3 relationship R^2 exceeds that reported by Riley et al. (2016) with the exception of the PM measurements. The relationship between NO_2 and O_3 was similar for all study periods, with the highest R^2 (0.88) when a daily average concentration was calculated from the AM, Noon and PM measurements, however this high relationship was anticipated as O_3 is used to correct for the NO_2 instrument cross-sensitivity to ozone.

This suggests that it may be possible to estimate the concentrations of multiple pollutants based on a single pollutant measurement however the success of any estimate may be

dependent on the time of day the measurements were made during, with generally more accurate estimates during rush hour periods. The more repeat measurements used, the greater the ability to explain a higher proportion of the variance in another pollutant concentrations meaning the estimates are likely to be more accurate than relationships derived from a fewer number of repeat measurements.

3.4. Spot measurements vs. passive samplers

When all measurement periods are considered, the particle metrics have the greatest relationship with the longer-term PDT NO_2 concentrations and not, as anticipated, the gaseous pollutants (Figure 4). The measurements made during AM or daily-average have the highest R^2 values for the relationship and have the lowest scatter in the data. The relationship between BC, PN and PDT for the all weekly studies is slightly better than our previous study (this study average R^2 (BC, PN) = 0.45, 0.32; previous study R^2 (BC, PN) = 0.28, 0.07) (Gillespie et al., 2017), and greater than the BC-PDT relationship reported by Riley et al. (2016) for winter measurements (R^2 = 0.38).

The relationship between the study-average concentrations at each site is greater for all pollutants than when all measurement periods considered independently, highlighting the importance of repeat measurements (Figure 5). The relationship between BC and PDT is similar between the different measurement times (range of R^2 0.69 – 0.71) and is of similar magnitude to our previously published work (Gillespie et al., 2017), while for PN the relationship is more variable (R^2 range 0.51 – 0.83), however is improved on our previous study (Gillespie et al., 2017). The relationship between these particle metric and NO_2 measured using passive samplers are within the range of values reported from the ESCAPE and SAPALDIA studies, which co-located NO_2 and $PM_{2.5}$ measurements for 14 days (R^2 ranging from 0.21 to 0.79) (Durant et al., 2014; Eeftens et al., 2015), and, for the SAPALDIA study only, R^2 range 0.47 – 0.82 for NO_2 and PN (Eeftens et al., 2015). This suggests that longer-term concentrations of NO_2 can be estimated using short-duration (6-minute) particle measurements, with more accurate estimates expected when BC measurements are used compared to PN measurements.

The O_3 and PDT measurements are anti-correlated (as anticipated), with the highest agreement during the Noon studies when O_3 concentrations are higher (Figure 5). This relationship, however, is much poorer than the results of Riley et al. (2016), which could be attributed to fewer number of data points and the different sampling methods used between the two studies. The relationship between spot and PDT NO_2 is improved when the study-average concentrations are used compared to the all study data, however the R^2 values are still < 0.2 for Noon and PM studies. There is an elevated spot NO_2 concentration during these studies at site 1 (Figure 3) which is inconsistent with the spatial trends of the BC, PN and PDT concentrations. The Aeroqual instruments were left running in a laboratory between the AM, Noon and PM measurements and we suggest the elevated concentrations could be a result of rapid changes in exposure conditions when the Aeroqual instruments were moved from indoor to outdoor environment. Removing this outlier increases the R^2 > 0.65 (data not shown)), highlighting the limitation of this type of short, peripatetic measurement where a single outlier can have large influences on the results. We suggest that the Aeroqual instrument requires some time to equilibrate before use when moving the instrument between indoor and outdoor environments in order to prevent these non-representative measurements.

The relationship between the short spot measurements and the longer-term NO_2 concentrations suggest that mobile monitoring using BC, PN (to a lesser degree of confidence) and NO_2 could be used as an indicative measure of pollution concentrations in an area. However, O_3 did not produce a significant relationship with PDT to be able to

confidently estimate longer-term NO_2 concentrations. If long term pollution concentrations are required it would still be advisable to deploy monitors for long term at sites of interest, however the mobile monitoring could be used to help identify the sites where further monitoring should take place.

4. Conclusions

Hand-held instruments, measuring BC, PN, NO_2 and O_3, were used to make short duration (6 minute) measurements at 10 sites around Glasgow city centre, and additionally longer term (1 week) monitoring of NO_2 was carried out at the sites using passive samplers (PDT). Measurements were made during morning peak time (AM), mid-day (Noon) and evening peak time (PM) to assess if measurement time has an impact on the relationships.

Those measurements made next to an urban background automatic monitoring station showed good agreement with concentrations measured by the reference analysers which were similar to previously published longer duration studies. After accounting for changes in background concentrations, the spatial trends measured each week were similar, with roadside sites having elevated concentrations in comparison to sites located further from traffic sources, and those measurements made during Noon generally had lower concentrations for BC, PN and NO_2. The spatial trends measured by the hand-held BC, PN and NO_2 instruments were similar to those concentrations measured by the week-exposed PDTs, showing the ability of short, mobile measurements to provide estimates of spatial trends over a geographical area.

Relationship were observed between hand-held instruments measuring different pollutants, with the relationship between PN and BC being most pronounced, as anticipated since these are both measures of particles. When all study weeks were considered independently the relationships between pollutants were less clear than when study-average concentrations for the sites were considered. The relationship between the hand-held particle and gas instruments were highest during the AM measurements, with R^2 values of 0.92 (BC-PN), 0.44 (BC-O_3), 0.70 (BC-NO_2), 0.35 (PN-O_3), 0.56 (PN-NO_2). The relationship between NO_2 and O_3 was similar for all study periods, with the highest R^2 (0.88) when a daily average concentration was calculated from the AM, Noon and PM measurements, however this high relationship was anticipated as O_3 is used to correct for the NO_2 instrument cross-sensitivity to ozone. This suggests that estimates of PN and NO_2 concentrations can be derived from BC measurements, with the most accurate estimates being measured in during the morning peak time.

The short-duration hand-held measurements gave varying agreement with weekly-average NO_2 concentrations from PDTs, with consistently high correlation between PDT and BC regardless of measurement time (R^2 = 0.69 – 0.71), suggesting that BC is a representative indicator of longer term NO_2 concentrations. The PDT-NO_2 relationship was poorer than anticipated considering these measure the same pollutants (max R^2 = 0.41 during AM), which was suggested to be due to an elevated NO_2 concentration at site 1 during the spot measurement, highlighting the limitation of this type of short, peripatetic measurement which can be influenced by atypical pollution occurrences during measurements. We suggest that, if moving the Aeroqual instruments from sampling indoors to outdoors, some equilibration of the instrument in the outdoor environment may be required. The relationship between PDT-PN and PDT-O_3 were variable, with the highest agreements during noon (R^2 = 0.83 and R^2 = 0.24 respectively), suggesting that PN could provide an estimate of longer term NO_2 (but with lower confidence than BC) but O_3 cannot be used for reliable estimates.

The highest relationship between the different hand-held instruments, and between the hand-held instruments and the PDTs, was observed when the study-average concentration was used for each site, rather than using all measurements from each site independently. This

highlights the importance of making repeat measurements at a site over a period in order to get the best characterisation of the pollution trends and also minimising the impact of any atypical measurements.

Acknowledgements

Nicola Masey is funded through a UK Natural Environment Research Council CASE PhD studentship (NE/K007319/1), with support from Ricardo Energy and Environment. Eliani Ezani is funded through a PhD scholarship from the Malaysian Ministry of Higher Education. Jonathan Gillespie is funded through an Engineering and Physical Sciences Research Council Doctoral Training Grant (EPSRC DTG EP/L505080/1 and EP/K503174/1) studentship, with support from the University of Strathclyde and Ricardo Energy and Environment.

References

Apte, J.S., Kirchstetter, T.W., Reich, A.H., Deshpande, S.J., Kaushik, G., Chel, A., Marshall, J.D., Nazaroff, W.W., 2011. Concentrations of fine, ultrafine, and black carbon particles in auto-rickshaws in New Delhi, India. Atmos. Environ. 45, 4470–4480.

Beckerman, B., Jerrett, M., Brook, J.R., Verma, D.K., Arain, M.A., Finkelstein, M.M., 2008. Correlation of nitrogen dioxide with other traffic pollutants near a major expressway. Atmos. Environ. 42, 275–290.

Cheng, Y.-H., 2013. Real-Time Performance of the microAeth® AE51 and the Effects of Aerosol Loading on Its Measurement Results at a Traffic Site. Aerosol Air Qual. Res. doi:10.4209/aaqr.2012.12.0371

Delgado-Saborit, J.M., 2012. Use of real-time sensors to characterise human exposures to combustion related pollutants. J. Environ. Monit. 14, 1824. doi:10.1039/c2em10996d

Deville Cavellin, L., Weichenthal, S., Tack, R., Ragettli, M.S., Smargiassi, A., Hatzopoulou, M., 2016. Investigating the Use Of Portable Air Pollution Sensors to Capture the Spatial Variability Of Traffic-Related Air Pollution. Environ. Sci. Technol. 50, 313–320. doi:10.1021/acs.est.5b04235

Dons, E., Temmerman, P., Van Poppel, M., Bellemans, T., Wets, G., Int Panis, L., 2013. Street characteristics and traffic factors determining road users' exposure to black carbon. Sci. Total Environ. 447, 72–79.

Durant, J.L., Beelen, R., Eeftens, M., Meliefste, K., Cyrys, J., Heinrich, J., Bellander, T., Lewné, M., Brunekreef, B., Hoek, G., 2014. Comparison of ambient airborne PM2.5, PM2.5 absorbance and nitrogen dioxide ratios measured in 1999 and 2009 in three areas in Europe. Sci. Total Environ. 487, 290–298. doi:10.1016/j.scitotenv.2014.04.019

Eeftens, M., Phuleria, H.C., Meier, R., Aguilera, I., Corradi, E., Davey, M., Ducret-Stich, R., Fierz, M., Gehrig, R., Ineichen, A., Keidel, D., Probst-Hensch, N., Ragettli, M.S., Schindler, C., Künzli, N., Tsai, M.-Y., 2015. Spatial and temporal variability of ultrafine particles, NO2, PM2.5, PM2.5 absorbance, PM10 and PMcoarse in Swiss study areas. Atmos. Environ. 111, 60–70. doi:10.1016/j.atmosenv.2015.03.031

Gillespie, J., Beverland, I.J., Hamilton, S., Padmanabhan, S., 2016. Development, Evaluation, and Comparison of Land Use Regression Modeling Methods to Estimate

Residential Exposure to Nitrogen Dioxide in a Cohort Study. Environ. Sci. Technol. 50, 11085–11093. doi:10.1021/acs.est.6b02089

Gillespie, J., Masey, N., Heal, M.R., Hamilton, S., Beverland, I.J., 2017. Estimation of spatial patterns of urban air pollution over a 4-week period from repeated 5-min measurements. Atmos. Environ. 150, 295–302. doi:10.1016/j.atmosenv.2016.11.035

Hankey, S., Marshall, J.D., 2015. On-bicycle exposure to particulate air pollution: Particle number, black carbon, PM2.5, and particle size. Atmos. Environ. 122, 65–73. doi:10.1016/j.atmosenv.2015.09.025

Heal, M.R., 2008. The effect of absorbent grid preparation method on precision and accuracy of ambient nitrogen dioxide measurements using Palmes passive diffusion tubes. J. Environ. Monit. 10, 1363–1369. doi:10.1039/b811230d

Klompmaker, J.O., Montagne, D.R., Meliefste, K., Hoek, G., Brunekreef, B., 2015. Spatial variation of ultrafine particles and black carbon in two cities: Results from a short-term measurement campaign. Sci. Total Environ. 508, 266–275. doi:10.1016/j.scitotenv.2014.11.088

Lin, C., Feng, X., Heal, M.R., 2016. Temporal persistence of intra-urban spatial contrasts in ambient NO2, O3 and Ox in Edinburgh, UK. Atmospheric Pollut. Res. 7, 734–741. doi:10.1016/j.apr.2016.03.008

Lin, C., Gillespie, J., Schuder, M.D., Duberstein, W., Beverland, I.J., Heal, M.R., 2015. Evaluation and calibration of Aeroqual series 500 portable gas sensors for accurate measurement of ambient ozone and nitrogen dioxide. Atmos. Environ. 100, 111–116.

Masey, N., Ezani, E., Gillespie, J., Lin, C., Wu, H., Ferguson, N.S., Heal, M.R., Hamilton, S., Beverland, I.J., In preparation. Temporal changes in field calibration relationships for Aeroqual S500 NO2 and O3 sensors.

Masey, N., Gillespie, J., Heal, M.R., Hamilton, S., Beverland, I.J., Submitted. Influence of wind-speed on short duration NO2 measurements using Palmes and Ogawa passive diffusion samplers.

Montagne, D.R., Hoek, G., Klompmaker, J.O., Wang, M., Meliefste, K., Brunekreef, B., 2015. Land Use Regression Models for Ultrafine Particles and Black Carbon Based on Short-Term Monitoring Predict Past Spatial Variation. Environ. Sci. Technol. 49, 8712–8720. doi:10.1021/es505791g

Norris, G., Larson, T., 1999. Spatial and temporal measurements of NO2 in an urban area using continuous mobile monitoring and passive samplers. J. Expo. Anal. Environ. Epidemiol. 9, 586–593. doi:10.1038/sj.jea.7500063

Riley, E.A., Schaal, L., Sasakura, M., Crampton, R., Gould, T.R., Hartin, K., Sheppard, L., Larson, T., Simpson, C.D., Yost, M.G., 2016. Correlations between short-term mobile monitoring and long-term passive sampler measurements of traffic-related air pollution. Atmos. Environ. 132, 229–239. doi:10.1016/j.atmosenv.2016.03.001

Targa, J., Loader, A., 2008. Diffusion Tubes for Ambient NO2 Monitoring: A Practical Guide (No. AEA/ENV/R/2504 – Issue 1a). AEA Energy and Environment.

Van den Bossche, J., Peters, J., Verwaeren, J., Botteldooren, D., Theunis, J., De Baets, B., 2015. Mobile monitoring for mapping spatial variation in urban air quality: Development and validation of a methodology based on an extensive dataset. Atmos. Environ. 105, 148–161. doi:10.1016/j.atmosenv.2015.01.017

Viana, M., Rivas, I., Reche, C., Fonseca, A.S., Pérez, N., Querol, X., Alastuey, A., Álvarez-Pedrerol, M., Sunyer, J., 2015. Field comparison of portable and stationary instruments for outdoor urban air exposure assessments. Atmos. Environ. 123, Part A, 220–228. doi:10.1016/j.atmosenv.2015.10.076

World Health Organization, 2013. Review of evidence on health aspects of air pollution – REVIHAAP project: final technical report.

Tables and Graphs

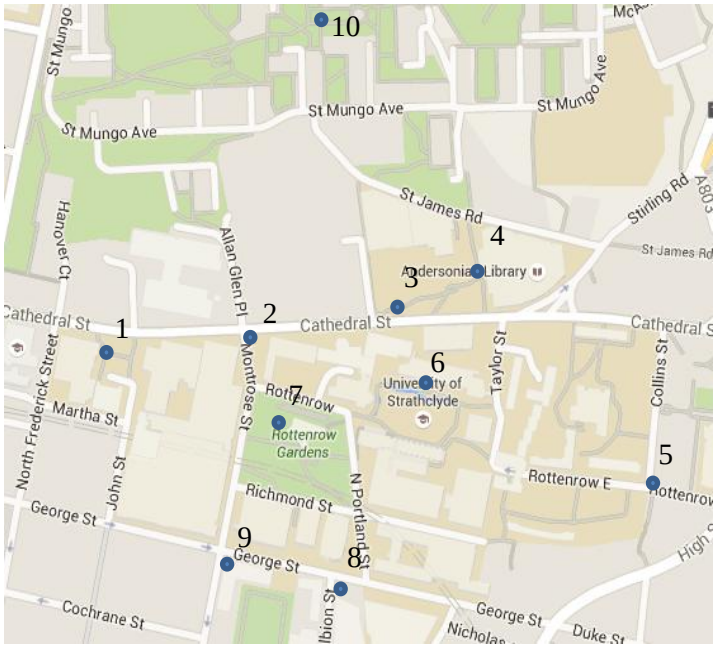

Figure 1: Location of the sites where six minute ‘spot’ and weekly-passive sampler measurements were made.

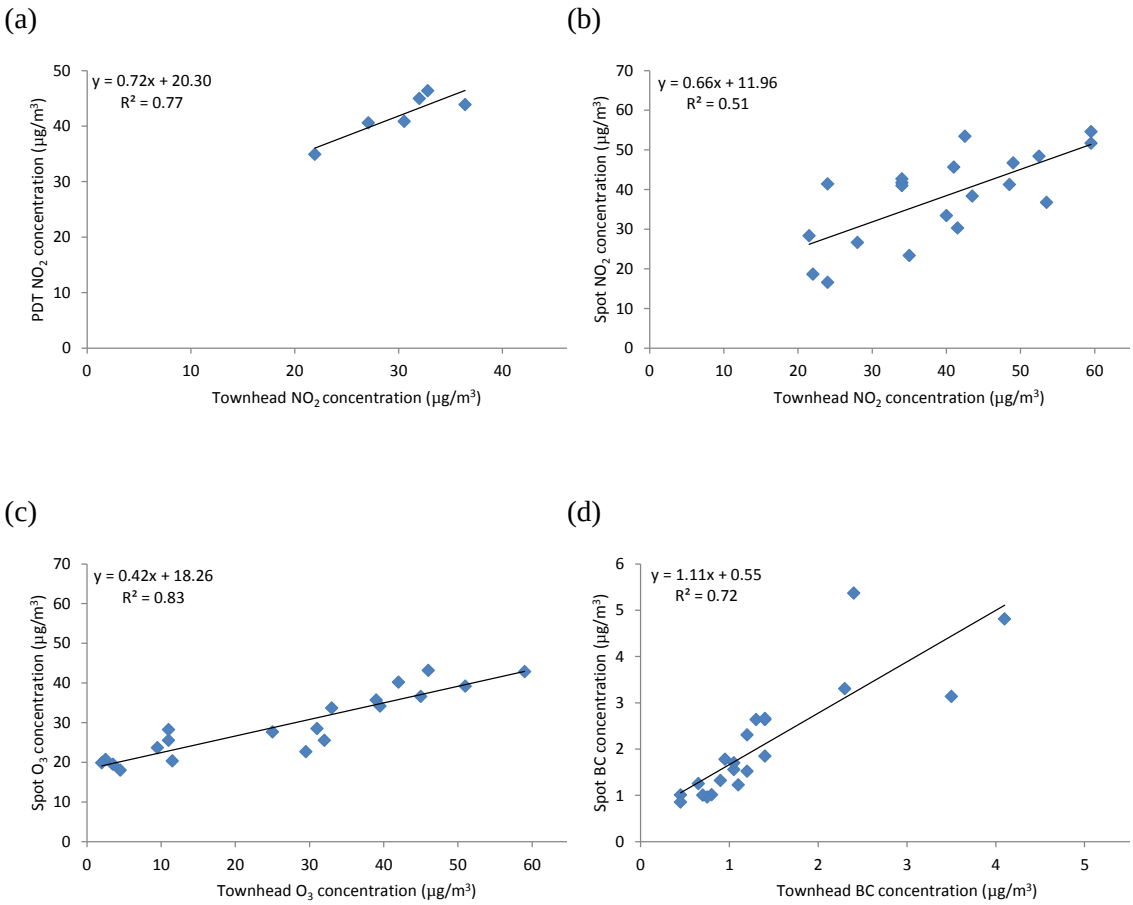

Figure 2: Agreement between measurements made at site 10 and concentrations recorded by the automatic analysers at the Townhead AURN station at the same site: (a) weekly average NO_2 concentrations measured by PDTs and analyser; and hand-held instrument spot measurement of (b) NO_2, (c) O_3 and (d) BC compared to average concentration measured at Townhead during the 2-hour window spot measurements were made during.

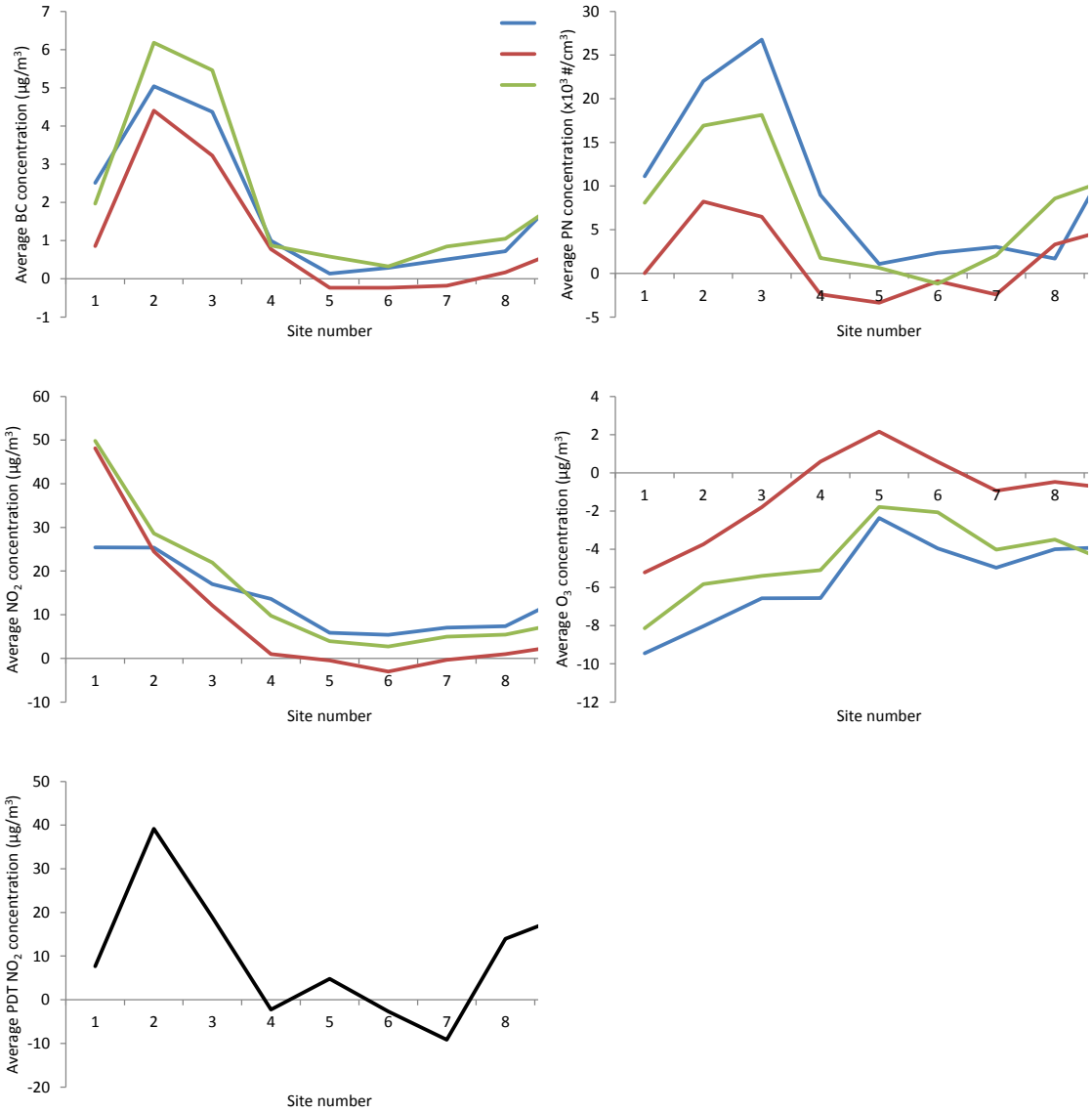

Figure 3: Average concentrations of pollutants measured at each site during the 7 'spot' measurements and 6 weekly passive sampler measurements. These are shown for each time of day that the spot measurements were made.

AM

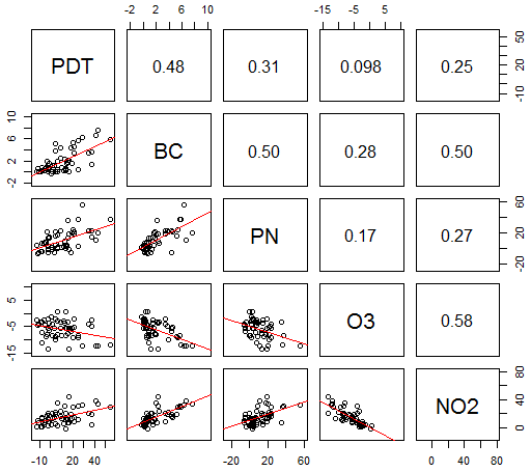

Noon

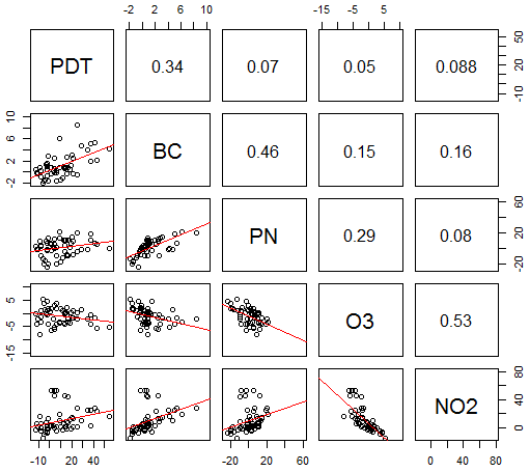

PM

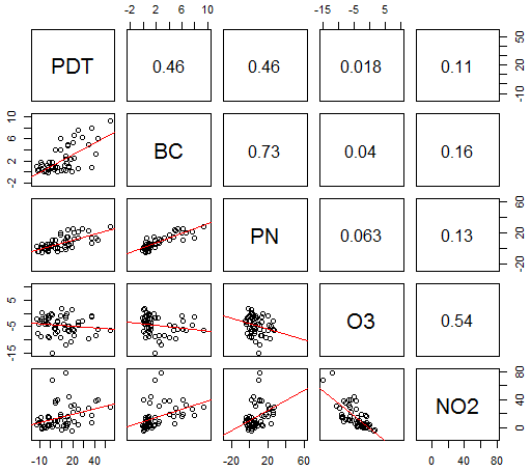

Average

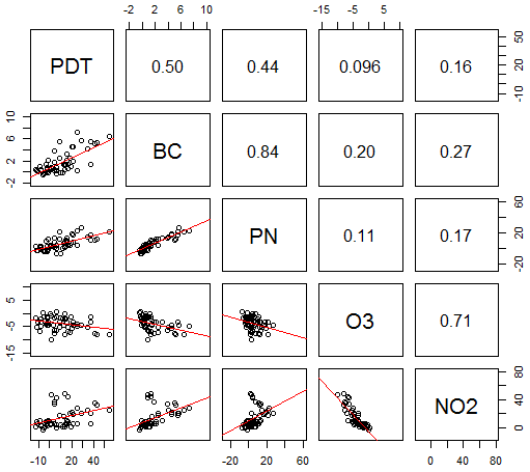

Figure 4: Correlation between spot measurements and passive sampler measurements for each of the different time periods the spot measurements were made at. This is shown for all data points (n = 60) and the spot measurements correspond to the average measurement made at the start and end of the PDT exposure time. The coefficient of determination is also shown.

AM

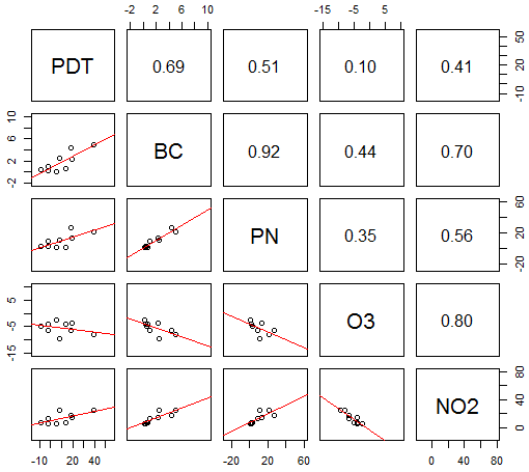

Noon

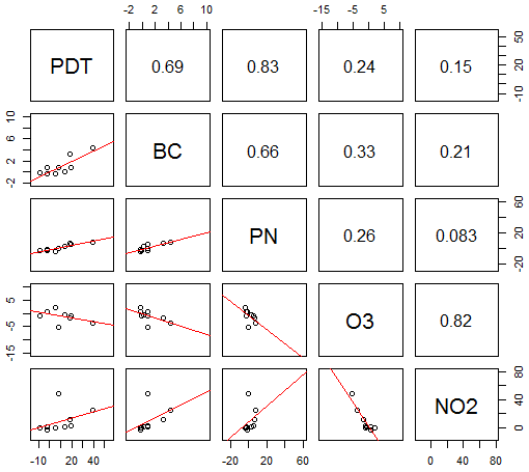

PM

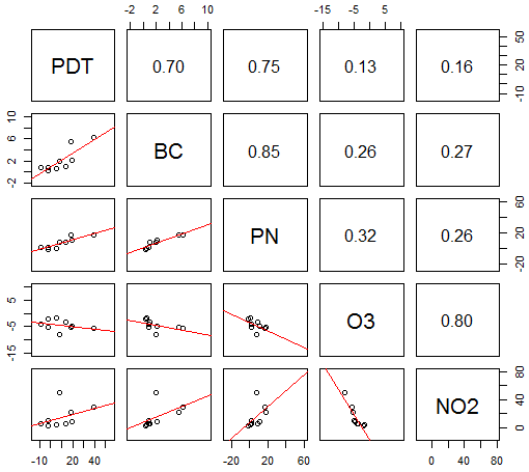

Average

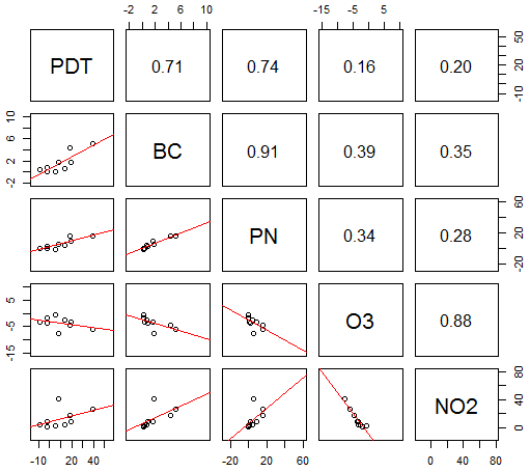

Figure 5: Correlation between the average spot measurement made at each site for each of the different times of day tested and the passive sampler measurements at the site (n = 10). The coefficient of determination is also shown.

Table 1: Correction equations derived for Aeroqual NO_2 instrument for each study period.

Month	$NO_{2\_aq\_corrected}$
October	$NO_{2\_aq} - (0.98*O_{3\_aq} - 59.70)$
November	$NO_{2\_aq} - (1.60*O_{3\_aq} - 66.11)$
December	$NO_{2\_aq} - (1.45*O_{3\_aq} - 61.26)$

Table 2: Average coefficient of determination between concentrations measured during each week measurements and the average concentrations measured during all weeks of spot measurement at each site (n = 7).

Pollutant	AM R^2 (min – max)	Noon R^2 (min – max)	PM R^2 (min – max)	Av R^2 (min – max)
BC	0.60 (0.24 – 0.80)	0.65 (0.37 – 0.96)	0.61 (0.01 – 0.92)	0.79 (0.56 – 0.94)
PN	0.58 (0.11 – 0.85)	0.35 (0.09 – 0.68)	0.52 (0.17 – 0.73)	0.62 (0.30 – 0.91)
O_3	0.66 (0.38 – 0.94)	0.53 (0.09 – 0.80)	0.44 (0.32 – 0.66)	0.74 (0.50 – 0.92)
NO_2	0.47 (0.14 – 0.80)	0.89 (0.76 – 0.97)	0.90 (0.83 – 0.17)	0.91 (0.84 – 0.98)
PDT	-	-	-	0.88 (0.72 – 0.97)

Table 3: Ratio of within site to between site variation from this study compared to other published studies (based on table published by Klompmaker et al. (2015).

Study (Within:Between)	BC	PN	O_3	NO_2	PDT
This study – AM	0.13	0.33	1.26	0.63	-
This study - Noon	0.20	1.88	0.35	0.04	-
This study – PM	0.15	0.22	0.91	0.09	-
This study – av	0.07	0.19	0.17	0.03	0.04
JG	0.28	1.17	-	-	0.14
MUSiC	3.25	2.21	-	-	-
ESCAPE	0.39	-	-	-	-
RUPIOH	-	0.5	-	-	-
VE3SPA	2.55	na	-	-	-

A (4): AEROSOL SCIENCE CONFERENCE (BIRMINGHAM, UK)

This poster won the Young Researchers' Best Poster Presentation (received an award plaque and a monetary prize of £150).

Exposure to Traffic-Related Air Pollution: Are Children More Exposed Than Adults?

University of Strathclyde Engineering

Eliani Ezani[1,2], Iain J. Beverland[1], Nicola Masey [1], Scott Hamilton[3] and David Sykes[3]

1- Department of Civil & Environmental Engineering, University of Strathclyde, Glasgow, UK
2- Department of Environmental and Occupational Health, Faculty of Medicine & Health Sciences, University Putra Malaysia, Serdang, Malaysia
3- Ricardo-AEA Ltd, 18 Blythswood Square, Glasgow UK
Email: nor-eliani-binti-ezani@strath.ac.uk, iain.beverland@strath.ac.uk

Background

Traffic-related pollution has been consistently associated with adverse effects on human health. Children's exposure to air pollutant may be greater because they are closer to the height of most traffic exhaust emissions.

A trolley was used in this study to assess exposure to $PM_{2.5}$, NO_2 and bioaerosols at two heights (0.8 m and 1.68 m- approximately the height of an adult pushing a child in a buggy) through repeated walks along a city centre route in Glasgow. NO_2 concentrations were measured at three days intervals at the same heights using passive diffusion tubes (PDTs) on lamp posts.

Methods

Figure 1: The Traffic Trolley

Figure 2: Location of study area within Glasgow city centre. The highlighted roads (red) show the route followed by the mobile trolley. The points on the map show the locations and names of the static monitoring sites (blue), where NO_2 measurements were made at the dual heights. The points on the map (green) show the Automatic Analysers (AUN) sites.

Results

Mobile Measurements

Figure 2: The measurements made at the lower (0.8 m) and upper (1.68 m) heights for the pollutants measured during each of the mobile trolley studies. The error bars shown are the standard deviation of the measurements.

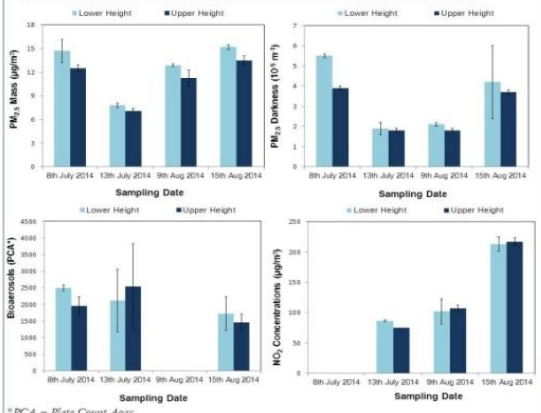

*PCA = Plate Count Agar

Static Measurements

Figure 4: Concentrations of NO_2 measured by the static PDTs located at upper (1.68 m) and lower (0.8 m) heights at 8 fixed sites in Glasgow City Centre. NO_2 measurements from Automatic Urban Network (AUN) sites are also shown. The error bars shown are the standard deviation of the measurements.

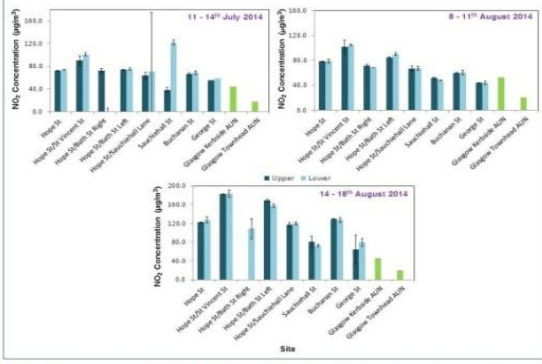

Key Summary

- Consistently increased $PM_{2.5}$ mass concentrations (13.6 % increase in mean), $PM_{2.5}$ darkness (19.2 % increase in mean) and bioaerosols (10% increase in mean) were observed at 0.8 m compared to 1.68 m.
- This study suggests that children may have greater exposure than adults to airborne particles close to roads.

APPENDIX A (4) : BOHS ANNUAL OCCUPATIONAL HYGIENE CONFERENCE (GLASGOW, UK)

Field Comparison of Instruments for Measurement of Personal Exposure to Black Carbon and Nitrogen Dioxide

Eliani Ezani[1,2], Akinola O. Idowu[1] and Iain J. Beverland[1]

1- Department of Civil & Environmental Engineering, University of Strathclyde, Glasgow, UK
2- Department of Environmental and Occupational Health, Faculty of Medicine & Health Sciences, University Putra Malaysia, Serdang, Malaysia
Email: nor-eliani-binti-ezani@strath.ac.uk, iain.beverland@strath.ac.uk

Background

Combustion-related air pollution has been consistently associated with adverse effects on human health. Personal exposure often varies substantially in space and time. Improved exposure measurement methods may be particularly beneficial characterising associations between pollution and health in people exposed to high concentrations of traffic-related air pollution, including professional drivers, vehicle maintenance personnel and traffic wardens.

This study presents measurements of black carbon (BC) and nitrogen dioxide (NO_2) using real-time instruments while walking on a pre-defined route in Glasgow City Centre. Instruments were placed in a backpack and data collected during repeat walks on the same route with position recorded by a GPS watch.

Measurement methods

Figure 1: Aeroqual NO_2 and Aethlabs black carbon sensors.

Results

Black carbon observations

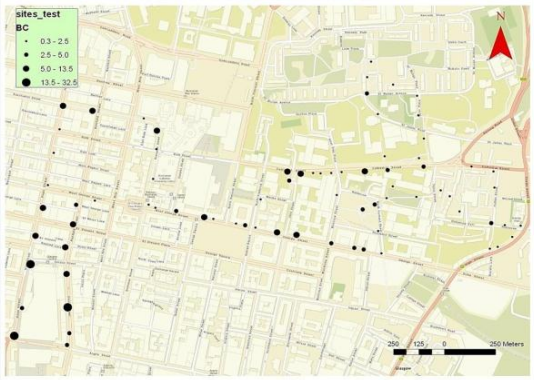

Figure 2: 1-minute average BC concentrations ($\mu g\ m^{-3}$) measured on a pre-defined route in Glasgow City Centre on 24th July 2015.

Results

Relationships between different devices & pollutants

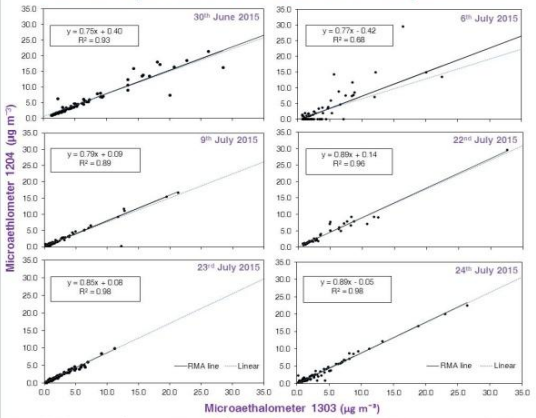

Figure 3: Comparison between MicroAeth 1303 and MicroAeth 1204 for 1-minute average of BC concentration ($\mu g\ m^{-3}$) using RMA line. The BC data were corrected to account for changes in attenuation value of AE51.

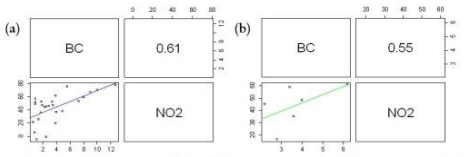

Figure 4: Comparison between average BC and NO_2 measurement for **(a)** 15-min time resolutions and **(b)** one-day measurements. Pearson correlation also shown.

Nitrogen dioxide observations

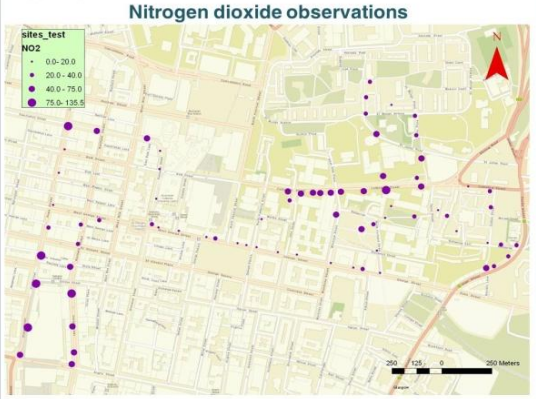

Figure 5: 1-minute NO_2 concentrations ($\mu g\ m^{-3}$) measured on a pre-defined route in Glasgow City Centre on 24th July 2015.

Conclusions

- Duplicate black carbon measurements showed a good inter-instrument precision and a similar spatio-temporal pattern to simultaneous measurements of NO_2.
- Occupational and environmental exposure to combustion-related air pollutants can be characterised by these portable instruments.

Assessment of Personal Exposure to Black Carbon and Nitrogen Dioxide in Contrasting Industrial (Fracking) and Urban (Road Traffic) Environments

Eliani Ezani[1,2], Iain J. Beverland[1], Tara K. Beattie[1], Megan Tailford[1], Akinola O. Idowu[1]

[1] Department of Civil & Environmental Engineering, University of Strathclyde, Glasgow, UK
[2] Department of Environmental and Occupational Health, Faculty of Medicine & Health Sciences, University Putra Malaysia, Serdang, Malaysia
Email: nor-eliani-binti-ezani@strath.ac.uk, iain.beverland@strath.ac.uk

Aim

This study used portable real-time monitors to assess and compare occupational and environmental exposure to black carbon (BC), nitrogen dioxide (NO_2) and ozone (O_3) in contrasting industrial and urban environments in Poland and Glasgow.

Methods

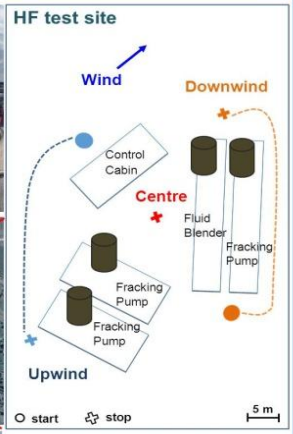

Figure 2 (a) Experimental fracking site in Poland. **(b)** Measurements were made at upwind (blue line), centre (red cross) and downwind (orange line) locations. **(c)** Continuously recording monitors were carried in a backpack and time of measurements was recorded at designated points.

- Occupational exposures to diesel exhaust from fracking equipment at a site in Poland were compared to pedestrian exposures to traffic-related air pollution in Glasgow, UK.
- Mobile measurements at different distances from sources were made using AE51 aethalometers (BC) & Aeroqual S500 sensors (NO_2 & O_3).
- Duplicate BC measurements were compared with NO_2 observations, after correction of NO_2 sensor response for O_3 interference effects.

Results

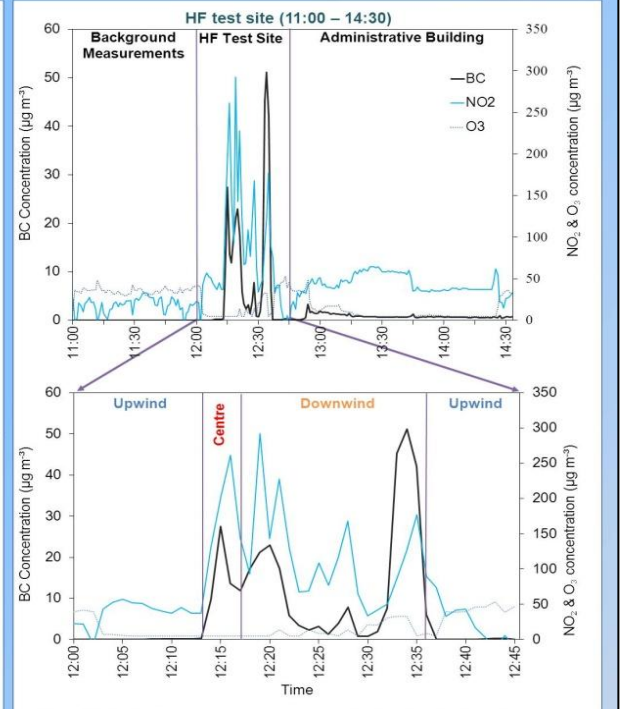

Figure 3 BC and NO_2 concentrations measured in vicinity of HF diesel-fuelled machinery.

Results

Table 1 BC and NO_2 concentrations measured at hydraulic fracking test site in Poland, and walking route in Glasgow city centre, UK.

Monitoring site	BC concentration (µg m⁻³)			NO_2 concentration (µg m⁻³)		
	Min	Max	Mean (SD*)	Min	Max	Mean (SD)
HF test site (downwind)	0.7	51.2	14.1 (15.9)	33.7	292.3	116.6 (66.1)
HF test site (upwind)	0.1	6.1	0.7 (1.9)	0.0	89.7	28.6 (34.5)
Glasgow city centre	0.1	44.4	3.7 (4.9)	0.9	280.6	53.1 (32.4)

*SD = standard deviation

- Average BC & NO_2 concentrations downwind of HF site were approximately 4 times higher than concentrations in Glasgow city centre.
- Duplicate BC instruments provided very similar real-time measurements, which in turn were relatively highly correlated with NO_2 observations at 1-minute temporal resolution at the HF experimental site (R^2 = 0.65) and on Glasgow city centre walking route (R^2 = 0.88).

Conclusions

- Marked elevations of BC and NO_2 concentrations were observed downwind of industrial fracking equipment and traffic sources.
- Exposure to diesel engine exhaust emissions from fracking equipment appears to present important risk to people working on HF sites.
- Short-time resolution portable instruments enabled identification of sources of occupational & environmental exposure to combustion-related air pollutants.

APPENDIX A (5) : IMAGE OF RESEARCH COMPETITION

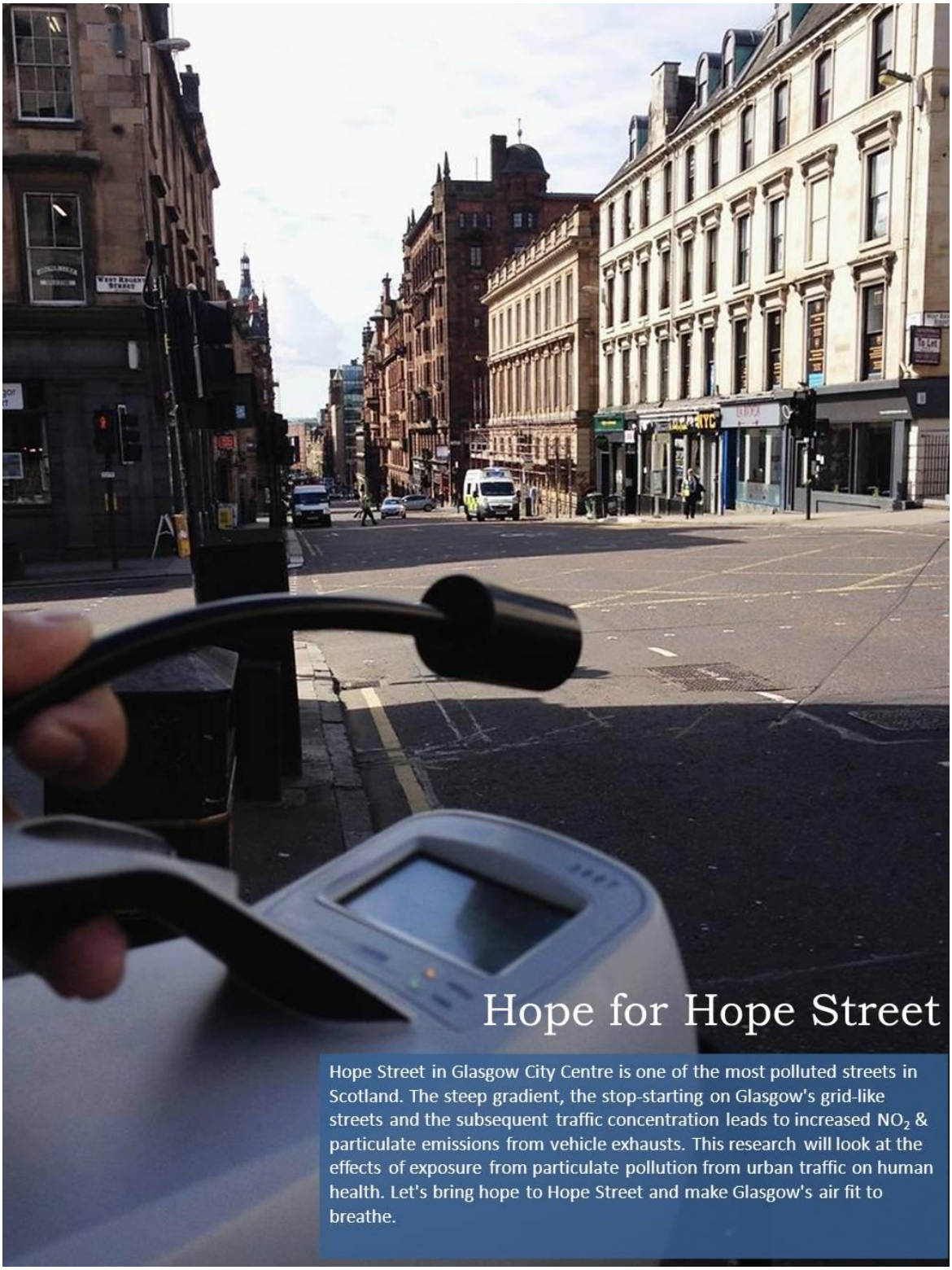

Figure 9A: Image can be found from http://www.imagesofresearch.strath.ac.uk/2015/gallery.php.

APPENDIX B HEALTH & SAFETY: RISK ASSESSMENT FORM

B (1): Working at AUN site risk assessment (RA) form.

B (2): Indoor RA form (DCEE).

B (3): Indoor RA form (ISC Building).

B (4): Outdoor RA form.

B (5): Outdoor RA form.

B (6): Poland fieldwork RA form.

B (1): Working at AUN site risk assessment (RA) form.

University of Strathclyde Glasgow

GENERAL RISK ASSESSMENT FORM (S20)

Persons who undertake risk assessments must have a level of competence commensurate with the significance of the risks they are assessing. It is the responsibility of each Head of Department or Director of Service to ensure that all staff are adequately trained in the techniques of risk assessment. The University document "Guidance on Carrying Out Risk Assessments" will be available, in due course, to remind assessors of the current practice used by the University. However, reading the aforementioned document will not be a substitute for suitable training.

Prior to the commencement of any work involving non-trivial hazards, a suitable and sufficient assessment of risks should be made and where necessary, effective measures taken to control those risks.

Individuals working under this risk assessment have a legal responsibility to ensure they follow the control measures stipulated to safeguard the health and safety of themselves and others.

SECTION 1

1.1 OPERATION / ACTIVITY			Complete the relevant details of the activity being assessed.
Title:	Deployment of air quality monitoring equipment on roof of government monitoring site		
Department:	Civil & Environmental Engineering		
Location(s) of work:	Townhead monitoring site, Kennedy Path, Glasgow	**Ref No.**	

Brief description:
Deployment of OSIRIS particle monitors and enclosures (11 kg); Aeroqual gas sensors (< 1 kg); AE51 microaethalometers (< 1kg); NO_2 passive diffusion devices (<1 kg)

1.2 PERSON RESPONSIBLE FOR MANAGING THIS WORK			
Name:	Iain Beverland	**Position:**	Senior Lecturer
Signature:		**Date:**	17 Mar 2016
Department:	Civil & Environmental Engineering		

1.3 PERSON CONDUCTING THIS ASSESSMENT			
Name:	Eliani Ezani	**Signature:**	
Name:	Iain Beverland	**Signature:**	
Name:		**Signature:**	
Date risk assessment undertaken:	17 Mar 2016		

1.4 ASSESSMENT REVIEW HISTORY

This assessment should be reviewed immediately if there is any reason to suppose that the original assessment is no longer valid. Otherwise, the assessment should be reviewed annually. The responsible person must ensure that this risk assessment remains valid.

	Review 1	Review 2	Review 3	Review 4
Due date:				
Date conducted: **Conducted by:**				

B (2): Indoor RA form (DCEE).

University of Strathclyde Glasgow

GENERAL RISK ASSESSMENT FORM (S20)

Persons who undertake risk assessments must have a level of competence commensurate with the significance of the risks they are assessing. It is the responsibility of each Head of Department or Director of Service to ensure that all staff are adequately trained in the techniques of risk assessment. The University document "Guidance on Carrying Out Risk Assessments" will be available, in due course, to remind assessors of the current practice used by the University. However, reading the aforementioned document will not be a substitute for suitable training.

Prior to the commencement of any work involving non-trivial hazards, a suitable and sufficient assessment of risks should be made and where necessary, effective measures taken to control those risks.

Individuals working under this risk assessment have a legal responsibility to ensure they follow the control measures stipulated to safeguard the health and safety of themselves and others.

SECTION 1

1.1 OPERATION / ACTIVITY			Complete the relevant details of the activity being assessed.
Title:	Deployment of Air Monitoring Equipment		
Department:	Civil and Environmental Engineering		
Location(s) of work:	Indoor (Level 5 JW Building)	**Ref No.**	
Brief description: Indoor particulate matter (PM10) and Nitrogen Dioxide concentration are determined through deployment of air sampling pump and diffusion tubes in the open plan office and cubicle at North JW Building. PM10 and NO_2 concentration for urban background will be determine at the same time by hanging the sampler head outside one of the window in JW building (north).			

1.2 PERSON RESPONSIBLE FOR MANAGING THIS WORK			
Name:	Eliani Ezani	**Position:**	PhD Student
Signature:		**Date:**	
Department:	Civil and Environmental Engineering		

1.3 PERSON CONDUCTING THIS ASSESSMENT			
Name:	Eliani Ezani	**Signature:**	
Name:	Nur Yahya	**Signature:**	
Name:	David Sykes	**Signature:**	
Date risk assessment undertaken:	July 2014		

1.4 ASSESSMENT REVIEW HISTORY

This assessment should be reviewed immediately if there is any reason to suppose that the original assessment is no longer valid. Otherwise, the assessment should be reviewed annually. The responsible person must ensure that this risk assessment remains valid.

	Review 1	Review 2	Review 3	Review 4
Due date:				
Date conducted: **Conducted by:**				

B (3): Indoor RA form (ISC Building).

University of Strathclyde Glasgow

GENERAL RISK ASSESSMENT FORM (S20)

Persons who undertake risk assessments must have a level of competence commensurate with the significance of the risks they are assessing. It is the responsibility of each Head of Department or Director of Service to ensure that all staff are adequately trained in the techniques of risk assessment. The University document "Guidance on Carrying Out Risk Assessments" will be available, in due course, to remind assessors of the current practice used by the University. However, reading the aforementioned document will not be a substitute for suitable training.

Prior to the commencement of any work involving non-trivial hazards, a suitable and sufficient assessment of risks should be made and where necessary, effective measures taken to control those risks.

Individuals working under this risk assessment have a legal responsibility to ensure they follow the control measures stipulated to safeguard the health and safety of themselves and others.

SECTION 1

1.1 OPERATION / ACTIVITY

Complete the relevant details of the activity being assessed.

Title:	Deployment of Air Quality Monitoring Equipment
Department:	Indoor (Graham Hills – Offices of the International Study Centre)
Location(s) of work:	Indoor **Ref No.**

Brief description: Particulate matter (PM2.5), Black carbon, nitrogen dioxide, ozone, temperature and humidity can be assessed by deploying handheld air quality monitors. The CP11 Rotronic, Aeroqual, AE51 aethalometer and MicroPEM indoor air monitors will be used in two rooms on the 8th floor of the Graham Hills building. The two rooms will be assessed over 48 hours, and then both monitors will be deployed in the room with the highest concentrations of carbon dioxide to assess the calibration of the monitors. This will take place over another 48 hour period.

1.2 PERSON RESPONSIBLE FOR MANAGING THIS WORK

Name:	Eliani Ezani	**Position:**	PhD Student
Signature:		**Date:**	
Department:	Civil and Environmental Engineering		

1.3 PERSON CONDUCTING THIS ASSESSMENT

Name:	Eliani Ezani	**Signature:**	
Name:	Jessica McQueen	**Signature:**	
Name:		**Signature:**	
Date risk assessment undertaken:	15th May 2015		

1.4 ASSESSMENT REVIEW HISTORY

This assessment should be reviewed immediately if there is any reason to suppose that the original assessment is no longer valid. Otherwise, the assessment should be reviewed annually. The responsible person must ensure that this risk assessment remains valid.

	Review 1	Review 2	Review 3	Review 4
Due date:				
Date conducted:				

B (4): Outdoor RA form.

University of Strathclyde Glasgow

GENERAL RISK ASSESSMENT FORM (S20)

Persons who undertake risk assessments must have a level of competence commensurate with the significance of the risks they are assessing. It is the responsibility of each Head of Department or Director of Service to ensure that all staff are adequately trained in the techniques of risk assessment. The University document "Guidance on Carrying Out Risk Assessments" will be available, in due course, to remind assessors of the current practice used by the University. However, reading the aforementioned document will not be a substitute for suitable training.

Prior to the commencement of any work involving non-trivial hazards, a suitable and sufficient assessment of risks should be made and where necessary, effective measures taken to control those risks.

Individuals working under this risk assessment have a legal responsibility to ensure they follow the control measures stipulated to safeguard the health and safety of themselves and others.

SECTION 1

1.1 OPERATION / ACTIVITY			Complete the relevant details of the activity being assessed.
Title:	Deployment/Retrieval of Passive Diffusion Tubes		
Department:	Civil and environmental engineering		
Location(s) of work:	Outdoors	**Ref No.**	
Brief description: Atmospheric NO_2 concentration is determined through deployment of passive diffusion tubes sensitive to NO2. The tubes are attached to lampposts (or similar) at heights ranging from 0.5 m to just above head height by means of a cable tie and plastic clip and left exposed to the atmosphere for a period of up to 4 weeks. After this time the tubes are collected and stored for analysis in the laboratory.			

1.2 PERSON RESPONSIBLE FOR MANAGING THIS WORK			
Name:	Eliani Ezani	**Position:**	PhD Student
Signature:		**Date:**	
Department:	Civil and Environmental Engineering		

1.3 PERSON CONDUCTING THIS ASSESSMENT			
Name:	Eliani Ezani	**Signature:**	
Name:	Nicola Masey	**Signature:**	
Name:	David Sykes	**Signature:**	
Date risk assessment undertaken:	7th July 2014		

1.4 ASSESSMENT REVIEW HISTORY

This assessment should be reviewed immediately if there is any reason to suppose that the original assessment is no longer valid. Otherwise, the assessment should be reviewed annually. The responsible person must ensure that this risk assessment remains valid.

	Review 1	Review 2	Review 3	Review 4
Due date: **Date conducted:**				
Conducted by:				

B (5): Outdoor RA form

University of Strathclyde Glasgow

GENERAL RISK ASSESSMENT FORM (S20)

Persons who undertake risk assessments must have a level of competence commensurate with the significance of the risks they are assessing. It is the responsibility of each Head of Department or Director of Service to ensure that all staff are adequately trained in the techniques of risk assessment. The University document "Guidance on Carrying Out Risk Assessments" will be available, in due course, to remind assessors of the current practice used by the University. However, reading the aforementioned document will not be a substitute for suitable training.

Prior to the commencement of any work involving non-trivial hazards, a suitable and sufficient assessment of risks should be made and where necessary, effective measures taken to control those risks.

Individuals working under this risk assessment have a legal responsibility to ensure they follow the control measures stipulated to safeguard the health and safety of themselves and others.

SECTION 1

1.1 OPERATION / ACTIVITY			Complete the relevant details of the activity being assessed.
Title:	Measurement air pollution during commuting along Glasgow city centre		
Department:	Civil and environmental engineering		
Location(s) of work:	Outdoors	**Ref No.**	

Brief description: Atmospheric black carbon (BC), nitrogen dioxide (NO_2) and ozone concentrations are measured using transportable monitoring devices that will be carried in a backpack while walking along predefined routes to and from the University of Strathclyde. Several repetitions of these routes will be undertaken.
Passive diffusion tubes (PDTs) will also be set up to record ambient NO_2 along the same routes.

1.2 PERSON RESPONSIBLE FOR MANAGING THIS WORK			
Name:	Eliani Ezani	**Position:**	PhD Student
Signature:		**Date:**	
Department:	Civil and Environmental Engineering		

1.3 PERSON CONDUCTING THIS ASSESSMENT			
Name:	Eliani Ezani	**Signature:**	
Name:	Akinola Idowu	**Signature:**	
Name:		**Signature:**	
Date risk assessment undertaken:	3th June 2015		

1.4 ASSESSMENT REVIEW HISTORY

This assessment should be reviewed immediately if there is any reason to suppose that the original assessment is no longer valid. Otherwise, the assessment should be reviewed annually. The responsible person must ensure that this risk assessment remains valid.

	Review 1	Review 2	Review 3	Review 4
Due date:				
Date conducted:				
Conducted by:				

B (6): Poland fieldwork RA form

University of Strathclyde Glasgow

GENERAL RISK ASSESSMENT FORM (S20)

Persons who undertake risk assessments must have a level of competence commensurate with the significance of the risks they are assessing. It is the responsibility of each Head of Department or Director of Service to ensure that all staff are adequately trained in the techniques of risk assessment. The University document "Guidance on Carrying Out Risk Assessments" will be available, in due course, to remind assessors of the current practice used by the University. However, reading the aforementioned document will not be a substitute for suitable training.

Prior to the commencement of any work involving non-trivial hazards, a suitable and sufficient assessment of risks should be made and where necessary, effective measures taken to control those risks.

Individuals working under this risk assessment have a legal responsibility to ensure they follow the control measures stipulated to safeguard the health and safety of themselves and others.

SECTION 1

1.1 OPERATION / ACTIVITY			Complete the relevant details of the activity being assessed.
Title:	Recording of air pollution data at unconventional natural gas operation site		
Department:	Civil and environmental engineering		
Location(s) of work:	Outdoors	**Ref No.**	
Brief description: Atmospheric black carbon (BC), nitrogen dioxide (NO_2) and ozone concentrations will be measured using mobile monitors over the course of a day at a model unconventional natural gas (UNG) operation site in Poland.			

1.2 PERSON RESPONSIBLE FOR MANAGING THIS WORK			
Name:	Eliani Ezani	**Position:**	PhD student
Signature:		**Date:**	
Department:			

1.3 PERSON CONDUCTING THIS ASSESSMENT			
Name:	Eliani Ezani	**Signature:**	
Name:	Megan Tailford	**Signature:**	
Name:		**Signature:**	
Date risk assessment undertaken:	16th June 2015		

1.4 ASSESSMENT REVIEW HISTORY

This assessment should be reviewed immediately if there is any reason to suppose that the original assessment is no longer valid. Otherwise, the assessment should be reviewed annually. The responsible person must ensure that this risk assessment remains valid.

Due date:	Review 1	Review 2	Review 3	Review 4
Date conducted:				
Conducted by:				

APPENDIX C: R SCRIPT

```
install.packages (zoo)
install.packages (plotKML)
require (zoo)
require (plotKML)
# function to interpolatie GPX files to 1 second.  Uses linear interpolation and assumes
interpolate_GPS <- function(file = file.choose(), name = "output.csv"){
  #function to convert zoo object back into a dataframe
  zoo.to.data.frame <- function(x, index.name="date.time") {
    stopifnot(is.zoo(x))
    xn <- if(is.null(dim(x))) deparse(substitute(x)) else colnames(x)
    setNames(data.frame(index(x), x, row.names=NULL), c(index.name,xn))
  }
  # read the GPX file and convert to a dataframe
  df1 <- readGPX (file)
  df2 <- data.frame (df1[4])
  names (df2) <- c("lat", "lon", "elevation", "date.time")
  df <- df2 [c(4,1,2)]
  #create POSIXct (date format) column within dataframe
  df$date.time <- with(df,as.POSIXct(date.time,format="%Y-%m-%dT%H:%M:%S.000Z", tz
= "GMT"))
  #extrapolate the time series to include all mising seconds
  full.time    <- with(df,seq(date.time[1],tail(date.time,1),by=1))
  #convert to zoo object
  df.zoo <- zoo(df[,2:3],df$date.time)
  #interpolate the missing values
  result <- na.approx(df.zoo,xout=full.time)
  # convert back to data frame and write the output as a csv
  return (write.csv (zoo.to.data.frame (result), name))
}
```